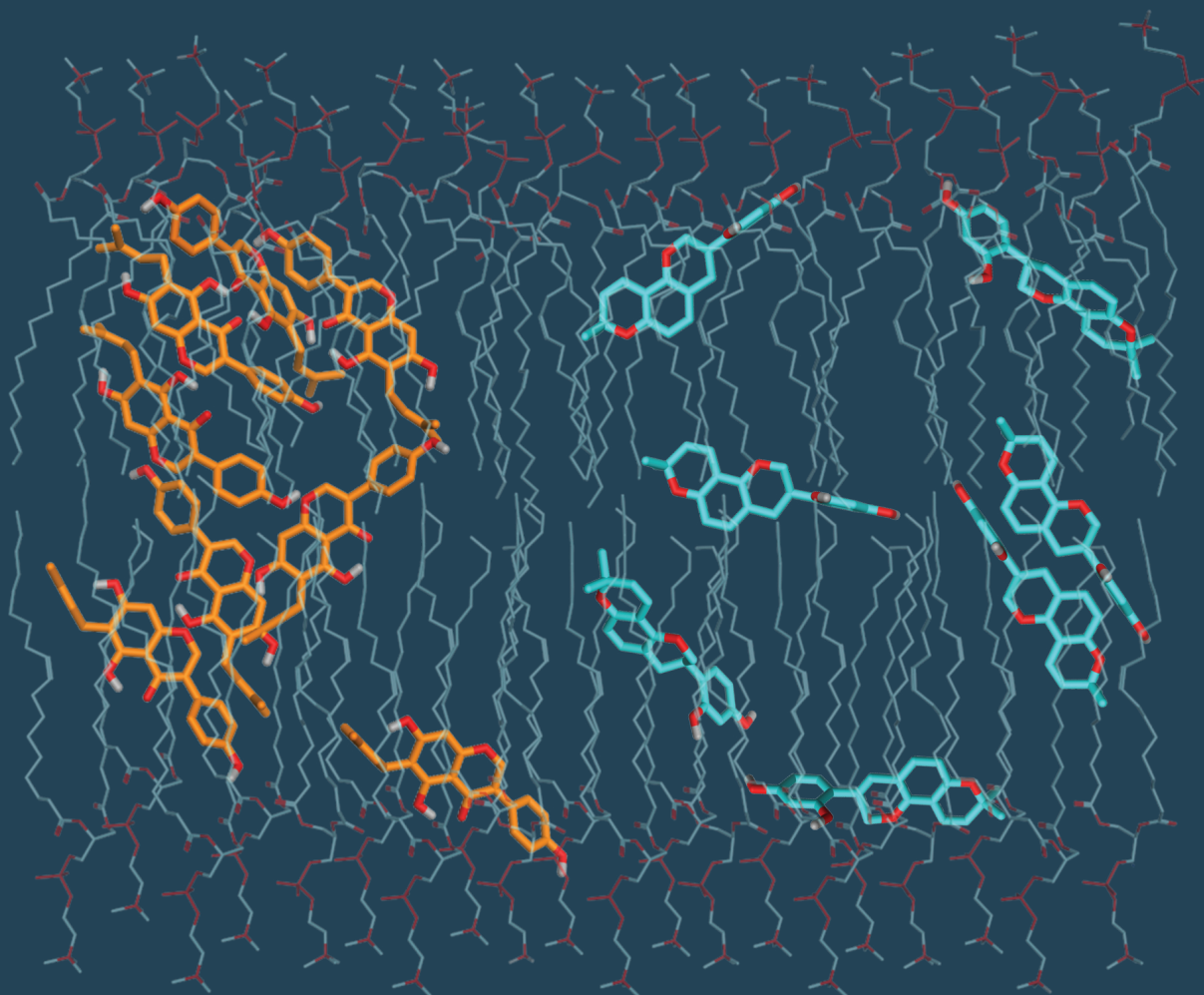


Prenylated (iso)flavonoids as antimicrobial agents

Production, activity and mode of action



Sylvia Kalli-Angel

Propositions

1. Mono-prenylated isoflavonoids can serve as promising antimicrobials against Gram-positive bacteria and yeasts.
(this thesis)
2. The concepts of priming and elicitation cannot be distinguished on the basis of defence metabolite production.
(this thesis)
3. The exponentially growing developments in genetic engineering will revolutionize the way we approach the Human Enhancement Question ("what do we want to become?").
based on Yuval Noah Harari, *Sapiens: A Brief History of Humankind*
4. The olympic motto - *Citius, Altius, Fortius* (faster, higher, stronger) - is getting increasingly applicable to science.
5. Emotional intelligence should be raised through compulsory activities already in early stages of education.
6. Music disturbs inertia and comforts chaos.

Propositions belonging to the thesis, entitled:

Prenylated (iso)flavonoids as antimicrobial agents

Production, activity and mode of action

Sylvia Kalli-Angel

Wageningen, 28 May 2021

Prenylated (iso)flavonoids as antimicrobial agents

Production, activity and mode of action

Sylvia Kalli-Angel

Thesis committee

Promotor

Prof. Dr J.-P. Vincken
Professor of Food Chemistry
Wageningen University & Research

Co-promotor

Dr C. Araya-Cloutier
Assistant professor, Laboratory of Food Chemistry
Wageningen University & Research

Other members

Prof. Dr T. Abee, Wageningen University & Research
Dr V. Fotopoulos, Cyprus University of Technology, Limassol, Cyprus
Prof. Dr N. Martin, University of Leiden
Prof. Dr H.-G. Janssen, Wageningen University & Research

This research was conducted under the auspices of the Graduate School VLAG (Advanced studies in Food Technology, Agrobiotechnology, Nutrition and Health Sciences).

Prenylated (iso)flavonoids as antimicrobial agents

Production, activity and mode of action

Sylvia Kalli-Angel

Thesis

submitted in fulfilment of the requirements for the degree of doctor
at Wageningen University

by the authority of the Rector Magnificus,

Prof. Dr A.P.J. Mol,

in the presence of the

Thesis Committee appointed by the Academic Board

to be defended in public

on Friday 28 May 2021

at 11 a.m. in the Aula.

Sylvia Kalli-Angel
Prenylated (iso)flavonoids as antimicrobial agents
Production, activity and mode of action
214 pages.

PhD thesis, Wageningen University, Wageningen, The Netherlands (2021)
With references, with summary in English

ISBN 978-94-6395-679-6
DOI <https://doi.org/10.18174/538785>

To my father

Στον μπαμπά μου

*που τον αναζήτησα πολλές
φορές αυτά τα τέσσερα χρόνια*

Abstract

Prenylated flavonoids and isoflavonoids (i.e. (iso)flavonoids) are typically produced in the legume (Fabaceae) family as part of plant's defence mechanism. Prenylation, i.e. the substitution with a C5-isoprenoid moiety, is acknowledged for conferring the antimicrobial properties of prenylated (iso)flavonoids. The first aim of this thesis was to enhance the amounts and diversity of prenylated (iso)flavonoids *in planta* using the well-studied legume, soybean. Second, the antimicrobial properties of prenylated (iso)flavonoids against the Gram-positive pathogen, methicillin-resistant *Staphylococcus aureus* (MRSA) and the food spoilage yeast, *Zygosaccharomyces parabailii* were explored. Lastly, insights into the mode of action of antimicrobial prenylated (iso)flavonoids were sought through *in silico* and *in vitro* means.

Sensitization of soybean seedlings with reactive oxygen species (ROS), generated through H₂O₂ and FeSO₄, prior to microbial elicitation enhanced the production of prenylated isoflavonoids (glyceollins), compared to the traditional fungal elicitation without priming. Application of the most stable ROS, H₂O₂, together with AgNO₃, prior to microbial elicitation enhanced the production of prenylated isoflavones and a coumestan with promising antibacterial activity, in addition to glyceollins. A systematic study on 106 prenylated (iso)flavonoids tested against MRSA showed that 75% of the di-prenylated (iso)flavonoids and 40% of the mono-prenylated ones were active with minimum inhibitory concentrations (MIC) \leq 25 μ g/mL. Formal and partial charge, hydrophobic volume and uneven distribution of hydrophobic moieties were correlated to antimicrobial activity. The different molecular properties suggested potentially distinct interactions of the different prenylated (iso)flavonoid subclasses with the microbial membrane. Two mono-prenylated isoflavonoids from different subclasses were found to be very active towards the food spoiler and weak organic acid-resistant *Z. parabailii* (MIC \leq 12.5 μ g/mL, pH 4.0). Killing of *Z. parabailii* was evidenced within 15 min of exposure to these compounds, accompanied with different deformations of the yeast membrane. Prenylated (iso)flavonoids can be powerful antimicrobials to be used as therapeutics or food preservatives, when their toxicity profile against human cells has been verified. The quantitative models developed provide useful information on the design of new antimicrobial prenylated (iso)flavonoids.

Table of contents

Chapter 1	General Introduction	1
Chapter 2	Enhanced biosynthesis of the natural antimicrobial glyceollins in soybean seedlings by priming and elicitation	31
Chapter 3	Induction of promising antibacterial prenylated isoflavonoids from different subclasses by sequential elicitation of soybean	53
Chapter 4	Prenylated (iso)flavonoids as agents against methicillin-resistant <i>Staphylococcus aureus</i> - Insights into the molecular properties underlying antibacterial activity	85
Chapter 5	Prenylated (iso)flavonoids as antifungal agents against the food spoiler <i>Zygosaccharomyces parabailii</i>	139
Chapter 6	General Discussion	175
Summary		203
Acknowledgements		207
About the author		211

CHAPTER

1

General Introduction

The quest for promising, naturally-derived antimicrobial agents with fundamentally different modes of action from the traditional antimicrobials, is imperative. Molecules with more than one phenolic ring, the so-called polyphenols, are specialized metabolites constitutively present in plants. These polyphenols can be decorated with a C5-isoprenoid (*prenyl*) moiety as a result of the plant's strategy to defend itself from invaders. This property may render prenylated phenolic compounds interesting antimicrobial properties. Although effort has been put into exploring the mode of action of these molecules, only small steps have been made. Prenylated phenolics are a diverse group of molecules that can possess different backbones which are decorated with the prenyl group, as well as other functional groups, at different locations and various configurations. However, this large molecular diversity cannot be easily covered in clear-cut structure activity relationships (SARs), which would be the first step in understanding the mode of action of these molecules. In addition, all the different features decorating prenylated phenolics can make a difference in their antimicrobial properties. Hence, investigation and better understanding of overall molecular properties contributing to antimicrobial activity is necessary. Despite the large chemical diversity of prenylated phenolics, their abundance, even in stressed plants, is low which limits their use. Novel, non-laborious ways for efficient production of chemically diverse prenylated phenolics are still under investigation. The need for natural agents that possess antimicrobial activities towards key microorganisms and ways of enhancing their production will be elaborated in this chapter.

1.1. Increased demand for novel, natural and promising antimicrobial agents

1.1.1. Food preservation

Microbial food spoilage is related to food borne illnesses, food waste, substantial economic losses and to a negative impact on brand names, posing a major health and economic challenge.

The most common spoilage and pathogenic bacteria in foods are *Listeria monocytogenes*, *Escherichia coli* O157, *Salmonella typhimurium*, *Staphylococcus aureus*, *Bacillus cereus*, *Campylobacter jejuni*, *Clostridium perfringens* [1]. Yeasts become more relevant than bacteria during food preservation. Yeast species such as *Zygosaccharomyces bailii*, *Zygosaccharomyces rouxii*, *Debaryomyces hansenii*, *Kluyveromyces lactis* and *Saccharomyces cerevisiae* are often encountered in high sugar and/or acid products such as salad dressings, fruit juices, wine, mayonnaise, chocolate and soft drinks [2].

To prevent the growth of these problematic microorganisms, various preservation techniques are employed in the food industry, together with regular quality, safety and hygienic controls [3-5]. Thermal processing, packaging, irradiation, water activity decrease, and the use of chemical preservatives are some of the means utilized to ensure food safety and stability. Heat treatment and synthetic preservatives are thought to be the most effective means to control the growth of notorious microorganisms [6,7].

Weak organic acids, such as sorbic and benzoic acid are extensively used in large-scale food and soft drink preservation, as they are highly effective against most microbial species especially at low pH [8]. However, major safety concerns about these molecules have led to restriction in their use and to a negative reputation among consumers [8,9]. Furthermore, spoilage yeasts have developed several resistance mechanisms towards carboxylate weak acids, such as enzymatic degradation, limitation of diffusional entry of the acid, activation of efflux pumps [8], and phenotypic heterogeneity [10]. This necessitates the addition of these molecules in very high and unpermitted levels (mM concentrations) in food products [8].

Although, single preservation techniques can be powerful, they might compromise food quality [11] and/or they are poorly perceived by the consumers [8]. Nowadays, where interactions between the different techniques are better known, combinations are frequently used [12]. This so-called "hurdle technology" pertains the sequential use of multiple preservation "hurdles" against the growth of problematic microorganisms. These hurdles are thought to act synergistically balancing food safety, stability and quality [13]. However, certain microorganisms might still survive hurdle technology [14].

The need to employ more sustainable food preservation practices without compromising the quality and safety of food products has led to a growing demand

for novel, milder yet effective preservation alternatives. In this thesis, prenylated (iso)flavonoids are explored as promising, alternative food preservatives.

1.1.2. Clinical setting

The use of antibiotics for the treatment of infectious diseases is one of the most revolutionary breakthroughs of modern medicine. With the advent of penicillin (1929) and then actinomycin (1940), antibiotics faced a golden discovery era for approximately 30 years ^[15]. In the late '60s, the discovery rate of novel scaffolds dropped and mainly relied on optimization/modification of already existing ones ^[16]. This, along with the (irrational) use of antibiotics in multiple settings (clinical, agricultural, food, and veterinary) ^[17], led to antimicrobial resistance (AMR). Around this time, the clinical usage of methicillin to treat *Staphylococcus aureus* (SA) began and soon after, SA started to develop resistance towards this antibiotic (MRSA strain). Similarly, 20 years later, the emergence of vancomycin-resistant enterococci (VRE) MDR-*Mycobacterium tuberculosis* emerged and gradually spread in clinical settings and communities worldwide. After the 1990s, AMR started to supersede drug discovery and scaffold optimization ^[18]. The wide range of AMR mechanisms include enzymatic inactivation of the drug e.g. by acetylation, adenylation and phosphorylation ^[19], modification of drug targets, changing cell permeability through porin loss or increase in expression of efflux pumps, and mechanical protection provided by biofilm formation ^[20]. Being in the AMR era already for a decade, severe, unprecedented complications peril public health, environmental and economic welfare ^[21]. At the moment, drug-resistant diseases cause the death of at least 700,000 people annually (33% of which die from multidrug-resistant tuberculosis) ^[22]. The World Health Organization has named AMR as one of the three most important public health threats of the 21st century ^[22]. This thesis deals with the potency of prenylated (iso)flavonoids as novel, natural antimicrobial agents.

1.2. Yeast and bacterial cell envelop

The microbial cell envelop is a complex multi-layered structure (**Figure 1.1**) that protects microorganisms from their hostile environment ^[23]. For Gram-positive bacteria and yeasts, the cell envelop consists of an outermost layer, the cell wall, which is the first barrier that antimicrobials need to cross, and the cytoplasmic (plasma) membrane, which keeps the interior of the cell separate from the extracellular environment ^[23]. Gram-negatives, however, possess an additional outer membrane that is separated from the inner one by the periplasm ^[24]. Although the overall make-up of the cell envelop is similar across bacteria and fungi (yeasts), the composition of the two cell envelop constituents, i.e. cell wall and cytoplasmic membrane, is markedly different.

The cell wall of Gram-positive bacteria is composed of a thick peptidoglycan layer (accounts for 50% of the weight of the wall ^[25]) through which teichoic acids (which can account for up to 50% of the mass of the cell wall ^[26]) are threaded.

Teichoic acids are negatively charged and this charge is screened by divalent cations (mainly Ca^{2+} and Mg^{2+}). Teichoic acids do not influence the permeation of charged molecules ^[27] and have minimal effect on the penetration of hydrophobic substances. An important form of teichoic acid is the lipoteichoic acids, which connect the cell wall to the cytoplasmic membrane ^[27]. In contrast, the yeast cell wall is an ensemble of cross linked β -1,3 and β -1,6 glucans (35-55% of wall mass) with mannoproteins and a layer of chitin (1.5-6.0% wall mass in *S. cerevisiae* ^[28]) bound to the glucan network. Mannoproteins form a fibrillar layer in the most external part of the yeast cell walls ^[29].

The cytoplasmic membrane of Gram-positive and Gram-negative bacteria is primarily made of phospholipids, whereas that of yeasts (e.g. *S. cerevisiae*), additionally contains approximately 30% of sphingolipids ^[30] and a significant, yet undefined amount of sterols ^[31]. In the membrane of these microbial types, integral proteins, influx transporters and transmembrane efflux pumps are located ^[19,23,32].

Even though the inner membrane and the inner leaflet of the outer membrane (OM) of Gram-negatives are primarily made of phospholipids, the outer leaflet of the OM is mostly made of negatively charged lipopolysaccharides (LPS), which are stabilized on the surface of the OM by divalent cations. Contrary to teichoic acids in Gram-positives, LPS are thought to limit the penetration of hydrophobic molecules more in Gram-negatives ^[23,33]. Moreover, small hydrophilic channels, known as porins, exert additional size and hydrophobicity barriers in the Gram-negatives ^[33]. Porins have also been identified in some Gram-positive mycobacteria ^[34-36] and at least one porin has been reported in yeasts, mainly transporting water and glycerol ^[37]. The efflux pumps present in Gram-negatives efficiently extrude compounds both from the cytoplasm and the periplasm as they span from the inner to the outer membrane ^[38].

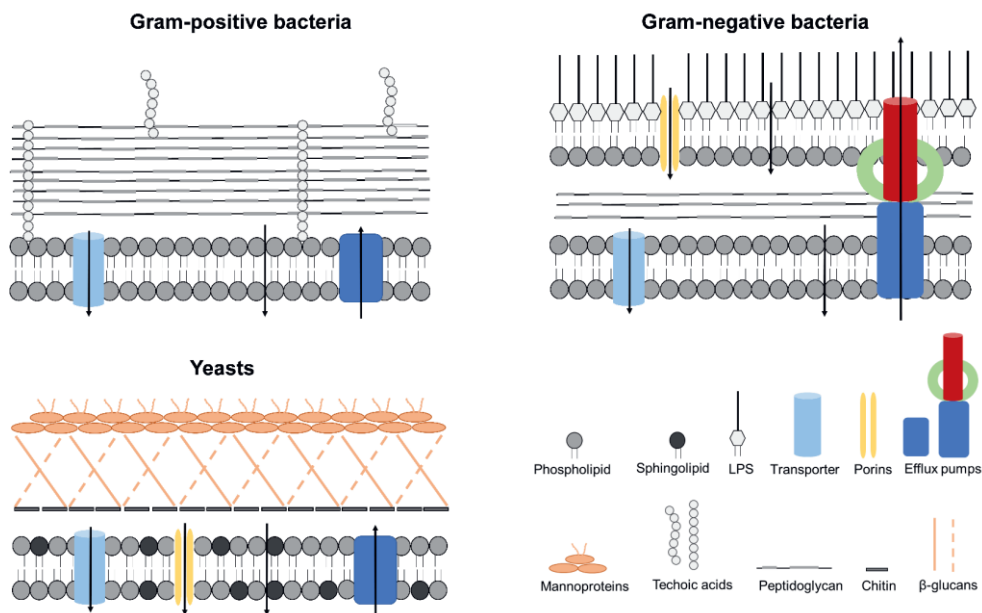


Figure 1.1. Simplified representation of bacterial and yeast cell envelop focusing on the main similarities and differences in architecture. Arrows indicate routes of antimicrobial influx and efflux. Based on Silhavy *et al.* (2010) and Schreuder *et al.* (1996) [23,39].

1.3. Opportunities offered by plants - prenylated (iso)flavonoids as potent antimicrobials

Due to the growing prevalence of drug-resistant pathogens and preservative-resistant food-spoilage microorganisms, novel, powerful antimicrobial agents with fundamentally different modes of action from the currently used substances are sought. A promising alternative can be offered by plants.

Plants have been acknowledged as sources of essential oils and extracts used for food preservation and as therapeutics since prehistory [40,41]. Rational drug discovery started with the isolation of morphine, the famous painkiller and sleep-inducer from opium. This discovery triggered the discovery of a series of plant-derived therapeutics [42]. Subramani *et al.* (2017) has provided an overview of plant-derived molecules and extracts reported during 2005-2015, which have been used against multi-drug-resistant pathogens [43]. Triterpenes from the leaves *Planchonia careya* [44] and flavonoids from the roots of *Sophora flavescens* targeted both MRSA and VRE [45,46].

The Fabaceae (Leguminosae) is the third largest plant family [47] and was listed as one of the most important medicinal plant families on a worldwide scale [48], with more than 490 medicinal plant species [49]. Recently, the Leguminosae was ranked as the family with the most species (in total 28) able to cure tuberculosis [50]. The main secondary metabolites in legumes include alkaloids, cyanogens,

peptides, phenolic compounds, polyketides, and terpenoids [51]. The *Papilionoideae* subfamily of Fabaceae is the largest producer of prenylated flavonoids and isoflavonoids (collectively termed in this thesis as (iso)flavonoids) [52,53]. Prenylated (iso)flavonoids are appreciated for their wide range of bioactivities, including antioxidant, (anti)estrogenic, anti-inflammatory, antitumor and antimicrobial activities [54].

1.3.1. Structural diversity of prenylated (iso)flavonoids

(Iso)flavonoids are synthesized through the phenylpropanoid pathway (**Figure 1.2**) using phenylalanine as a building block. Phenylalanine is converted into *p*-coumaroyl-CoA through cinnamate [55]. *p*-Coumaroyl-CoA is condensed with three malonyl-CoA units, either by chalcone synthase (CHS) to yield chalconaringenin, or by CHS and chalcone reductase (CHR) to yield isoliquiritigenin. These two chalcones are further cyclized into the corresponding 2-aryl benzopyrans (flavonoids), naringenin and liquiritigenin. Isoflavonoids (3-aryl benzopyrans) derive after aryl rearrangement from the C2 to the C3 of the benzopyran moiety of the flavonoid. This rearrangement is catalysed by 2-hydroxyisoflavanone synthase (2-HIS) and 2-hydroxyisoflavanone dehydratase (2-HID) and yields the simplest isoflavonoids, daidzein and genistein, from liquiritigenin and naringenin, respectively [56]. Because (iso)flavonoids contain a C6–C3–C6 framework, they are often related to xanthones (C6–C1–C6) [57], but xanthones are synthesized via the acetate-shikimate pathway in plants [58].

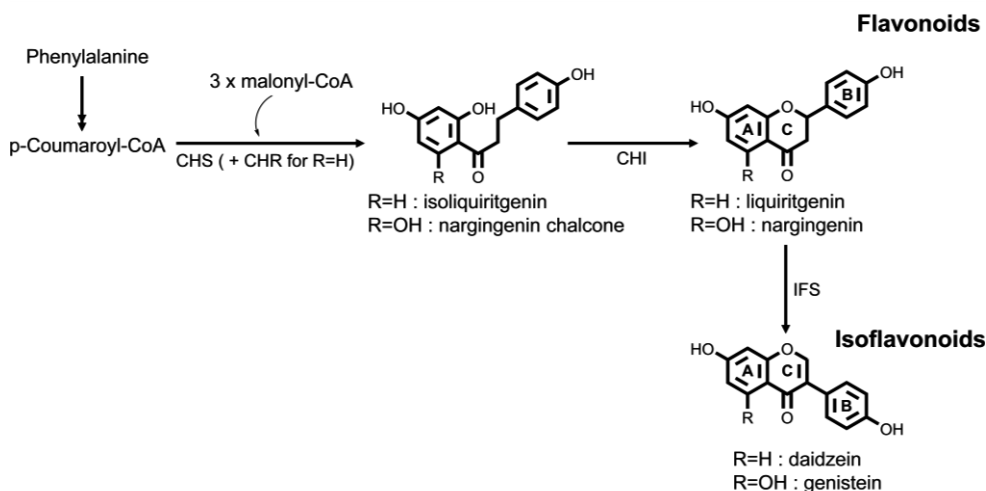


Figure 1.2. Simplified biosynthetic pathway of (iso)flavonoids. The main enzymes involved are: CHS, chalcone synthase; CHR: chalcone reductase; CHI, chalcone isomerase; 2-HIS: 2-hydroxyisoflavanone synthase; 2-HID: 2-hydroxyisoflavanone dehydratase. Adapted from Dixon *et al.* (1999) [59].

To date, 8 and 13 different subclasses have been described for flavonoids and isoflavonoids, respectively. This chemical diversity mainly stems from the level of oxidation of the C-ring [60,61]. Isoflavonoid subclasses with an additional heterocyclic ring (D-ring) are also encountered in legumes, which account for their increased diversity compared to flavonoids [62,63]. The main (iso)flavonoid subclasses frequently encountered in legumes are shown in **Figure 1.3**.

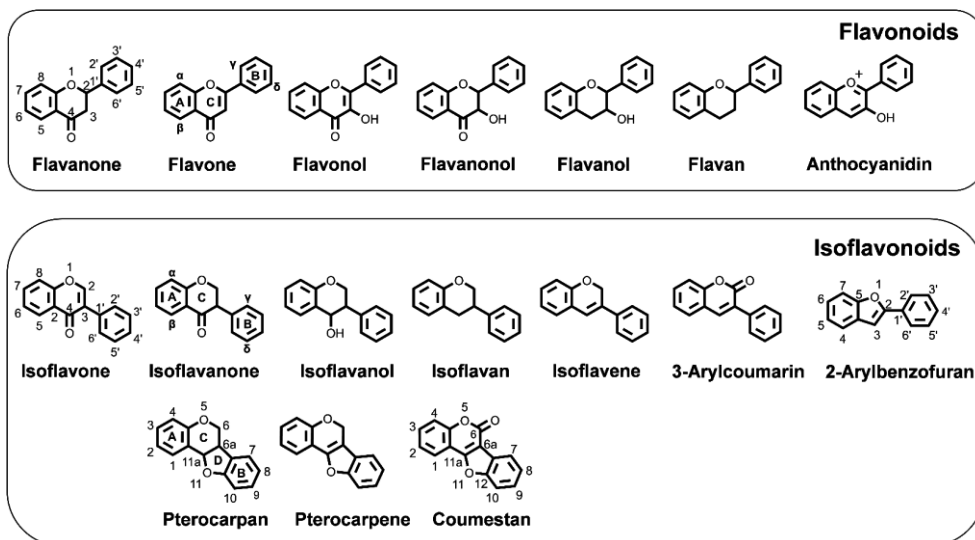


Figure 1.3. Most frequently encountered (iso)flavonoid subclasses. The subclass-dependent IUPAC numbering is also demonstrated. For the subclasses where the numbering is not shown, these are numbered similarly to first subclass in the row. Greek letters denote possible positions for prenyl substitution in flavonoids and isoflavonoids, independent of the subclass.

The extensive chemical diversity of (iso)flavonoids generated from the different subclasses becomes even larger due the occurrence of different substituents on the (iso)flavonoid backbone. The most common decoration in (iso)flavonoids involves hydroxyl, *O*-methyl, glycosyl and, as mentioned, prenyl-groups. Prenyl-substituted (iso)flavonoids are the main focus of this thesis.

Prenylation refers to substitution of a molecule with five-carbon (prenyl), ten-carbon (geranyl or lavandulyl) or fifteen carbon (farnesyl) isoprenoid moieties. This thesis exclusively deals with five-carbon isoprenoid groups. Prenyl groups can adopt multiple configurations; a chain (3-dimethylallyl or 3-methylbut-2-enyl) or a five-membered ring (2"-isopropenylfuran) or a six-membered ring (2,2-dimethylpyran) coupled to a vicinal hydroxyl group (**Figure 1.4**). Additional chain prenyl-configurations depending on the presence of hydroxylation and position of unsaturation, such as 2-methylbut-3-en-2-yl [64], 3-methylbut-1-enyl [65] have been also encountered in nature.

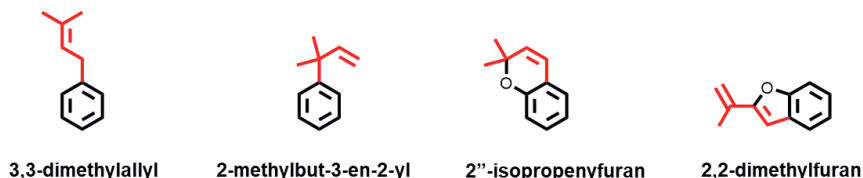


Figure 1.4. Prenyl configurations encountered in this thesis (in red).

Both C- and O-prenylation have been described in plants, but C-prenylation is more dominant ^[66]. Furthermore, prenylation mainly occurs at the A- and the B-rings, although prenylation at the C-ring can be also encountered ^[67].

1.3.2. Enhancing the biosynthesis of prenylated (iso)flavonoids

1.3.2.1. Induction of plant's defence mechanism as an alternative to chemical or enzymatic production systems

To study SARs and mode of action of prenylated (iso)flavonoids extensive structural variation is essential. Still, the quantities and induced chemical diversity of prenylated (iso)flavonoids are restrictive. Several strategies have been employed to increase the yields of and diversify the prenylated (iso)flavonoids produced. Chemical synthesis ^[68-71], biotransformation using transgenic yeasts expressing either plant prenyltransferases ^[72,73] or microbial prenyltransferases ^[74-76] have been employed. Nevertheless, complications like limited scaffold diversity ^[77], expensive and environment-unfriendly reagents and harsh conditions have been associated with chemical synthesis ^[65]. Similarly, the high substrate- and regio-specificity of plant prenyltransferases may prevent the achievement of wide structural diversity ^[78]. The low conversion yields (<10%) ^[74] and the possible antifungal activities of the resulting compounds limit the use of microbial production systems.

Higher plants can be considered as a biochemical factory of prenylated (iso)flavonoids as part of their defence mechanism. This defence mechanism can be mobilized *in vivo* leading to enhanced amounts and/or chemical diversity of prenylated (iso)flavonoids. Elicitation, for example, has been described as one of the most practically feasible techniques for the production of specialized metabolites. Elicitation is defined as the application of a small concentration of a substance, which induces or improves the biosynthesis of metabolites ^[79]. Elicitation proceeds through activation of a signal-transduction cascade that leads to activation or *de novo* biosynthesis of transcription factors, which in turn regulate the expression of biosynthetic genes involved in specialized metabolites ^[80]. Factors such as type and concentration of elicitor, treatment duration, plant's age and cultivar can crucially influence the effectiveness of elicitation ^[81,82].

Elicitors are conventionally classified into biotic and abiotic agents depending on their nature (**Figure 1.5**). Biotic elicitors can be exogenous such as live microorganisms or their constituents (e.g. yeast cell wall or fungal cell wall oligosaccharides ^[83,84]) or endogenous, such as plant-derived fragments ^[79,85,86]. Abiotic elicitors include chemical and physical stressors or plant's signalling molecules (the latter are sometimes classified under biotic elicitors).

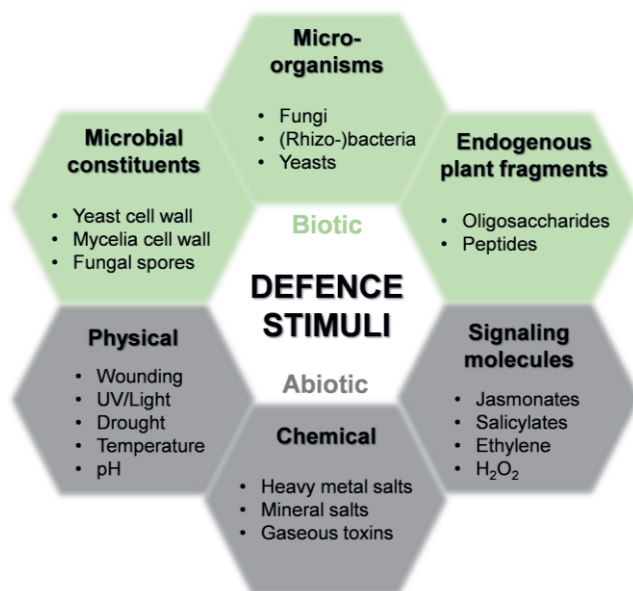


Figure 1.5. Overview of agents that stimulate plant's defense mechanism. Based on Shakya *et al.* (2019) ^[87].

Besides elicitors, plant's defence mechanism can also be conditioned by so-called primers. Interestingly, the same agents that can function as elicitors can also act as primers ^[88], making priming and elicitation two highly intertwined concepts. Priming is a low-cost (although there might be some allocation and/or ecological costs) defensive state, activated by a priming stimulus and functions as a warning signal for a subsequent stress (challenging stimulus, i.e. elicitation). Primed plants are reported to deploy defence responses in a faster, stronger, and/or more sustained manner after the perception of a later elicitor ^[89,90]. In contrast, elicitation, without prior priming, leads plants into an immediate, fully activated defence state which is accompanied with high fitness costs. Priming *per se* is traditionally thought to involve minimal or no gene expression changes ^[91-94]. It should however be noted that advanced analytical tools (e.g. -omics) ^[95] showed that priming can induce direct defensive changes in the plant ^[88], rendering the concepts of priming and elicitation more strongly intertwined than already suggested by the similarity in the sensitizing agents. It is postulated that a primed

plant stores defence-related information until exposure to a challenging stimulus (i.e. elicitation). In the time span between the perception of the priming and the elicitation stimulus, the so-called memory, the defence responses, which are marginally induced upon priming, return to basal levels^[96]. Nevertheless it is not clear whether fitness costs also return to basal levels when memory is asserted. Defence responses include alterations in signalling pathways and associated molecules and production of specialized metabolites e.g. phenolics^[95]. Overall, priming is anticipated to lead to a positive cost-benefit balance upon a subsequent elicitation. The effects of priming on the memory, fitness and robustness of defence responses are shown in **Figure 1.6**.

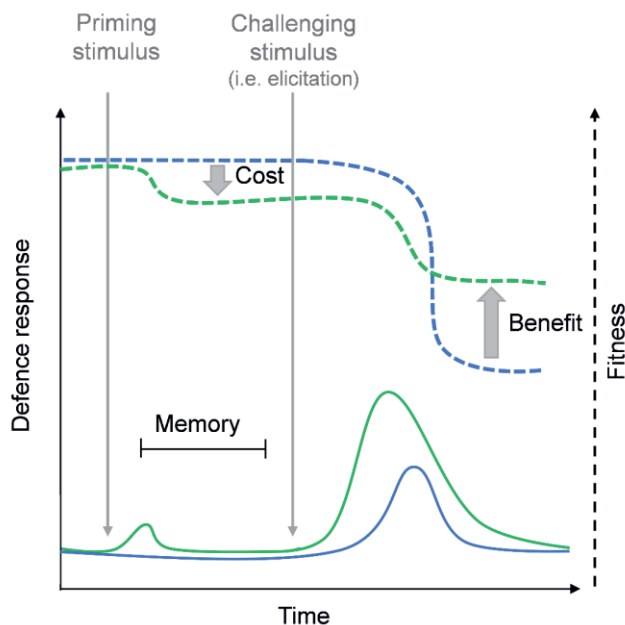


Figure 1.6. Effect of priming on the memory, fitness and defence responses of a plant. Primed (green) and unprimed (blue) plants are subjected to a challenging stimulus (i.e. elicitation). The area under the curve represents the extent of induction of defence responses. Adapted from Martinez-Medina *et al.* (2016)^[96].

1.3.2.2. *In planta methods for the biosynthesis of prenylated phenolics*

Several techniques have been employed for the production of prenylated phenolics in plants (**Table 1.1**). Soybeans, mostly in the form of seedlings, are the most studied legume with respect to the production of prenylated isoflavonoids. 6a-OH-pterocarpan (glyceollins) are predominantly induced in elicited soybeans, occasionally followed by the induction of prenylated isoflavones and prenylated coumestans^[97,98]. The highest amounts of prenylated isoflavonoids reported in

soybean, is 2 mg daidzein equivalents/g DW obtained in *Rhizopus*-elicited seedlings [97,98]. However, elicitation of plant cell and organ cultures of *Hypericum perforatum* [99] or in peanuts [100] resulted in 50 times higher yields of prenylated xanthones and of prenylated stilbenoids, respectively. In general, elicitation with microorganisms is considered highly successful, but it relies on the intricate interactions between the plant and the microorganism. For example, glyceollins are produced only in incompatible interactions (successful plant defence) [101,102] and not in compatible interactions (successful infection leading to disease) [103].

Abiotic agents can be alternatively used for the induction of prenylated phenolics (**Table 1.1**) as an effort to limit the biological variability that might arise both from the plant and the live microbial elicitors. Degousee *et al.* (1994), for example, used reactive oxygen species (ROS), the key signalling molecules accumulated in response to abiotic and biotic stresses [104] to specifically stimulate the production of glyceollins [105].

Some more sophisticated treatments have been also applied to increase the biosynthesis of prenylated isoflavonoids in soybeans. Combination of different elicitors, such as a live preparation of a fungus or a fungal cell wall glucan elicitor (WGE) with abiotic agents, such as UV-light or heavy metal salts [98,106], have been reported (**Table 1.1**). WGE combined with AgNO₃ resulted in an additive accumulation of glyceollin I [106]. The two agents were found to act via different modes. WGE induced major changes in gene transcripts related to the biosynthesis of glyceollins (mimicking basically the mode of action of the live fungus [107,108]), whereas AgNO₃ inhibited the degradation of glyceollin I while accelerating the hydrolysis of a glycosylated isoflavonoid precursor. Light combined with fungal elicitation resulted in a synergistic accumulation of prenylated isoflavonoids (60% higher than fungal elicitation alone) [98]. Light was reported to stimulate the production of the precursors, malonyl-CoA and coumaroyl-CoA [109] enhancing the levels of isoflavonoid precursors (e.g. daidzein) available for prenylation [98].

Furthermore, priming prior to elicitation is sometimes used. For example, signalling molecules were used to prime *H. perforatum* before fungal elicitation for the enhanced production of xanthones and flavonoids [110]. Likewise, signalling molecules were employed to both prime and elicit broccoli for the production of glucosinolates [111].

In contrast, priming followed by elicitation has not been reported for soybean. However, as seen in **Table 1.1**, some reports that claim simple elicitation of soybeans, use forms of wounded seedlings (incised or crumbled) prior to elicitation [106,112]. Wounding is a widely acknowledged priming stimulus which is associated with minimal (or no) induction of defence responses *per se* [98,113]. Thus, some treatments from **Table 1.1** should have been termed as priming plus elicitation treatments. This is an example of how easily the concept of priming can be ignored.

In this thesis, we aimed to use sophisticated treatments, including sensitization of seedlings before the traditional microbial elicitation, to improve the amounts and diversity of prenylated isoflavonoids biosynthesized in soybeans. We

used important signalling molecules such as ROS or the most stable ROS representative, H₂O₂ and the heavy metal salt, AgNO₃, as abiotic agents and the fungus, *Rhizopus oligosporus/oryzae* (benchmark treatment) or a rhizobacterium (*Bacillus subtilis*) as biotic agents.

For the sake of consistency, we distinguish the concepts of priming and elicitation for the sensitization treatment on the basis of defence responses. When a sensitization stimulus induces lower production of defence metabolites, i.e. prenylated isoflavonoids, than the benchmark treatment, this will be called a priming treatment. If the sensitization stimulus induces equal or higher production of prenylated isoflavonoids than the benchmark, then this treatment is considered an elicitation treatment.

1.3.3. Antimicrobial potency of prenylated (iso)flavonoids induced

Substantial amount of evidence has demonstrated the remarkable antimicrobial potency of prenylated (iso)flavonoids against bacteria, fungi, and yeasts ^[120-123]. Based on Gibbons *et al.* (2004), purified compounds with MIC values equal or lower than 15 µg/mL are considered as compounds with very high antimicrobial activity; compounds with MIC values from 15 up to and including 25 µg/mL are considered as having good activity, whereas compounds with MIC values from 25 up to and including 100 µg/mL are considered as having moderate antibacterial activity. Pure compounds with MIC values higher than 100 µg/mL are usually considered as having low activity ^[124]. In **Figure 1.7** and **Table 1.2**, examples of prenylated (iso)flavonoids with high antimicrobial activity are depicted.

The antimicrobial potency of prenylated (iso)flavonoids is comparable to, and in some cases even better than, conventional antibiotics (**Table 1.2**). For example, sedonan C showed a MIC value of 7.6 µg/mL against *S. cerevisiae* which is comparable to the MIC value of fluconazole ^[125]. Gancaonin Q had an MIC value of 0.6 µg/mL, whereas the antibiotic gentamycin had a 2-fold higher MIC ^[126]. Interestingly, when prenylated (iso)flavonoids are tested against more than one strain of the same species, they show activity within a very narrow range (usually 2-fold difference at the most). In contrast, antibiotics can have larger ranges of MIC values across different strains. For example, erybraedin A and eryzerin C showed MIC values of 1.6-3.1 µg/mL and 6.3 µg/mL against 4 strains of VRE, respectively, whereas vancomycin inhibited the VRE strains at concentrations of 12.5-100 µg/mL ^[127]. Similarly, candidone and neobavaisoflavone inhibited the growth of two strains of *Klebsiella pneumoniae* at a concentration of 8 µg/mL, whereas chloramphenicol showed a MIC range of 16-128 µg/mL against these two strains ^[128].

Table 1.1. Overview of induction methods for the production of prenylated phenolic. * DW and FW stand for dry, fresh weight, respectively.

Treatment	Agents	Plant species	Plant form	Induced prenylated phenolics	Induced amounts*	Subclass	Ref.
Abiotic elicitation							
	Acid (pH 3.0)	Soybean (<i>G. max</i>)	roots	Glyceollin I-III	0.3 mg/g seedlings or 1.7 mg /g roots	6a-OH pterocarpan	[114]
	AgNO ₃	Soybean (<i>G. max</i>)	incised seeds	Glyceollin I	0.2 mg/g FW	6a-OH pterocarpan	[106]
	ROS (1 M H ₂ O ₂ + 1 mM FeSO ₄)	Soybean (<i>G. max</i>)	hypocotyl/radicle	Glyceollin I	0.2 mg/g FW	6a-OH pterocarpan	[105]
	Sodium acetate	Peanut (<i>A. hypogaea</i>)	hairy root cultures	<i>Trans</i> -resveratrol, <i>trans</i> -arachidin-1 & 3	0.02 mg/g DW root	pterocarpan Stilbenoids	[115]
Biotic elicitation							
Fungus	<i>A. sojae</i>	Soybean (<i>G. max</i>)	crumbled seeds	Glyceollin I-II, glycofuran, A ^{prenyl} -daidzein and B ^{prenyl} -glycitein	No absolute quantified amounts (25–89% increase in prenylated isoflavonoids compared to control)	6a-OH pterocarpan, isoflavones	[116]
Fungus	<i>A. caelatus</i>	Peanut (<i>A. hypogaea</i>)	sliced seeds	Chiricanine A, arachidin 1-3, apahypin 1-5, SB-1, IPD	2.1 mg/g FW seed	Stilbenoids	[117]
Fungus	<i>R. oryzae</i>	Soybean (<i>G. max</i>)	seedlings	Glyceollin I-V, glyceollidins I-II, A ^{prenyl} - and B ^{prenyl} - daidzein and genistein, B ^{prenyl} -glycitein, phaseol	1.9 mg DE/g DW prenylated pterocarpan, 0.30 mg DE/g DW prenylated isoflavones, 0.09 mg DE/g DW phaseol	6a-OH pterocarpan	[97]
Fungal fragments	(Cell) wall glucan elicitor (WGE)	Soybean (<i>G. max</i>)	incised seeds	Glyceollin I	0.45 mg/g FW	6a-OH pterocarpan	[106]
Bacterium	<i>A. tumefaciens</i>	<i>H. perforatum</i>	cell culture	1,3,6,7-Tetrahydroxy-8-prenyl xanthone, 1,3,6,7-Tetrahydroxy-2-prenyl xanthone, 1,3,7-Trihydroxy-6-methoxy-8-prenyl xanthone	4.08 mg/g DW (13x more total prenylated xanthenes than control)	Xanthenes	[118]
Bacterium	<i>A. tumefaciens</i> or <i>rhizogenes</i>	<i>H. perforatum</i>	cell culture	Various prenylated xanthenes	90 mg/g DW (10x more total prenylated xanthenes than control)	Xanthenes	[99]

Table 1.1. Continued.

Treatment	Agents	Plant species	Plant form	Induced prenylated phenolics	Induced amounts*	Subclass	Ref.
Biotic elicitation							
Bacterium	<i>A. tumefaciens</i> or <i>rhizogenes</i>	<i>H. perforatum</i>	cell culture	Various prenylated xanthones	90 mg/g DW (10x more total prenylated xanthones than control)	Xanthones	[99]
Bacterial fragments	Mannans or acidic polysaccharides	<i>S. flavescentis</i>	callus cultures	Sophoraflavanone G and lehmanning	1-3 mg/g DW (5x higher than control)	Flavanones	[119]
Sophisticated elicitation							
Priming & elicitation	MeJA or SA and <i>H. perforatum</i> C. <i>gloeosporioides</i>		cell culture	1,3,7-Trihydroxy-6-methoxy-8-prenylxanthone, γ -mangostin	7 mg/g DW total xanthones (12x higher than the control)	Xanthones	[110]
Combined elicitation	WGE + AgNO ₃	Soybean (G. <i>max</i>)	incised seeds	Glyceollin I	0.64 mg/g FW	6a-OH pterocarpan Stilbenoids	[106]
Combined elicitation	methyl- β -cyclodextrin + 125 μ M MeJA + H ₂ O ₂ + MgCl ₂	Peanut (<i>A. hypogaea</i>)	hairy root cultures	Arachidin-1, arachidin-2, arachidin-3 and arachidin-5	107 mg/g DW		[100]
Combined elicitation	<i>R. oryzae</i> + light	Soybean (G. <i>max</i>)	seedlings	Glyceollin I-IV, glyceollidins II, glyceofuran, A ^{prenyl} - and B ^{prenyl} - daidzein/genistein, phaseol	2.3 mg DE/g DW prenylated pterocarpan, 0.9 mg DE/g DW prenylated isoflavones, 0.08 mg DE/g DW prenylated coumestan	6a-OH pterocarpan, isoflavones, coumestan	[98]

Double chain prenylated (iso)flavonoids are highly effective against Gram-positive bacteria, due to their efficient partitioning in the membrane ^[129]. In contrast, chain, mono-prenylated (iso)flavonoids have shown high potency towards Gram-negative bacteria, as they do not suffer from hydrophobicity restrictions posed by porin-mediated influx, as di-prenylated isoflavonoids do ^[129]. In this respect, Araya-Cloutier *et al.* (2018) found that mono-prenylated isoflavonoids exert their activity towards *E. coli* only under the presence of an efflux pump inhibitor (EPI) ^[129]. However, other studies which demonstrated the activity of prenylated (iso)flavonoids against Gram-negatives do not mention the use of an EPI ^[128,130]. The antimicrobial potency of prenylated (iso)flavonoids against yeasts is far less studied than that against bacteria. To date, both mono- and di-prenylated compounds, have been acknowledged for their remarkable antifungal activities (**Figure 1.7**), although, much less evidence is available for the latter.

From **Figure 1.7** and **Table 1.2**, it becomes also apparent that the antimicrobial potency of prenylated (iso)flavonoids is not specific to certain subclasses or degree of hydroxylation.

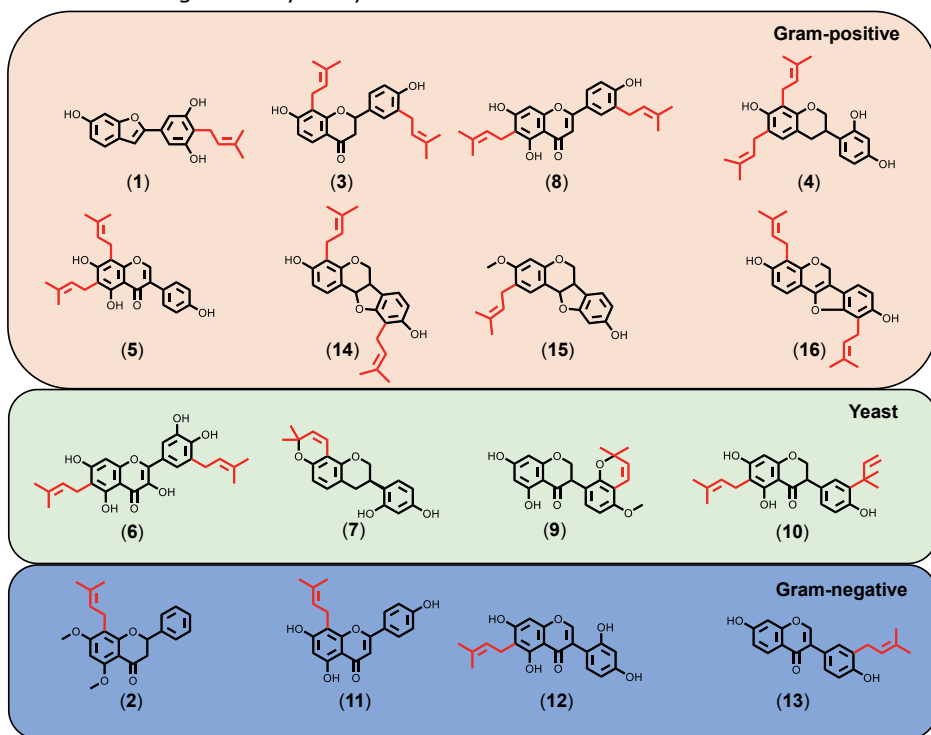


Figure 1.7. Examples of prenylated (iso)flavonoids with high antimicrobial activity ($\text{MIC} \leq 25 \mu\text{g/mL}$) grouped based on the targeted microbial species (i.e. Gram-positive, Gram-negative, and yeast). Numbers refer to those in **Table 1.2**. Molecule 12 was tested in the presence of an efflux pump inhibitor ^[129].

Table 1.2. Highly potent prenylated (iso)flavonoids against bacteria and yeasts. N.m. stands for not mentioned. * assessed in the presence of 25 µg/mL efflux pump inhibitor. Compounds are ordered based on (iso)flavonoid subclass.

No.	Subclass	Name	No. prenyl groups	Plant origin	MIC (µg/mL)	MIC (µM)	Microorganism	Determination method	Inoculum size (CFU/mL)	MIC (µg/mL) (antibiotic)	Ref.
1	2-Arylbenzofuran	Moracin C	1	<i>M. alba</i>	3.1	10	<i>B. subtilis</i>	Agar dilution	n.m.	0.1 (amoxicillin)/ 0.4 (vancomycin)	[131]
2	Flavanone	Candidone	1	<i>E. giganteuseus</i>	8.0	23	<i>K. pneumoniae</i>	colorimetric assay	1.5 × 10 ⁶	16-128 (chloramphenicol)	[128]
3	Flavanone	Glabrol	2	<i>G. glabra</i>	6.3	16	<i>L. monocytogenes</i>	Broth microdilution	10 ³	10 (ampicillin)	[129]
4	Flavone	Gancaonin Q	2	<i>D. angusticornis</i>	0.6	6	<i>B. cereus</i>	Macrodilution	1.5 × 10 ⁶	1.22 (gentamycin)	[126]
5	Flavone	Licoflavone C	1	<i>R. raetam</i>	7.8	23	<i>E. coli</i>	Broth microdilution	1.5 × 10 ⁸	0.1 (ofloxacin)	[130]
6	Flavonol	Papyriflavonol A	2	<i>B. papyrifera</i>	12.5 25.0	35 71	<i>S. cerevisiae</i> <i>C. albicans</i>	Broth microdilution	10 ⁴	1.3 (amphotericin B/miconazole)	[132]
7	Isoflavan	Glabridin	1	<i>G. glabra</i>	12.5	39	<i>C. albicans</i>	Broth microdilution	5 × 10 ⁴	2.5 (nystatin)	[133]
8	Isoflavan	Eryzerin C	2	<i>E. zeyheri</i>	6.3	16	VRE	Agar dilution	10 ⁶	12.5-100 (vancomycin)	[127]
9	Isoflavanone	Sedonan A	1	<i>D. formosa</i>	7.6	21	<i>S. cerevisiae</i>	Broth microdilution	n.m.	> 6.1 (fluconazole)	[125]
10	Isoflavanone	Sedonan C	2	<i>D. formosa</i>	15.2	37	<i>S. cerevisiae</i>	Broth microdilution	n.m.	> 6.1 (fluconazole)	[125]
11	Isoflavone	6,8-diprenyl genistein	2	<i>G. uralensis</i>	6.3	15	<i>L. monocytogenes</i>	Broth microdilution	10 ³	10 (ampicillin)	[129]
12	Isoflavone	Luteone*	1	<i>L. luteus</i>	10.0	28	<i>E. coli</i>	Broth microdilution	10 ⁴	10 (ampicillin)	[129]
13	Isoflavone	Neobavaisoflavone	1	<i>P. corylifolia</i>	8.0	25	<i>K. pneumoniae</i>	colorimetric assay	1.5 × 10 ⁶	16-128 (chloramphenicol)	[128]
14	Pterocarpan	Erybraedin A	2	<i>E. zeyheri</i>	3.1	8	VRE	Agar dilution	10 ⁶	12.5-100 (vancomycin)	[127]
15	Pterocarpan	Orientanol B	1	<i>E. varegiata</i>	6.3	18	MRSA	Agar dilution	10 ⁶	0.8-1.6 (vancomycin)	[134]
16	Pterocarpene	Eryvarin W	2	<i>E. varegiata</i>	3.1	8	MRSA	Broth microdilution	n.m.	0.8-1.6 (vancomycin)	[135]

1.3.4. SARs of prenylated (iso)flavonoids as antimicrobials

Several efforts have been made to identify correlations between molecular structures and (bio)activity in a so-called structure-activity relationships study (SARs). Prenylation has always been the classical explanation for the increased antimicrobial potency of prenylated (iso)flavonoids, representing one of the most known SARs. Another frequently shown SAR supports that hydroxylation of the prenyl group is detrimental for activity ^[131,136]. Moreover, double prenylation has been correlated with high antimicrobial activity against Gram-positive bacteria and the absence of activity against Gram-negative bacteria ^[129,137]. Notably, most diprenylated (iso)flavonoids were found to be inactive against yeasts ^[126,138]. However, not all prenylated (iso)flavonoids are potent antimicrobials and not all double prenylated (iso)flavonoids are active against Gram-positives ^[139,140] and inactive against yeasts ^[67,125,141].

Furthermore, (iso)flavonoid subclasses do not always follow the same SARs. For example, even though prenylation at the C6 position is more favourable than at the C8 in isoflavones ^[142], the opposite applies for flavanones ^[138,143]. Similarly, C3'-prenylation is preferred over C6-prenylation in flavanones, but C6 is the preferred prenylation position in isoflavones ^[129]. In the same way, O-methylation has been shown detrimental for prenylated pterocarpenes and isoflavanones ^[144,145], beneficial for prenylated pterocarpans, isoflavans and flavanones ^[146] and indifferent in the activity of prenylated isoflavones.

All the above show that often SARs, based on the presence and location of substituents, fail to explain the entire correlation between chemical diversity and antimicrobial properties of prenylated (iso)flavonoids. Overall molecular properties (such as hydrophobicity, shape and hydrogen bonding) have been shown important determinants for activity ^[129,147].

1.3.5. Mode of action of prenylated (iso)flavonoids

The mode of antimicrobial action of prenylated (iso)flavonoids has not been elucidated. Nevertheless, a few reports have provided insights in how prenylated (iso)flavonoids exert their activity. Most evidence supports disruption of membrane's integrity by for example, permeabilization ^[148-151] or alteration of membrane's fluidity ^[152,153] or its thermotropic properties ^[154]. Moreover, inhibition of efflux pumps ^[155], disruption of membrane phospholipid synthesis ^[151], DNA fragmentation ^[156], inhibition of the bacterial respiratory chain ^[157] and direct interaction with the bacterial peptidoglycan layer ^[149] have been demonstrated for prenylated (iso)flavonoids. Most mechanistic information derives from investigations on bacterial cells and model systems. Information on the mechanism of action of prenylated (iso)flavonoids against yeasts is scarce and limited to *Candida* species ^[121,156]. In this thesis, we investigated the mode of membrane-activity of prenylated (iso)flavonoids against a notorious food spoilage yeast.

1.4. *In silico* tools to complement antimicrobial research

To rationalize the correlation between chemical diversity and antimicrobial properties and to get insights in their mode of action, *in silico* (computational) tools are increasingly explored in science. *In silico* tools are intended to complement *in vivo* and *in vitro* experimentation rather than standing alone ^[158,159].

Depending on the availability of structural information, a structure-based and/or a ligand-based approach can be employed ^[160]. When 3D-information on the target is available, then the structure-based approach can estimate the interaction energies for all molecules under investigation ^[159]. Structure-based approaches mainly include molecular docking and structure-based pharmacophore modelling ^[161]. Ligand-based approaches circumvent all kinds of limitations associated with the target, making them easier to implement and thus highly beneficial in early drug discovery ^[162]. These approaches rely on the analysis of features of structurally similar ligands with respect to their biological activity ^[163]. Ligand-based approaches include QSAR, virtual screening and ligand-based pharmacophore modelling ^[161]. In this thesis, a ligand-based approach is employed, as for many natural antimicrobials, including prenylated (iso)flavonoids, the target has not yet been established.

QSAR remains an efficient method for building mathematical models, which attempts to find a statistically significant correlation between the chemical structure and a continuous (pMIC, pEC50, Ki, etc.) or categorical/binary (active-inactive, toxic-nontoxic, etc.) biological property using regression and classification techniques, respectively ^[164]. QSAR analyses can be a useful *in silico* tool to identify important molecular signatures underlying the antimicrobial potency of prenylated (iso)flavonoids. Molecular signatures in computational studies are captured by mathematical representations known as molecular descriptors ^[165].

Robust QSAR models are built on a large set of compounds (at least 25 compounds or data points) covering a wide chemical space ^[166]. The modelling set is split into the training set (80%) and the test set (20%). Ideally, this division must be performed in a way that data points representing both the training and the test set are distributed within the whole descriptor space occupied by the entire dataset. Furthermore, each point of the test set should be close to at least one point of the training set. This approach ensures that the similarity principle can be employed for the activity prediction of the test set ^[166]. This rational splitting is usually performed with the help of clustering algorithms, such as hierarchical clustering, maximum dissimilarity method, Kennard-Stone method, etc. ^[166]. The training set is used to construct models using different numbers of descriptors. The statistical internal performance of the models, together with their predictive ability against the test set, determines the best model. Generally, the statistically compliant model with the lowest number of descriptors is selected to prevent overfitted and/or difficult to interpret models ^[167]. Nonetheless, for mechanistic

interpretations of the QSAR models, the frequency of the selected descriptors in all statistical compliant models is analysed.

In principle, any robust and highly predictive model can predict any compound that fits in the applicability domain (AD) of the model ^[168]. The AD represents the space formed by the knowledge or information of the training set and for which it is appropriate to make predictions for new compounds ^[169]. The AD can be visualized through a William's plot where the boundaries on the x-axis are defined by the critical leverage value (h^*) and the boundaries on the y-axis by 3 times the standard deviation of the standardized residuals of the molecules. The h^* equals $3p'/n$ where p' is the number of variables in the model plus one and n the number of training objects ^[170].

The importance of an external validation set to additionally assess the predictive power of the selected, best model is increasingly highlighted ^[171]. The external validation set can be any set of molecules which has not entered model's training and selection process ^[172,173] but fits in the AD of the selected model. The QSAR modelling and validation workflow is displayed in **Figure 1.8**.

Araya-Cloutier *et al.* (2017) used *in silico* ligand-based methods, such as QSAR and pharmacophore modelling with 30 molecules to elucidate the molecular properties important for antibacterial activity ^[129]. This QSAR analysis indicated the importance of hydrophobicity and shape in the antibacterial activity of prenylated (iso)flavonoids against *L. monocytogenes* and *E. coli*. However, the QSAR model was built on the entire dataset (i.e. without performing any splitting) due to the limited database size. More recently, Sadgrove *et al.* (2020) performed QSAR modelling of 74 (prenylated) (iso)flavonoids from the *Erythrina* species against (MR)SA ^[147]. The large dataset employed facilitated the splitting of the modelling dataset into a training and a test set (but no external evaluation was performed). The model correlated activity with properties such as hydrogen-bonding, hydrophobicity, primary oxygens and charge distribution. Unfortunately, the outcomes of the model were not used for mechanistic interpretation ^[147].

The focus of this thesis is to perform a QSAR study on an extended, strictly defined set of prenylated (iso)flavonoids tested against MRSA and mechanistically relate the findings to the mode of action.

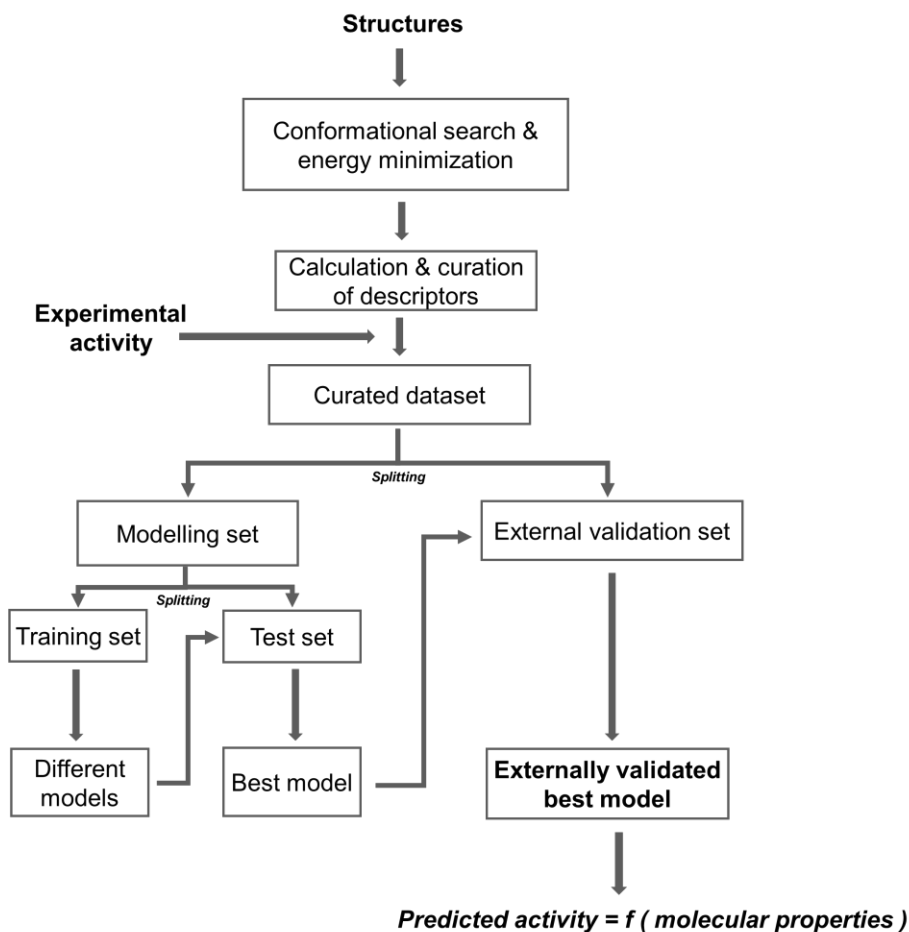


Figure 1.8. Predictive QSAR modeling and validation workflow based on Golbraikh *et al.* (2000) [166].

1.5. Aim and outline of the thesis

The aim of this thesis is binary. The first aim is to improve and diversify the *in planta* production of prenylated (iso)flavonoids in the well-studied legume, soybean. The second aim is to explore the antimicrobial properties of prenylated (iso)flavonoids and their mode of action by using *in vitro* and *in silico* means against pathogenic and spoilage microorganisms.

In **Chapter 2**, the concept of priming prior to, the commonly used, elicitation is employed to enhance the production of prenylated pterocarpans, usually present in elicited soybeans. This was investigated by using different agents to prime the seedlings of one soybean cultivar and evaluate the robustness of the most effective treatment for a second cultivar. Liquid chromatography coupled to mass

spectrometry was used to identify and quantify the prenylated isoflavonoids and their precursor isoflavonoids in the extracts. In **Chapter 3**, we further optimized the most effective treatment described in **Chapter 2**, to diversify the production of prenylated isoflavonoids. The newly induced molecules, belonging to the isoflavone subclass, were predicted as potent antibacterials based on previously developed QSAR models. In **Chapter 4**, QSAR and pharmacophore modelling were performed with an extended set of 77 prenylated (iso)flavonoids to elucidate, understand and mechanistically correlate the properties underlying antibacterial activity against MRSA. In **Chapter 5**, the antifungal properties of prenylated (iso)flavonoids against a notorious food spoilage yeast *Z. parabailii* were investigated and insights into their mode of action were obtained. Finally, in **Chapter 6**, the main findings of this PhD research are discussed and possibilities in utilising prenylated (iso)flavonoids as antimicrobials are given.

1.6. References

- [1] Food, U. & Administration, D. *Draft guidance for industry: hazard analysis and risk-based preventive controls for human food*, www.fda.gov/Food/GuidanceRegulation/GuidanceDocumentsRegulatoryInformation/ucm517412.htm. (2017).
- [2] Shwaiki, L. N., Arendt, E. K., Lynch, K. M. & Thery, T. L. Inhibitory effect of four novel synthetic peptides on food spoilage yeasts. *International Journal of Food Microbiology* **300**, 43-52 (2019).
- [3] Farkas, J. Physical methods of food preservation. in *Food Microbiology: Fundamentals and Frontiers, Third Edition* 685-712 (American Society of Microbiology, 2007).
- [4] Davidson, P. M., Taylor, T. M. & Schmidt, S. E. Chemical preservatives and natural antimicrobial compounds. in *Food microbiology* 765-801 (American Society of Microbiology, 2013).
- [5] Walker, M. & Phillips, C. A. The effect of preservatives on *Alicyclobacillus acidoterrestris* and *Propionibacterium cyclohexanicum* in fruit juice. *Food Control* **19**, 974-981 (2008).
- [6] Zheng, L., Bae, Y.-M., Jung, K.-S., Heu, S. & Lee, S.-Y. Antimicrobial activity of natural antimicrobial substances against spoilage bacteria isolated from fresh produce. *Food Control* **32**, 665-672 (2013).
- [7] Calo, J. R., Crandall, P. G., O'Bryan, C. A. & Ricke, S. C. Essential oils as antimicrobials in food systems—A review. *Food Control* **54**, 111-119 (2015).
- [8] Piper, P. W. Resistance of yeasts to weak organic acid food preservatives. in *Advances in Applied Microbiology* Vol. 77 97-113 (Elsevier, 2011).
- [9] Carocho, M., Morales, P. & Ferreira, I. C. Natural food additives: Quo vadis? *Trends in Food Science & Technology* **45**, 284-295 (2015).
- [10] Stratford, M., Steels, H., Nebe-von-Caron, G., Novodvorska, M., Hayer, K. & Archer, D. B. Extreme resistance to weak-acid preservatives in the spoilage yeast *Zygosaccharomyces bailii*. *International Journal of Food Microbiology* **166**, 126-134 (2013).
- [11] Choi, L. H. & Nielsen, S. S. The effects of thermal and nonthermal processing methods on apple cider quality and consumer acceptability. *Journal of Food quality* **28**, 13-29 (2005).
- [12] Singh, S. & Shalini, R. Effect of hurdle technology in food preservation: a review. *Critical Reviews in Food Science and Nutrition* **56**, 641-649 (2016).
- [13] Aguilera, J. & Chirife, J. Combined methods for the preservation of foods in Latin America and the CYTED-D project. in *Water in Foods* 433-444 (Elsevier, 1994).

- [14] Leistner, L. Basic aspects of food preservation by hurdle technology. *International Journal of Food Microbiology* **55**, 181-186 (2000).
- [15] Lyddiard, D., Jones, G. L. & Greatrex, B. W. Keeping it simple: lessons from the golden era of antibiotic discovery. *FEMS Microbiology Letters* **363** (2016).
- [16] Walsh, C. T. & Wencewicz, T. A. Prospects for new antibiotics: a molecule-centered perspective. *The Journal of Antibiotics* **67**, 7 (2014).
- [17] Radhouani, H., Silva, N., Poeta, P., Torres, C., Correia, S. & Igrejas, G. Potential impact of antimicrobial resistance in wildlife, environment and human health. *Frontiers in Microbiology* **5**, 23 (2014).
- [18] Cheesman, M. J., Ilanko, A., Blonk, B. & Cock, I. E. Developing new antimicrobial therapies: are synergistic combinations of plant extracts/compounds with conventional antibiotics the solution? *Pharmacognosy Reviews* **11**, 57 (2017).
- [19] Munita, J. M. & Arias, C. A. Mechanisms of antibiotic resistance. *Virulence Mechanisms of Bacterial Pathogens*, 481-511 (2016).
- [20] Gupta, P. D. & Birdi, T. J. Development of botanicals to combat antibiotic resistance. *Journal of Ayurveda and Integrative Medicine* **8**, 266-275 (2017).
- [21] Aslam, B., Wang, W., Arshad, M. I., Khurshid, M., Muzammil, S., Rasool, M. H., Nisar, M. A., Alvi, R. F., Aslam, M. A. & Qamar, M. U. Antibiotic resistance: A rundown of a global crisis. *Infection and Drug Resistance* **11**, 1645 (2018).
- [22] Organization, W. H. New report calls for urgent action to avert antimicrobial resistance crisis. *Joint News Release* **29** (2019).
- [23] Silhavy, T. J., Kahne, D. & Walker, S. The bacterial cell envelope. *Cold Spring Harbor perspectives in biology* **2**, a000414 (2010).
- [24] Miller, S. I. & Salama, N. R. The gram-negative bacterial periplasm: size matters. *PLoS Biology* **16**, e2004935 (2018).
- [25] Koch, M. A., Schuffenhauer, A., Scheck, M., Wetzels, S., Casaulta, M., Odermatt, A., Ertl, P. & Waldmann, H. Charting biologically relevant chemical space: a structural classification of natural products (SCONP). *Proceedings of the National Academy of Sciences* **102**, 17272-17277 (2005).
- [26] Vollmer, W., Blanot, D. & De Pedro, M. A. Peptidoglycan structure and architecture. *FEMS Microbiology Reviews* **32**, 149-167 (2008).
- [27] Lambert, P. Cellular impermeability and uptake of biocides and antibiotics in Gram-positive bacteria and mycobacteria. *Journal of Applied Microbiology* **92**, 46S-54S (2002).
- [28] Klis, F. M., Boorsma, A. & De Groot, P. W. Cell wall construction in *Saccharomyces cerevisiae*. *Yeast* **23**, 185-202 (2006).
- [29] Garcia-Rubio, R., de Oliveira, H. C., Rivera, J. & Trevijano-Contador, N. The fungal cell wall: *Candida*, *Cryptococcus*, and *Aspergillus* Species. *Frontiers in Microbiology* **10**, 2993 (2020).
- [30] Pilkington, B. J. & Rose, A. H. Accumulation of sulphite by *Saccharomyces cerevisiae* and *Zygosaccharomyces bailii* as affected by phospholipid fatty-acyl unsaturation and chain length. *Microbiology* **135**, 2423-2428 (1989).
- [31] Lindberg, L., Santos, A. X., Riezman, H., Olsson, L. & Bettiga, M. Lipidomic profiling of *Saccharomyces cerevisiae* and *Zygosaccharomyces bailii* reveals critical changes in lipid composition in response to acetic acid stress. *PLoS One* **8**, e73936 (2013).
- [32] Claus, S., Jezierska, S. & Van Bogaert, I. N. A. Protein-facilitated transport of hydrophobic molecules across the yeast plasma membrane. *FEBS Letters* **593**, 1508-1527 (2019).
- [33] Denyer, S. P. & Maillard, J. Y. Cellular impermeability and uptake of biocides and antibiotics in Gram-negative bacteria. *Journal of Applied Microbiology* **92**, 35S-45S (2002).
- [34] Trias, J., Jarlier, V. & Benz, R. Porins in the cell wall of mycobacteria. *Science* **258**, 1479-1481 (1992).
- [35] Trias, J. & Benz, R. Characterization of the channel formed by the mycobacterial porin in lipid bilayer membranes. Demonstration of voltage gating and of negative

- point charges at the channel mouth. *Journal of Biological Chemistry* **268**, 6234-6240 (1993).
- [36] Trias, J. & Benz, R. Permeability of the cell wall of *Mycobacterium smegmatis*. *Molecular Microbiology* **14**, 283-290 (1994).
- [37] Sabir, F., Loureiro-Dias, M. C. & Prista, C. Comparative analysis of sequences, polymorphisms and topology of yeasts aquaporins and aquaglyceroporins. *FEMS Yeast Research* **16**, fow025 (2016).
- [38] Blair, J. M. & Piddock, L. J. Structure, function and inhibition of RND efflux pumps in Gram-negative bacteria: an update. *Current Opinion in Microbiology* **12**, 512-519 (2009).
- [39] Schreuder, M. P., Mooren, A. T., Toschka, H. Y., Verrips, C. T. & Klis, F. M. Immobilizing proteins on the surface of yeast cells. *Trends in Biotechnology* **14**, 115-120 (1996).
- [40] Hammer, K. A., Carson, C. F. & Riley, T. V. Antimicrobial activity of essential oils and other plant extracts. *Journal of Applied Microbiology* **86**, 985-990 (1999).
- [41] Calvo, M., Arosemena, E., Shiva, C. & Adelantado, C. Antimicrobial activity of plant natural extracts and essential oils. *Science Against Microbial Pathogens: Communicating Current Research and Technological Advances*, 1179-1185 (2011).
- [42] Potterat, O. & Hamburger, M. Drug discovery and development with plant-derived compounds. in *Natural Compounds as Drugs Volume I* 45-118 (Springer, 2008).
- [43] Subramani, R., Narayanasamy, M. & Feussner, K.-D. Plant-derived antimicrobials to fight against multi-drug-resistant human pathogens. *3 Biotech* **7**, 172 (2017).
- [44] McRae, J. M., Yang, Q., Crawford, R. J. & Palombo, E. A. Antibacterial compounds from *Planchonia careya* leaf extracts. *Journal of Ethnopharmacology* **116**, 554-560 (2008).
- [45] Lee, G.-S., Kim, E.-S., Cho, S.-I., Kim, J.-H., Choi, G., Ju, Y.-S., Park, S.-H., Jeong, S.-I. & Kim, H.-J. Antibacterial and synergistic activity of prenylated chalcone isolated from the roots of *Sophora flavescens*. *Journal of the Korean Society for Applied Biological Chemistry* **53**, 290-296 (2010).
- [46] Cha, J. D., Moon, S. E., Kim, J. Y., Jung, E. K. & Lee, Y. S. Antibacterial activity of sophoraflavanone G isolated from the roots of *Sophora flavescens* against methicillin-resistant *Staphylococcus aureus*. *Phytotherapy Research: An International Journal Devoted to Pharmacological and Toxicological Evaluation of Natural Product Derivatives* **23**, 1326-1331 (2009).
- [47] Stevens, P. F. Angiosperm phylogeny website. Version 13. *Angiosperm Phylogeny Website. Version 13*. (2016).
- [48] Royal Botanic Gardens, K. State of the world's plants. (Royal Botanic Gardens, 2016).
- [49] Gao, T., Yao, H., Song, J., Liu, C., Zhu, Y., Ma, X., Pang, X., Xu, H. & Chen, S. Identification of medicinal plants in the family Fabaceae using a potential DNA barcode ITS2. *Journal of Ethnopharmacology* **130**, 116-121 (2010).
- [50] Sharifi-Rad, J., Salehi, B., Stojanović-Radić, Z. Z., Fokou, P. V. T., Sharifi-Rad, M., Mahady, G. B., Sharifi-Rad, M., Masjedi, M.-R., Lawal, T. O. & Ayatollahi, S. A. Medicinal plants used in the treatment of tuberculosis-Ethnobotanical and ethnopharmacological approaches. *Biotechnology Advances*, 107629 (2020).
- [51] Wink, M. Evolution of secondary metabolites in legumes (*Fabaceae*). *South African Journal of Botany* **89**, 164-175 (2013).
- [52] Botta, B., Menendez, P., Zappia, G., de Lima, R. A., Torge, R. & Monache, G. D. Prenylated isoflavonoids: botanical distribution, structures, biological activities and biotechnological studies. An update (1995-2006). *Current Medicinal Chemistry* **16**, 3414-3468 (2009).
- [53] Yazaki, K., Sasaki, K. & Tsurumaru, Y. Prenylation of aromatic compounds, a key diversification of plant secondary metabolites. *Phytochemistry* **70**, 1739-1745 (2009).

- [54] Chen, X., Mukwaya, E., Wong, M.-S. & Zhang, Y. A systematic review on biological activities of prenylated flavonoids. *Pharmaceutical Biology* **52**, 655-660 (2014).
- [55] Vogt, T. Phenylpropanoid biosynthesis. *Molecular Plant* **3**, 2-20 (2010).
- [56] Dewick, P. M. Isoflavonoids. in *The Flavonoids Advances in Research Since 1986* 117-238 (Routledge, 2017).
- [57] Negi, J., Bisht, V., Singh, P., Rawat, M. & Joshi, G. Naturally occurring xanthenes: chemistry and biology. *Journal of Applied Chemistry* **2013** (2013).
- [58] El-Awaad, I. A. M. *Cytochrome P450 enzymes involved in xanthone biosynthesis in Hypericum species* PhD thesis, (2016).
- [59] Dixon, R. A. & Steele, C. L. Flavonoids and isoflavonoids—a gold mine for metabolic engineering. *Trends in Plant Science* **4**, 394-400 (1999).
- [60] Veitch, N. C. Isoflavonoids of the Leguminosae. *Natural Product Reports* **24**, 417-464 (2007).
- [61] Veitch, N. C. & Grayer, R. J. Flavonoids and their glycosides, including anthocyanins. *Natural Product Reports* **28**, 1626-1695 (2011).
- [62] Simons, R., Gruppen, H., Bovee, T. F., Verbruggen, M. A. & Vincken, J.-P. Prenylated isoflavonoids from plants as selective estrogen receptor modulators (phytoSERMs). *Food & Function* **3**, 810-827 (2012).
- [63] Veitch, N. C. Isoflavonoids of the Leguminosae. *Natural Product Reports* **30**, 988-1027 (2013).
- [64] Hatano, T., Yasuhara, T., Fukuda, T., Noro, T. & Okuda, T. Phenolic constituents of licorice. II.: structures of licopyranocoumarin, licoaryl coumarin and glisoflavone, and inhibitory effects of licorice phenolics on xanthine oxidase. *Chemical and Pharmaceutical Bulletin* **37**, 3005-3009 (1989).
- [65] Yang, X., Jiang, Y., Yang, J., He, J., Sun, J., Chen, F., Zhang, M. & Yang, B. Prenylated flavonoids, promising nutraceuticals with impressive biological activities. *Trends in Food Science & Technology* **44**, 93-104 (2015).
- [66] Epifano, F., Genovese, S., Menghini, L. & Curini, M. Chemistry and pharmacology of oxyprenylated secondary plant metabolites. *Phytochemistry* **68**, 939-953 (2007).
- [67] Sohn, H. Y., Son, K. H., Kwon, C. S., Kwon, G. S. & Kang, S. S. Antimicrobial and cytotoxic activity of 18 prenylated flavonoids isolated from medicinal plants: *Morus alba* L., *Morus mongolica* Schneider, *Broussonetia papyrifera* (L.) Vent, *Sophora flavescens* Ait and *Echinosophora koreensis* Nakai. *Phytomedicine* **11**, 666-672 (2004).
- [68] Luniwal, A., Khupse, R., Reese, M., Liu, J., El-Dakdouki, M., Malik, N., Fang, L. & Erhardt, P. Multigram synthesis of glyceollin I. *Organic Process Research & Development* **15**, 1149-1162 (2011).
- [69] Gester, S., Metz, P., Zierau, O. & Vollmer, G. An efficient synthesis of the potent phytoestrogens 8-prenylnaringenin and 6-(1, 1-dimethylallyl) naringenin by europium (III)-catalyzed Claisen rearrangement. *Tetrahedron* **57**, 1015-1018 (2001).
- [70] Tischer, S. & Metz, P. Selective C-6 prenylation of flavonoids via europium (III)-catalyzed claisen rearrangement and cross-metathesis. *Advanced Synthesis & Catalysis* **349**, 147-151 (2007).
- [71] Kawamura, T., Hayashi, M., Mukai, R., Terao, J. & Nemoto, H. An efficient method for C8-prenylation of flavonols and flavanones. *Synthesis* **44**, 1308-1314 (2012).
- [72] Sasaki, K., Tsurumaru, Y. & Yazaki, K. Prenylation of flavonoids by biotransformation of yeast expressing plant membrane-bound prenyltransferase SfN8DT-1. *Bioscience, Biotechnology, and Biochemistry* **73**, 759-761 (2009).
- [73] Levisson, M., Araya-Cloutier, C., De Bruijn, W. J., Van Der Heide, M., Salvador López, J. M., Daran, J.-M., Vincken, J.-P. & Beekwilder, J. Toward developing a yeast cell factory for the production of prenylated flavonoids. *Journal of Agricultural and Food Chemistry* **67**, 13478-13486 (2019).

- [74] Araya-Cloutier, C., Martens, B., Schaftenaar, G., Leipoldt, F., Gruppen, H. & Vincken, J.-P. Structural basis for non-genuine phenolic acceptor substrate specificity of *Streptomyces roseochromogenes* prenyltransferase CloQ from the ABBA/PT-barrel superfamily. *PLoS One* **12**, e0174665 (2017).
- [75] Ozaki, T., Mishima, S., Nishiyama, M. & Kuzuyama, T. NovQ is a prenyltransferase capable of catalyzing the addition of a dimethylallyl group to both phenylpropanoids and flavonoids. *The Journal of Antibiotics* **62**, 385-392 (2009).
- [76] Kumano, T., Richard, S. B., Noel, J. P., Nishiyama, M. & Kuzuyama, T. Chemoenzymatic syntheses of prenylated aromatic small molecules using *Streptomyces* prenyltransferases with relaxed substrate specificities. *Bioorganic & Medicinal Chemistry Letters* **16**, 8117-8126 (2008).
- [77] Schmidt, B., Ribnicky, D. M., Poulev, A., Logendra, S., Cefalu, W. T. & Raskin, I. A natural history of botanical therapeutics. *Metabolism* **57**, S3-S9 (2008).
- [78] de Bruijn, W. J., Levisson, M., Beekwilder, J., van Berkel, W. J. & Vincken, J.-P. Plant Aromatic Prenyltransferases: Tools for Microbial Cell Factories. *Trends in Biotechnology* (2020).
- [79] Radman, R., Saez, T., Bucke, C. & Keshavarz, T. Elicitation of plants and microbial cell systems. *Biotechnology and Applied Biochemistry* **37**, 91-102 (2003).
- [80] Zhao, J., Davis, L. C. & Verpoorte, R. Elicitor signal transduction leading to production of plant secondary metabolites. *Biotechnology Advances* **23**, 283-333 (2005).
- [81] Halder, M., Sarkar, S. & Jha, S. Elicitation: A biotechnological tool for enhanced production of secondary metabolites in hairy root cultures. *Engineering in Life Sciences* **19**, 880-895 (2019).
- [82] Ramirez-Estrada, K., Vidal-Limon, H., Hidalgo, D., Moyano, E., Golenioswki, M., Cusidó, R. M. & Palazon, J. Elicitation, an effective strategy for the biotechnological production of bioactive high-added value compounds in plant cell factories. *Molecules* **21**, 182 (2016).
- [83] Nicolaou, K., Winssinger, N., Pastor, J. & DeRoose, F. A general and highly efficient solid phase synthesis of oligosaccharides. Total synthesis of a heptasaccharide phytoalexin elicitor (HPE). *Journal of the American Chemical Society* **119**, 449-450 (1997).
- [84] Namdeo, A. Plant cell elicitation for production of secondary metabolites: a review. *Pharmacognosy Reviews* **1**, 69-79 (2007).
- [85] Huffaker, A., Pearce, G., Veyrat, N., Erb, M., Turlings, T. C., Sartor, R., Shen, Z., Briggs, S. P., Vaughan, M. M. & Alborn, H. T. Plant elicitor peptides are conserved signals regulating direct and indirect antiherbivore defense. *Proceedings of the National Academy of Sciences* **110**, 5707-5712 (2013).
- [86] Ferrari, S., Savatin, D. V., Sicilia, F., Gramegna, G., Cervone, F. & De Lorenzo, G. Oligogalacturonides: plant damage-associated molecular patterns and regulators of growth and development. *Frontiers in Plant Science* **4**, 49 (2013).
- [87] Shakya, P., Marslin, G., Siram, K., Beerhues, L. & Franklin, G. Elicitation as a tool to improve the profiles of high-value secondary metabolites and pharmacological properties of *Hypericum perforatum*. *Journal of Pharmacy and Pharmacology* **71**, 70-82 (2019).
- [88] Mauch-Mani, B., Baccelli, I., Luna, E. & Flors, V. Defense priming: an adaptive part of induced resistance. *Annual Review of Plant Biology* **68**, 485-512 (2017).
- [89] Hilker, M., Schwachtje, J., Baier, M., Balazadeh, S., Bäurle, I., Geiselhardt, S., Hincha, D. K., Kunze, R., Mueller-Roeber, B. & Rillig, M. C. Priming and memory of stress responses in organisms lacking a nervous system. *Biological Reviews* **91**, 1118-1133 (2016).
- [90] Conrath, U., Beckers, G. J., Langenbach, C. J. & Jaskiewicz, M. R. Priming for enhanced defense. *Annual Review of Phytopathology* **53**, 97-119 (2015).

- [91] Katz, V. A., Thulke, O. U. & Conrath, U. A benzothiadiazole primes parsley cells for augmented elicitation of defense responses. *Plant Physiology* **117**, 1333-1339 (1998).
- [92] Zimmerli, L., Jakab, G., Métraux, J.-P. & Mauch-Mani, B. Potentiation of pathogen-specific defense mechanisms in *Arabidopsis* by β -aminobutyric acid. *Proceedings of the National Academy of Sciences* **97**, 12920-12925 (2000).
- [93] Zimmerli, L., Métraux, J.-P. & Mauch-Mani, B. β -Aminobutyric acid-induced protection of *Arabidopsis* against the necrotrophic fungus *Botrytis cinerea*. *Plant Physiology* **126**, 517-523 (2001).
- [94] Slaughter, A., Daniel, X., Flors, V., Luna, E., Hohn, B. & Mauch-Mani, B. Descendants of primed *Arabidopsis* plants exhibit resistance to biotic stress. *Plant Physiology* **158**, 835-843 (2012).
- [95] Balmer, A., Pastor, V., Gamir, J., Flors, V. & Mauch-Mani, B. The 'prime-ome': towards a holistic approach to priming. *Trends in Plant Science* **20**, 443-452 (2015).
- [96] Martinez-Medina, A., Flors, V., Heil, M., Mauch-Mani, B., Pieterse, C. M., Pozo, M. J., Ton, J., van Dam, N. M. & Conrath, U. Recognizing plant defense priming. *Trends in Plant Science* **21**, 818-822 (2016).
- [97] Simons, R., Vincken, J.-P., Roidos, N., Bovee, T. F., van Iersel, M., Verbruggen, M. A. & Gruppen, H. Increasing soy isoflavonoid content and diversity by simultaneous malting and challenging by a fungus to modulate estrogenicity. *Journal of Agricultural and Food Chemistry* **59**, 6748-6758 (2011).
- [98] Aisyah, S., Gruppen, H., Madzora, B. & Vincken, J.-P. Modulation of isoflavonoid composition of *Rhizopus oryzae* elicited soybean (*Glycine max*) seedlings by light and wounding. *Journal of Agricultural and Food Chemistry* **61**, 8657-8667 (2013).
- [99] Tusevski, O., Stanoeva, J. P., Stefova, M. & Simic, S. G. *Agrobacterium* enhances xanthone production in *Hypericum perforatum* cell suspensions. *Plant Growth Regulation* **76**, 199-210 (2015).
- [100] Fang, L., Yang, T. & Medina-Bolivar, F. Production of prenylated stilbenoids in hairy root cultures of peanut (*Arachis hypogaea*) and its wild relatives *A. ipaensis* and *A. duranensis* via an optimized elicitation procedure. *Molecules* **25** (2020).
- [101] Glazebrook, J. Contrasting mechanisms of defense against biotrophic and necrotrophic pathogens. *Annual Review of Phytopathology* **43**, 205-227 (2005).
- [102] Mohr, P. G. & Cahill, D. M. Relative roles of glyceollin, lignin and the hypersensitive response and the influence of ABA in compatible and incompatible interactions of soybeans with *Phytophthora sojae*. *Physiological and Molecular Plant Pathology* **58**, 31-41 (2001).
- [103] Ponzio, C., Weldegergis, B. T., Dicke, M. & Gols, R. Compatible and incompatible pathogen-plant interactions differentially affect plant volatile emissions and the attraction of parasitoid wasps. *Functional Ecology* **30**, 1779-1789 (2016).
- [104] Demidchik, V. Mechanisms of oxidative stress in plants: from classical chemistry to cell biology. *Environmental and Experimental Botany* **109**, 212-228 (2015).
- [105] Degousee, N., Triantaphylidès, C. & Montillet, J.-L. Involvement of oxidative processes in the signaling mechanisms leading to the activation of glyceollin synthesis in soybean (*Glycine max*). *Plant Physiology* **104**, 945-952 (1994).
- [106] Farrell, K., Jahan, M. A. & Kovinich, N. Distinct mechanisms of biotic and chemical elicitors enable additive elicitation of the anticancer phytoalexin glyceollin I. *Molecules* **22**, 1261 (2017).
- [107] Akashi, T., Sasaki, K., Aoki, T., Ayabe, S.-i. & Yazaki, K. Molecular cloning and characterization of a cDNA for pterocarpan 4-dimethylallyltransferase catalyzing the key prenylation step in the biosynthesis of glyceollin, a soybean phytoalexin. *Plant Physiology* **149**, 683-693 (2009).
- [108] Moy, P., Qutob, D., Chapman, B. P., Atkinson, I. & Gijzen, M. Patterns of gene expression upon infection of soybean plants by *Phytophthora sojae*. *Molecular Plant-Microbe Interactions* **17**, 1051-1062 (2004).

- [109] Kim, E., Kim, S., Chung, J., Chi, H., Kim, J. & Chung, I. Analysis of phenolic compounds and isoflavones in soybean seeds (*Glycine max* (L.) Merrill) and sprouts grown under different conditions. *European Food Research and Technology* **222**, 201 (2006).
- [110] Conceição, L. F., Ferreres, F., Tavares, R. M. & Dias, A. C. Induction of phenolic compounds in *Hypericum perforatum* L. cells by *Colletotrichum gloeosporioides* elicitation. *Phytochemistry* **67**, 149-155 (2006).
- [111] Baenas, N., Villaño, D., García-Viguera, C. & Moreno, D. A. Optimizing elicitation and seed priming to enrich broccoli and radish sprouts in glucosinolates. *Food Chemistry* **204**, 314-319 (2016).
- [112] Sobolev, V. S., Neff, S. A. & Gloer, J. B. New stilbenoids from peanut (*Arachis hypogaea*) seeds challenged by an *Aspergillus caelatus* strain. *Journal of Agricultural and Food Chemistry* **57**, 62-68 (2008).
- [113] Galis, I., Gaquerel, E., Pandey, S. P. & Baldwin, I. T. Molecular mechanisms underlying plant memory in JA-mediated defence responses. *Plant, Cell & Environment* **32**, 617-627 (2009).
- [114] Jahan, M. A. & Kovinich, N. 1 Acidity stress for the systemic elicitation of glyceollin phytoalexins in soybean plants. *Plant Signaling & Behavior* **14** (2019).
- [115] Condori, J., Sivakumar, G., Hubstenberger, J., Dolan, M. C., Sobolev, V. S. & Medina-Bolivar, F. Induced biosynthesis of resveratrol and the prenylated stilbenoids arachidin-1 and arachidin-3 in hairy root cultures of peanut: Effects of culture medium and growth stage. *Plant Physiology and Biochemistry* **48**, 310-318 (2010).
- [116] John, K. M., Jung, E. S., Lee, S., Kim, J.-S. & Lee, C. H. Primary and secondary metabolites variation of soybean contaminated with *Aspergillus sojae*. *Food research international* **54**, 487-494 (2013).
- [117] Sobolev, V. S., Neff, S. A. & Gloer, J. B. New stilbenoids from peanut (*Arachis hypogaea*) seeds challenged by an *Aspergillus caelatus* strain. *Journal of Agricultural and Food Chemistry* **57**, 62-68 (2009).
- [118] Franklin, G., Conceição, L. F., Kombrink, E. & Dias, A. C. Xanthone biosynthesis in *Hypericum perforatum* cells provides antioxidant and antimicrobial protection upon biotic stress. *Phytochemistry* **70**, 60-68 (2009).
- [119] Yamamoto, H., Ichimura, M. & Inoue, K. Stimulation of prenylated flavanone production by mannans and acidic polysaccharides in callus culture of *Sophora flavescens*. *Phytochemistry* **40**, 77-81 (1995).
- [120] Farhadi, F., Khameneh, B., Iranshahi, M. & Iranshahy, M. Antibacterial activity of flavonoids and their structure-activity relationship: An update review. *Phytotherapy Research* **33**, 13-40 (2019).
- [121] Liu, W., Li, L. P., Zhang, J. D., Li, Q., Shen, H., Chen, S. M., He, L. J., Yan, L., Xu, G. T. & An, M. M. Synergistic antifungal effect of glabridin and fluconazole. *PLoS One* **9**, e103442 (2014).
- [122] Ammar, M. I., Nenaah, G. E. & Mohamed, A. H. H. Antifungal activity of prenylated flavonoids isolated from *Tephrosia apollinea* L. against four phytopathogenic fungi. *Crop Protection* **49**, 21-25 (2013).
- [123] Jin, Y.-S. Recent advances in natural antifungal flavonoids and their derivatives. *Bioorganic & Medicinal Chemistry Letters* **29**, 126589 (2019).
- [124] Gibbons, S. Anti-staphylococcal plant natural products. *Natural Product Reports* **21**, 263-277 (2004).
- [125] Belofsky, G., Kolaczowski, M., Adams, E., Schreiber, J., Eisenberg, V., Coleman, C. M., Zou, Y. & Ferreira, D. Fungal ABC transporter-associated activity of isoflavonoids from the root extract of *Dalea formosa*. *Journal of Natural Products* **76**, 915-925 (2013).
- [126] Kuete, V., Simo, I. K., Ngameni, B., Bigoga, J. D., Watchueng, J., Kapguez, R. N., Etoa, F.-X., Tchaleu, B. N. & Beng, V. P. Antimicrobial activity of the methanolic extract, fractions and four flavonoids from the twigs of *Dorstenia angusticornis* Engl.(Moraceae). *Journal of Ethnopharmacology* **112**, 271-277 (2007).

- [127] Sato, M., Tanaka, H., Oh-Uchi, T., Fukai, T., Etoh, H. & Yamaguchi, R. Antibacterial activity of phytochemicals isolated from *Erythrina zeyheri* against vancomycin-resistant *enterococci* and their combinations with vancomycin. *Phytotherapy Research: An International Journal Devoted to Pharmacological and Toxicological Evaluation of Natural Product Derivatives* **18**, 906-910 (2004).
- [128] Mbaveng, A. T., Sandjo, L. P., Tankeo, S. B., Ndifor, A. R., Pantaleon, A., Nagdju, B. T. & Kuete, V. Antibacterial activity of nineteen selected natural products against multi-drug resistant Gram-negative phenotypes. *SpringerPlus* **4**, 823 (2015).
- [129] Araya-Cloutier, C., Vincken, J. P., van de Schans, M. G. M., Hageman, J., Schaftenaar, G., den Besten, H. M. W. & Gruppen, H. QSAR-based molecular signatures of prenylated (iso)flavonoids underlying antimicrobial potency against and membrane-disruption in Gram positive and Gram negative bacteria. *Scientific Reports* **8**, 9267 (2018).
- [130] Edziri, H., Mastouri, M., Mahjoub, M. A., Mighri, Z., Mahjoub, A. & Verschaeye, L. Antibacterial, antifungal and cytotoxic activities of two flavonoids from *Retama raetam* flowers. *Molecules* **17**, 7284-7293 (2012).
- [131] Fukai, T., Kaitou, K. & Terada, S. Antimicrobial activity of 2-arylbenzofurans from *Morus* species against methicillin-resistant *Staphylococcus aureus*. *Fitoterapia* **76**, 708-711 (2005).
- [132] Sohn, H.-Y., Kwon, C.-S. & Son, K.-H. Fungicidal effect of prenylated flavonol, papyriflavonol a, isolated from *Broussonetia papyrifera* (L.) vent. against *Candida albicans*. *Journal of Microbiology and Biotechnology* **20**, 1397-1402 (2010).
- [133] Messier, C. & Grenier, D. Effect of licorice compounds licochalcone A, glabridin and glycyrrhizic acid on growth and virulence properties of *Candida albicans*. *Mycoses* **54**, e801-e806 (2011).
- [134] Tanaka, H., Sato, M., Fujiwara, S., Hirata, M., Etoh, H. & Takeuchi, H. Antibacterial activity of isoflavonoids isolated from *Erythrina variegata* against methicillin-resistant *Staphylococcus aureus*. *Letters in Applied Microbiology* **35**, 494-498 (2002).
- [135] Tanaka, H., Atsumi, I., Shiota, O., Sekita, S., Sakai, E., Sato, M., Murata, J., Murata, H., Darnaedi, D. & Chen, I. S. Three new constituents from the roots of *Erythrina variegata* and their antibacterial activity against methicillin-resistant *Staphylococcus aureus*. *Chemistry & biodiversity* **8**, 476-482 (2011).
- [136] Chukwuikwu, J., Van Heerden, F. & Van Staden, J. Antibacterial activity of flavonoids from the stem bark of *Erythrina caffra* thunb. *Phytotherapy Research* **25**, 46-48 (2011).
- [137] Raksat, A., Maneerat, W., Andersen, R. J., Pyne, S. G. & Laphookhieo, S. Antibacterial prenylated isoflavonoids from the stems of *Millettia extensa*. *Journal of Natural Products* **81**, 1835-1840 (2018).
- [138] Tahara, S., Katagiri, Y., Ingham, J. L. & Mizutani, J. Prenylated flavonoids in the roots of yellow lupin. *Phytochemistry* **36**, 1261-1271 (1994).
- [139] Rukachaisirikul, T., Innok, P., Aroonrerk, N., Boonamnuyaylap, W., Limrangsun, S., Boonyon, C., Woonjina, U. & Suksamrarn, A. Antibacterial pterocarpanes from *Erythrina subumbrans*. *Journal of Ethnopharmacology* **110**, 171-175 (2007).
- [140] Taniguchi, M. & Kubo, I. Ethnobotanical drug discovery based on medicine men's trials in the African savanna: screening of east African plants for antimicrobial activity II. *Journal of Natural Products* **56**, 1539-1546 (1993).
- [141] Özçelik, B., Orhan, I. & Toker, G. Antiviral and antimicrobial assessment of some selected flavonoids. *Zeitschrift für Naturforschung C* **61**, 632-638 (2006).
- [142] Sato, M., Tanaka, H., Tani, N., Nagayama, M. & Yamaguchi, R. Different antibacterial actions of isoflavones isolated from *Erythrina poeppigiana* against methicillin-resistant *Staphylococcus aureus*. *Letters in Applied Microbiology* **43**, 243-248 (2006).
- [143] Tahara, S., Katagiri, Y., Ingham, J. L. & Mizutani, J. Prenylated flavonoids in the roots of yellow lupin. *Phytochemistry* **36**, 1261-1271 (1994).

- [144] Rahman, M. M., Gibbons, S. & Gray, A. I. Isoflavanones from *Uraria picta* and their antimicrobial activity. *Phytochemistry* **68**, 1692-1697 (2007).
- [145] Osawa, K., Yasuda, H., Maruyama, T., Morita, H., Takeya, K. & Itokawa, H. Isoflavanones from the heartwood of *Swartzia polyphylla* and their antibacterial activity against cariogenic bacteria. *Chemical and Pharmaceutical Bulletin* **40**, 2970-2974 (1992).
- [146] Yin, S., Fan, C.-Q., Wang, Y., Dong, L. & Yue, J.-M. Antibacterial prenylflavone derivatives from *Psoralea corylifolia*, and their structure-activity relationship study. *Bioorganic & Medicinal Chemistry* **12**, 4387-4392 (2004).
- [147] Sadgrove, N. J., Oliveira, T. B., Khumalo, G. P., Vuuren, S. F. v. & van Wyk, B.-E. Antimicrobial isoflavones and derivatives from *Erythrina* (Fabaceae): structure activity perspective (sar & qsar) on experimental and mined values against *Staphylococcus Aureus*. *Antibiotics* **9**, 223 (2020).
- [148] Araya-Cloutier, C., Vincken, J.-P., van Ederen, R., den Besten, H. M. & Gruppen, H. Rapid membrane permeabilization of *Listeria monocytogenes* and *Escherichia coli* induced by antibacterial prenylated phenolic compounds from legumes. *Food Chemistry* **240**, 147-155 (2018).
- [149] Mun, S.-H., Joung, D.-K., Kim, S.-B., Park, S.-J., Seo, Y.-S., Gong, R., Choi, J.-G., Shin, D.-W., Rho, J.-R. & Kang, O.-H. The mechanism of antimicrobial activity of sophoraflavanone B against methicillin-resistant *Staphylococcus aureus*. *Foodborne Pathogens and Disease* **11**, 234-239 (2014).
- [150] Sianglum, W., Muangngam, K., Joycharat, N. & Voravuthikunchai, S. P. Mechanism of action and biofilm inhibitory activity of lupinifolin against multidrug-resistant enterococcal clinical isolates. *Microbial Drug Resistance* **25**, 1391-1400 (2019).
- [151] Pang, D., Liao, S., Wang, W., Mu, L., Li, E., Shen, W., Liu, F. & Zou, Y. Destruction of the cell membrane and inhibition of cell phosphatidic acid biosynthesis in *Staphylococcus aureus*: an explanation for the antibacterial mechanism of morusin. *Food & Function* **10**, 6438-6446 (2019).
- [152] Tsuchiya, H. & Iinuma, M. Reduction of membrane fluidity by antibacterial sophoraflavanone G isolated from *Sophora exigua*. *Phytomedicine* **7**, 161-165 (2000).
- [153] Selvaraj, S., Krishnaswamy, S., Devashya, V., Sethuraman, S. & Krishnan, U. M. Influence of membrane lipid composition on flavonoid-membrane interactions: Implications on their biological activity. *Progress in Lipid Research* **58**, 1-13 (2015).
- [154] Hendrich, A. B., Malon, R., Pola, A., Shirataki, Y., Motohashi, N. & Michalak, K. Differential interaction of Sophora isoflavonoids with lipid bilayers. *European Journal of Pharmaceutical Sciences* **16**, 201-208 (2002).
- [155] Peralta, M. A., Calise, M., Fornari, M. C., Ortega, M. G., Diez, R. A., Cabrera, J. L. & Pérez, C. A prenylated flavanone from *Dalea elegans* inhibits rhodamine 6 G efflux and reverses fluconazole-resistance in *Candida albicans*. *Planta Medica* **78**, 981-987 (2012).
- [156] Moazeni, M., Hedayati, M., Nabili, M., Mousavi, S., Gohar, A. A. & Gholami, S. Glabridin triggers over-expression of MCA1 and NUC1 genes in *Candida glabrata*: is it an apoptosis inducer? *Journal de Mycologie Medicale* **27**, 369-375 (2017).
- [157] Haraguchi, H., Tanimoto, K., Tamura, Y., Mizutani, K. & Kinoshita, T. Mode of antibacterial action of retrochalcones from *Glycyrrhiza inflata*. *Phytochemistry* **48**, 125-129 (1998).
- [158] Danchick, R. The Delphic Boat: what genomes tell us. (Harvard University Press, 2002).
- [159] Kalyaanamoorthy, S. & Chen, Y.-P. P. Structure-based drug design to augment hit discovery. *Drug Discovery Today* **16**, 831-839 (2011).
- [160] Drwal, M. N. & Griffith, R. Combination of ligand-and structure-based methods in virtual screening. *Drug Discovery Today: Technologies* **10**, 395-401 (2013).

- [161] Lu, P., Bevan, D. R., Leber, A., Hontecillas, R., Tubau-Juni, N. & Bassaganya-Riera, J. Computer-aided drug discovery. in *Accelerated Path to Cures* 7-24 (Springer, 2018).
- [162] Merz Jr, K. M., Ringe, D. & Reynolds, C. H. Drug design: structure-and ligand-based approaches. (Cambridge University Press, 2010).
- [163] Kurogi, Y. & Guner, O. F. Pharmacophore modeling and three-dimensional database searching for drug design using catalyst. *Current Medicinal Chemistry* **8**, 1035-1055 (2001).
- [164] Cherkasov, A., Muratov, E. N., Fourches, D., Varnek, A., Baskin, I. I., Cronin, M., Dearden, J., Gramatica, P., Martin, Y. C. & Todeschini, R. QSAR modeling: where have you been? Where are you going to? *Journal of Medicinal Chemistry* **57**, 4977-5010 (2014).
- [165] Chandrasekaran, B., Abed, S. N., Al-Attaqchi, O., Kuche, K. & Tekade, R. K. Computer-aided prediction of pharmacokinetic (ADMET) properties. in *Dosage Form Design Parameters* 731-755 (Elsevier, 2018).
- [166] Golbraikh, A. & Tropsha, A. Predictive QSAR modeling based on diversity sampling of experimental datasets for the training and test set selection. *Molecular Diversity* **5**, 231-243 (2000).
- [167] Arakawa, M., Hasegawa, K. & Funatsu, K. The recent trend in QSAR modeling-variable selection and 3D-QSAR methods. *Current Computer-Aided Drug Design* **3**, 254-262 (2007).
- [168] Netzeva, T. I., Worth, A. P., Aldenberg, T., Benigni, R., Cronin, M. T., Gramatica, P., Jaworska, J. S., Kahn, S., Klopman, G. & Marchant, C. A. Current status of methods for defining the applicability domain of (quantitative) structure-activity relationships: The report and recommendations of ecvam workshop 52. *Alternatives to Laboratory Animals* **33**, 155-173 (2005).
- [169] Jaworska, J., Nikolova-Jeliazkova, N. & Aldenberg, T. QSAR applicability domain estimation by projection of the training set in descriptor space: a review. *Alternatives to Laboratory Animals* **33**, 445-459 (2005).
- [170] Gramatica, P. Principles of QSAR models validation: internal and external. *QSAR & Combinatorial Science* **26**, 694-701 (2007).
- [171] Golbraikh, A. & Tropsha, A. Beware of q²! *Journal of Molecular Graphics and Modelling* **20**, 269-276 (2002).
- [172] Faulon, J.-L. & Bender, A. Handbook of chemoinformatics algorithms. (CRC press, 2010).
- [173] Tropsha, A. Best practices for QSAR model development, validation, and exploitation. *Molecular Informatics* **29**, 476-488 (2010).

Enhanced biosynthesis of the natural antimicrobial glyceollins in soybean seedlings by priming and elicitation

Glyceollins are a class of antimicrobial prenylated pterocarpanes produced in soybean seedlings upon fungus elicitation. Priming with reactive oxygen species (ROS) prior to elicitation with *Rhizopus oligosporus/oryzae* (*R*) was investigated for its potential to enhance glyceollin production. ROS-priming prior to *R*-elicitation (ROS + *R*) increased glyceollin production ($8.6 \pm 0.9 \mu\text{mol/g}$ dry weight (DW)) more than 4-fold compared to elicitation without priming ($1.9 \pm 0.4 \mu\text{mol/g}$ DW). Furthermore, ROS-priming was superior to two physical primers which were used as benchmark, namely slicing ($5.0 \pm 0.6 \mu\text{mol glyceollins/g DW}$) and sonication ($4.8 \pm 1.0 \mu\text{mol glyceollins/g DW}$). Subsequently, the robustness of ROS + *R* was assessed by applying it to another soybean cultivar, where it also resulted in a significantly higher glyceollin content than *R*-elicitation without priming. ROS-priming prior to elicitation provides opportunities for improving the yield in large-scale production of natural antimicrobials due to the ease of application and the robustness of the effect across cultivars.

Based on: Kalli, S.; Araya-Cloutier, C.; Lin, Y.; de Bruijn, W. J. C.; Chapman, J.; & Vincken, J.-P. Enhanced biosynthesis of the natural antimicrobial glyceollins in soybean seedlings by priming and elicitation. *Food Chemistry*, **317**, 126389 (2020).

2.1. Introduction

Leguminosae is one of the largest plant families and many of its species are known to be excellent sources of potent antimicrobial compounds. Soybeans (*Glycine max*) are able to produce isoflavonoids. A family of C5-isoprenoid (prenyl)-substituted isoflavonoids with a pterocarpan backbone, collectively known as glyceollins, is accumulated in stressed soybeans ^[1-3]. The production of antimicrobial glyceollins is one of soybeans' main defence responses to counteract stress. Glyceollins have been well documented to exert bioactivities, including antibacterial and antifungal properties ^[4-6]. Due to their antimicrobial properties, glyceollins can serve as promising candidates for natural food preservation.

Glyceollins exist predominantly as a mixture of three isomers: the pyran-ring prenylated isomers, glyceollins I and II, and the furan-ring prenylated isomer, glyceollin III. Glyceollin I is a C4-prenylated pterocarpan, whereas glyceollins II and III are C2-prenylated pterocarpanes. Glyceollins derive from daidzein, the simplest, non-prenylated isoflavone which is further transformed into the pterocarpan, glycinol (**Figure 2.1A**). In some soybean cultivars, glyceollin induction is accompanied by a minor induction of prenylated isoflavones, which are also acknowledged for their high antimicrobial potency ^[2,6].

It has been widely reported that plants transiently sensitized prior to fungus infection (the latter also commonly known as elicitation, **Figure 2.1B**), demonstrate enhanced expression of their defence responses, including the production of antimicrobial compounds (**Figure 2.1C**). This sensitization process, known as priming, enables the plant to mount a faster and/or stronger activation of defence responses to a subsequent elicitation ^[7]. In this way, plants minimize their energy expenditure to respond to elicitation and are able to induce stronger responses upon subsequent stress ^[8]. It is hypothesized that inactive signal amplifiers are accumulated in the plant during priming, which are activated upon subsequent elicitation (**Figure 2.1C**) ^[9,10].

Priming can be achieved by external application of chemicals, colonization of the roots by beneficial microbes or by physical damage to the plant (e.g. wounding) ^[11]. Chemical priming usually involves the external application of endogenous signalling molecules ^[12]. Reactive oxygen species (ROS), for example, serve a multifaceted role in plants' defence mechanism. They follow successful microbial infection ^[13] as they are rapidly and transiently produced in an "oxidative burst". In this way, they act as intracellular signalling molecules that regulate defence gene activation. ROS is also the main regulator of whether the plant will enter the cell death phase due to a prolonged oxidative phase, or whether it will enter the "primed" state upon adequate redox scavenging ^[14].

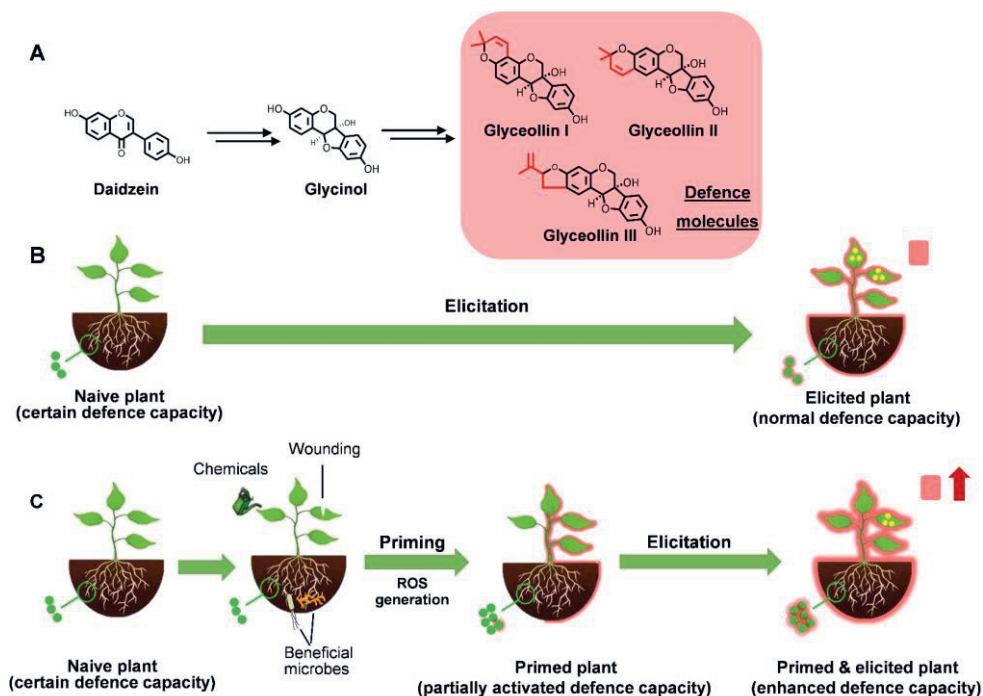


Figure 2.1. Defensive prenylated isoflavonoids produced in soybeans to counteract stress. These defensive molecules in soybeans derive from the isoflavone, daidzein and the pterocarpan, glycinol [2] (A). Effect of direct elicitation on plant's defence responses (in the form of antimicrobial compound production) and overall fitness of the plant (B). Effect of plant-priming prior to elicitation on plant's defence responses (in the form of antimicrobial compound production) and overall fitness of the plant (C). Priming can be induced by chemicals, by physical damage, or by beneficial microorganisms. The intensity of the red glow surrounding the plant refers to the extent to which its defence mechanism is activated. The red boxes represent the production of antimicrobials. Green dots represent inactive signal amplifiers that become activated (green dots with red glow) upon elicitation, while yellow dots show disease symptoms of the plant. Adapted from Conrath *et al.* (2009) [14].

The main distinctive characteristics of the processes of priming and elicitation are summarized in **Table 2.1**. Priming always takes place prior to elicitation, as it activates dormant defence mechanisms in anticipation of a major stress response, which is then triggered by elicitation [15]. The intensity by which the two processes stimulate the defence mechanisms is another major difference. The short-term and transient nature of priming results in weak and local activation of the signal transduction pathway, whereas the more prolonged nature of elicitation leads to strong and more systemic activation of defence signal cascades. Furthermore, it has been shown that primed and elicited plants demonstrated lower fitness costs, i.e. increased growth rates [8], leading to increased secondary metabolism compared to directly elicited plants. The main similarity of the two concepts is that agents that are used for priming can be used for elicitation and vice versa.

One molecule that acts as a direct elicitor in one species, can act as a primer in others [9].

Table 2.1. Main distinctive characteristics of priming and elicitation in plants [8,9,16-18].

Process	Duration of event	Way of application	Activation of defence responses (incl. production of antimicrobials)	Plant's fitness costs
Priming	Short (h)	Imbibition	+	Low
Elicitation	Long (d)	Spraying	++	High
Priming + elicitation	Short (h), Long (d)	Imbibition + Spraying	+++	Moderate

The multifaceted, central role of ROS in signal transduction pathway prompted us to use ROS as a primer of soybean seedlings prior to *Rhizopus*-elicitation. The priming effect of ROS is compared with that of wounding, which is considered a traditional primer [19]. We hypothesize that priming prior to elicitation enhances the diversity and the quantities of glyceollins produced by soybean seedlings. Additionally, we expect that ROS-priming is more robust and less laborious than wounding. The robustness of ROS-priming prior to *Rhizopus*-elicitation was examined across two soybean cultivars. To our knowledge, this is the first report on the use of reactive oxygen species prior to fungus elicitation to enhance the biosynthesis of potent natural antimicrobials, glyceollins.

2.2. Materials and methods

2.2.1. Materials

A mixture of soybeans (*Glycine max*) from different soybean lines of unknown origin (mixCv) was kindly provided by FRANK Food Products (Twello, the Netherlands). Soybeans (*Glycine max*) from the cultivar 'Envy' were purchased from Vreeken's Zaden (Dordrecht, the Netherlands). Tempeh starter culture (a mixture of *Rhizopus oligosporus* and *Rhizopus oryzae*) was purchased from TopCultures (Zoersel, Belgium). H₂O₂ (30 % (w/w) and standards of daidzein (≥ 98 %) and genistein (≥ 98 %) were purchased from Sigma Aldrich Chemie B.V. (Zwijndrecht, the Netherlands). ULC-MS grade acetonitrile (ACN) with 0.1 % (v/v) formic acid (FA), water with 0.1 % (v/v) FA, methanol (MeOH) were purchased from Biosolve BV (Valkenswaard, the Netherlands). Iron (II) sulfate heptahydrate, sodium hypochlorite 14% (v/v) n-Hexane and ethanol 96% (v/v) were purchased from VWR International B.V. (Amsterdam, the Netherlands) and NaCl was purchased from Fisher Scientific (Landsmeer, the Netherlands). Peptone physiological salt solution (PPS) was purchased from Tritium Microbiologie (Eindhoven, the Netherlands).

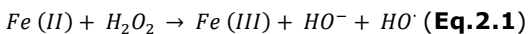
2.2.2. Methods

2.2.2.1. Germination, priming, and elicitation

Soybeans were treated in a modified sprouting machine (MikroFarm™ EQMM; Easy-Green, San Diego, CA, USA). The machine was modified to provide appropriate experimental conditions for both the soybeans and the fungus. The temperature was maintained at 30 °C by a heating mat with a thermostat and by a styrofoam box covering and insulating the machine. Humid air was generated by a fog generator (minifogger; Conrad, Hirschau, Germany) placed in the equipment's water compartment. Fog was generated every 3 h, with a duration of 15 min. In addition, a fan attached to the machine homogeneously distributed the fog for 4 s per 20 s.

In all treatments, seeds were subjected to three phases: soaking (1 day), germination (2 days i.e. "early", unless stated otherwise), elicitation (1-5 days) (**Figure 2.2**). Prior to the soaking step, the seeds (50 g) were surface sanitized with 4 % (w/v) NaOCl for 5 min at room temperature and then thoroughly rinsed with demineralized water. The surface-sterilized seeds were soaked for 24 h at 25 °C in demineralized water. The soaked seeds were placed in sterilized cartridges, which were then placed in the sprouting machine. Before this, the machine was sterilized according to the cleaning protocol provided by the manufacturer. After soaking, seeds were drained and germinated for 2 days at 30 °C and 100 % RH. In "Early" priming experiments, priming and elicitation treatments were sequentially applied on 2-day old germinated seeds (seedlings) (**Figure 2.2**). In "Late" priming experiments, the treatments were performed on the 4-day old germinated seedlings. "Late" priming experiments were performed only in 'Envy'. For wounding-based priming, two wounding methods were used: slicing (S) and sonication (SO). Slicing was performed by cutting each cotyledon individually with a sterilized knife. First, the opposite side of the hilum was longitudinally cut to separate the cotyledon. Next, the newly-exposed cotyledon surface was cut in two parallel slices to form approximately 2-mm thick slices ^[3]. For SO-priming, seeds were immersed in demineralized water and were sonicated for 10 seconds. Wounding-based priming was performed only on mixCv.

For ROS-priming of the seedlings, seedlings were immersed in 1 mM FeSO₄ solution (10 mL/g dry seed) for 30 min and continuously swirled. Then, the metal solution was drained and the seedlings were immersed in 1 M H₂O₂ solution (10 mL/g dry seed) for another 30 min and continuously swirled to generate ROS according to Degousee *et al.* (1994) ^[13]. Subsequently, the H₂O₂ solution was drained and the seedlings were thoroughly rinsed with water.



Wounded or ROS-treated seedlings were then immediately inoculated with a suspension of fungal sporangia (*Rhizopus*-elicitation) of approximately 10⁷ CFU/mL in PPS (0.4 mL/g dry seed). All treatments were performed in the dark and in three independent replicates.

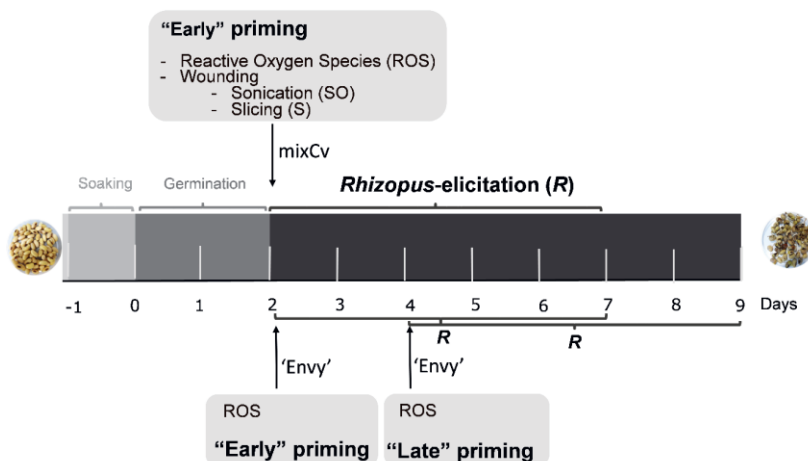


Figure 2.2. Timeline of priming and elicitation experiments in soybean seedlings of two cultivars; mixCv and ‘Envy’.

2.2.2.2. Soybean seedling extraction

Seedlings were freeze-dried and subsequently milled in a bead mill (Cryomill MM440; Retsch GmbH, Haan, Germany) into fine powder with large beads of 20 mm at a frequency of 30 s⁻¹, for 30 s. Seedling extraction was performed using a speed extractor (E-916; Büchi, Flawil, Switzerland). Approximately 300 mg of the powder was mixed with fat-free quartz sand (0.3-0.9 mm, Büchi) and filled into the extraction cells. Samples were defatted in a two-cycle programme (55 min, 40 °C, 100 atm) with 25.5 mL 96 % (v/v) n-hexane per cycle, and (iso)flavonoids were extracted in a three-cycle programme (75 min, 40 °C, 100 atm) with 25.5 mL 96 % (v/v) EtOH per cycle. The ethanol extract was evaporated under reduced pressure in a Syncore evaporator at 40 °C. The dried extract was re-dissolved to a concentration of 5 mg/mL in MeOH and stored at -20 °C. All samples were centrifuged (15,000g, 5 min; room temperature) prior to analysis. The hexane extract was found to be isoflavonoid-free and was not considered further.

2.2.2.3. Compositional analysis by RP-UHPLC-PDA-ESI-MS

Samples were analysed by RP-UHPLC-MS on an Accela UHPLC system (Thermo Scientific, San Jose, CA, USA) equipped with a pump, autosampler, PDA detector, and ESI-ion trap-MS. Injection volume was 1 µL and the extract was separated on an Acquity UPLC BEH C18 column (2.1 mm i.d. × 150 mm, 1.7 µm particle size; Waters, Milford, MA, USA) with a VanGuard (5mm × 2.1mm i.d., 1.7 µm) guard column of the same material (Waters, Milford, MA). Water acidified with 0.1 % (v/v) formic acid and 1 % (v/v) ACN, eluent A, and ACN acidified with 0.1 % (v/v) formic acid, eluent B, were used as solvents at a flow rate of 300 µL/min. The following elution gradient was used: 0-1 min, isocratic at 9% B; 1-3 min, linear

gradient from 9-25% B; 3-10 min, linear gradient from 25-50% B; 10-13 min, isocratic at 50% B; 13-23 min, linear gradient from 50-100% B; 23-28 min, isocratic at 100% B; 28-29 min, linear gradient from 100-9% B; 29-34 min, isocratic at 9% B. Column oven and autosampler temperatures were set at 45 °C and 15 °C, respectively. The PDA detector was set to measure from 200-600 nm.

Mass spectrometric analysis was performed on a Velos Pro (Thermo Scientific) equipped with a heated ESI-MS probe coupled to *in-line* to the RP-UHPLC system. Nitrogen was used as a sheath and an auxiliary gas. Spectra were acquired over an *m/z* range of 150 – 1,500 Da in both positive ionization (PI) and negative ionization (NI) modes. Data-dependent MS² analysis was performed on the most intense ion by collision-induced dissociation (CID) with normalized collision energy of 40%. For both modes, the ion transfer tube (ITT) temperature was 350 °C. The S-lens RF level 55 and the source voltage was 3.5 kV for NI and 4.0 kV for PI mode. A dynamic mass exclusion approach was used, in which a compound detected 3 times as most intense was subsequently excluded for the following 5 s, allowing data-dependent MS² of less intense co-eluting compounds. The system was tuned with genistein in both PI and NI mode via automatic tuning using Tune Plus (Xcalibur 2.1, Thermo Scientific).

2.2.2.4. Tentative annotation and quantification of phytochemicals

Isoflavonoids were tentatively annotated based on UV_{max} and MS spectral data, obtained by Xcalibur (v.2.2, Thermo Scientific). The identities of the peaks were previously determined in our laboratory [1,3,20]. In brief, full MS and MS² scans provided information regarding the molecular weight of the isoflavonoids and substitutions of the phenolic skeleton by means of characteristic neutral losses. The configuration of the prenyl group (chain or ring-closed) attached to the skeleton was determined by typical neutral losses in MS² positive mode: a neutral loss of 56 Da (C₄H₈) was used to distinguish a prenyl chain, whereas a ring-closed prenyl typically showed neutral losses of 42 Da (C₃H₆), 56 Da (C₄H₆), 70 Da (C₃H₆ + H₂O) and 15 Da (CH₃).

The quantification of (iso)flavonoids was based on the ultraviolet (UV) absorbance at 280 nm. A standardized six-point (1-100 µg/mL) calibration curve based on an external standard of daidzein (*R*² = 0.995) was used for the quantification of (iso)flavonoids. Compounds were first converted to mg daidzein equivalents per g of dry weight of the seedling (mg DE /g dry weight (DW)). Then, the quantities of each compound were corrected for the differences in molar extinction coefficients between the standards and the compounds of interest, using Lambert-Beer's law (Eq.2.2) (see Table S2.1 for an overview of the molar extinction coefficients used [1,20,21]).

$$\varepsilon_A C_A = \varepsilon_B C_B \quad (\text{Eq.2.2})$$

Ultimately, the quantities of the compounds were expressed in µmol isoflavonoid per gram of seedling's dry weight (µmol/g DW).

2.2.2.5. Statistical analysis

Statistical analysis was performed using the SPSS Statistics (version 23, IBM, Armonk, NY, USA). Differences in the amounts of isoflavonoid subclasses between pairs of treatments were evaluated for significance ($p < 0.05$) with independent samples t-test. Over-time differences in the amounts of isoflavonoid subclasses within the same treatment were assessed with Tukey's *post hoc* multiple comparison test ($p < 0.05$).

2.3. Results and Discussion

2.3.1. Chromatographic profile of germinated and treated soybean seedlings

The composition of the extracts of germinated (control), *Rhizopus*-elicited (*R*), ROS-primed (ROS) and ROS-primed before *Rhizopus*-elicited (ROS + *R*) soybeans of mixCv is shown in **Figure 2.3**. UHPLC-PDA-MS analysis of the extracts from germinated and treated soybeans showed that (iso)flavonoid profiles were modulated upon priming and/or elicitation, as expected [3,22]. The diversity of compounds increased when germinated seedlings were *R*-elicited or primed with ROS. Peaks **2** and **10-12** (**Figure 2.3**) were mainly induced upon the treatments. The diversity of the compounds increased further when seedlings were treated with ROS + *R* (peaks **6**, **7** and **9**).

2.3.2. Annotation of isoflavonoids in treated soybean seedlings

In total, 12 isoflavonoids, belonging to the subclasses of pterocarpan and isoflavones, were annotated in mixCv seedlings. Saponins (peak **13** and **14**, **Table S2.2**) were also present in the extracts but due to their weak antimicrobial potential [20], they were not considered further.

The germinated control soybeans predominantly contained the glycoside daidzin (**1**) and malonylated glycosides of daidzein (**3**) and genistein (**4**), the two major isoflavones present in soybean. Upon *R*-elicitation, soybeans of mixCv accumulated glycinol (**2**), the non-prenylated pterocarpin precursor of all glyceollins (**Figure 2.3**) and the three main glyceollin isomers (i.e. glyceollin I-III) (**10-12**). Upon ROS-treatment, the aglycones daidzein (**5**) and genistein (**8**) were also annotated. ROS + *R* led to accumulation of glycitein (**6**), a methoxy-isoflavone, glyceofuran (**7**), the detoxification product of glyceollin II [3] and glyceollidin II (**9**), the chain-prenylated glycinol, which is an intermediate to glyceollins II and III. Prenylated isoflavones and prenylated coumestans were not detected in mixCv, contrary to what was anticipated [2].

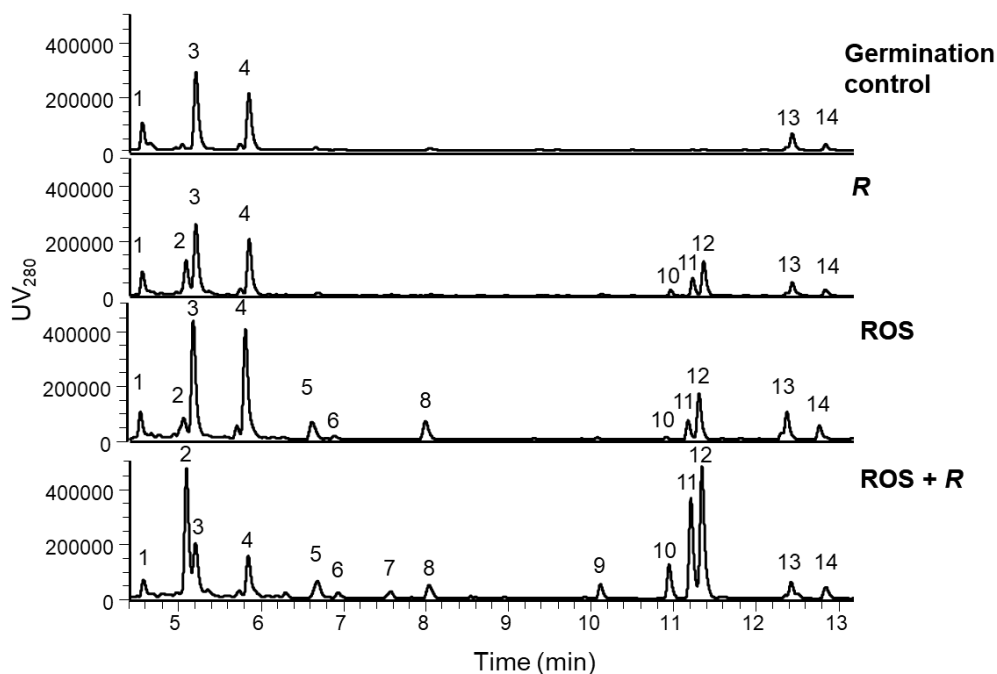


Figure 2.3. RP-UHPLC-PDA (UV 280 nm) profiles of ethanol extracts of germinated (control), *Rhizopus* (*R*)-elicited, reactive oxygen species (ROS)-primed, and ROS-primed prior to *Rhizopus* elicitation, (ROS + *R*)-treated seedlings of soybean mixCv. The chromatograms refer to seedlings three days after priming and/or elicitation. Peak numbers refer to compounds in **Table S2.2**.

2.3.3. ROS-priming is superior to physical priming

The glyceollin content of the seedlings was monitored daily for five days after applying the different treatments, to determine the optimal end-time with respect to maximum glyceollin induction. The content of glyceollins together with the levels of their biosynthetic precursors in the treated mixCv-soybeans over five days are shown in **Figure S2.1** and **Figure S2.2**. The (ROS + *R*)-treated seedlings of mixCv showed a gradual increase in the glyceollin accumulation over time, reaching a clear maximum of $8.6 \pm 0.9 \mu\text{mol/g DW}$ on the 3rd day after fungus inoculation (**Figure S2.2**). This finding is in line with a study where maximal glyceollin levels were observed 40 h after elicitation of 3d-old soybean seedlings with hydroperoxides [13]. A maximum after 3 days was also observed for the glyceollin content of the seedlings upon other treatments (**Figure S2.2**), thus henceforth all treatments were compared based on the samples taken three days after fungus inoculation.

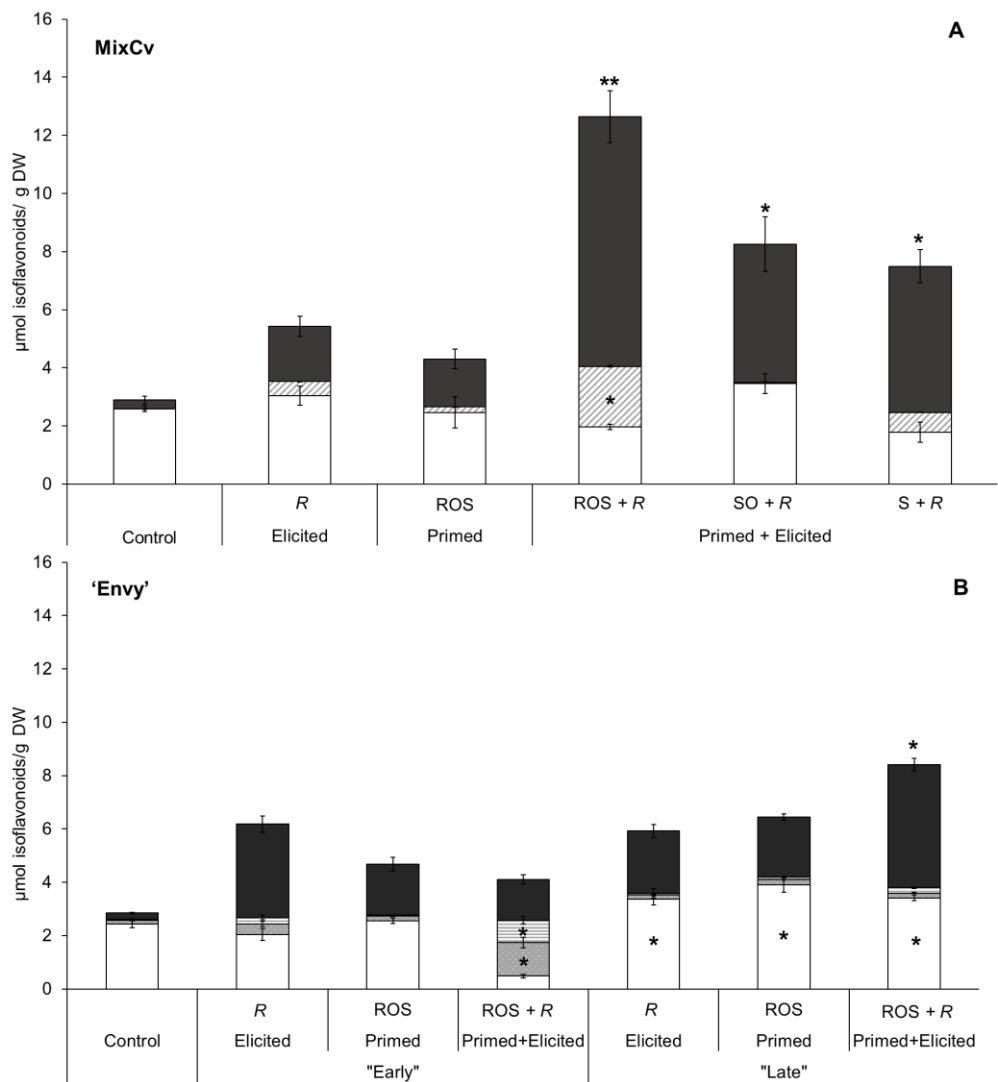


Figure 2.4. Content ($\mu\text{mol/g DW}$) of glycosylated isoflavonoids (white bars) and glyceollins (black bars) in seedlings of the two soybean cultivars, mixCv and 'Envy'. Vertically striped grey bars represent the non-prenylated pterocarpin precursor of glyceollins, glycinol, in mixCv (A), grey dotted bars represent the non-prenylated aglycone, daidzein and horizontally striped grey bars represent daidzein's hydroxylated derivative, genistein in 'Envy'. For "Early" treatments, the metabolite content on 4th day after priming and/or elicitation is shown, whereas for "Late" treatments that on the 3rd after priming and/or elicitation is shown (B). Asterisks signify the statistical increase between the treatments and the benchmark *Rhizopus*-elicited sample on the corresponding isoflavonoid subclass in each cultivar ($p < 0.05$). Error bars indicate the standard deviation of the three biological replicates. The germination controls are presented for comparison.

In **Figure 2.4A**, the glyceollin content of the seedlings upon different treatments is compared. Glyceollin levels in ROS + *R*-treated seedlings were more than four times higher ($8.6 \pm 0.9 \mu\text{mol/g DW}$) than those in the ROS-treated seedlings ($1.6 \pm 0.3 \mu\text{mol/g DW}$) and the *R*-elicited seedlings ($1.9 \pm 0.3 \mu\text{mol/g DW}$). ROS + *R* stimulated the accumulation of both glyceollin subclasses, i.e. C2- and C4-prenylated, compared to *R*-elicited seedlings (**Figure 2.5**). The extent of increase was larger for the C2-glyceollins (five-fold increase) than for C4-glyceollins (three-fold increase). ROS + *R* also accumulated significantly more glycinol on the 3rd day after fungus inoculation (**Figure 2.4A**). The induction of glycinol in the (ROS + *R*)-treated seedlings was thrice more than that in the ROS-treated seedlings ($0.2 \pm 0.01 \mu\text{mol glycinol/g DW}$) and the *R*-elicited seedlings ($0.5 \pm 0.01 \mu\text{mol glycinol/g DW}$).

Priming by sonication or slicing prior to *Rhizopus* elicitation (SO + *R* or S + *R*) yielded similar amounts of glyceollins, i.e. $4.8 \pm 0.9 \mu\text{mol/g DW}$ for SO+*R* and $5.0 \pm 0.6 \mu\text{mol/g DW}$ for S+*R* (**Figure 2.4A**). Overall, all three types of priming prior to *Rhizopus*-elicitation significantly increased the glyceollin levels of elicited seedlings, compared to *R*-elicitation without priming. In mixCv, ROS-priming was almost twice as effective as physical priming (i.e. sonication or slicing) prior to *Rhizopus*-elicitation in stimulating glyceollin production (**Figure 2.4A**).

Additionally, ROS + *R* yielded more reproducible inductions than physical priming (SO + *R* or S + *R*) in time (**Figure S2.2**). This might be attributed to the more systemic and homogeneous effect that imbibition of the seedlings in the ROS solution, compared to the more localized effect of slicing.

2.3.4. ROS + *R* protocol for induction of glyceollins in mixCv is not directly extrapolatable to 'Envy'

To assess the robustness of ROS + *R*, the treatment was also applied to a second soybean cultivar, 'Envy'. This soybean cultivar possessed the capacity to produce a wider variety of prenylated (iso)flavonoids (**Figure S2.3** and **Table S2.2**).

Overall, the isoflavonoid profile of seedlings of 'Envy' was similar to that of mixCv. The main differences between 'Envy' and mixCv were that 'Envy' constitutively contained the 4-prenyl coumestrol, phaseol (**15**) and that it accumulated four prenylated isoflavones (**17-20**) upon priming and/or elicitation. These prenylated isoflavones were tentatively annotated as B_{prenyl} daidzein (**17**), A_{prenyl} daidzein (**18**), A_{prenyl} genistein (**19**) and B_{prenyl} genistein (**20**)^[3] (**Table S2.2**). Due to the absence of treatment effects on phaseol and the inconsistent treatment effects on prenylated isoflavones (**Figure S2.3**), these compounds are not further discussed in this study.

Remarkably, the primed and/or elicited seedlings of 'Envy' did not accumulate glycinol, as opposed to the findings for mixCv. ROS + *R* on 'Envy' led to maximal glyceollin accumulation of $1.5 \pm 0.3 \mu\text{mol/g DW}$ on the 4th day after the fungus inoculation (**Figure S2.4**), which was lower than those in the unprimed *R*-elicited seedlings and similar to those of the ROS-treated seedlings (**Figure 2.4B**,

“Early”). However, ROS + R synergistically induced non-prenylated aglycones ($2.2 \pm 0.3 \mu\text{mol/g DW}$) compared to *Rhizopus*-elicited ($0.7 \pm 0.1 \mu\text{mol/g DW}$) and ROS-treated seedlings ($0.2 \pm 0.01 \mu\text{mol/g DW}$) (**Figure 2.4B, “Early”**). This synergistic accumulation of non-prenylated aglycones, mainly comprised of daidzein and genistein, was observed in all time points of ROS + R (**Figure S2.4**). It seemed as if the ROS + R-treated seedlings were not sufficiently prepared to make use of the large biosynthetic pool of aglycone isoflavonoids for the production of prenylated derivatives.

2.3.5. ROS + R was adaptable to elicit prenylated isoflavonoid production in both soybean cultivars

Unexpectedly, ROS + R, as such, was not successful in enhancing the glyceollin content more than R without priming in ‘Envy’, as opposed to its effect in mixCv. However, the increase in the non-prenylated precursors in the ‘Envy’-soybean seedlings urged us to apply the treatments at a later stage of seedling germination. Seedlings’ age has been established to affect their competency to accumulate glyceollins [23]. Therefore, the treatment was applied also on the 4th day of germination of ‘Envy’ (“Late” application) in addition to the 2nd day (“Early” application) that has been shown so far for both cultivars (**Figure 2.4B**). The aim was to investigate whether perhaps the ideal time point of elicitation was different for ‘Envy’ than mixCv and whether ROS + R could prove to be applicable in ‘Envy’ for glyceollin enhancement.

In **Figure 2.4B** the effect of later application of the treatments on the different isoflavonoid subclasses in ‘Envy’ is compared. “Late” ROS + R had an enhancing effect on the accumulation of glyceollins compared to “Late” ROS or “Late” R. The treatment yielded the highest average of $4.6 \pm 0.3 \mu\text{mol glyceollins/g DW}$ on the 3rd day after fungus inoculation, even though there was no significant change in glyceollin levels over time (**Figure S2.5**). This finding is in line with the optimal day for glyceollin accumulation found in ROS + R-treated seedlings of mixCv.

In comparison to “Early” application, “Late” ROS + R-treated seedlings accumulated far less non-prenylated aglycone isoflavonoids (**Figure 2.4B**). It seems that the seedlings of ‘Envy’ needed to be more developed to process the increased levels of non-prenylated biosynthetic precursors that accumulated upon the “Early” ROS + R-treatment. Moreover, glyceollin accumulation in “Late” R was lower compared to that in “Early” R, therefore “Early” R was used as a benchmark for assessing the effectiveness of the “Late” ROS + R-treatment (**Figure 2.4B**). “Late” ROS + R was statistically better with respect to glyceollin induction than the R-benchmark. Similar to mixCv, the treatment significantly enhanced the accumulation of both C2- and C4-glyceollins in ‘Envy’ compared to R (**Figure 2.5**). It is interesting to note that the two cultivars intrinsically accumulated different ratios of C2:C4-glyceollins (**Figure 2.5, R-elicited**). Thus, we propose that ROS + R enlarges the diversity of generated potent antimicrobials, despite the intrinsic

tendency of soybean seedlings of different cultivars to favour the accumulation of a specific glyceollin subclass over the other.

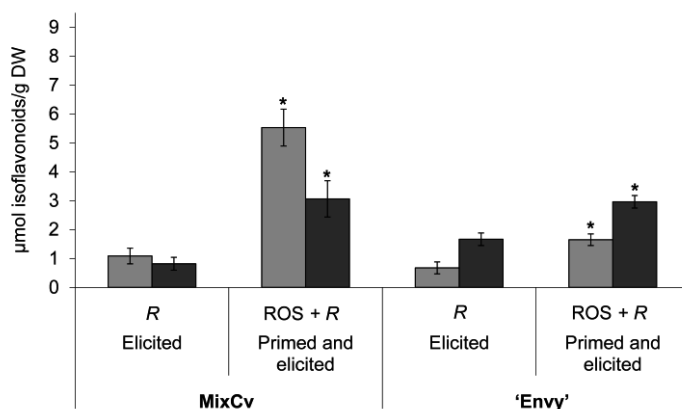


Figure 2.5. Influence of ROS-priming prior to *R*-elicitation (ROS + *R*) on the synthesis of the C2- (striped bars) and C4- (dotted bars) glyceollins in both soybean cultivars employed in this study. For 'Envy', the "Late" ROS + *R* is being shown. Error bars indicate the standard deviation of three biological replicates. Asterisks signify the statistical difference in each glyceollin subclass between *R* and ROS + *R* ($p < 0.05$).

Overall, "Late" ROS + *R* was the superior treatment in 'Envy', yielding the highest overall metabolite content and the highest glyceollin content. ROS + *R* outperformed *R* with respect to the production of potent antimicrobials (i.e. glyceollins) three days after fungus inoculation, in both soybean cultivars employed in this study. The non-laborious application and the robustness of ROS across two soybean cultivars renders it promising as a priming candidate for large scale applications.

2.3.6. ROS + *R* stimulated accumulation of non-prenylated aglycone biosynthetic precursors of glyceollins

The similar effects of ROS + *R* in the two cultivars gives an insight on the possible effect of the treatment on the biosynthetic pathway of glyceollins. In both cultivars, "Early" ROS + *R* samples consistently accumulated less glycosylated isoflavonoids compared to the germination control and *R* samples (**Figure 2.4**). The increased accumulation of glycosylated isoflavonoids in the "Late" ROS + *R* is most likely due to the older age of the seedlings, rather than the treatment itself, since all treatments applied later induced higher accumulation of glycosides (**Figure 2.4**, **Figure S2.4** and **S2.5**). Glycosylated isoflavonoids are the dormant isoflavonoid reserves in plants that become biologically active upon stress by splitting their sugar moiety [24]. In both cultivars, the decreased levels of glycosylated isoflavonoids were accompanied with an increase in aglycone isoflavonoids upon

"Early" ROS + R. In mixCv, deglycosylation resulted in the synergistic accumulation of the aglycone glycinol, which was produced at three times higher quantities than the additive response in ROS and R (**Figure 2.4A**). In 'Envy', daidzein was synergistically induced upon ROS + R treatment (two times more than the calculated additive response in ROS and R) (**Figure 2.4B, "Early"**), whereas glycinol was not detected at all. Based on the consistent decrease in glycosides and the concomitant increase in non-prenylated aglycones upon ROS + R, it seems that the treatment promotes deglycosylation of isoflavones. Moreover, the unequal reduction in molar content of glycosides and the simultaneous increase in glycinol in mixCv (**Figure 2.4A**) as well as the absence of glycinol in 'Envy' suggest that ROS + R may also stimulate *de novo* biosynthesis of daidzein in both cultivars. Similarly, increased accumulation of distant and more downstream precursors of defence-related secondary metabolites has been also reported during the post-challenge primed stage of sorghum seedlings ^[25]. Given the increased accumulation of daidzein, we infer that conversion of daidzein to glycinol might be the rate-limiting step in 'Envy'. Most likely, this is also the reason why 'Envy' was able to accumulate prenylated isoflavones. Prenylated isoflavones and glyceollins share daidzein as their non-prenylated aglycone precursor ^[26].

2.4. Conclusions

In this work, we employed a key molecule in plant's defence response (ROS) as a priming agent prior to *Rhizopus*-elicitation to stimulate the synthesis of soybean's potent antimicrobials, glyceollins. Priming of soybean seedlings with reactive oxygen species (ROS + R) was almost twice as effective as physical priming (sonication or slicing) at stimulating the production of the natural potent antimicrobials, glyceollins. ROS + R enhanced the production of antimicrobial glyceollins 1.3 to 4-fold compared to unprimed *Rhizopus*-elicitation. The treatment had a stimulating effect on the content of non-prenylated aglycone precursors of glyceollins. Lastly, ROS + R stimulated prenylation at both positions (C2 and C4) of the glyceollin backbone, generating larger diversity of prenylated pterocarpanes. This, together with the possibility for large-scale applicability and the robustness across cultivars of the ROS + R method, make ROS a promising primer for triggering the synthesis of antimicrobial compounds in soybean.

2.5. References

- [1] Van De Schans, M. G., Vincken, J.-P., De Waard, P., Hamers, A. R., Bovee, T. F. & Gruppen, H. Glyceollins and dehydroglyceollins isolated from soybean act as SERMs and ER subtype-selective phytoestrogens. *The Journal of Steroid Biochemistry and Molecular Biology* **156**, 53-63 (2016).
- [2] Simons, R., Vincken, J. P., Bohin, M. C., Kuijpers, T. F., Verbruggen, M. A. & Gruppen, H. Identification of prenylated pterocarpanes and other isoflavonoids in *Rhizopus* spp. elicited soya bean seedlings by electrospray ionisation mass spectrometry. *Rapid Communications in Mass Spectrometry* **25**, 55-65 (2011).

- [3] Aisyah, S., Gruppen, H., Madzora, B. & Vincken, J.-P. Modulation of isoflavonoid composition of *Rhizopus oryzae* elicited soybean (*Glycine max*) seedlings by light and wounding. *Journal of Agricultural and Food Chemistry* **61**, 8657-8667 (2013).
- [4] Nwachukwu, I. D., Luciano, F. B. & Udenigwe, C. C. The inducible soybean glyceollin phytoalexins with multifunctional health-promoting properties. *Food Research International* **54**, 1208-1216 (2013).
- [5] Lee, M. R., Kim, J. Y., Chun, J., Park, S., Kim, H. J., Kim, J.-S., Jeong, J.-I. & Kim, J. H. Induction of glyceollins by fungal infection in varieties of Korean soybean. *Journal of Microbiology and Biotechnology* **20**, 1226-1229 (2010).
- [6] Araya-Cloutier, C., Vincken, J.-P., van de Schans, M. G., Hageman, J., Schaftenaar, G., den Besten, H. M. & Gruppen, H. QSAR-based molecular signatures of prenylated (iso) flavonoids underlying antimicrobial potency against and membrane-disruption in Gram positive and Gram negative bacteria. *Scientific Reports* **8**, 9267 (2018).
- [7] Graham, T. & Graham, M. Role of hypersensitive cell death in conditioning elicitation competency and defense potentiation. *Physiological and Molecular Plant Pathology* **55**, 13-20 (1999).
- [8] van Hulten, M., Pelser, M., Van Loon, L., Pieterse, C. M. & Ton, J. Costs and benefits of priming for defense in Arabidopsis. *Proceedings of the National Academy of Sciences* **103**, 5602-5607 (2006).
- [9] Conrath, U., Beckers, G. J., Flors, V., García-Agustín, P., Jakab, G., Mauch, F., Newman, M.-A., Pieterse, C. M., Poinssot, B. & Pozo, M. J. Priming: getting ready for battle. *Molecular Plant-Microbe Interactions* **19**, 1062-1071 (2006).
- [10] Beckers, G. J., Jaskiewicz, M., Liu, Y., Underwood, W. R., He, S. Y., Zhang, S. & Conrath, U. Mitogen-activated protein kinases 3 and 6 are required for full priming of stress responses in *Arabidopsis thaliana*. *The Plant Cell* **21**, 944-953 (2009).
- [11] Martinez-Medina, A., Flors, V., Heil, M., Mauch-Mani, B., Pieterse, C. M., Pozo, M. J., Ton, J., van Dam, N. M. & Conrath, U. Recognizing plant defense priming. *Trends in Plant Science* **21**, 818-822 (2016).
- [12] Savvides, A., Ali, S., Tester, M. & Fotopoulos, V. Chemical priming of plants against multiple abiotic stresses: mission possible? *Trends in Plant Science* **21**, 329-340 (2016).
- [13] Degousee, N., Triantaphylidès, C. & Montillet, J.-L. Involvement of oxidative processes in the signaling mechanisms leading to the activation of glyceollin synthesis in soybean (*Glycine max*). *Plant Physiology* **104**, 945-952 (1994).
- [14] Conrath, U. Priming of induced plant defense responses. *Advances in Botanical Research* **51**, 361-395 (2009).
- [15] Mauch-Mani, B., Baccelli, I., Luna, E. & Flors, V. Defense priming: an adaptive part of induced resistance. *Annual Review of Plant Biology* **68**, 485-512 (2017).
- [16] Baenas, N., Villaño, D., García-Viguera, C. & Moreno, D. A. Optimizing elicitation and seed priming to enrich broccoli and radish sprouts in glucosinolates. *Food Chemistry* **204**, 314-319 (2016).
- [17] Conceição, L. F., Ferreres, F., Tavares, R. M. & Dias, A. C. Induction of phenolic compounds in *Hypericum perforatum* L. cells by *Colletotrichum gloeosporioides* elicitation. *Phytochemistry* **67**, 149-155 (2006).
- [18] Conrath, U., Beckers, G. J., Langenbach, C. J. & Jaskiewicz, M. R. Priming for enhanced defense. *Annual Review of Phytopathology* **53** (2015).
- [19] Galis, I., Gaquerel, E., Pandey, S. P. & Baldwin, I. T. Molecular mechanisms underlying plant memory in JA-mediated defence responses. *Plant, Cell & Environment* **32**, 617-627 (2009).
- [20] Araya-Cloutier, C., den Besten, H. M., Aisyah, S., Gruppen, H. & Vincken, J.-P. The position of prenylation of isoflavonoids and stilbenoids from legumes (Fabaceae) modulates the antimicrobial activity against Gram positive pathogens. *Food Chemistry* **226**, 193-201 (2017).

- [21] Murphy, P. A., Barua, K. & Hauck, C. C. Solvent extraction selection in the determination of isoflavones in soy foods. *Journal of Chromatography B* **777**, 129-138 (2002).
- [22] Namdeo, A. Plant cell elicitation for production of secondary metabolites: a review. *Pharmacognosy Reviews* **1**, 69-79 (2007).
- [23] Abbasi, P., Graham, M. & Graham, T. Effects of soybean genotype on the glyceollin elicitation competency of cotyledon tissues to *Phytophthora sojae* glucan elicitors. *Physiological and Molecular Plant Pathology* **59**, 95-105 (2001).
- [24] Miadoková, E. Isoflavonoids—an overview of their biological activities and potential health benefits. *Interdisciplinary Toxicology* **2**, 211-218 (2009).
- [25] Tugizimana, F., Steenkamp, P. A., Piater, L. A., Labuschagne, N. & Dubery, I. A. Unravelling the metabolic reconfiguration of the post-challenge primed state in sorghum bicolor responding to *Colletotrichum sublineolum* infection. *Metabolites* **9**, 194 (2019).
- [26] Yoneyama, K., Akashi, T. & Aoki, T. Molecular characterization of soybean pterocarpan 2-dimethylallyltransferase in glyceollin biosynthesis: local gene and whole-genome duplications of prenyltransferase genes led to the structural diversity of soybean prenylated isoflavonoids. *Plant and Cell Physiology* **57**, 2497-2509 (2016).

2.6. Supplementary information

2.6.1. Supplementary figures

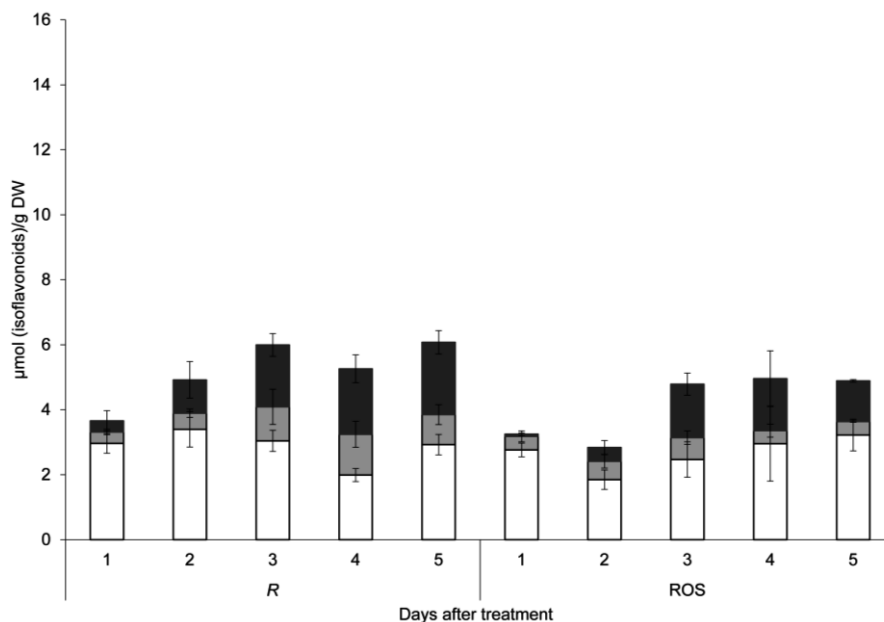


Figure S2.1. Content (μmol/g DW) of R-elicited and ROS-primed seedlings of mixCv in glycosylated isoflavonoids (white bars), non-prenylated aglycone isoflavonoids (grey bars) and glyceollins (black bars) over five days. Error bars indicate the standard deviation of the three biological replicates. No statistical difference was proven for the amounts of the different isoflavonoid subclasses over time for any of the treatments (Tukey's test, $p < 0.05$).

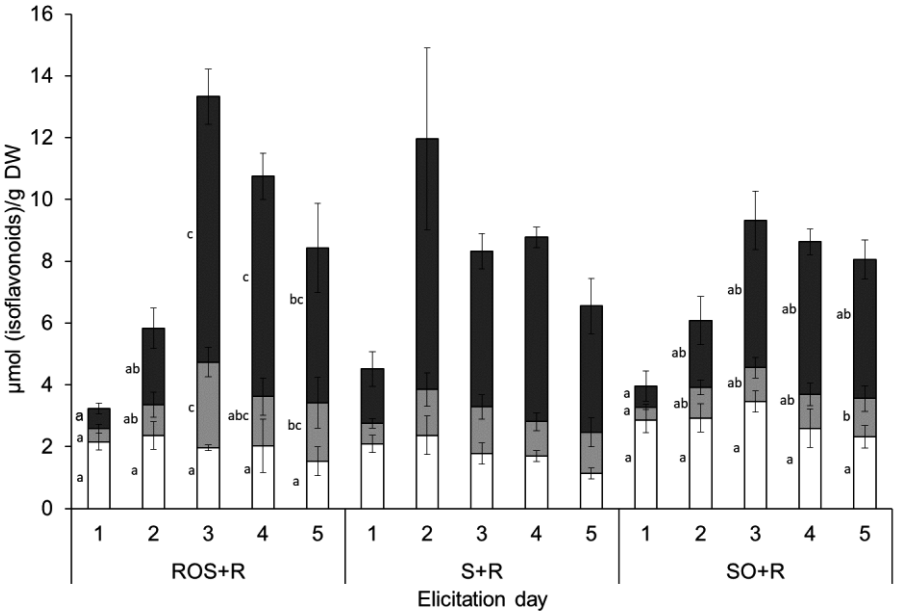


Figure S2.2. Content (μmol/g DW) of ROS + R-, S+R- and SO+R-elicited seedlings of mixCv in glycosylated isoflavonoids (white bars), non-prenylated aglycone isoflavonoids (grey bars) and glyceollins (black bars) over five days. Error bars indicate the standard deviation of the three replicates. Bars with a different letter show significant day-to-day differences in the isoflavonoid content within the same treatment (Tukey's test, $p < 0.05$). For demonstration purposes, isoflavonoid subclasses that were not influenced by the treatment over time were not statistically labeled.

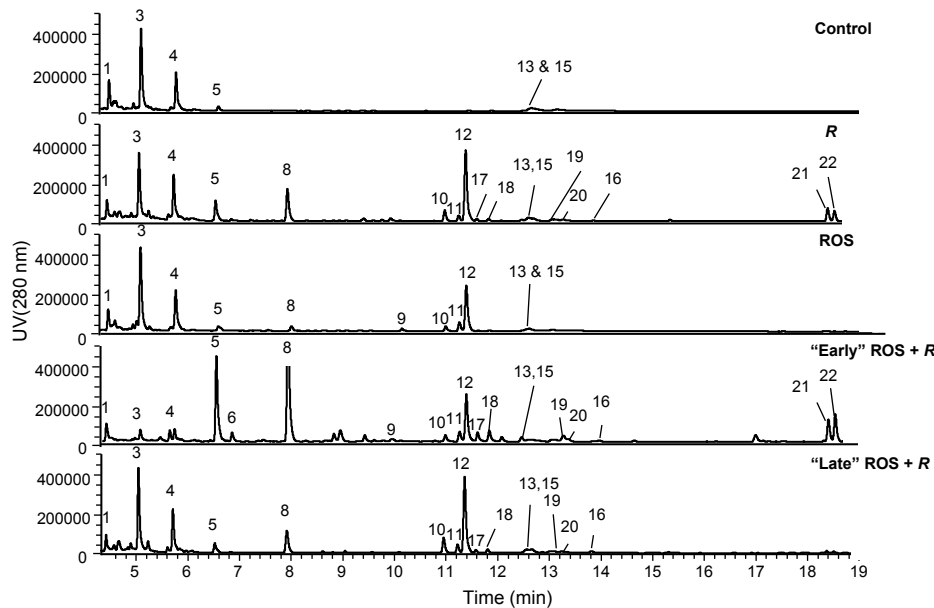


Figure S2.3. RP-UHPLC-PDA (UV 280 nm) of EtOH extracts of germinated (G), *Rhizopus* (R)-elicited, reactive oxygen species (ROS)-primed and ROS-primed prior to *Rhizopus* elicitation, ROS + R seedlings of the soybean ‘Envy’ cultivar. The ROS + R-treatment was applied at an “Early” and a “Late” stage of the germination course. Peak numbers refer to compounds in **Table S2.2**.

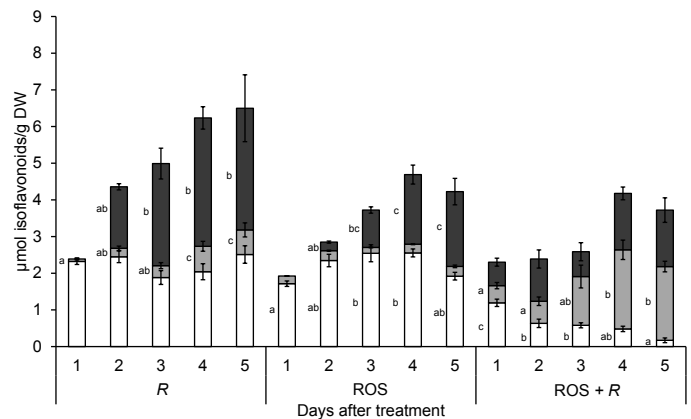


Figure S2.4. Content (μmol/g DW) in “Early” R-, ROS- and ROS + R-seedlings of ‘Envy’ cultivar in glycosylated isoflavonoids (white bars), non-prenylated aglycone isoflavonoids (grey bars) and glyceollins (black bars) over five days. Error bars indicate the standard deviation of the three biological replicates. Bars with a different letter show significant day-to-day differences in the isoflavonoid content within the same treatment (Tukey’s test, $p < 0.05$). For demonstration purposes, isoflavonoid subclasses that were not statistically influenced by the treatment over time were not statistically labeled.

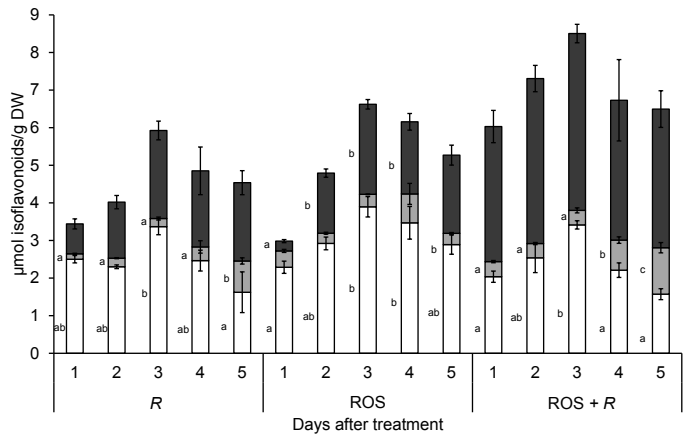


Figure S2.5. Content ($\mu\text{mol/g DW}$) in “Late” *R*-, *ROS*- and *ROS + R*-seedlings of ‘Envy’ cultivar in glycosylated isoflavonoids (white bars), non-prenylated aglycone isoflavonoids (grey bars) and glyceollins (black bars) over five days. Error bars indicate the standard deviation of the three biological replicates. Bars with a different letter show significant day-to-day differences in the isoflavonoid content within the same treatment (Tukey’s test, $p < 0.05$). For demonstration purposes, isoflavonoid subclasses that were not statistically influenced by the treatment over time were not statistically labeled.

2.6.2. Supplementary tables

Table S2.1. Molar extinction coefficients (ϵ) of isoflavonoids used for the quantification of compounds in soybean seedling extracts.

Compound	Subclass	ϵ (AU/M·cm)	Ref.
Daidzein	Isoflavone	13782	[1]
Glycinol*	Pterocarpan		
Glycitein	Isoflavone	25388	[2]
Genistein	Isoflavone	31623	[3]
Glyceollidin II	Pterocarpan	4487	[4]
Glyceollin III	Pterocarpan	5115	[4]
Glyceollin II	Pterocarpan	6288	[4]
Glyceollin I	Pterocarpan	8634	[4]
Glyceollin IV	Pterocarpan	7377	[4]
Glyceofuran	Pterocarpan	4512	[4]

* Glycinol was quantified using the ϵ of daidzein

Table S2.2. Phenolic compounds tentatively annotated by RP-UHPLC-UV-MS present in soybean seedling extracts of mixCv and 'Envy'. Annotation of isoflavonoids was based on the annotation of Simons *et al.*, (2011), Aisyah *et al.*, (2013) ^[56], while annotation of saponins was based on Decroos *et al.* (2007) ^[7]. The identification of oxylipins was based on Feng *et al.*, (2007) ^[6]. Values in bold face refer to the most abundant ions.

No.	RT (min)	λ_{max} (nm)	[M-H] ⁻	MS ² NI product ion (relative abundance)	[M+H] ⁺	MS ² PI product ion (relative abundance)	Tentative annotation	Subclass
1	4.55	260,310	415	253	417	255	Daidzin	Isoflavone
2	5.09	284	271	161 ,256(38),227(34)	273	199 ,227(62),237(13)	Glycinol	Pterocarpan
3	5.20	258	501	253	503	255	Malonyl-daidzin	Isoflavone
4	5.71	259,325	517	225 ,241(28),269(11)	519	271 ,433(7)	Malonyl-genistein	Isoflavone
5	6.66	301,351	253	209 ,225(77),253(28)	255	199 ,137(75),227(60),237(20)	Daidzein	Isoflavone
6	6.94	285	283	268 ,255(15)	285	270 ,225(12),229(15)	Glycitein	Isoflavone
7	7.57	286	353	335 ,149(27),161(3)	355	309 ,319(80),188(42),215(11)	Glyceofuran	Pterocarpan
8	8.02	260,342	269	225 ,201(74),241(51),269(9)	271	153 ,215(81),243(76),253(32)	Genistein	Isoflavone
9	10.11	285	339	161 ,324(53),295(21),270(12)	341	267	Glyceollidin II	Pterocarpan
10	10.94	290	337	319 ,293(62),282(15),149(86)	321	306 ,279(96),293(62),303(44)	Glyceollin III	Pterocarpan
11	11.22	283,307, 316	337	319 ,293(88),282(64),149(19)	321	279 ,251(85),306(80)	Glyceollin II	Pterocarpan
12	11.35	283	337	319 ,149(82),293(42)	321	303 ,306(80),293(36)	Glyceollin I	Pterocarpan
13	12.44	295	1067.5	967 ,741(78),1049(78),879(72),9 21(35),583(26),651(24)	1069.5	n.d.	Soyasaponin β g	Saponin
14	12.85	291	1037.5	937 ,741(80),733(70),849(40), 1019(68)	1039.5	n.d.	Soyasaponin β a	Saponin
15	12.67	306,342	335	280 ,291(6)	337	281	Phaseol	Coumestan
16	13.60	284	353	335 ,149(20)	337	281 ,269(65)	Glyceollin IV	Pterocarpan
17	11.58	268,310, 350	321	265 ,266(30),252(8)	323	267 ,255(16)	Bprenyl daidzein	Isoflavone
18	11.80	260,306	321	266	323	267	Apreryl daidzein	Isoflavone
19	13.23	262	337	282 ,283(18),293(5),309(5),322 (2)	339	283 ,284(20)	Apreryl genistein	Isoflavone
20	13.33	262	337	281 ,293(48),309(30)	339	283 ,271(18)	Bprenyl genistein	Isoflavone
21	18.62	278	293	249 ,113(68),275(28),179(24), 167(18),185(16),197(12),141(12), 149(8)	295	277 ,179(12)	9-oxooctadecadienoic acids	Oxylipin
22	18.78	275	293	277 ,171(66)	295	277 ,179(8),241(8),259(6),161 (5),151(4)	9-oxooctadecadienoic acids	Oxylipin

Table S2.3. Characteristics of ROS + R on two soybean cultivars with different composition of inducible isoflavonoids. Upward and downward arrows represent statistically significant increase and decrease ($p < 0.05$) compared to the benchmark, R, respectively. Dashes refer to statistically insignificant change.

	ROS + R
Prenylated isoflavonoids	
C2-glyceollins	↑
C4-glyceollins	↑
Prenylated isoflavones	-
Non-prenylated aglycone isoflavonoids	↑
Glycosylated isoflavonoids	↓
Optimal day after fungus inoculation*	3

* with respect to maximum glyceollin accumulation

2.6.3 Supplementary references

- [1] Tahara, S., Ingham, J. L. & Mizutani, J. New coumaronochromones from white lupin, *Lupinus albus* L. (*Leguminosae*). *Agricultural and Biological Chemistry* **49**, 1775-1783 (1985).
- [2] Murphy, P. A., Barua, K. & Hauck, C. C. Solvent extraction selection in the determination of isoflavones in soy foods. *Journal of Chromatography B* **777**, 129-138 (2002).
- [3] Araya-Cloutier, C., den Besten, H. M., Aisyah, S., Gruppen, H. & Vincken, J.-P. The position of prenylation of isoflavonoids and stilbenoids from legumes (*Fabaceae*) modulates the antimicrobial activity against Gram positive pathogens. *Food Chemistry* **226**, 193-201 (2017).
- [4] Van De Schans, M. G., Vincken, J.-P., De Waard, P., Hamers, A. R., Bovee, T. F. & Gruppen, H. Glyceollins and dehydroglyceollins isolated from soybean act as SERMs and ER subtype-selective phytoestrogens. *The Journal of Steroid Biochemistry and Molecular Biology* **156**, 53-63 (2016).
- [5] Simons, R., Vincken, J.-P., Roidos, N., Bovee, T. F., van Iersel, M., Verbruggen, M. A. & Gruppen, H. Increasing soy isoflavonoid content and diversity by simultaneous malting and challenging by a fungus to modulate estrogenicity. *Journal of Agricultural and Food Chemistry* **59**, 6748-6758 (2011).
- [6] Aisyah, S., Gruppen, H., Madzora, B. & Vincken, J.-P. Modulation of isoflavonoid composition of *Rhizopus oryzae* elicited soybean (*Glycine max*) seedlings by light and wounding. *Journal of Agricultural and Food Chemistry* **61**, 8657-8667 (2013).
- [7] Decroos, K., Vincken, J.-P., Van Koningsveld, G. A., Gruppen, H. & Verstraete, W. Preparative chromatographic purification and surfactant properties of individual soyasaponins from soy hypocotyls. *Food Chemistry* **101**, 324-333 (2007).
- [8] Feng, S., Saw, C. L., Lee, Y. K. & Huang, D. Fungal-stressed germination of black soybeans leads to generation of oxooctadecadienoic acids in addition to glyceollins. *Journal of Agricultural and Food Chemistry* **55**, 8589-8595 (2007).

CHAPTER 3

Induction of promising antibacterial prenylated isoflavonoids from different subclasses by sequential elicitation of soybean

Elicited soybean seedlings can produce prenylated isoflavonoids from different subclasses. Recently, we showed that priming with reactive oxygen species (ROS) specifically stimulated the production of glyceollins in *Rhizopus* spp.-elicited soybean seedlings (ROS + *R*). Herein, we achieved diversification of the inducible subclasses of prenylated isoflavonoids in soybean, by additional stimulation of two prenylated isoflavones and one prenylated coumestan. This was achieved by using a combination of the relatively long-lived ROS representative, H₂O₂, with AgNO₃ prior to microbial elicitation. Microbial elicitation was performed with a live preparation of either a phytopathogenic fungus, *Rhizopus* spp. or a symbiotic bacterium, *Bacillus subtilis*. *B. subtilis* induced 30% more prenylated isoflavones than *Rhizopus* spp. in (H₂O₂ + AgNO₃)-treated seedlings, without significantly compromising the total levels of glyceollins, compared to (ROS + *R*)-treated seedlings. The most abundant prenylated isoflavone induced (60% of the total prenylated isoflavones), 6-prenyl daidzein and a prenylated coumestan, phaseol, were predicted to be promising antimicrobials based on previously developed quantitative structure-activity relationship (QSAR) models. Overall, we show that treatment with H₂O₂ and AgNO₃ prior to microbial elicitation leads to the production of promising antibacterial isoflavonoids from different subclasses. Extracts rich in prenylated isoflavonoids may potentially be applied as natural antimicrobial agents.

Based on: Kalli, S.; Araya-Cloutier, C.; de Bruijn, W.J.C.; Chapman, J., & Vincken, J.-P. Induction of promising antibacterial prenylated isoflavonoids from different subclasses by sequential elicitation of soybean. *Phytochemistry*, **179**, 112496 (2020).

3.1. Introduction

The increasing demand for novel, natural antimicrobials for food preservation ^[1] and for combating drug-resistant pathogens ^[2] has triggered research to find methods for efficient production of structurally diverse, yet chemically-related compounds. Stressed soybeans (*Glycine max* (L.) Merrill, Leguminosae) produce different subclasses of prenylated isoflavonoids as part of their defence metabolism, from their non-prenylated biosynthetic precursors, daidzein and genistein (**Figure 3.1**). Prenylated pterocarpan (glyceollins) and prenylated isoflavones are the most important subclasses, but prenylated coumestans have been also found in stressed soybeans ^[3-5].

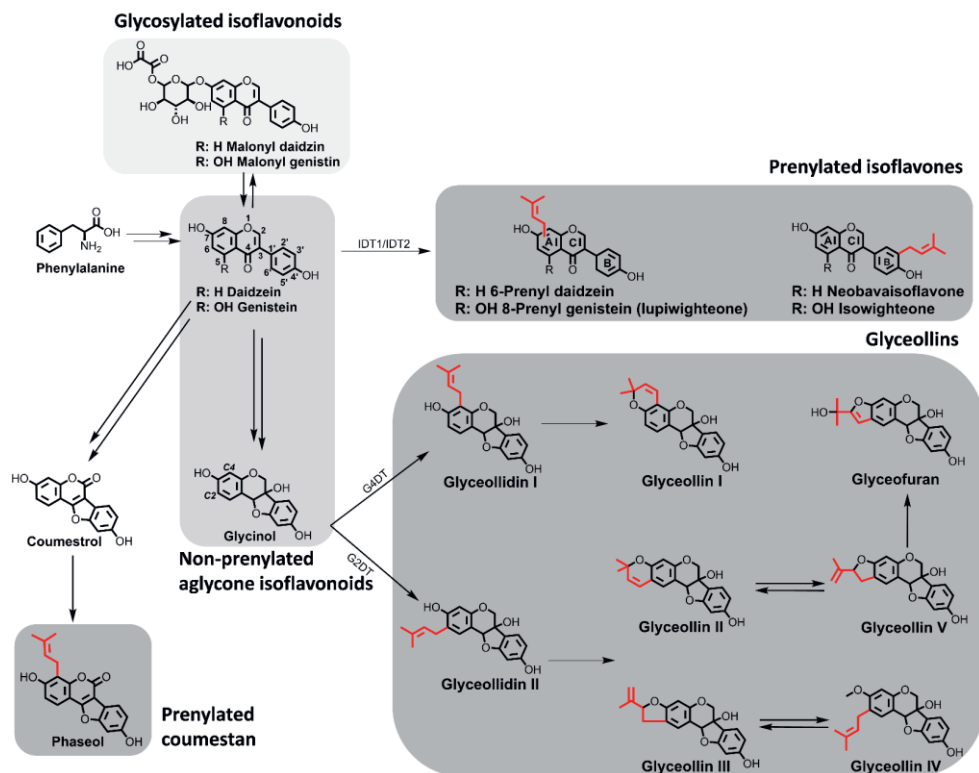


Figure 3.1. Simplified biosynthetic pathway of the main prenylated isoflavonoids and their corresponding subclasses encountered in stressed soybeans (*Glycine max*). The prenyl group in its different configurations is highlighted in red. The different prenyltransferases involved in the biosynthesis of the two main subclasses of prenylated isoflavonoids (i.e. glyceollins and prenylated isoflavones) are demonstrated. Both possible prenylation positions (C2 and C4) on the glycinol backbone for the synthesis of glyceollins are also depicted. Based on Suzuki *et al.* (2006), Yonevama *et al.* (2016) and Dewick *et al.* (1982) [6–8].

Glyceollins as such, are mainly known for their antifungal properties ^[9], whereas they serve as absolute precursors of the powerful antibacterials,

dehydroglyceollins ^[10]. Some dehydroglyceollins, for example, were shown to be active against the Gram-positive bacterium, *Listeria monocytogenes*, with minimum inhibitory concentrations (MICs) of 15 µg/mL (47 µM), while for their precursors, MICs higher than 50 µg/mL were found. In contrast, the prenylated isoflavones, wighteone and isowighteone were found to be very potent against both *L. monocytogenes* and *Escherichia coli* (MICs 10-25 µg/mL, 30-74 µM) ^[10]. So far, the antimicrobial activity of prenylated coumestans is not well documented. Prenylated coumestans have been reported as moderately or no potent against Gram-positives ^[11,12], but potent against Gram-negatives ^[13].

The amounts of defence metabolites in plants are relatively low and dependent on plant's physiological and developmental stage ^[14-17] as well as on environmental factors ^[18,19]. Plant elicitation, i.e. the stimulation of biosynthesis of these metabolites upon the addition of small amounts of elicitors ^[20], is one of the most practically feasible techniques for the induction of these molecules ^[21]. Elicitation is often intertwined with priming, as the agents that can induce elicitation can act also act as primers ^[21,22]. Priming refers to a physiological state that a plant acquires in response to warning signals (e.g. microbially-derived, physical and chemical stimuli) in its environment ^[22,23]. Contrary to elicitation, priming involves short (and sometimes repetitive) ^[24,25] exposure to the stimuli, preserves the fitness of the plant and involves no or minimal induction of defensive genes ^[26]. After priming, plant's defence mechanisms are more effectively induced upon subsequent attack ^[22,23].

Different classes of agents, such as biotic, including live microorganisms or fragments thereof, and abiotic, including metal ions and endogenous signalling molecules can stimulate defence responses in different ways ^[27,28]. Regarding microbial stress, fungal elicitation is the most employed strategy to stimulate production of prenylated isoflavonoids in legumes ^[29-32]. On the contrary, reports on the efficiency of bacterial elicitation are scarce and often contradicting ^[33-36]. The most relevant and systematic study on soybean elicitation with plant-growth promoting (PGPR) bacteria was reported by Ramos-Solano *et al.* (2010) ^[34]. It was suggested that *Bacillus spp.* cause mobilization of non-prenylated aglycone isoflavones from soybeans' roots to shoots where they may play a role in defence. This effect did not compromise soybeans' growth. However, no subsequent analysis on prenylated isoflavonoids was performed.

Plants might respond differently to microbial stresses due to variability in pathogen recognition ^[37,38] and discrepancies have been observed even between different hosts of the same plant species ^[39]. Therefore, alternatives to microbial stress are sought for more controllable and reliable inductions ^[40]. Exogenous application of chemicals is readily used as an abiotic stimulator of plants' secondary metabolism ^[21,41,42]. Farrell *et al.* (2017), for example, reported specific biosynthesis of glyceollin I in soybean seeds by 1 mM silver nitrate (AgNO₃) but not with the same concentration of CuCl₂ ^[28]. Later, 1 mM AgNO₃ was shown to upregulate prenyltransferases involved in the production of both glyceollins and

prenylated isoflavones in soybean [43]. Furthermore, endogenous signalling molecules are also exploited to chemically stress plants. Reactive oxygen species (ROS) generated through Fenton's reaction ($\text{H}_2\text{O}_2 + \text{Fe (II)}$), have been exogenously applied alone [44] or as a primer prior to fungus elicitation to stimulate glyceollin biosynthesis [39].

In this study, a combination of H_2O_2 and AgNO_3 was selected to treat soybean seedlings prior to microbial elicitation to stimulate the production of prenylated isoflavonoids from different subclasses, including the more antibacterial prenylated isoflavones. H_2O_2 , the freely diffusible and relatively long-lived representative of ROS, is expected to regulate the fast entry of the plant into the primed state [45]. AgNO_3 is expected to specifically target the biosynthesis of prenylated isoflavonoids [28,43]. Ag (I) does not participate in Fenton's reaction [46], as is known for Fe (II) [39,44], thus H_2O_2 and AgNO_3 should act independently. As microbial elicitors, a phytopathogenic, live fungus preparation (a mixture of *Rhizopus oligosporus* and *Rhizopus oryzae*) [47,48] or a live bacterial preparation of a symbiotic bacterium (*Bacillus subtilis*) [49] were used. We hypothesized that the symbiont will affect less the fitness of soybeans seedlings, thereby allowing more extensive secondary metabolism. Last, the effect of soybeans' development stage on the induction of prenylated isoflavonoids was also investigated, by applying the treatments in 2d- and 4d- old soybean seedlings. The treatments and the sequence by which they were applied to the seedlings are depicted in **Figure 3.2**.

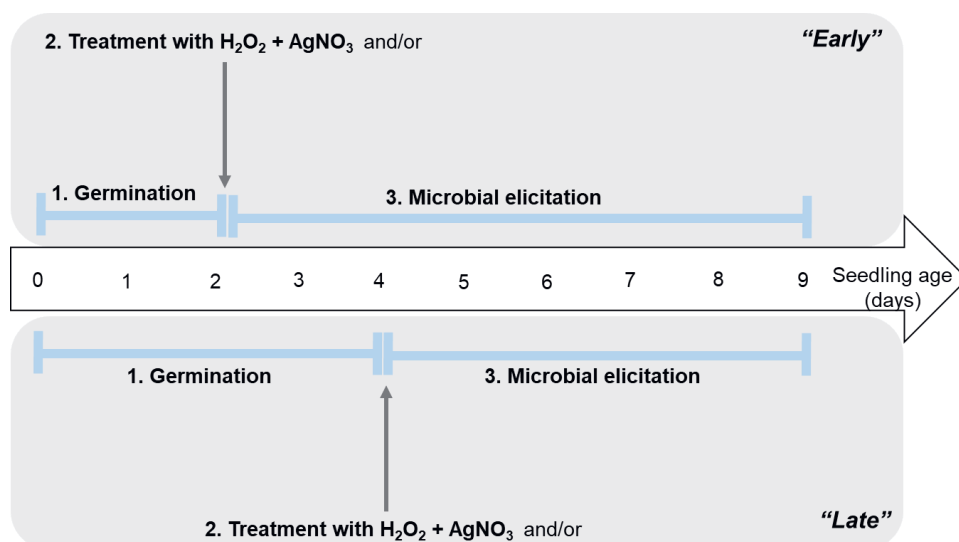


Figure 3.2. Timeline of ($\text{H}_2\text{O}_2 + \text{AgNO}_3$)-treatment with or without subsequent microbial elicitation of soybean seedlings. Microbial elicitation was performed with a live preparation of either a phytopathogenic fungus, *Rhizopus* spp. or a symbiotic bacterium, *Bacillus subtilis*. "Early" and "Late" refer to the time point of application of the ($\text{H}_2\text{O}_2 + \text{AgNO}_3$)-treatment to 2d- and 4d-germinated seedlings, respectively.

3.2. Materials and methods

3.2.1. Materials

Soybeans (*Glycine max* (L.) Merrill, Leguminosae) from the cultivar Envy were purchased from Vreeken's Zaden (Dordrecht, the Netherlands). Tempeh starter culture (mixture of *Rhizopus spp. oligosporus* and *Rhizopus spp. oryzae*) was purchased from TopCultures (Zoersel, Belgium). H₂O₂ (30 % (w/w)) and standards of daidzein (≥ 98 %) and genistein (≥ 98 %) were purchased from Sigma Aldrich Chemie B.V. (Zwijndrecht, The Netherlands). ULC-MS grade acetonitrile (ACN) with 0.1 % (v/v) formic acid (FA), water with 0.1 % (v/v) FA, and methanol (MeOH) were purchased from Biosolve BV (Valkenswaard, the Netherlands). AgNO₃ ($\geq 99.0\%$) was purchased from VWR International B.V. (Amsterdam, the Netherlands) and NaCl was purchased from Sigma Aldrich Chemie B.V.. *n*-Hexane and 96% (v/v) aqueous ethanol were obtained from VWR International B.V.. *Bacillus subtilis* (ATCC 6633) was kindly provided by the Laboratory of Food Microbiology of Wageningen University and Research (Wageningen, the Netherlands). Brain heart infusion broth was purchased from BD (Franklin Lakes, NJ, USA), malt extract agar (CM59) and bacteriological agar from Oxoid Ltd (Basingstoke, UK). Peptone physiological salt solution (PPS) was purchased from Tritium Microbiologie (Eindhoven, the Netherlands). Standards of prenylated isoflavones (lupiwighteone, isowighteone and neobavaisoflavone) were purchased from Plantech UK (Berkshire, UK).

3.2.2. Methods

3.2.2.1. Application of (H₂O₂ + AgNO₃)-treatments to soybean seedlings

Soybeans were treated in a modified sprouting machine (MikroFarm™ EQMM; Easy-Green, San Diego, CA, USA) as described previously [39]. In all treatments, 50 g of seeds (~ 250) were subjected to three phases: soaking (1 day), germination (2 or 4 days), elicitation (1-5 days) as described by Kalli *et al.* (2020) [39].

Elicitation treatments were sequentially applied on 2-day old ("Early" application) or 4-day old ("Late" application) germinated seedlings. The (iso)flavonoid content of the sequentially elicited seedlings was subsequently monitored daily for five days. A time-line of the experimental set-up can be found in **Figure 3.2**.

Treatment with H₂O₂ + AgNO₃ was performed by first immersing the seedlings in 1 mM AgNO₃ solution (10 mL/g dry seed) for 30 min under continuous swirling. Then, the seedlings were drained from the metal ion solution and subsequently immersed in a 1 M H₂O₂ solution (10 mL/g dry seed) for another 30 min and continuously swirled. Subsequently, the H₂O₂ solution was drained and the seedlings thoroughly rinsed with water. (H₂O₂ + AgNO₃)-treated seedlings were subjected to microbial elicitation with either with the fungus, *Rhizopus*

oligosporus/oryzae (in brief, *Rhizopus* spp.) or with the rhizobacterium, *Bacillus subtilis*. For the fungal inoculation, a suspension of fungal sporangia was prepared by scrapping off the *Rhizopus* spp. culture, grown in malt extract agar plates, for 7 days at 30 °C in the dark (approximately 10⁷ CFU/mL). Bacterial cell suspensions were prepared by streaking *Bacillus subtilis* from a -80°C glycerol stock onto a brain heart infusion (BHI) agar plate and incubated for 24 h at 30°C in the dark. One colony was transferred to BHI broth (10 mL) and further incubated for 18 h at 30°C in the dark. The overnight bacterial culture was diluted with BHI (approximately 10⁷ CFU/mL). The microbial spore/cell suspensions (0.4 mL/g dry seed) were poured over the germinated seedlings and the inoculated seedlings were incubated for a maximum of 5 days at 30 °C and 100 % RH. All treatments were performed in the dark and in three independent replicates. An overview of the elicitation treatments discussed in this work can be found in **Table 3.1**.

Table 3.1. Elicitation treatments performed on 2d-old (“Early” application) and 4d-old (“Late” application) soybean seedlings.

Process	Treatment ^a
Abiotic elicitation	H ₂ O ₂ + AgNO ₃
Microbial elicitation	R
	B
Sequential elicitation	(H ₂ O ₂ + AgNO ₃) + R
	(H ₂ O ₂ + AgNO ₃) + B

^a R: *Rhizopus* spp., B: *Bacillus subtilis*

3.2.2.2. Ethanolic extraction of defatted soybean seedlings

Seedlings were extracted according to an established protocol [39]. In short, seedlings were freeze-dried and milled. The powder was defatted with hexane and extracted with 96% (v/v) aqueous ethanol. The ethanol extract was dried under reduced pressure, resolubilised in methanol at a concentration of 5 mg/mL and stored at -20 °C until analysis. All samples were centrifuged (15,000g, 5 min; room temperature) prior to analysis.

3.2.2.3. Compositional analysis of ethanolic, seedling extracts by RP-UHPLC-PDA-ESI-MS

Samples were analysed by RP-UHPLC-MS on an Accela UHPLC system (Thermo Scientific, San Jose, CA, USA) equipped with a pump, autosampler, PDA detector, and ESI-ion trap-MS. Identical column, eluents, and gradient elution program were used as reported as described elsewhere [39]. Mass spectrometric analysis was performed on a Velos Pro (Thermo Scientific) equipped with an heated ESI-MS probe coupled to *in-line* to the RP-UHPLC system as described elsewhere [39].

3.2.2.4. Tentative annotation and quantification of isoflavonoids

Annotation and quantification of phytochemicals was performed as described previously by Kalli *et al.* (2020) [39]. In short, isoflavonoids were tentatively annotated based on MS spectral data and identified based on the ultraviolet (UV) absorbance at 280 nm.

A standardized six-point (1-100 µg/mL) calibration curve based on an external standard of daidzein ($R^2 = 0.995$) was used for the quantification of (iso)flavonoids. Compounds were first converted to mg daidzein equivalents per g of dry weight of the seedling (mg DE /g DW). Then, the quantities of each compound were corrected for the differences in molar extinction coefficients between the standards and the compounds of interest, using Lambert-Beer's law (**Eq.3.1**), using the molar extinction coefficients reported by Kalli *et al.* (2020) [39].

$$\varepsilon_A C_A = \varepsilon_B C_B \text{ (Eq.3.1)}$$

Ultimately, the quantities of the compounds were expressed in µmol isoflavonoid per gram of seedling's dry weight (µmol/g DW).

3.2.2.5. Statistical analysis

Statistical analysis was performed using the SPSS Statistics software package (version 23, IBM, Armonk, NY, USA). Differences in the amounts of isoflavonoid subclasses between pairs of treatments were evaluated for significance ($p < 0.05$) with independent samples t-test. Over-time differences in the amounts of isoflavonoid subclasses within the same treatment were assessed with Tukey's *post hoc* multiple comparison test ($p < 0.05$).

3.2.2.6. Prediction of antibacterial potency of 6-prenyl daidzein and phaseol

The antibacterial potency of 6-prenyl daidzein and phaseol was predicted based on two already developed QSAR models for the bacteria, *L. monocytogenes* (Gram-positive) and *E. coli* (Gram-negative) [10]. First, chemical structures were drawn in the modelling software (Molecular Operating Environment, MOE, v.2019.08, Chemical Computing Group). A conformational search (LowModeMD, RSM gradient 0.1 kcal/mol/Å, other settings default) was performed and the conformation with the lowest energy was further refined using MOPAC force field (RSM gradient 0.01 kcal/mol/Å). Optimized chemical structures were used to calculate different molecular descriptors available in MOE.

Already proposed QSAR models for the prediction of prenylated (iso)flavonoids against *L. monocytogenes* (**Eq.3.2**) and *E. coli* (**Eq.3.3**) were used to calculate the minimum inhibitory concentrations (MICs) of 6-prenyl daidzein and phaseol.

$$y = 2.71 + 0.4 * KierA3 + 1.13 * rsynth - 0.07 * vsurf_DD12 - 0.16 * vsurf_IW4 + 0.29 * vsurf_ID8 \text{ (Eq.3.2)}$$

$$y = 1.60 + b_count * 0.06 + 1.54 * std_dim3 + 0.74 * vsurf_IW2 + 0.80 * rgyr - 0.28 * vsurf_IW4 \text{ (Eq.3.3)}$$

Both compounds were found to fit within the applicability domains of the models, as determined by the standardization method ^[50].

3.3. Results and discussion

3.3.1. Chromatographic profile and annotation of isoflavonoids in (H₂O₂ + AgNO₃)-treated soybean seedlings

The RP-UHPLC-PDA chromatograms of ethanol extracts of (H₂O₂ + AgNO₃)-treated (and subsequently elicited) soybean seedlings are shown in **Figure 3.3** and compared to the recently proposed ROS + *R*, i.e. (H₂O₂ + Fe (II)), which is used as a benchmark in this study. Treatment with (H₂O₂ + AgNO₃) stimulated the production of **12** and **13** which were tentatively annotated as neobavaisoflavone (3'-prenyldaidzein) and 6-prenyl daidzein ^[51], respectively. When (H₂O₂ + AgNO₃)-treated seedlings were subsequently elicited with *Rhizopus* spp. or *Bacillus subtilis*, the levels of prenylated isoflavones increased significantly. In addition to **12** and **13**, they also substantially accumulated phaseol (4-prenylcoumestrol) ^[3,5] (**15**), lupiwighteone (8-prenyl genistein) (**16**), isowighteone (3'-prenyl genistein) ^[51] (**17**) and the C2-glyceollin, glyceollin IV (**18**) ^[52]. Interestingly, compounds **12-17** were weakly or not consistently induced over-time in ROS + *R* ^[39].

All treated seedlings accumulated the three main glyceollin isomers, namely the only C4-glyceollin present in the extracts, glyceollin I (**11**) and the C2-glyceollins, glyceollin II and III (**9** and **10**). In addition, the C2-glyceollins, glyceofuran (**6**) and glyceollidin II (**8**) were also identified ^[29]. The concomitant production of the newly induced prenylated isoflavones and prenylated coumestans together with glyceollins shows that the latter were not sacrificed at the expense of the former two ^[29,39]. This finding shows that (H₂O₂ + AgNO₃)-treatment prior to microbial elicitation results in diversification in the induced subclasses of prenylated isoflavonoids; from mainly glyceollins as induced by ROS + *R* ^[39] to the additional induction of prenylated isoflavones and of a prenylated coumestan (**Figure 3.3**).

The major non-prenylated isoflavonoids typically found in soybeans, namely daidzein (**4**) and genistein (**7**) ^[6], together with their glycosides, daidzin (**1**), the malonylated glycoside of daidzein (6"-O-malonyldaidzin) (**2**) and of genistein (6"-O-malonylgenistin) (**3**), were also identified in the extracts and represented more than 90% of the annotated peaks in the germination control (**Figure 3.3**). Soyasaponin βg (**14**), constitutively present in the soybeans, was not considered further due to its weak antimicrobial potential ^[51]. The annotated isoflavonoids all (H₂O₂ + AgNO₃)-treated seedlings can be found in **Table S3.1**.

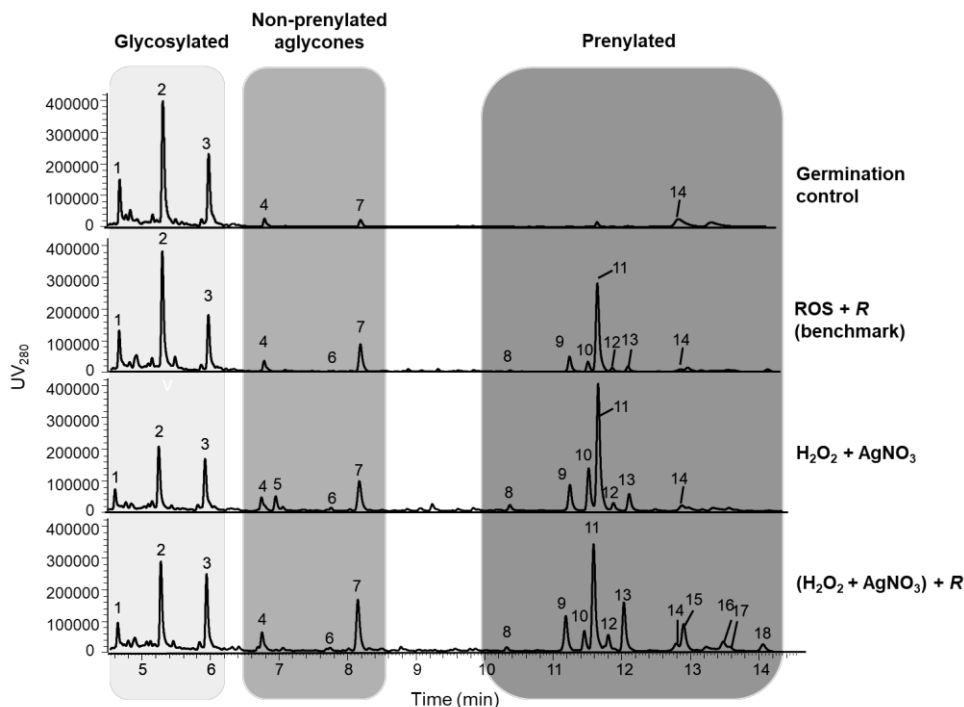


Figure 3.3. RP-UHPLC-PDA (280 nm) profiles of 96% (v/v) EtOH extracts of germinated (without any treatment application), ROS-primed and subsequently *Rhizopus* spp. (*R*)-elicited [39], (H₂O₂ + AgNO₃)-treated and (H₂O₂ + AgNO₃)-treated and subsequently *R*-elicited soybean seedlings. Extracts correspond to 7d-old seedlings, where treatments (if any) were applied on the 4th day of germination. Peak numbers refer to compounds in **Table S3.1**.

3.3.2. Abiotic elicitation with H₂O₂ + AgNO₃ alone can circumvent biotic agents in the induction of glyceollins

The effect of soybeans' developmental stage on the induction of the different subclasses of prenylated isoflavonoids by the (H₂O₂ + AgNO₃)-treatments was studied. For this, the treatments were applied to the seedlings at different moments, i.e. after 2 days of germination ("early") and after 4 days of germination ("late") (**Figure 3.2**). "Late" treatment with H₂O₂ + AgNO₃ without subsequent elicitation triggered a 1.5-times increase in glyceollin levels compared to "Early" application, with a maximum of 4.5 ± 0.3 $\mu\text{mol/g DW}$ on the 4th day after the treatment (**Figure 3.4A**). This finding further corroborates the fact that older soybean seedlings respond better to elicitation treatments with respect to glyceollin induction than their younger counterparts [14,17,39]. "Late" (H₂O₂ + AgNO₃)-treatment without subsequent elicitation performed similarly to "Late" ROS + *R* in the induction of glyceollins (4.6 ± 0.3 $\mu\text{mol glyceollins/g DW}$) when applied in 4d- and 3d- old seedlings, respectively, of the same soybean cultivar (**Figure 3.4A**). This finding suggests that the purely chemical treatment resembles more

to elicitation than to priming, despite the short exposure of the seedlings to the agents. Furthermore, the "Late" ($\text{H}_2\text{O}_2 + \text{AgNO}_3$)-elicitation resulted in similar induction of C2- and C4- glyceollins (48:52, **Table S3.3**) whereas the "Late" ROS + *R* was found to favour more the production of C4- glyceollins (36:64) ^[39] on the optimal day of the treatments. This finding shows that the newly proposed abiotic treatment might also lead to higher diversity of the induced glyceollins compared to the recently published ROS + *R*.

Along with the increased levels of glyceollins, the treatment with $\text{H}_2\text{O}_2 + \text{AgNO}_3$ alone slightly triggered the production of approximately $0.3 \pm 0.05 \mu\text{mol/g DW}$ prenylated isoflavones (on the 4th day after elicitation), regardless the time of application of elicitation ("Early" or "Late") (**Figure 3.4A**).

Last, seedlings treated with $\text{H}_2\text{O}_2 + \text{AgNO}_3$ consistently contained more than 50% less glycosylated isoflavonoids (**Figure 3.4A**) compared to ROS + *R* (**Figure S3.1**) ^[39]. The most affected compound was 6"-O-malonyldaidzin (**2**) (**Table S3.2** and **S3.5**), which was approximately 75% less in the ($\text{H}_2\text{O}_2 + \text{AgNO}_3$)-treatment. This seems to corroborate the hypothesis that AgNO_3 stimulates specific deglycosylation of 6"-O-malonyldaidzin and subsequent generation of precursors for prenylation ^[28].

Overall, we suggest the potential of a combined, purely abiotic elicitation treatment ($\text{H}_2\text{O}_2 + \text{AgNO}_3$) to circumvent microbial agents (ROS + *R*) in the induction of glyceollins. Since all plants seem to share a similar signal transduction pathway, elicitation with chemicals will enable a more universally applicable and controllable approach than approaches involving biotic agents.

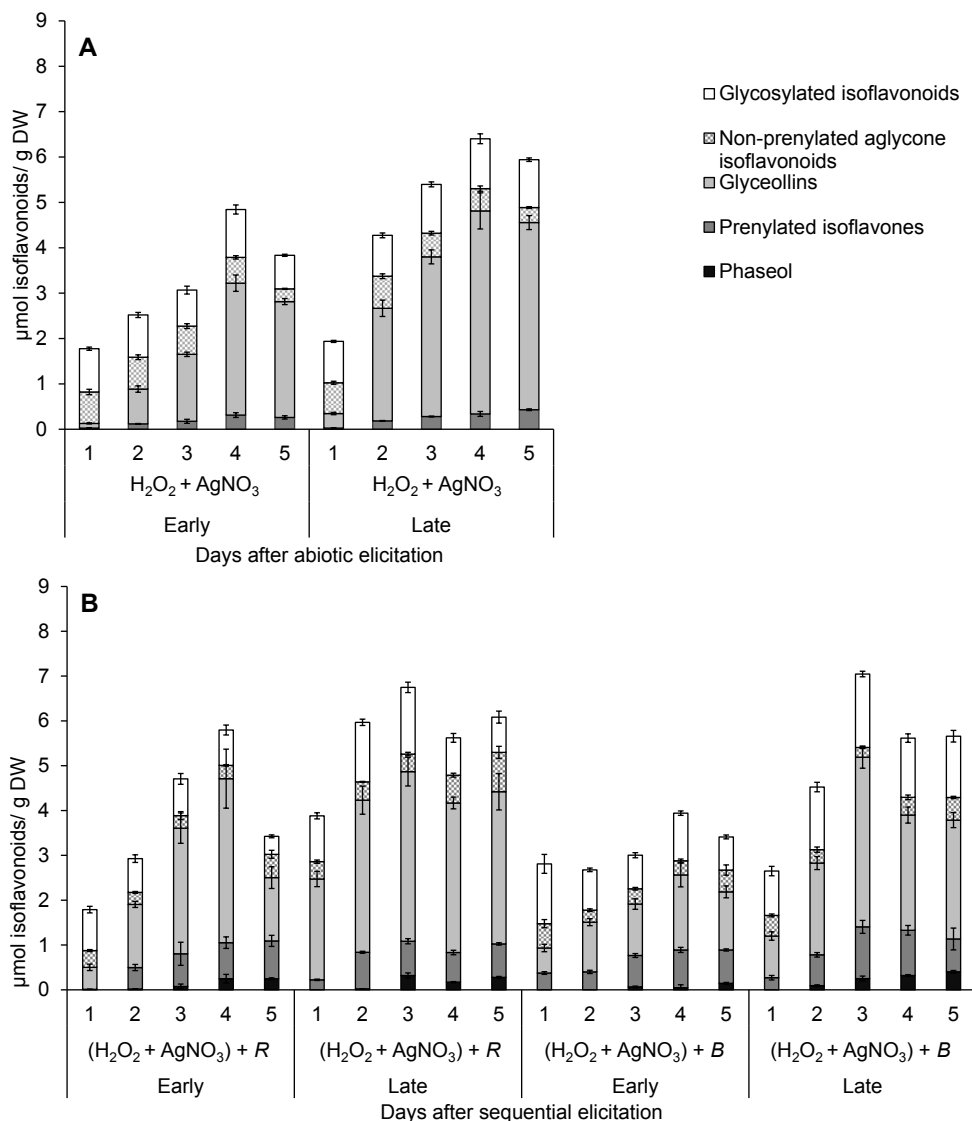


Figure 3.4. Isoflavonoid content ($\mu\text{mol/g DW}$) of “early” and “late” ($\text{H}_2\text{O}_2 + \text{AgNO}_3$)-treated (**A**) and ($\text{H}_2\text{O}_2 + \text{AgNO}_3$)-elicited prior to *R*- or *B*- elicited (**B**) soybean seedlings over five days. Isoflavonoids are classified into four main families (from top to bottom); i.e. glycosylated isoflavonoids (white), non-prenylated aglycones (patterned), glyceollins (light grey) and prenylated isoflavones (dark grey). Phaseol contents (black) are also depicted for sequential elicitation treatments (**B**). Error bars indicate the standard deviation of three biological replicates. Quantification of the individual isoflavonoids over-time per treatment can be found in **Tables S3.2-S3.4**. Statistical analysis (Tukey’s test, $p < 0.05$) of the over-time differences in each isoflavonoid subclass within the same treatment can be found in **Table S3.8**.

3.3.3. Microbial elicitation after (H₂O₂ + AgNO₃)-elicitation boosts the production of prenylated isoflavones and of the prenylated coumestan, phaseol

Elicitation with (H₂O₂ + AgNO₃) without a subsequent microbial elicitation had a stimulatory effect on the induction of glyceollins and a smaller triggering effect on the production of isoflavones. When chemical elicitation was followed by microbial elicitation, the biosynthesis of prenylated isoflavones was enhanced further by 3-4 times. *Bacillus subtilis* was more effective in inducing prenylated isoflavones than *Rhizopus* spp. when applied "late" in (H₂O₂ + AgNO₃)-elicited seedlings, at all time-points (**Figure 3.4B**). On the contrary, both microorganisms induced similar glyceollin levels in (H₂O₂ + AgNO₃)-elicited seedlings over time (**Figure 3.4B**). Interestingly, *Rhizopus* spp. (phytopathogenic) generally outperformed *Bacillus subtilis* (symbiont) in terms of glyceollin production when these were applied alone without prior elicitation (**Figure S3.2**). This discrepancy in the effects of the microorganisms, when used as direct elicitors or after elicitation, has not been reported before. It might be related to the differential recognition of *B. subtilis* as a symbiont or as a pathogen by non-elicited or already elicited soybeans, respectively. This differential recognition may have an effect on the balance between maintaining plant's vitality and inducing the production of defensive metabolites [53,54].

Unlike glyceollins, prenylated isoflavones were already maximally induced upon "early" application of the sequential elicitation treatment. Later application of the treatment did not lead to a consistent increase in prenylated isoflavones. Prenylation of isoflavonoids in soybean is catalysed via two classes of prenyltransferases, the glycinol prenyltransferases yielding glyceollins and the isoflavone prenyltransferases yielding prenylated isoflavones (**Figure 3.1**) [7]. Early induction of prenyltransferases involved in direct prenylation of isoflavones by AgNO₃ has been shown before [43].

The increased prenylated isoflavone accumulation in sequentially elicited seedlings, compared to only (H₂O₂ + AgNO₃)-elicited ones, can be partially explained by the comparably low levels of glycosylated isoflavonoids observed in both cases (**Figure 3.4A and B**), compared to ROS + R (**Figure S3.1**). Nevertheless, the combined treatments seem to additionally upregulate the activity of isoflavone-specific prenyltransferase(s).

Sequential elicitation treatments additionally stimulated the synthesis of phaseol (**Figure 3.4B**). Phaseol (4-prenyl coumestrol) derives from daidzein as a distant precursor [8], similarly to glyceollins and to prenylated isoflavones (**Figure 3.1**). Seedlings accumulated more pronounced levels of phaseol upon late application of sequential elicitation, regardless the microbe used (**Figure 3.4B**). Even though phaseol has been reported before in soybean seedlings [3,4], there is no information on its antimicrobial potency.

3.3.4. “Late” elicitation with ($\text{H}_2\text{O}_2 + \text{AgNO}_3$) prior to biotic elicitation, the new protocol for induction of a wide array of prenylated isoflavonoids subclasses

Overall, abiotic elicitation prior to microbial elicitation and seedlings’ age seem important in improving the biosynthetic capacity of the soybean seedlings. Since the “Late” treatments resulted in maximum accumulation of all subclasses of prenylated (iso)flavonoids, i.e. glyceollins, prenylated isoflavones and the prenylated coumestan, the “Late” treatments are considered as optimal and are further compared (**Figure 3.5**).

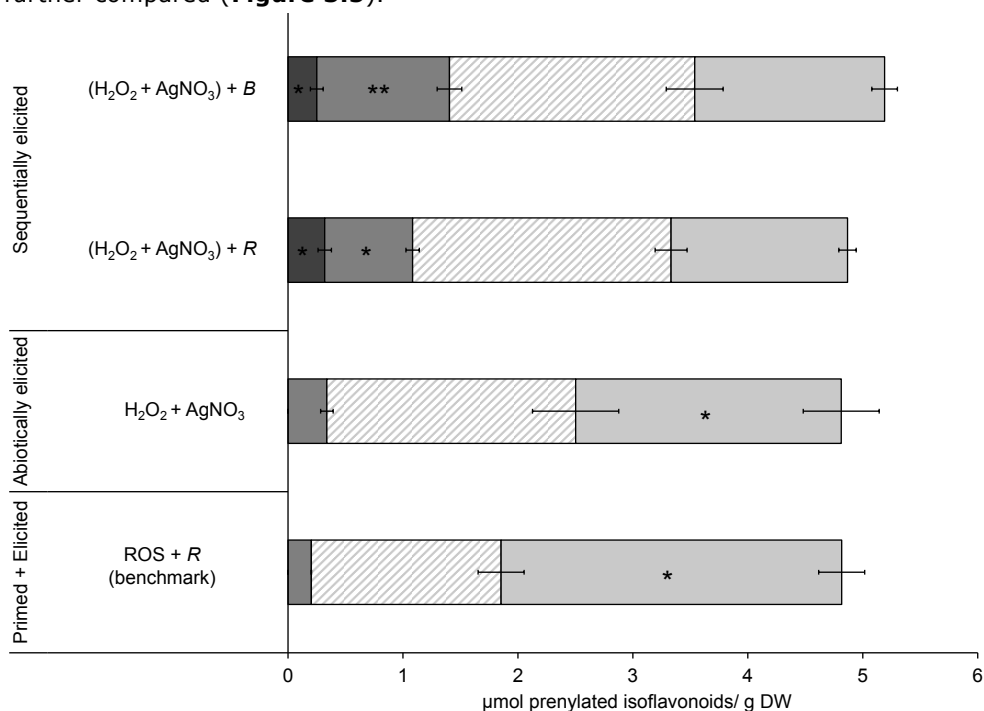


Figure 3.5. Content ($\mu\text{mol/g DW}$) of prenylated isoflavonoids in ($\text{H}_2\text{O}_2 + \text{AgNO}_3$)-elicited (and subsequently *B. subtilis* (B)- or *Rhizopus* spp. (R)- elicited) soybean seedlings in comparison to the recently proposed priming and elicitation treatment, ROS + R published by Kalli *et al.* (2020) [39]. Prenylated isoflavonoids were classified into (from right to left): C4-glyceollins (light grey), C2-glyceollins (light grey striped), prenylated isoflavones (grey), and phaseol (dark grey). Treatments are shown at their optimum day (4d for ($\text{H}_2\text{O}_2 + \text{AgNO}_3$)-elicited and 3d for the sequentially elicited or ROS + R treatments) after “late” application with respect to maximum prenylated isoflavonoid accumulation. Error bars indicate the standard deviation of the three biological replicates. Asterisks signify a statistically higher accumulation of a specific prenylated isoflavonoid subclass compared to the rest of the treatments ($p < 0.05$).

Treatments that involved microbial elicitation after ($\text{H}_2\text{O}_2 + \text{AgNO}_3$)-elicitation stimulated the levels of prenylated isoflavones more than 4-fold compared to ROS + R ($0.2 \pm 0.02 \mu\text{mol/g DW}$) on their optimal day (3rd after the treatment). Among

the studied microorganisms, *B. subtilis* induced the accumulation of 30% more prenylated isoflavones than *Rhizopus* spp. in (H₂O₂ + AgNO₃)-elicited seedlings (0.8 ± 0.1 µmol/g DW and 1.2 ± 0.1 µmol/g DW for *R*- and *B*- elicitation, respectively) (**Figure 3.5**). This increase in prenylated isoflavones was mainly attributed to the enhanced accumulation of 6-prenyl daidzein (60% of the total induced prenylated isoflavones, **Table S3.4**). Neobavaisoflavone was the second most strongly induced prenylated isoflavone (over 25% of the total induced prenylated isoflavones, **Table S3.4**) in sequentially elicited seedlings. Isowighteone and lupiwighteone make up the complete prenylated isoflavone pool (**Table S3.4**). Along with prenylated isoflavones, the prenylated coumestan, phaseol was induced at levels of 0.3 ± 0.06 µmol/g DW in sequentially elicited seedlings on the optimal day (3rd after the treatment) (**Figure 3.5**).

Maximal induction of prenylated isoflavones upon the “late” subsequent elicitation treatments occurred without significantly compromising the levels of total induced glyceollins (3.8 ± 0.3 µmol/g DW for both *R*- and *B*- elicitation) compared to ROS + *R* (4.6 ± 0.3 µmol/g DW). This indicates that (H₂O₂ + AgNO₃)-elicitation prior to microbial elicitation is able to specifically induce prenylated isoflavones (**Figure 3.5**), whereas ROS-priming prior to *R*-elicitation targeted mainly glyceollin production [39].

Overall, we propose elicitation of 4d-old (instead of 2d-old) soybean seedlings with H₂O₂ and AgNO₃ before microbial elicitation for the simultaneous enhanced production of three subclasses of prenylated isoflavonoids (i.e. pterocarpan, isoflavones and coumestans) in soybean seedlings. The symbiont, *B. subtilis* was shown to be more effective than the phytopathogenic, *Rhizopus* spp. in the induction of prenylated isoflavones in sequentially elicited seedlings.

As might be expected, the use of AgNO₃ can rise safety and environmental concerns as metallic silver is anticipated to be deposited on the seedlings in the presence of H₂O₂ [46] and subsequently in the rinsing water (**section 3.2.2.1**). Cost-effective, simple technologies that recover silver from waste waters, minimizing its environmental impact are available (for an example, see [55] and for a review, see [56]). Furthermore, co-extraction of any residual silver present in the seedlings with the compounds of interest should be limited when pure organic solvents (e.g. ethyl acetate), known to maximize the extractability of prenylated isoflavonoids, are used [57].

3.3.5. QSAR-based prediction of the antibacterial potency of 6-prenyl daidzein and phaseol

In this study, treated seedlings were extracted with 96% (v/v) EtOH to obtain and study the entire range of isoflavonoid families (glycosylated, aglycone and prenylated). As the antimicrobial activity of crude extracts (containing glycosylated and aglycone isoflavonoids) is low [51], enrichment of the extracts in prenylated isoflavonoids or purification of prenylated isoflavonoids are suitable strategies to

obtain potent, natural antimicrobials. Several reports on the antibacterial activity of purified prenylated isoflavonoids is available in literature [10,58,59]. In particular, certain prenylated isoflavones have been shown to be powerful antibacterial agents against the food-borne Gram-positive pathogen *L. monocytogenes* and the clinically-relevant Gram-negative pathogen *E.coli* [10]. Among the most abundant prenylated isoflavones induced by our proposed sequential elicitation protocol, neobavaisoflavone has showed high potency towards *E.coli* (20 µg/mL, 59 µM), in the presence of an efflux pump inhibitor, and more moderate activity against *L. monocytogenes* (50 µg/mL, 155 µM) [10].

The most strongly induced prenylated isoflavone by sequential elicitation, 6-prenyl daidzein, and the prenylated coumestan, phaseol, have not been tested for their antimicrobial potency yet. To predict their antibacterial potency, the structures of molecules were inputted to MOE (Molecular Operating Environment) and molecular descriptors corresponding to these structures were calculated (Table S3.9). With these descriptors, the antibacterial potency of these two compounds against *L. monocytogenes* and *E. coli* was predicted by using QSAR models already developed against these two bacteria (Eq.3.2 and Eq.3.3, section 3.2.2.6). The predicted antibacterial activity of 6-prenyl daidzein and phaseol can be found in Table 3.2. 6-Prenyl daidzein was predicted as very active, having a MIC value of 6.9 µg/ mL (21 µM) and 9.1 µg/ mL (28 µM) against *L. monocytogenes* and *E. coli*, respectively. Phaseol was predicted to be potent having a MIC value of 36 µg/ mL (108 µM) and 23 µg/mL (69 µM) against the two bacteria, respectively. Based on these predictions, it is worthwhile to evaluate *in-vitro* the antibacterial activity of the purified compounds.

Table 3.2. Antibacterial activity of 6-prenyl daidzein and phaseol as predicted by using already developed QSAR models for *L. monocytogenes* and *E. coli* [10].

Bacterium	Predicted antibacterial activity	
	pMIC in M (MIC, µM)	
	6-Prenyl daidzein	Phaseol
<i>L. monocytogenes</i>	4.67 (21)	3.97 (108)
<i>E. coli</i> *	4.55 (28)	4.16 (69)

* Activity predicted in the presence of an efflux pump inhibitor (PAβN)

3.4. Conclusions

A combination of H₂O₂ and AgNO₃ was used to induce different subclasses of prenylated isoflavonoids in microbially-elicited soybean seedlings. (H₂O₂ + AgNO₃)-treatment without subsequent microbial elicitation was as effective in inducing glyceollins (4.5 ± 0.3 µmol/ g DW) as the recently proposed, priming and elicitation treatment (ROS + R). This finding suggests that abiotic elicitation may circumvent the use of microbial agents for glyceollin production. Additionally, treatment with H₂O₂ and AgNO₃ triggered the synthesis of prenylated isoflavones,

which were substantially boosted (3-4 fold) by subsequent microbial elicitation. Elicitation with the symbiotic bacterium, *Bacillus subtilis*, induced 30% more prenylated isoflavones in (H_2O_2 + AgNO_3)-treatment seedlings than with the phytopathogenic fungus, *Rhizopus* spp. This increase was mainly attributed to the production of 6-prenyl daidzein (60% of the total induced prenylated isoflavones). Besides this, the prenylated coumestrol, phaseol was boosted by the sequential elicitation treatments. The antibacterial potency of the newly induced 6-prenyl daidzein and phaseol was predicted by previously developed QSAR models. Both compounds were predicated to be promising antibacterials against *L. monocytogenes* and *E.coli*, although 6-prenyl daidzein was predicted to be 2-5 times more potent than phaseol.

We propose elicitation of 4d-old soybean seedlings with H_2O_2 and AgNO_3 before *B. subtilis* elicitation for the simultaneous induction of the three isoflavonoid subclasses: prenylated pterocarpan (glyceollins), isoflavones and coumestans. These results show that sequential elicitation can be used to produce extracts containing prenylated isoflavonoids from different subclasses, which, after enrichment or purification, may be used as natural antibacterial agents.

3.5. Acknowledgement

The authors are thankful to Yiran Lin for her help in performing screening elicitation experiments.

3.6. References

- [1] Hintz, T., Matthews, K. K. & Di, R. The use of plant antimicrobial compounds for food preservation. *BioMed research international* **2015** (2015).
- [2] Subramani, R., Narayanasamy, M. & Feussner, K.-D. Plant-derived antimicrobials to fight against multi-drug-resistant human pathogens. *3 Biotech* **7**, 172 (2017).
- [3] Caballero, P., Smith, C. M., Fronczek, F. R. & Fischer, N. H. Isoflavones from an insect-resistant variety of soybean and the molecular structure of afrormosin. *Journal of Natural Products* **49**, 1126-1129 (1986).
- [4] Yuk, H. J., Lee, J. H., Curtis-Long, M. J., Lee, J. W., Kim, Y. S., Ryu, H. W., Park, C. G., Jeong, T.-S. & Park, K. H. The most abundant polyphenol of soy leaves, coumestrol, displays potent α -glucosidase inhibitory activity. *Food Chemistry* **126**, 1057-1063 (2011).
- [5] Simons, R., Vincken, J. P., Bohin, M. C., Kuijpers, T. F., Verbruggen, M. A. & Gruppen, H. Identification of prenylated pterocarpan and other isoflavonoids in *Rhizopus* spp. elicited soya bean seedlings by electrospray ionisation mass spectrometry. *Rapid Communications in Mass Spectrometry* **25**, 55-65 (2011).
- [6] Suzuki, H., Takahashi, S., Watanabe, R., Fukushima, Y., Fujita, N., Noguchi, A., Yokoyama, R., Nishitani, K., Nishino, T. & Nakayama, T. An isoflavone conjugate-hydrolyzing β -Glucosidase from the roots of soybean (*Glycine max*) seedlings purification, gene cloning, phylogenetics, and cellular localization. *Journal of Biological Chemistry* **281**, 30251-30259 (2006).
- [7] Yoneyama, K., Akashi, T. & Aoki, T. Molecular characterization of soybean pterocarpan 2-dimethylallyltransferase in glyceollin biosynthesis: local gene and whole-genome duplications of prenyltransferase genes led to the structural diversity of soybean prenylated isoflavonoids. *Plant and Cell Physiology* **57**, 2497-2509 (2016).

- [8] Dewick, P., Barz, W. & Grisebach, H. Biosynthesis of coumestrol in *Phaseolus aureus*. *Phytochemistry* **9**, 775-783 (1970).
- [9] Lee, M. R., Kim, J. Y., Chun, J., Park, S., Kim, H. J., Kim, J.-S., Jeong, J.-I. & Kim, J. H. Induction of glyceollins by fungal infection in varieties of Korean soybean. *Journal of Microbiology and Biotechnology* **20**, 1226-1229 (2010).
- [10] Araya-Cloutier, C., Vincken, J. P., van de Schans, M. G. M., Hageman, J., Schaftenaar, G., den Besten, H. M. W. & Gruppen, H. QSAR-based molecular signatures of prenylated (iso)flavonoids underlying antimicrobial potency against and membrane-disruption in Gram positive and Gram negative bacteria. *Scientific Reports* **8**, 9267 (2018).
- [11] Eerdunbayaer, M. A., Aoyama, H., Kuroda, T. & Hatano, T. Structures of new phenolics isolated from licorice, and the effectiveness of licorice phenolics on vancomycin-resistant *Enterococci*. *Molecules* **19**, 13027 (2014).
- [12] Tanaka, H., Sato, M., Fujiwara, S., Hirata, M., Etoh, H. & Takeuchi, H. Antibacterial activity of isoflavonoids isolated from *Erythrina variegata* against methicillin-resistant *Staphylococcus aureus*. *Letters in Applied Microbiology* **35**, 494-498 (2002).
- [13] Khatune, N. A., Islam, M. E., Haque, M. E., Khondkar, P. & Rahman, M. M. Antibacterial compounds from the seeds of *Psoralea corylifolia*. *Fitoterapia* **75**, 228-230 (2004).
- [14] Abbasi, P. & Graham, T. Age-related regulation of induced isoflavonoid responses in soybean lines differing in inherent elicitation competency. *Physiological and Molecular Plant Pathology* **59**, 143-152 (2001).
- [15] Dixon, R. A. Natural products and plant disease resistance. *Nature* **411**, 843-847 (2001).
- [16] Oksman-Caldentey, K.-M. & Inzé, D. Plant cell factories in the post-genomic era: new ways to produce designer secondary metabolites. *Trends in Plant Science* **9**, 433-440 (2004).
- [17] Aisyah, S., Gruppen, H., Slager, M., Helmink, B. & Vincken, J. P. Modification of prenylated stilbenoids in peanut (*Arachis hypogaea*) seedlings by the same fungi that elicited them: the fungus strikes back. *Journal of Agricultural and Food Chemistry* **63**, 9260-9268 (2015).
- [18] Yang, L., Wen, K. S., Ruan, X., Zhao, Y. X., Wei, F. & Wang, Q. Response of plant secondary metabolites to environmental factors. *Molecules* **23** (2018).
- [19] Isah, T. Stress and defense responses in plant secondary metabolites production. *Biological Research* **52**, 39 (2019).
- [20] Radman, R., Saez, T., Bucke, C. & Keshavarz, T. Elicitation of plants and microbial cell systems. *Biotechnology and Applied Biochemistry* **37**, 91-102 (2003).
- [21] Namdeo, A. Plant cell elicitation for production of secondary metabolites: a review. *Pharmacognosy Reviews* **1**, 69-79 (2007).
- [22] Mauch-Mani, B., Baccelli, I., Luna, E. & Flors, V. Defense priming: an adaptive part of induced resistance. *Annual Review of Plant Biology* **68**, 485-512 (2017).
- [23] Pastor, V., Luna, E., Mauch-Mani, B., Ton, J. & Flors, V. Primed plants do not forget. *Environmental and Experimental Botany* **94**, 46-56 (2013).
- [24] Baenas, N., Villafañ, D., García-Viguera, C. & Moreno, D. A. Optimizing elicitation and seed priming to enrich broccoli and radish sprouts in glucosinolates. *Food Chemistry* **204**, 314-319 (2016).
- [25] Singh, P., Yekondi, S., Chen, P.-W., Tsai, C.-H., Yu, C.-W., Wu, K. & Zimmerli, L. Environmental history modulates *Arabidopsis* pattern-triggered immunity in a histone acetyl transferase1-dependent manner. *The Plant Cell* **26**, 2676-2688 (2014).
- [26] Slaughter, A., Daniel, X., Flors, V., Luna, E., Hohn, B. & Mauch-Mani, B. Descendants of primed *Arabidopsis* plants exhibit resistance to biotic stress. *Plant Physiology* **158**, 835-843 (2012).
- [27] Yoshikawa, M. Diverse modes of action of biotic and abiotic phytoalexin elicitors. *Nature* **275**, 546 (1978).

- [28] Farrell, K., Jahan, M. A. & Kovinich, N. Distinct mechanisms of biotic and chemical elicitors enable additive elicitation of the anticancer phytoalexin glyceollin I. *Molecules* **22**, 1261 (2017).
- [29] Aisyah, S., Gruppen, H., Madzora, B. & Vincken, J.-P. Modulation of isoflavonoid composition of *Rhizopus oryzae* elicited soybean (*Glycine max*) seedlings by light and wounding. *Journal of Agricultural and Food Chemistry* **61**, 8657-8667 (2013).
- [30] Feng, S., Saw, C. L., Lee, Y. K. & Huang, D. Fungal-stressed germination of black soybeans leads to generation of oxooctadecadienoic acids in addition to glyceollins. *Journal of Agricultural and Food Chemistry* **55**, 8589-8595 (2007).
- [31] Simons, R., Vincken, J.-P., Roidos, N., Bovee, T. F., van Iersel, M., Verbruggen, M. A. & Gruppen, H. Increasing soy isoflavonoid content and diversity by simultaneous malting and challenging by a fungus to modulate estrogenicity. *Journal of Agricultural and Food Chemistry* **59**, 6748-6758 (2011).
- [32] Sobolev, V. S., Neff, S. A. & Gloer, J. B. New stilbenoids from peanut (*Arachis hypogaea*) seeds challenged by an *Aspergillus caelatus* strain. *Journal of Agricultural and Food Chemistry* **57**, 62-68 (2008).
- [33] Hynes, R., Hill, J., Reddy, M. & Lazarovits, G. Phytoalexin production by wounded white bean (*Phaseolus vulgaris*) cotyledons and hypocotyls in response to inoculation with rhizobacteria. *Canadian Journal of Microbiology* **40**, 548-554 (1994).
- [34] Ramos-Solano, B., Algar, E., Garcia-Villaraco, A., Garcia-Cristobal, J., Lucas Garcia, J. A. & Gutierrez-Mañero, F. J. Biotic elicitation of isoflavone metabolism with plant growth promoting rhizobacteria in early stages of development in *Glycine max* var. Osumi. *Journal of Agricultural and Food chemistry* **58**, 1484-1492 (2010).
- [35] Dakora, F. & Phillips, D. Diverse functions of isoflavonoids in legumes transcend anti-microbial definitions of phytoalexins. *Physiological and Molecular Plant Pathology* **49**, 1-20 (1996).
- [36] Mañero, F. J. G., Algar, E., Martín Gómez, M. S., Saco Sierra, M. D. & Solano, B. R. Elicitation of secondary metabolism in *Hypericum perforatum* by rhizosphere bacteria and derived elicitors in seedlings and shoot cultures. *Pharmaceutical Biology* **50**, 1201-1209 (2012).
- [37] Berenbaum, M. R. The chemistry of defense: theory and practice. *Proceedings of the National Academy of Sciences* **92**, 2-8 (1995).
- [38] Ferrari, S. Biological elicitors of plant secondary metabolites: mode of action and use in the production of nutraceuticals in *Bio-Farms for Nutraceuticals*, 152-166 (Springer, 2010).
- [39] Kalli, S., Araya-Cloutier, C., Lin, Y., de Bruijn, W. J., Chapman, J. & Vincken, J.-P. Enhanced biosynthesis of the natural antimicrobial glyceollins in soybean seedlings by priming and elicitation. *Food Chemistry*, 126389 (2020).
- [40] Poulev, A., O'Neal, J. M., Logendra, S., Pouleva, R. B., Timeva, V., Garvey, A. S., Gleba, D., Jenkins, I. S., Halpern, B. T. & Kneer, R. Elicitation, a new window into plant chemodiversity and phytochemical drug discovery. *Journal of Medicinal Chemistry* **46**, 2542-2547 (2003).
- [41] Ghosh, A., Saha, I., Dolui, D., De, A. K., Sarkar, B. & Adak, M. K. Silver can induce oxidative stress in parallel to other chemical elicitors to modulate the ripening of Chili cultivars. *Plants* **9**, 238 (2020).
- [42] Thakur, M., Bhattacharya, S., Khosla, P. K. & Puri, S. Improving production of plant secondary metabolites through biotic and abiotic elicitation. *Journal of Applied Research on Medicinal and Aromatic Plants* **12**, 1-12 (2019).
- [43] Sukumaran, A., McDowell, T., Chen, L., Renaud, J. & Dhaubhadel, S. Isoflavonoid-specific prenyltransferase gene family in soybean: GmPT01, a pterocarpan 2-dimethylallyltransferase involved in glyceollin biosynthesis. *The Plant Journal* **96**, 966-981 (2018).

- [44] Degousee, N., Triantaphylidès, C. & Montillet, J.-L. Involvement of oxidative processes in the signaling mechanisms leading to the activation of glyceollin synthesis in soybean (*Glycine max*). *Plant Physiology* **104**, 945-952 (1994).
- [45] Graham, T. & Graham, M. Role of hypersensitive cell death in conditioning elicitation competency and defense potentiation. *Physiological and Molecular Plant Pathology* **55**, 13-20 (1999).
- [46] Nishimoto, M., Abe, S. & Yonezawa, T. Preparation of Ag nanoparticles using hydrogen peroxide as a reducing agent. *New Journal of Chemistry* **42**, 14493-14501 (2018).
- [47] Ghosh, B. & Ray, R. R. Current commercial perspective of *Rhizopus oryzae*: a review. *Journal of Applied Sciences* **11**, 2470-2486 (2011).
- [48] Partida-Martinez, L. P., Groth, I., Schmitt, I., Richter, W., Roth, M. & Hertweck, C. *Burkholderia rhizoxinica* sp. nov. and *Burkholderia endofungorum* sp. nov., bacterial endosymbionts of the plant-pathogenic fungus *Rhizopus microsporus*. *International Journal of Systematic and Evolutionary Microbiology* **57**, 2583-2590 (2007).
- [49] Nagórska, K., Bikowski, M. & Obuchowski, M. Multicellular behaviour and production of a wide variety of toxic substances support usage of *Bacillus subtilis* as a powerful biocontrol agent. *Acta Biochimica Polonica-English Edition* **54**, 495 (2007).
- [50] Roy, K., Kar, S. & Ambure, P. On a simple approach for determining applicability domain of QSAR models. *Chemometrics and Intelligent Laboratory Systems* **145**, 22-29 (2015).
- [51] Araya-Cloutier, C., den Besten, H. M., Aisyah, S., Gruppen, H. & Vincken, J.-P. The position of prenylation of isoflavonoids and stilbenoids from legumes (Fabaceae) modulates the antimicrobial activity against Gram positive pathogens. *Food Chemistry* **226**, 193-201 (2017).
- [52] Van De Schans, M. G., Vincken, J.-P., De Waard, P., Hamers, A. R., Bovee, T. F. & Gruppen, H. Glyceollins and dehydroglyceollins isolated from soybean act as SERMs and ER subtype-selective phytoestrogens. *The Journal of Steroid Biochemistry and Molecular Biology* **156**, 53-63 (2016).
- [53] Berg, G. Plant-microbe interactions promoting plant growth and health: perspectives for controlled use of microorganisms in agriculture. *Applied Microbiology and Biotechnology* **84**, 11-18 (2009).
- [54] González-Lamothe, R., Mitchell, G., Gattuso, M., Diarra, M., Malouin, F. & Bouarab, K. Plant antimicrobial agents and their effects on plant and human pathogens. *International journal of molecular sciences* **10**, 3400-3419 (2009).
- [55] Zou, H.-S., Chu, Z.-Q. & Gang, L. A novel recovery technology of trace precious metals from waste water by combining agglomeration and adsorption. *Transactions of Nonferrous Metals Society of China* **17**, 858-863 (2007).
- [56] Syed, S. Silver recovery aqueous techniques from diverse sources: Hydrometallurgy in recycling. *Waste Management* **50**, 234-256 (2016).
- [57] Simons, R., Vincken, J. P., Bakx, E. J., Verbruggen, M. A. & Gruppen, H. A rapid screening method for prenylated flavonoids with ultra-high-performance liquid chromatography/electrospray ionisation mass spectrometry in licorice root extracts. *Rapid Communications in Mass Spectrometry: An International Journal Devoted to the Rapid Dissemination of Up-to-the-Minute Research in Mass Spectrometry* **23**, 3083-3093 (2009).
- [58] Djeussi, D. E., Sandjo, L. P., Noumedem, J. A., Omosa, L. K., Ngadjui, B. T. & Kuete, V. Antibacterial activities of the methanol extracts and compounds from *Erythrina sismoidea* against Gram-negative multi-drug resistant phenotypes. *BMC Complementary and Alternative Medicine* **15**, 453 (2015).
- [59] Mbaveng, A. T., Sandjo, L. P., Tankeo, S. B., Ndifor, A. R., Pantaleon, A., Nagdjui, B. T. & Kuete, V. Antibacterial activity of nineteen selected natural products against multi-drug resistant Gram-negative phenotypes. *SpringerPlus* **4**, 823 (2015).

3.7. Supplementary information

3.7.1. Supplementary figures

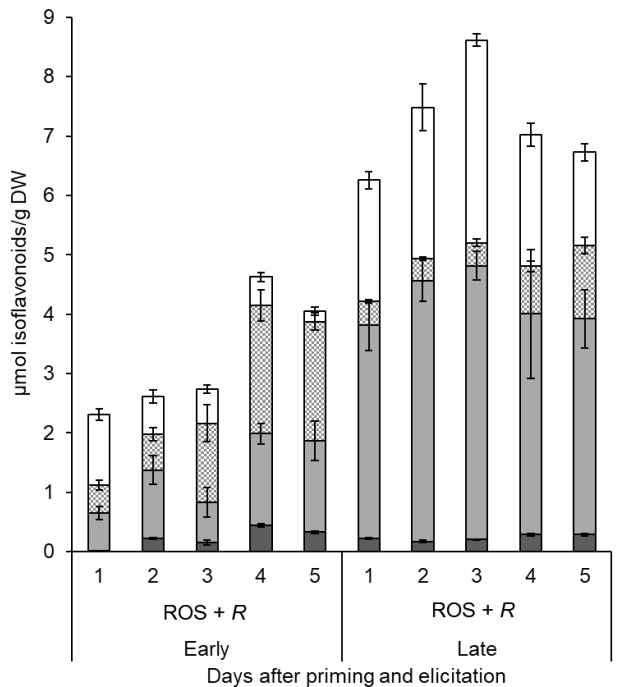


Figure S3.1. Isoflavonoid content ($\mu\text{mol/g DW}$) of “early” and “late” ROS + R- treated soybean seedlings over five days published earlier by Kalli *et al.* (2020) ^[1]. Isoflavonoids are classified into four main families, i.e. glycosylated isoflavonoids (white), non-prenylated aglycones (patterned), glyceollins (grey) and prenylated isoflavones (dark grey). Error bars indicate the standard deviation of three biological replicates.

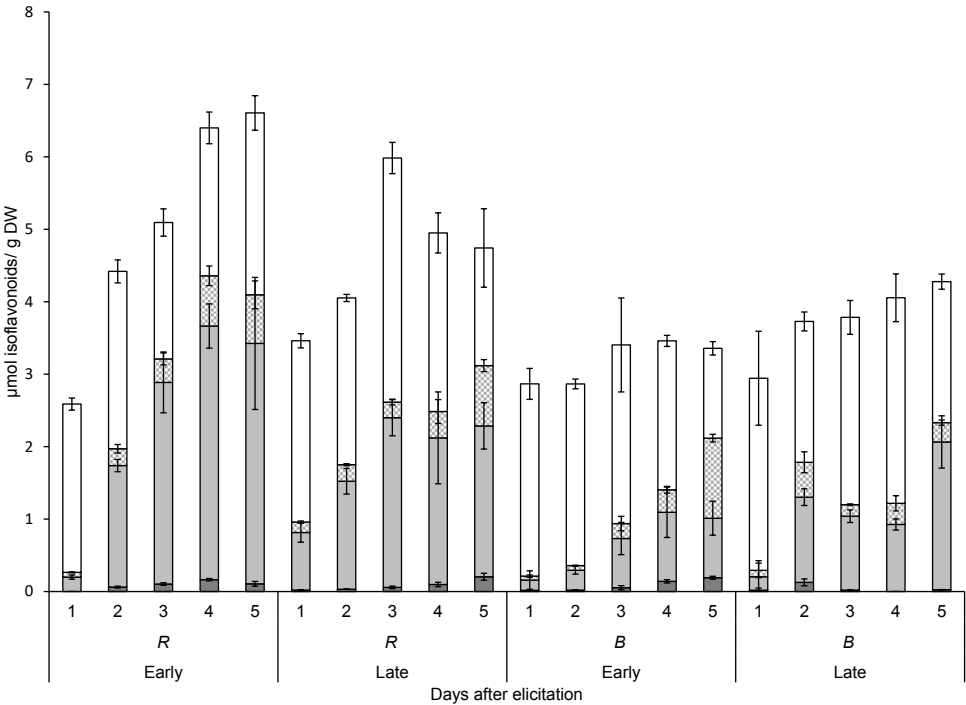


Figure S3.2. Isoflavonoid content ($\mu\text{mol/g DW}$) of “early” and “late” *R*- or *B*- elicited soybean seedlings over five days. Isoflavonoids are classified into four main families, i.e. glycosylated isoflavonoids (white), non-prenylated aglycones (patterned), glyceollins (grey) and prenylated isoflavones (dark grey). Error bars indicate the standard deviation of three biological replicates. Quantification of the individual isoflavonoids over-time per treatment can be found in Tables **S3.5-S3.7**. Statistical analysis (Tukey’s test, $p < 0.05$) of the over-time differences in each isoflavonoid subclass within the same treatment can be found in **Table S3.8**.

3.7.2. Supplementary tables

Table S3.1. Phenolic compounds tentatively annotated by RP-UHPLC-PDA-MS present in soybean seedling extracts. ^a Most abundant product ion is shown in **bold**. ^b Annotation of isoflavonoids was based on the annotation by Simons *et al.* (2009) ^[2], Aisyah *et al.* (2013) ^[3] and Araya-Cloutier *et al.* (2017) ^[4], while saponin annotation was based on Decroos *et al.* (2007) ^[5].

No.	RT (min)	λ_{\max} (nm)	[M-H] ⁻	MS ² NI product ion (relative abundance) ^a	[M+H] ⁺	MS ² PI product ion (relative abundance) ^a	Tentative annotation ^b	Subclass
1	4.55	260,310	415	253	417	255	Daidzin	Isoflavone
2	5.20	258	501	253	503	255	Malonyl-daidzin	Isoflavone
3	5.71	259,325	517	225 , 241(28), 269(11)	519	271 , 433(7)	Malonyl-genistin	Isoflavone
4	6.66	301,351	253	209 , 225(77), 253(28)	255	199 , 137(75), 227(60), 237(20)	Daidzein	Isoflavone
5	6.94	285	283	268 , 255(15)	285	270 , 225(12), 229(15)	Glycitein	Isoflavone
6	7.57	286	353	335 , 149(27), 161(3)	355	309 , 319(80), 188(42), 215(11)	Glyceofuran	Pterocarpan
7	8.02	260,342	269	225 , 201(74), 241(51), 269(9)	271	153 , 215(81), 243(76), 253(32)	Genistein	Isoflavone
8	10.11	285	339	161 , 324(53), 295(21), 270(12)	341	267	Glyceollidin II	Pterocarpan
9	10.94	290	337	319 , 293(62), 282(15), 149(86)	321	306 , 279(96), 293(62), 303(44)	Glyceollin III	Pterocarpan
10	11.22	283, 307,316	337	319 , 293(88), 282(64), 149(19)	321	279 , 251(85), 306(80)	Glyceollin II	Pterocarpan
11	11.35	283	337	319 , 149(82), 293(42)	321	303 , 306(80), 293(36)	Glyceollin I	Pterocarpan
12	11.58	268,310 ,350	321	265 , 266(30), 277(15), 252(8)	323	267 , 255(16)	Neobavaisoflavone	Isoflavone
13	11.80	260,306	321	266	323	267	6-prenyl daidzein	Isoflavone
14	12.44	295	1067.5	967 , 741(78), 1049(78), 879(72), 921(35), 583 (26), 651(24)	1069.5	n.d.	Soyasaponin β g	Saponin
15	12.67	306,342	335	280 , 291(6)	337	281	Phaseol	Coumestan
16	13.23	262	337	282 , 283(18), 293(5), 309(5), 322(2)	339	283 , 284(20)	Lupiwighteone	Isoflavone
17	13.33	262	337	281 , 293(48), 309(30)	339	283 , 271(18)	Isowighteone	Isoflavone
18	13.60	284	353	335 , 149(20)	337	281 , 269(65)	Glyceollin IV	Pterocarpan

Table S3.2. Quantification (in $\mu\text{mol/g DW}$) of individual non-prenylated isoflavonoids present in $\text{H}_2\text{O}_2 + \text{AgNO}_3$ -treated seedling extracts. <LOQ stands for below limit of quantification.

Time-point	Treatment	Day	Daidzin	6"-O-Malonyl/daidzin	6"-O-Malonyl/genistein	Daidzein	Glycitein	Genistein
Early	$(\text{H}_2\text{O}_2 + \text{AgNO}_3) + B$	1	0.161 \pm 0.030	0.799 \pm 0.181	0.348 \pm 0.104	0.292 \pm 0.073	0.020 \pm 0.003	0.231 \pm 0.055
		2	0.095 \pm 0.009	0.535 \pm 0.035	0.243 \pm 0.018	0.162 \pm 0.027	<LOQ	0.106 \pm 0.011
		3	0.113 \pm 0.022	0.380 \pm 0.049	0.226 \pm 0.016	0.195 \pm 0.027	0.012 \pm 0.002	0.134 \pm 0.014
		4	0.109 \pm 0.008	0.587 \pm 0.048	0.302 \pm 0.006	0.161 \pm 0.037	0.015 \pm 0.003	0.120 \pm 0.013
		5	0.104 \pm 0.033	0.370 \pm 0.025	0.217 \pm 0.012	0.266 \pm 0.098	0.017 \pm 0.002	0.185 \pm 0.059
Late	$(\text{H}_2\text{O}_2 + \text{AgNO}_3) + B$	1	0.121 \pm 0.029	0.557 \pm 0.093	0.283 \pm 0.039	0.303 \pm 0.011	0.026 \pm 0.007	0.131 \pm 0.030
		2	0.191 \pm 0.023	0.810 \pm 0.098	0.331 \pm 0.032	0.151 \pm 0.053	0.015 \pm 0.010	0.132 \pm 0.027
		3	0.290 \pm 0.008	0.969 \pm 0.061	0.300 \pm 0.012	0.019 \pm 0.003	0.152 \pm 0.017	0.117 \pm 0.043
		4	0.199 \pm 0.008	0.757 \pm 0.086	0.283 \pm 0.040	0.162 \pm 0.024	0.012 \pm 0.005	0.158 \pm 0.033
		5	0.235 \pm 0.012	0.781 \pm 0.107	0.309 \pm 0.072	0.245 \pm 0.016	0.025 \pm 0.003	0.204 \pm 0.014
Early	$(\text{H}_2\text{O}_2 + \text{AgNO}_3) + R$	1	0.102 \pm 0.015	0.565 \pm 0.067	0.227 \pm 0.026	0.206 \pm 0.014	0.027 \pm 0.005	0.141 \pm 0.017
		2	0.069 \pm 0.002	0.528 \pm 0.055	0.253 \pm 0.032	0.140 \pm 0.027	0.014 \pm 0.002	0.122 \pm 0.018
		3	0.063 \pm 0.006	0.576 \pm 0.032	0.275 \pm 0.018	0.068 \pm 0.040	0.007 \pm 0.005	0.205 \pm 0.091
		4	0.082 \pm 0.017	0.427 \pm 0.098	0.220 \pm 0.048	0.142 \pm 0.012	0.014 \pm 0.002	0.126 \pm 0.004
		5	0.074 \pm 0.025	0.182 \pm 0.019	0.128 \pm 0.005	0.220 \pm 0.063	0.021 \pm 0.002	0.150 \pm 0.064
Late	$(\text{H}_2\text{O}_2 + \text{AgNO}_3) + R$	1	0.124 \pm 0.020	0.570 \pm 0.064	0.294 \pm 0.012	0.234 \pm 0.034	0.021 \pm 0.002	0.133 \pm 0.013
		2	0.137 \pm 0.019	0.788 \pm 0.066	0.350 \pm 0.014	0.153 \pm 0.007	<LOQ	0.216 \pm 0.004
		3	0.173 \pm 0.029	0.900 \pm 0.107	0.332 \pm 0.034	0.141 \pm 0.032	0.018 \pm 0.002	0.204 \pm 0.009
		4	0.071 \pm 0.007	0.480 \pm 0.087	0.223 \pm 0.043	0.270 \pm 0.028	0.014 \pm 0.001	0.255 \pm 0.032
		5	0.112 \pm 0.082	0.407 \pm 0.094	0.178 \pm 0.044	0.021 \pm 0.008	<LOQ	0.053 \pm 0.024
Early	$\text{H}_2\text{O}_2 + \text{AgNO}_3$	1	0.111 \pm 0.009	0.565 \pm 0.031	0.254 \pm 0.016	0.429 \pm 0.058	0.034 \pm 0.002	0.229 \pm 0.016
		2	0.108 \pm 0.008	0.558 \pm 0.045	0.246 \pm 0.032	0.399 \pm 0.049	0.015 \pm 0.001	0.288 \pm 0.020
		3	0.073 \pm 0.019	0.486 \pm 0.067	0.218 \pm 0.050	0.368 \pm 0.050	0.006 \pm 0.008	0.247 \pm 0.021
		4	0.103 \pm 0.016	0.604 \pm 0.088	0.295 \pm 0.045	0.269 \pm 0.019	0.091 \pm 0.021	0.209 \pm 0.024
		5	0.070 \pm 0.005	0.444 \pm 0.020	0.208 \pm 0.010	0.143 \pm 0.003	<LOQ	<LOQ
Late	$\text{H}_2\text{O}_2 + \text{AgNO}_3$	1	0.102 \pm 0.005	0.496 \pm 0.018	0.291 \pm 0.012	0.340 \pm 0.031	0.090 \pm 0.004	0.249 \pm 0.010
		2	<LOQ	0.600 \pm 0.051	0.259 \pm 0.017	0.417 \pm 0.044	0.022 \pm 0.002	0.269 \pm 0.027
		3	<LOQ	0.732 \pm 0.054	0.283 \pm 0.008	0.281 \pm 0.037	0.026 \pm 0.002	0.215 \pm 0.015
		4	0.135 \pm 0.019	0.679 \pm 0.101	0.250 \pm 0.036	0.207 \pm 0.046	0.083 \pm 0.015	0.202 \pm 0.033
		5	0.134 \pm 0.009	0.618 \pm 0.034	0.247 \pm 0.018	0.150 \pm 0.011	0.015 \pm 0.002	0.166 \pm 0.016

Table S3.3. Quantification (in $\mu\text{mol/g DW}$) of individual prenylated pterocarpanes present in H_2O_2 + AgNO_3 -treated seedling extracts. <LOQ stands for below limit of quantification.

Time-point	Treatment	Day	Glyceollidin II	Glyceollin III	Glyceollin II	Glyceollin I	Glyceollin IV	Glyceofuran
Early	$(\text{H}_2\text{O}_2 + \text{AgNO}_3) + B$	1	<LOQ	0.069 \pm 0.014	0.136 \pm 0.007	0.354 \pm 0.082	<LOQ	<LOQ
		2	0.043 \pm 0.004	0.188 \pm 0.061	0.190 \pm 0.025	0.684 \pm 0.041	<LOQ	<LOQ
		3	0.027 \pm 0.020	0.322 \pm 0.019	0.192 \pm 0.032	0.564 \pm 0.109	0.043 \pm 0.003	<LOQ
		4	0.068 \pm 0.010	0.479 \pm 0.082	0.273 \pm 0.106	0.728 \pm 0.229	0.072 \pm 0.006	0.054 \pm 0.018
		5	0.075 \pm 0.050	0.392 \pm 0.086	0.205 \pm 0.046	0.487 \pm 0.060	0.086 \pm 0.034	0.051 \pm 0.028
Late	$(\text{H}_2\text{O}_2 + \text{AgNO}_3) + B$	1	0.046 \pm 0.008	0.165 \pm 0.037	0.128 \pm 0.002	0.582 \pm 0.085	<LOQ	0.008 \pm 0.012
		2	0.087 \pm 0.011	0.540 \pm 0.051	0.336 \pm 0.041	0.998 \pm 0.128	0.042 \pm 0.007	0.045 \pm 0.006
		3	0.217 \pm 0.042	1.217 \pm 0.156	0.605 \pm 0.103	1.652 \pm 0.154	0.095 \pm 0.018	<LOQ
		4	0.151 \pm 0.031	0.847 \pm 0.104	0.402 \pm 0.085	0.918 \pm 0.111	0.134 \pm 0.013	0.120 \pm 0.028
		5	0.132 \pm 0.045	0.988 \pm 0.055	0.442 \pm 0.081	0.955 \pm 0.108	0.134 \pm 0.070	<LOQ
Early	$(\text{H}_2\text{O}_2 + \text{AgNO}_3) + R$	1	<LOQ	0.070 \pm 0.004	0.049 \pm 0.006	0.371 \pm 0.071	<LOQ	<LOQ
		2	0.082 \pm 0.008	0.318 \pm 0.031	0.215 \pm 0.046	0.765 \pm 0.203	0.022 \pm 0.004	0.034 \pm 0.024
		3	0.044 \pm 0.062	0.710 \pm 0.094	0.497 \pm 0.067	1.727 \pm 0.152	0.047 \pm 0.009	<LOQ
		4	0.170 \pm 0.038	1.015 \pm 0.309	0.719 \pm 0.261	1.476 \pm 0.515	0.126 \pm 0.049	0.152 \pm 0.040
		5	0.085 \pm 0.040	0.672 \pm 0.165	0.353 \pm 0.082	0.840 \pm 0.152	<LOQ	<LOQ
Late	$(\text{H}_2\text{O}_2 + \text{AgNO}_3) + R$	1	0.476 \pm 0.069	0.420 \pm 0.061	0.225 \pm 0.042	1.106 \pm 0.137	<LOQ	0.022 \pm 0.017
		2	0.119 \pm 0.020	0.840 \pm 0.240	0.469 \pm 0.072	1.801 \pm 0.188	0.079 \pm 0.008	0.087 \pm 0.014
		3	0.274 \pm 0.045	1.131 \pm 0.067	0.562 \pm 0.064	1.535 \pm 0.076	0.105 \pm 0.011	0.177 \pm 0.015
		4	0.200 \pm 0.056	1.075 \pm 0.096	0.364 \pm 0.027	1.264 \pm 0.042	0.236 \pm 0.030	0.198 \pm 0.042
		5	0.792 \pm 0.160	0.188 \pm 0.038	1.150 \pm 0.138	0.504 \pm 0.105	1.375 \pm 0.365	<LOQ
Early	$\text{H}_2\text{O}_2 + \text{AgNO}_3$	1	<LOQ	<LOQ	<LOQ	0.104 \pm 0.013	<LOQ	<LOQ
		2	<LOQ	0.068 \pm 0.011	0.133 \pm 0.017	0.568 \pm 0.068	<LOQ	<LOQ
		3	0.083 \pm 0.018	0.106 \pm 0.006	0.262 \pm 0.006	1.025 \pm 0.044	<LOQ	<LOQ
		4	0.100 \pm 0.015	0.264 \pm 0.049	0.599 \pm 0.078	1.944 \pm 0.155	<LOQ	<LOQ
		5	<LOQ	0.251 \pm 0.029	0.601 \pm 0.035	1.700 \pm 0.049	<LOQ	<LOQ
Late	$\text{H}_2\text{O}_2 + \text{AgNO}_3$	1	<LOQ	0.031 \pm 0.006	0.036 \pm 0.003	0.254 \pm 0.025	<LOQ	<LOQ
		2	0.108 \pm 0.016	0.357 \pm 0.071	0.412 \pm 0.036	1.604 \pm 0.162	<LOQ	<LOQ
		3	0.156 \pm 0.027	0.615 \pm 0.108	0.705 \pm 0.047	2.043 \pm 0.095	<LOQ	<LOQ
		4	0.202 \pm 0.055	0.835 \pm 0.113	0.980 \pm 0.180	2.311 \pm 0.330	0.023 \pm 0.004	0.124 \pm 0.026
		5	0.207 \pm 0.027	0.842 \pm 0.127	0.947 \pm 0.055	1.996 \pm 0.061	0.029 \pm 0.001	0.104 \pm 0.014

Table S3.4. Quantification (in $\mu\text{mol/g DW}$) of individual prenylated isoflavones and phaseol present in H_2O_2 + AgNO_3 -treated seedling extracts. <LOQ stands for below limit of quantification.

Time-point	Treatment	Day	Neobavaisoflavone	6-prenyl daidzein	Lupiwighteone	Isowighteone	Phaseol
Early	$(\text{H}_2\text{O}_2 + \text{AgNO}_3) + B$	1	0.122 \pm 0.026	0.153 \pm 0.011	0.069 \pm 0.009	0.031 \pm 0.007	<LOQ
		2	0.102 \pm 0.014	0.260 \pm 0.034	0.029 \pm 0.004	0.010 \pm 0.001	<LOQ
		3	0.104 \pm 0.009	0.499 \pm 0.023	0.088 \pm 0.032	0.010 \pm 0.014	0.066 \pm 0.018
		4	0.113 \pm 0.011	0.523 \pm 0.054	0.176 \pm 0.013	0.030 \pm 0.009	0.163 \pm 0.007
		5	0.097 \pm 0.013	0.458 \pm 0.009	0.155 \pm 0.018	0.035 \pm 0.002	0.144 \pm 0.021
Late	$(\text{H}_2\text{O}_2 + \text{AgNO}_3) + B$	1	0.099 \pm 0.013	0.120 \pm 0.008	0.044 \pm 0.049	0.007 \pm 0.000	<LOQ
		2	0.154 \pm 0.035	0.397 \pm 0.030	0.103 \pm 0.018	0.033 \pm 0.007	0.093 \pm 0.017
		3	0.295 \pm 0.050	0.695 \pm 0.135	0.118 \pm 0.009	0.047 \pm 0.006	0.250 \pm 0.056
		4	0.191 \pm 0.042	0.625 \pm 0.095	0.151 \pm 0.024	0.042 \pm 0.004	0.319 \pm 0.021
		5	0.134 \pm 0.070	0.534 \pm 0.230	0.065 \pm 0.033	0.000 \pm 0.000	0.402 \pm 0.029
Early	$(\text{H}_2\text{O}_2 + \text{AgNO}_3) + R$	1	0.003 \pm 0.000	0.008 \pm 0.000	<LOQ	<LOQ	<LOQ
		2	0.135 \pm 0.047	0.302 \pm 0.049	0.030 \pm 0.008	0.012 \pm 0.008	0.018 \pm 0.005
		3	0.133 \pm 0.079	0.247 \pm 0.110	0.341 \pm 0.219	0.007 \pm 0.010	0.075 \pm 0.053
		4	0.169 \pm 0.054	0.490 \pm 0.112	0.114 \pm 0.016	0.031 \pm 0.026	0.249 \pm 0.096
		5	0.201 \pm 0.062	0.485 \pm 0.077	0.097 \pm 0.069	0.061 \pm 0.028	0.247 \pm 0.020
Late	$(\text{H}_2\text{O}_2 + \text{AgNO}_3) + R$	1	0.165 \pm 0.015	0.058 \pm 0.003	<LOQ	<LOQ	<LOQ
		2	0.253 \pm 0.011	0.511 \pm 0.019	0.036 \pm 0.002	0.016 \pm 0.001	0.022 \pm 0.003
		3	0.205 \pm 0.015	0.517 \pm 0.056	0.043 \pm 0.004	<LOQ	0.319 \pm 0.058
		4	0.193 \pm 0.038	0.359 \pm 0.032	0.035 \pm 0.001	0.019 \pm 0.002	0.171 \pm 0.012
		5	0.180 \pm 0.021	0.498 \pm 0.014	0.055 \pm 0.008	0.014 \pm 0.000	0.278 \pm 0.044
Early	$\text{H}_2\text{O}_2 + \text{AgNO}_3$	1	<LOQ	0.025 \pm 0.001	<LOQ	<LOQ	<LOQ
		2	0.031 \pm 0.005	0.069 \pm 0.006	0.019 \pm 0.002	<LOQ	<LOQ
		3	0.057 \pm 0.003	0.073 \pm 0.033	0.078 \pm 0.030	0.004 \pm 0.003	<LOQ
		4	0.086 \pm 0.020	0.227 \pm 0.049	<LOQ	<LOQ	<LOQ
		5	0.041 \pm 0.016	0.207 \pm 0.032	0.013 \pm 0.003	<LOQ	<LOQ
Late	$\text{H}_2\text{O}_2 + \text{AgNO}_3$	1	<LOQ	0.026 \pm 0.002	<LOQ	<LOQ	<LOQ
		2	0.072 \pm 0.003	0.083 \pm 0.006	0.030 \pm 0.003	<LOQ	<LOQ
		3	0.081 \pm 0.002	0.149 \pm 0.010	0.039 \pm 0.003	0.011 \pm 0.001	<LOQ
		4	0.094 \pm 0.036	0.233 \pm 0.041	0.011 \pm 0.001	<LOQ	<LOQ
		5	0.073 \pm 0.009	0.272 \pm 0.011	0.070 \pm 0.011	0.016 \pm 0.001	<LOQ

Table S3.5. Quantification (in $\mu\text{mol/g DW}$) of individual non-prenylated isoflavonoids present in microbially-treated seedling extracts. <LOQ stands for below limit of quantification. * Published by Kalli *et al.* (2020) [1].

Time-point	Treatment	Day	Daidzin	6"-O-Malonyldaidzin	6"-O-Malonylgenistin	Daidzein	Glycitein	Genistein
Early	R	1	0.300 \pm 0.015	1.514 \pm 0.067	0.470 \pm 0.048	0.055 \pm 0.006	<LOQ	0.011 \pm 0.003
		2	0.389 \pm 0.052	1.524 \pm 0.148	0.422 \pm 0.022	0.125 \pm 0.055	0.006 \pm 0.004	0.064 \pm 0.020
		3	0.218 \pm 0.023	1.251 \pm 0.183	0.379 \pm 0.046	0.206 \pm 0.066	0.013 \pm 0.003	0.106 \pm 0.050
		4	0.329 \pm 0.028	1.223 \pm 0.211	0.353 \pm 0.048	0.401 \pm 0.100	0.022 \pm 0.007	0.238 \pm 0.091
		5	0.363 \pm 0.020	1.557 \pm 0.208	0.537 \pm 0.113	0.438 \pm 0.169	0.028 \pm 0.014	0.205 \pm 0.090
Late	R	1	0.318 \pm 0.023	1.597 \pm 0.088	0.516 \pm 0.036	0.132 \pm 0.015	<LOQ	0.012 \pm 0.002
		2	0.286 \pm 0.012	1.454 \pm 0.036	0.490 \pm 0.030	0.176 \pm 0.014	<LOQ	0.027 \pm 0.004
		3	0.493 \pm 0.085	2.072 \pm 0.186	0.622 \pm 0.069	0.160 \pm 0.034	0.003 \pm 0.005	0.052 \pm 0.020
		4	0.428 \pm 0.044	1.448 \pm 0.265	0.453 \pm 0.065	0.237 \pm 0.140	0.010 \pm 0.007	0.116 \pm 0.087
		5	0.298 \pm 0.023	0.768 \pm 0.530	0.435 \pm 0.110	0.525 \pm 0.058	0.029 \pm 0.005	0.278 \pm 0.059
Early	B	1	0.355 \pm 0.042	1.715 \pm 0.197	0.514 \pm 0.071	0.090 \pm 0.128	<LOQ	<LOQ
		2	0.376 \pm 0.025	1.645 \pm 0.061	0.439 \pm 0.015	0.057 \pm 0.005	<LOQ	0.008 \pm 0.001
		3	0.403 \pm 0.101	1.581 \pm 0.642	0.446 \pm 0.088	0.157 \pm 0.094	0.003 \pm 0.004	0.046 \pm 0.032
		4	<LOQ	1.514 \pm 0.076	0.501 \pm 0.005	0.198 \pm 0.045	<LOQ	0.112 \pm 0.013
		5	0.300 \pm 0.059	0.652 \pm 0.070	0.250 \pm 0.014	0.742 \pm 0.032	0.035 \pm 0.008	0.328 \pm 0.041
Late	B	1	0.412 \pm 0.101	1.710 \pm 0.642	0.486 \pm 0.088	0.078 \pm 0.094	0.000 \pm 0.004	0.011 \pm 0.032
		2	0.354 \pm 0.019	1.056 \pm 0.117	0.441 \pm 0.054	0.376 \pm 0.041	0.007 \pm 0.010	0.098 \pm 0.139
		3	0.369 \pm 0.036	1.665 \pm 0.218	0.435 \pm 0.075	0.102 \pm 0.010	<LOQ	0.057 \pm 0.004
		4	0.424 \pm 0.069	1.772 \pm 0.316	0.567 \pm 0.061	0.237 \pm 0.102	0.005 \pm 0.006	0.039 \pm 0.021
		5	0.309 \pm 0.028	1.210 \pm 0.094	0.329 \pm 0.036	0.182 \pm 0.035	<LOQ	0.084 \pm 0.005
Late	ROS + R* Germination control	7	0.669 \pm 0.025	2.237 \pm 0.106	0.471 \pm 0.031	0.163 \pm 0.056	<LOQ	0.218 \pm 0.036
		1	0.408 \pm 0.054	1.880 \pm 0.216	0.511 \pm 0.050	0.157 \pm 0.094	<LOQ	0.046 \pm 0.032
		2	0.520 \pm 0.047	1.862 \pm 0.106	0.484 \pm 0.075	0.107 \pm 0.021	<LOQ	0.107 \pm 0.021
		3	0.471 \pm 0.063	1.532 \pm 0.142	0.412 \pm 0.047	0.132 \pm 0.024	<LOQ	0.040 \pm 0.013

Table S3.6. Quantification (in $\mu\text{mol/g DW}$) of individual prenylated pterocarpanes present in present in microbially-treated seedling extracts. <LOQ stands for below limit of quantification. * Published by Kalli *et al.* (2020) ^[1]. Glyceollin I is a C4-glyceollin, whereas glyceollidin II, glyceollin II-IV and glyceofuran are C2-glyceollins.

Time-point	Treatment	Day	Glyceollidin II	Glyceollin III	Glyceollin II	Glyceollin I	Glyceollin IV	Glyceofuran
Early	R	1	<LOQ	0.012 \pm 0.016	<LOQ	0.188 \pm 0.024	<LOQ	<LOQ
		2	0.033 \pm 0.023	0.206 \pm 0.015	0.129 \pm 0.008	1.309 \pm 0.080	<LOQ	<LOQ
		3	<LOQ	0.411 \pm 0.091	0.245 \pm 0.086	2.113 \pm 0.401	0.013 \pm 0.004	<LOQ
		4	0.071 \pm 0.034	0.539 \pm 0.057	0.344 \pm 0.123	2.510 \pm 0.271	0.035 \pm 0.004	<LOQ
		5	<LOQ	0.491 \pm 0.130	0.251 \pm 0.100	2.521 \pm 0.897	0.053 \pm 0.021	<LOQ
Late	R	1	<LOQ	0.070 \pm 0.017	0.025 \pm 0.018	0.699 \pm 0.132	<LOQ	<LOQ
		2	0.056 \pm 0.015	0.185 \pm 0.023	0.101 \pm 0.011	1.148 \pm 0.175	<LOQ	<LOQ
		3	0.064 \pm 0.045	0.344 \pm 0.103	0.231 \pm 0.035	1.666 \pm 0.217	0.019 \pm 0.027	0.018 \pm 0.025
		4	0.055 \pm 0.039	0.343 \pm 0.173	0.200 \pm 0.094	1.366 \pm 0.600	0.061 \pm 0.044	<LOQ
		5	0.030 \pm 0.022	0.327 \pm 0.125	0.218 \pm 0.073	1.456 \pm 0.282	0.051 \pm 0.037	<LOQ
Early	B	1	<LOQ	0.090 \pm 0.128	<LOQ	0.051 \pm 0.011	<LOQ	<LOQ
		2	0.050 \pm 0.007	<LOQ	<LOQ	0.224 \pm 0.053	<LOQ	<LOQ
		3	<LOQ	0.124 \pm 0.092	0.050 \pm 0.038	0.505 \pm 0.199	<LOQ	<LOQ
		4	<LOQ	0.213 \pm 0.119	0.093 \pm 0.066	0.647 \pm 0.320	<LOQ	<LOQ
		5	<LOQ	0.151 \pm 0.057	0.078 \pm 0.031	0.576 \pm 0.225	0.017 \pm 0.013	<LOQ
Late	B	1	0.030 \pm 0.000	0.000 \pm 0.092	0.000 \pm 0.038	0.155 \pm 0.199	<LOQ	<LOQ
		2	<LOQ	0.190 \pm 0.015	0.145 \pm 0.020	0.841 \pm 0.112	<LOQ	<LOQ
		3	0.057 \pm 0.005	0.067 \pm 0.005	0.134 \pm 0.020	0.762 \pm 0.084	<LOQ	<LOQ
		4	<LOQ	0.115 \pm 0.012	0.072 \pm 0.007	0.739 \pm 0.076	<LOQ	<LOQ
		5	0.115 \pm 0.013	0.216 \pm 0.025	0.379 \pm 0.114	1.260 \pm 0.341	<LOQ	0.069 \pm 0.013
Late	ROS + R*	7	0.090 \pm 0.025	0.965 \pm 0.090	0.446 \pm 0.060	2.963 \pm 0.218	0.149 \pm 0.025	<LOQ
	Germination control	1	<LOQ	<LOQ	<LOQ	0.038 \pm 0.025	<LOQ	<LOQ
		2	<LOQ	<LOQ	<LOQ	0.087 \pm 0.040	<LOQ	<LOQ
		3	<LOQ	<LOQ	0.030 \pm 0.007	0.202 \pm 0.113	<LOQ	<LOQ

Table S3.7. Quantification (in $\mu\text{mol/g DW}$) of individual prenylated isoflavones and phaseol present in microbially-treated seedling extracts. <LOQ stands for below limit of quantification. * Published by Kalli *et al.* (2020) [1].

Time-point	Treatment	Day	Neobavaisoflavone	6-prenyl daidzein	Lupiwighteone	Isoiwighteone	Phaseol
Early	R	1	<LOQ	<LOQ	<LOQ	<LOQ	<LOQ
		2	0.005 \pm 0.007	0.034 \pm 0.002	0.022 \pm 0.010	<LOQ	<LOQ
		3	0.017 \pm 0.012	0.023 \pm 0.008	0.064 \pm 0.009	<LOQ	<LOQ
		4	0.030 \pm 0.006	0.062 \pm 0.007	0.060 \pm 0.010	0.012 \pm 0.009	<LOQ
		5	0.029 \pm 0.021	0.064 \pm 0.024	0.014 \pm 0.006	<LOQ	<LOQ
Late	R	1	<LOQ	0.020 \pm 0.002	<LOQ	<LOQ	<LOQ
		2	<LOQ	0.032 \pm 0.003	<LOQ	<LOQ	<LOQ
		3	0.009 \pm 0.013	0.048 \pm 0.011	<LOQ	<LOQ	<LOQ
		4	0.019 \pm 0.013	0.057 \pm 0.013	0.016 \pm 0.023	0.005 \pm 0.007	<LOQ
		5	0.050 \pm 0.015	0.087 \pm 0.027	0.050 \pm 0.035	0.017 \pm 0.012	<LOQ
Early	B	1	<LOQ	0.017 \pm 0.001	<LOQ	<LOQ	<LOQ
		2	<LOQ	0.020 \pm 0.001	<LOQ	<LOQ	<LOQ
		3	0.007 \pm 0.010	0.046 \pm 0.027	<LOQ	<LOQ	<LOQ
		4	0.021 \pm 0.016	0.066 \pm 0.016	0.054 \pm 0.006	<LOQ	<LOQ
		5	0.047 \pm 0.014	0.072 \pm 0.011	0.052 \pm 0.008	0.020 \pm 0.006	<LOQ
Late	B	1	0.000 \pm 0.010	0.019 \pm 0.027	<LOQ	<LOQ	<LOQ
		2	0.017 \pm 0.024	0.028 \pm 0.039	0.075 \pm 0.002	0.007 \pm 0.010	<LOQ
		3	<LOQ	0.020 \pm 0.002	<LOQ	<LOQ	<LOQ
		4	<LOQ	<LOQ	<LOQ	<LOQ	<LOQ
		5	<LOQ	0.026 \pm 0.002	<LOQ	<LOQ	<LOQ
Late	ROS + R* Germination control	7	0.056 \pm 0.002	0.122 \pm 0.000	0.025 \pm 0.001	<LOQ	<LOQ
		1	<LOQ	<LOQ	<LOQ	<LOQ	<LOQ
		2	<LOQ	<LOQ	<LOQ	<LOQ	<LOQ
		3	<LOQ	<LOQ	<LOQ	<LOQ	<LOQ

Table S3.8. Statistical labelling of the different isoflavonoid families in time within the same treatment. Quantitative differences were assessed with Tukey's *post hoc* multiple comparison test ($p < 0.05$). Different letters are used to indicate significant differences in the isoflavonoid families over-time. a represents the lowest quantity and c the highest.

Time-point	Treatment	Day	Glycosylated isoflavonoids	Non-prenylated aglycone isoflavonoids	Glyceollins	Prenylated isoflavones	Phaseol
Early	(H ₂ O ₂ +AgNO ₃) + B	1	b	a	a	a	a
		2	ab	a	ab	a	a
		3	a	a	ab	b	ab
		4	ab	a	b	b	ab
		5	a	a	ab	b	b
Late	(H ₂ O ₂ +AgNO ₃) + B	1	a	b	a	a	a
		2	ab	a	b	ab	ab
		3	b	a	c	b	b
		4	ab	b	bc	b	bc
		5	ab	b	bc	ab	c
Early	(H ₂ O ₂ +AgNO ₃) + R	1	b	a	a	a	a
		2	b	ab	ab	b	a
		3	b	ab	bc	b	a
		4	b	ab	c	b	b
		5	a	b	ab	b	b
Late	(H ₂ O ₂ +AgNO ₃) + R	1	ab	a	a	a	a
		2	bc	a	ab	c	a
		3	c	a	b	bc	c
		4	a	ab	ab	b	b
		5	a	b	ab	bc	c
Early	H ₂ O ₂ +AgNO ₃	1	a	b	a	a	n.d
		2	a	b	a	ab	n.d
		3	a	b	c	bc	n.d
		4	a	b	d	d	n.d
		5	a	a	d	cd	n.d
Late	H ₂ O ₂ +AgNO ₃	1	a	b	a	a	n.d
		2	a	b	b	b	n.d
		3	a	bc	bc	bc	n.d
		4	a	ab	c	cd	n.d
		5	a	a	c	d	n.d

Table S3.8. Continued

Time-point	Treatment	Day	Glycosylated isoflavonoids	Non-prenylated aglycone isoflavonoids	Glyceollins	Prenylated isoflavones	Phaseol
Early	R	1	a	a	a	a	n.d
		2	a	ab	ab	ab	n.d
		3	a	b	b	bc	n.d
		4	a	b	b	c	n.d
		5	a	b	b	bc	n.d
Late	R	1	ab	a	a	a	n.d
		2	ab	a	a	a	n.d
		3	b	a	a	a	n.d
		4	ab	a	a	a	n.d
		5	ab	b	a	a	n.d
Early	B	1	ab	a	a	a	n.d
		2	ab	a	a	a	n.d
		3	ab	ab	a	a	n.d
		4	ab	ab	a	b	n.d
		5	ab	b	a	c	n.d
Late	B	1	a	a	a	a	n.d
		2	a	b	b	b	n.d
		3	a	ab	ab	a	n.d
		4	a	ab	ab	a	n.d
		5	a	ab	c	a	n.d

Table S3.9. Descriptors used for the calculation of the predicted antibacterial activity (pMIC, M) of 6-prenyl daidzein and phaseol against *L. monocytogenes* (Gram-positive) and *E. coli* (Gram-negative) using already developed QSAR models (Eq.3.2 and 3.3, section 3.2.2.6).

		6-Prenyl daidzein	Phaseol
<i>L. monocytogenes</i>	<i>KierA3</i>	3.11	2.39
	<i>rsynth</i>	0.67	0.32
	<i>vsurf_DD12</i>	0.50	1.00
	<i>vsurf_IW4</i>	1.59	1.38
	<i>vsurf_ID8</i>	0.85	0.79
	pMIC in M (MIC, μM)	4.67 (21 μ M)	3.97 (108 μ M)
<i>E. coli</i>	<i>bcount</i>	44.0	44.0
	<i>std_dim3</i>	0.90	0.79
	<i>vsurf_IW2</i>	1.41	1.33
	<i>rgyr</i>	4.51	4.16
	<i>vsurf_ID8</i>	0.85	0.79
	pMIC in M (MIC, μM)	4.55 (28 μ M)	4.16 (69 μ M)

3.7.3. Supplementary references

- [1] Kalli, S., Araya-Cloutier, C., Lin, Y., de Bruijn, W. J., Chapman, J. & Vincken, J.-P. Enhanced biosynthesis of the natural antimicrobial glyceollins in soybean seedlings by priming and elicitation. *Food Chemistry*, 126389 (2020).
- [2] Simons, R., Vincken, J. P., Bakx, E. J., Verbruggen, M. A. & Gruppen, H. A rapid screening method for prenylated flavonoids with ultra-high-performance liquid chromatography/electrospray ionisation mass spectrometry in licorice root extracts. *Rapid Communications in Mass Spectrometry: An International Journal Devoted to the Rapid Dissemination of Up-to-the-Minute Research in Mass Spectrometry* **23**, 3083-3093 (2009).
- [3] Aisyah, S., Gruppen, H., Madzora, B. & Vincken, J. -P. Modulation of isoflavonoid composition of *Rhizopus oryzae* elicited soybean (*Glycine max*) seedlings by light and wounding. *Journal of Agricultural and Food Chemistry* **61**, 8657-8667 (2013).
- [4] Araya-Cloutier, C., den Besten, H. M., Aisyah, S., Gruppen, H. & Vincken, J. -P. The position of prenylation of isoflavonoids and stilbenoids from legumes (*Fabaceae*) modulates the antimicrobial activity against Gram positive pathogens. *Food Chemistry* **226**, 193-201 (2017).
- [5] Decroos, K., Vincken, J. -P., Van Koningsveld, G. A., Gruppen, H. & Verstraete, W. Preparative chromatographic purification and surfactant properties of individual soyasaponins from soy hypocotyls. *Food Chemistry* **101**, 324-333 (2007).

Prenylated (iso)flavonoids as agents against methicillin-resistant *Staphylococcus aureus*

The high resistance towards currently used antibiotics has urged the development of new, natural therapeutics towards methicillin-resistant *Staphylococcus aureus* (MRSA). Prenylated (iso)flavonoids, present mainly in the Fabaceae, can serve as promising candidates. Herein, the anti-MRSA properties of 23 prenylated (iso)flavonoids were assessed *in-vitro* and *in-silico*. The di-prenylated (iso)flavonoids, glabrol (flavanone) and 6,8-diprenyl genistein (isoflavone), together with the mono-prenylated, 4'-*O*-methyl glabridin (isoflavan), were the most active anti-MRSA compounds (minimum inhibitory concentrations (MIC) $\leq 10 \mu\text{g/mL}$, $30 \mu\text{M}$). The in-house activity data was complemented with literature data to yield an extended, curated dataset of 67 molecules for the development of robust QSAR prediction models. A model with four descriptors was obtained, having a good fit (R^2_{adj} 0.61), low average prediction errors and a good predictive power (Q^2) for the training (4% and Q^2_{LOO} 0.57, respectively) and the test set (5% and Q^2_{test} 0.75, respectively). Furthermore, the model predicted well the activity of an external validation set of 10 compounds (on average 5% prediction errors). Our best QSAR model was additionally assessed for its capacity to predict the level of activity (low, moderate, high) of prenylated (iso)flavonoids been tested against other Gram-positive bacteria. The model classified correctly 73% of these compounds. Last, a pharmacophore model was constructed and predicted the anti-MRSA activity all (77) prenylated (iso)flavonoids with an accuracy of 65%. Based on the QSAR analysis and the pharmacophore results, prenylated (iso)flavonoids with fundamentally different molecular properties, such as acidic or highly hydrophobic, appeared equally effective anti-MRSA agents, suggesting potentially different mode of action.

Based on: Kalli, S.; Araya-Cloutier, C.; Hageman, J.; Vincken, J.-P. Prenylated (iso)flavonoids as agents against methicillin-resistant *Staphylococcus aureus* - Insights into the molecular properties underlying antibacterial activity. **Submitted for publication.**

4.1. Introduction

Staphylococcus aureus (SA) and its oxacillin-resistant form (methicillin-resistant, MRSA) is one of the leading causes of healthcare-associated infections worldwide ^[1]. Furthermore, MRSA has also emerged as a major cause of community-associated and livestock infections ^[2]. In the United States, even though hospital-associated MRSA infections decreased by 5.4% from 2013 to 2016, community-associated infections increased by 1.6% ^[3]. In Europe, MRSA is a public health concern for Southern and Eastern European countries, in particular ^[4]. The World Health Organization has referred to MRSA as a high priority pathogen for the development of new therapeutics ^[5]. Over the last 30 years, only a few antibiotics have been approved as anti-MRSA agents, but MRSA has already developed resistance towards them ^[6].

Novel chemical scaffolds with different modes of action to currently used antibiotics are constantly being investigated ^[7]. Prenylated flavonoids and isoflavonoids, collectively termed as (iso)flavonoids, as well as stilbenoids, have shown promising antibacterial activity against clinically-relevant pathogens, including MRSA ^[8,9]. Prenylated phenolic compounds are a class of secondary defence metabolites produced by species of the Fabaceae family upon (a)biotic stress ^[10]. Attachment of the prenyl moiety (3,3-dimethylallyl) to a phenolic skeleton is known to increase its antibacterial potency, due to the increased hydrophobicity conferred to the molecule ^[11].

Several efforts have been made in correlating essential structural features of prenylated (iso)flavonoids with their anti-MRSA activity. Clear structure-activity relationships (SARs) remain difficult to be established due to the extensive structural diversity of prenylated (iso)flavonoids. This chemical diversity stems mainly from the different (iso)flavonoid subclasses (21 known to date). (Iso)flavones, (iso)flavanones, isoflavans, pterocarpanes, pterocarpenes, 3-arylcoumarins, and 2-arylbenzofurans are some of the main (iso)flavonoid subclasses encountered in Fabaceae ^[10,12]. Chemical diversity increases further by the presence of substituents other than the prenyl group (hydroxyl, methoxyl), as well as the different configuration that the prenyl group can have (chain, pyran or furan). Therefore, SARs that apply to one subclass of prenylated (iso)flavonoids might not apply to another.

Methylation is one of the most common decorations of prenylated (iso)flavonoids. Methylation at the C7, for example, slightly reduces the anti-MRSA activity of prenylated isoflavones ^[13,14], has no effect on the activity of prenylated isoflavans, while it was shown detrimental for prenylated coumarins ^[13]. Chain prenylation seems more favourable than ring prenylation in prenylated isoflavones with respect to anti-MRSA activity ^[14-16]. In contrast, the ring-prenylated pterocarpan, phaseollin (MIC 78 μ M) is active, whereas its chain-prenylated analogue, phaseollidin has lower anti-MRSA activity (MIC 154 μ M) ^[16]. Prenylation at C6 of isoflavones ^[14] is better for anti-MRSA activity than C8-prenylation ^[13],

whereas the opposite seems to be preferred for flavanones ^[17], consistent with the results for other G⁺ bacteria ^[18].

Since prenylation-dependent hydrophobicity is not the only determinant of antibacterial activity, more systematic SARs are necessary to rationally portray how the overall molecular characteristics influence anti-MRSA activity. *In silico* tools, such as QSAR and pharmacophore modelling ^[19] can aid the elucidation of these molecular characteristics. Properties, such as shape (flexibility and globularity) and surface (hydrophilic/hydrophobic regions) of prenylated (iso)flavonoids, have been shown to contribute to their antibacterial activity against the Gram-positive, *Listeria monocytogenes* ^[18]. To date, the most systematic (Q)SAR study on the activity of (iso)flavonoids against SA or MRSA has been performed by Sadgrove *et al.* (2020) ^[20]. However, this study considered molecules only from *Erythrina* species (Fabaceae) including non-prenylated, prenylated, geranylated (iso)flavonoids and a chromen-4-one derivative. By using regression QSAR modelling, the importance of hydrogen-bonding, hydrophobicity, primary oxygens and charge distribution was highlighted in this study ^[20]. However, the importance of these molecular properties with respect to the mechanism of action of these compounds was not addressed.

In this study, a multiple linear regression model was developed from a curated dataset of 67 prenylated (iso)flavonoids from 9 subclasses tested only against MRSA by using a QSAR approach. The model was externally validated with an additional set of 10 prenylated (iso)flavonoids and further assessed for its capacity to predict the level of activity of prenylated (iso)flavonoids against other Gram-positive bacteria (including SA, *Staphylococcus epidermis*, *Bacillus subtilis*, *Enterococcus faecalis*, and *Streptococcus mutans*). In addition, a 3D pharmacophore model was developed to visualize the structural requirements for anti-MRSA activity. Both *in-silico* approaches were based on molecules from both in-house and literature activity data. For the in-house data, the activity (MIC values) of 23 prenylated compounds belonging to 6 subclasses was determined.

4.2. Materials and methods

4.2.1. Materials

Prenylated isoflavonoids (glabrene, 3'-hydroxy-4'-O-methyl-glabridin, 4'-O-methyl-glabridin, hispaglabridin A, hispaglabridin B, glyceofuran, glyceollidin II, glyceollin I, glyceollin II, glyceollin III, glyceollin IV, glyceollin V, dehydroglyceollidin II, dehydroglyceollin I, dehydroglyceollin II, dehydroglyceollin, III, dehydroglyceollin IV) and one prenylated flavanone (glabrol) were previously purified and chemically characterized ^[21,22]. Wighteone, lupiwighteone, luteone, 2,3-dehydrokieveitone, licoisoflavone A, neobavaisoflavone, iso-osajin and 6,8-diprenygenistein were purchased from Plantech UK (Reading, UK). Isowighteone and anhydrotuberosin were purchased from ChemFaces (Wuhan, Hubei, China). 6-Prenylnaringenin and ampicillin were purchased from Sigma Aldrich (St. Louis, MO,

USA). Psoralidin and 8-prenylnaringenin were purchased from Sanbio B.V. (Uden, the Netherlands). Glabridin was purchased from Wako (Osaka, Japan). Bacto brain heart infusion (BHI) broth was purchased from BD (Franklin Lakes, NJ, USA), tryptone soya broth (TSB) and bacteriological agar from Oxoid Ltd (Basingstoke, UK), and peptone physiological salt solution (PPS) from Tritium Microbiologie (Eindhoven, the Netherlands). Ethanol absolute (EtOH) was purchased from Biosolve (Valkenswaard, the Netherlands).

4.2.2. Methods

4.2.2.1. Antibacterial susceptibility assay

Different prenylated (iso)flavonoids were tested for their antibacterial activity against MRSA 18HN (strain kindly provided by RIVM, Bilthoven, The Netherlands). Bacteria were streaked from a $-80\text{ }^{\circ}\text{C}$ glycerol stock onto a BHI agar plate and incubated 24 h at $37\text{ }^{\circ}\text{C}$. Next, one colony was transferred to BHI broth (10 mL) and further incubated for 18 h at $37\text{ }^{\circ}\text{C}$. These overnight cultures were diluted with TSB (final inoculum concentration $3.8 \pm 0.4\text{ log CFU/mL}$). Stock solutions of the different prenylated compounds were prepared in aqueous EtOH (70% v/v) or DMSO and subsequently diluted with TSB. A series of concentrations were tested ranging from 3.1 to 100 or 150 $\mu\text{g/mL}$ (2.1% v/v solvent max.) of prenylated (iso)flavonoids. Equal volumes (100 μL) of bacteria and prenylated compound solutions in TSB were mixed into a 96-well plate. The 96-well plate was incubated in a SpectraMax M2e (Molecular Devices, Sunnyvale, CA, USA) at $37\text{ }^{\circ}\text{C}$ with constant linear shaking. The optical density (OD) at 600 nm was measured every 5 min for 24 h.

Positive control (vancomycin, 2 $\mu\text{g/mL}$), negative control (TSB suspension of bacteria with 2.5% (v/v) max. solvent) and blanks (compounds and TSB medium with no bacteria) were considered for optical comparison and sterility control. Inhibition of growth was assessed by measuring the time to detection (TTD), i.e. the time to reach a change in OD of 0.05 units. When no change in OD (i.e. $\Delta\text{OD} < 0.05$) was observed after the 24 h of incubation, cell viability was verified by plate counting. Briefly, 100 μL of the well with no change in OD was decimally diluted in PPS solution and 100 μL of each dilution was spread onto BHI agar plates. Plates were incubated for 24 h at $37\text{ }^{\circ}\text{C}$ and colonies were counted. The minimum inhibitory concentration (MIC) was defined as the lowest concentration of compound that resulted in a bacterial count equal or lower than that of the initial inoculum. The minimum bactericidal concentration (MBC) was defined as the lowest concentration of compound that resulted in $> 99\%$ bacterial inactivation from the initial bacterial inoculum. Prenylated compounds were tested in two independent biological reproductions, each performed in duplicate.

4.2.2.2. Inactivation kinetics

An overnight MRSA culture was diluted to 4.4 ± 0.5 Log (CFU/mL) and mixed with prenylated phenolics at their MIC and 2xMIC. Samples were incubated in duplicate at 37 °C/125 rpm. At different time points (0, 2, 4, 6, 24 h), 100 µL of culture medium were taken and decimally diluted in PPS. Dilutions were spread on BHI agar plates and incubated overnight at 37 °C, after which colonies were counted. Vancomycin and ampicillin at 2 µg/mL were used as control antibiotics.

4.2.2.3. QSAR modelling

Database construction. An outline of the different steps followed for the QSAR modelling is demonstrated in **Figure S4.1**. First, 106 prenylated (iso)flavonoids together with their anti-MRSA activity were mined from 19 different studies (2000-2017, **Table S4.1**). These studies were chosen under the premise that agar or broth (micro) dilution assays were used to determine the anti-MRSA activity. The activity data of prenylated (iso)flavonoids from 16 studies was combined with the activity data of the prenylated (iso)flavonoids generated in-house, to obtain a large dataset of 94 molecules with reported MIC values. The activity data from the 3 other, randomly chosen, studies [23-25] was used to externally validate the model [26]. The choice for the construction of this independent external validation set was based on whole studies, instead of various molecules from different studies to minimize extreme experimental variability. Compounds where no specific MIC value was obtained (i.e. MIC was higher than the highest tested concentration), were excluded from the QSAR modelling study. When more than one MRSA strain was tested and a range of MIC values was given, or more than one MIC value per compound was available, the highest MIC value was used to consider the worst-case scenario. Activity data [MIC values (µM)] was converted to pMIC [-log MIC (M)] (to improve the normality of the data distribution).

Dataset curation. A defined dataset of 77 prenylated (iso)flavonoids with established MICs was intended to enter the training/test phase. To ensure uniform chemical diversity upon the splitting of the modelling set, two selection criteria were applied for the compounds used for the QSAR modelling. First, (iso)flavonoids with common chain prenylation (i.e. 3,3-dimethylallyl) and ring prenylation (2"-isopropenylfuran and/or 2,2-dimethylpyran) were exclusively considered (**criterion 1**). Second, for each subgroup of mono- and di-prenylated compounds (in each subclass) two representative compounds had to be present, otherwise the subgroup was excluded (**criterion 2**). After these two selection criteria were applied, the modelling set of 70 complying compounds was split into a training set (80%, for model development) and test set (20%, for model selection based on model's predictive power on the test set) [26] using the Kennard-Stone algorithm from the R-package prospectr (using principal components and retaining 95% explained variance) [27]. This procedure selects the best chemically representative

subset as a training set, avoiding overoptimistic splitting which might occur during random splitting [28].

Model development and validation. A genetic algorithm (GA) was used to select a small subset of descriptors best able to predict the antibacterial activity (pMIC). pMIC activity was modelled using multiple linear regression (MLR) using the selected descriptors. Model accuracy for a given set of predictors was determined by a leave-one-out cross validation (LOOCV) procedure and calculated as Q^2_{LOO} . To exclude lucky or unlucky GA runs, every run was repeated 12 times with different starting seeds. Combinations of predictors with a Variance Inflation Factor (VIF) > 5, indicating a strong inter-correlation, were effectively removed from the GA population by penalizing the fit during the GA run. GA parameters were optimised using a full factorial experimental design and were found to be population size=150, cross-over rate=0.6, mutation rate=0.3. The maximum number of iterations was set to 200 and elitism set to 8. The number of predictors to be selected during a GA run was fixed and varied between 2 and 7.

The applicability domain (AD) of the models was calculated by means of the William's plot. If the first GA run indicates the presence of outliers with high leverage then all outliers (including high residual outliers) are removed from the dataset and the GA is repeated until no high leverage outliers are detected. High leverage molecules are poorly fitting, highly impactful molecules that force the GA to accommodate them in the model, having great impact on its performance [29]. In our study, after the first GA-run, two molecules, glyceollin I (**87**) and glyceollin III (**89**) (**Table S4.1**) were flagged as high leverage molecules. Erysubin F (**55**) was highlighted as a high residual outlier. Erysubin F is reported to have an outstandingly low activity (MIC 100 $\mu\text{g/mL}$) for a double prenylated isoflavone [30]. All three molecules were removed from the dataset, the GA-MLR procedure was repeated once more and a new AD (AD') was defined. The final dataset used for the development and selection of the best QSAR model comprised 67 prenylated (iso)flavonoids from 9 different (iso)flavonoid subclasses: 2-arylbenzofurans, 3-arylcoumarins, flavanones, isoflavans, isoflavanones, isoflavenes, isoflavones, pterocarpanes and pterocarpenes.

Several internal and external statistical parameters which are typically used to assess the statistical performance of the models were calculated. Some of the internal ones include: the significance of the models and the descriptors individually ($p\text{-value} < 0.05$), the coefficient of determination, R^2 , and the adjusted R^2 (R^2_{adj}) which corrects for the difference in the number of descriptors, and the leave-one-out cross-validation coefficient of determination (Q^2_{LOO}) which is used to assess the model's internal predictivity. According to Tropsha *et al.* (2010), the R^2 and Q^2_{LOO} should be > 0.6 and > 0.5, respectively [31]. Furthermore, the maximum variance inflation factor (VIF_{max}), which indicates potential inter-correlation of the descriptors in the generated models, should preferably be < 5 [32]. The accuracy of the prediction of the test set was assessed by calculating the Q^2 for the test set

(Q^2_{test}) according to Consonni *et al.* (2009), a calculation based on the number of training objects [33]. For both sets, the % of prediction error was calculated with the following formula: $(\text{pMIC}_{\text{observed}} - \text{pMIC}_{\text{predicted}}) / \text{pMIC}_{\text{observed}} * 100$. Last, the best QSAR model was further validated with the external validation set; an independent set of 10 compounds with established MICs which were verified to belong to the applicability domain of the selected model (AD'). Since the external validation set is completely independent from the training and the test set, model's accuracy was assessed only by determining the prediction errors of this set. A threshold of 10% average prediction error was considered acceptable, which corresponds to maximum one 2-fold dilution difference between predicted and experimental values [34,35]. An average prediction error of 10% is also generally acceptable for the training set [36].

Prediction of activity of prenylated (iso)flavonoids against other Gram-positive bacteria. The best QSAR model for MRSA was also used to predict the level of activity (low, moderate, high) of prenylated (iso)flavonoids tested against other Gram-positive bacteria. Thus, the antibacterial activity of 71 prenylated (iso)flavonoids tested against other Gram-positive bacteria was mined from literature (studies from 1988-2020). The compounds were gathered under the premise that they fall within the applicability domain of our QSAR-MRSA model. Furthermore, only compounds from the same subclasses as the ones used to construct the QSAR-MRSA were used, to avoid extreme extrapolation of the model. When the compounds were tested against different Gram-positive bacteria or when more than one MIC was available per compound, then the highest MIC was taken into account to consider the worst-case scenario.

The quality of prediction was assessed by verifying that the compounds were still classified as active ($\text{MIC} \leq 25 \mu\text{g/mL}$), moderately active ($25 < \text{MIC} < 100 \mu\text{g/mL}$) or inactive ($\text{MIC} \geq 100 \mu\text{g/mL}$) after the prediction [37]. Based on the nature of the MIC determination method (agar or broth dilution assays), misclassified compounds for which their predicted activity differed from their experimentally measured activity by one two-fold dilution (acceptable experimental error in dilution assays [34,35]), were considered as correctly predicted.

4.2.2.4. Pharmacophore modelling

A pharmacophore model was built using the pharmacophore elucidation query module of MOE. Since no definite target site of these compounds is known, a ligand-based pharmacophore methodology was employed. This is performed by aligning the different active ligands and determining the essential common chemical queries necessary for activity. All 77 compounds (curated training, test and external validation set) were used to extract the pharmacophore features. An activity threshold of $\text{pMIC} \geq 4.1$ ($\text{MIC} \leq 25 \mu\text{g/mL}$) was set to distinguish the active from the moderate/inactive antibacterials. The quality of the model was assessed based on its capacity to discriminate the active from the moderately active or inactive molecules. The **overall accuracy** refers to the percentage of correct

predictions, including both actives and inactive molecules. The **positive accuracy** (sensitivity) refers to the proportion of correctly predicted actives, indicating the sensitivity of the model. The **negative accuracy** (specificity) is calculated based on the percentage of correctly predicted inactives showing the specificity of the model.

4.3. Results

4.3.1. Experimental anti-MRSA activity of prenylated (iso)flavonoids

Table 4.1 shows the antibacterial potency of prenylated (iso)flavonoids against MRSA 18HN. The classification of the compounds with respect to their anti-MRSA activity was based on literature of antimicrobial phytochemicals ^[37]. Compounds with MIC values ≤ 25 $\mu\text{g/mL}$ were considered active, with most active being the ones having a MIC of ≤ 10 $\mu\text{g/mL}$. Compounds with MIC values between 25 and 100 $\mu\text{g/mL}$ were considered moderately active, whereas those with MIC values ≥ 100 $\mu\text{g/mL}$ were classified as inactive. The most active compounds experimentally tested in this study were the isoflavone, 6,8-diprenylgenistein (**50**) and the di-prenylated flavanone, glabrol (**13**) which showed a MIC of 9 $\mu\text{g/mL}$, corresponding to 23 μM and 24 μM , respectively. These compounds share double chain prenylation in their backbones (**Figure S4.2**). The most active mono-prenylated compound was the ring-prenylated isoflavan, 4'-O-methylglabridin (**17**) with a MIC of 10 $\mu\text{g/mL}$ (30 μM). Inactive prenylated (iso)flavonoids with an established MIC tested were glyceollins I-III (**87-89**) (> 100 $\mu\text{g/mL}$, > 296 μM). The mono-prenylated compounds (**51, 63, 68, 76, 85, 91, 101**) and the di-prenylated hispaglabridin B (**26**) had negligible antibacterial activity against MRSA (TTD similar to that of the control at 100 $\mu\text{g/mL}$, therefore MIC $>> 100$ $\mu\text{g/mL}$) (**Table S4.1**).

Table 4.1. Minimum inhibitory concentration (MIC) and minimum bactericidal concentration (MBC) of prenylated (iso)flavonoids tested in this study against MRSA 18HN.

Subclass	Name	MIC μg/mL [μM]	MBC μg/mL [μM]
Flavanones	6-Prenylnaringenin (12)	38 [110]	44 [129]
	Glabrol (13)	9 [24]	19 [48]
	Sophoraflavanone B (14)	22 [64]	25 [73]
Isoflavans	3'-OH-4'-O-Methylglabridin (16)	16 [44]	26 [73]
	4'-O-Methylglabridin (17)	10 [30]	23 [66]
	Glabridin (22)	13 [39]	19 [58]
	Hispaglabridin A (25)	44 [111]	44 [111]
Isoflavones	6,8-Diprenylgenistein (50)	9 [23]	16 [38]
	Isowighteone (64)	22 [65]	34 [102]
	Licoisoflavone A (65)	25 [71]	50 [141]
	Luteone (69)	25 [71]	44 [123]
	Neobavaisoflavone (70)	38 [116]	50 [155]
	Wighteone (74)	16 [46]	22 [65]
Isoflavene	Glabrene (49)	25 [78]	44 [136]
Pterocarpanes	Glyceollidin II (86)	44 [129]	44 [129]
	Glyceollin I (87)	100 [296]	n.a.
	Glyceollin II (88)	150 [443]	n.a.
	Glyceollin III (89)	100 [296]	n.a.
	Glyceollin IV (90)	44 [123]	75 [212]
Pterocarpenes	Dehydroglyceollidin II (98)	22 [68]	22 [68]
	Dehydroglyceollin I (99)	16 [49]	22 [68]
	Dehydroglyceollin II (100)	19 [59]	19 [59]
	Dehydroglyceollin IV (102)	44 [130]	50 [149]

Figure 4.1 shows the inactivation kinetics of MRSA 18HN in the presence of the top three antibacterial prenylated (iso)flavonoids tested in this study. The di-prenylated (iso)flavonoids, 6,8-diprenylgenistein (**50**) and glabrol (**13**) inactivated MRSA by > 99% in the first 2 h of contact at 2 x their MIC, whereas the mono-prenylated isoflavan, 4'-O-methyl-glabridin (**17**) inactivated MRSA after 6 h also at 2 x its MIC. The control antibiotic vancomycin at its MIC decreased the initial inoculum by > 99% only after 24 h. The slow action of vancomycin against MRSA is in line with what has been shown before for MRSA and *Streptococcus pneumoniae* [38,39].

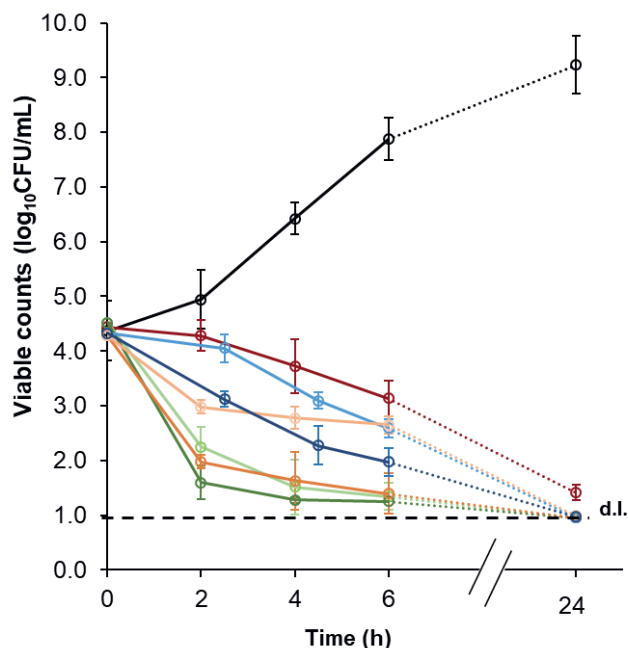


Figure 4.1. MRSA 18HN inactivation kinetics in the presence of the three most antibacterial prenylated (iso)flavonoids tested in this study, at their MIC (light shade) and 2xMIC (dark shade). Control (black), vancomycin (2 $\mu\text{g/mL}$, red), 4'-O-methylglabridin (**17**) (blue), glabrol (**13**) (orange) and 6,8-diprenylgenistein (**50**) (green).

4.3.2. Extended prenylated (iso)flavonoid dataset for QSAR modelling of anti-MRSA activity

A QSAR study was performed to pinpoint overall molecular properties contributing to the anti-MRSA activity. To construct robust and reliable QSAR models, the experimental data shown above was combined with literature data to enlarge and diversify our collection of prenylated (iso)flavonoids. In total, 76 prenylated (iso)flavonoids with established MICs from 10 subclasses were collected (**Table S4.1**). This diverse set of compounds was curated (see criteria 1 and 2, in **Dataset construction**), which resulted in 70 molecules in the modelling set (**Figure S4.1**). During the training phase, genetic algorithm (GA) flagged glyceollin I (**87**), glyceollin III (**89**) and erysubin F (**55**) as outliers. Thus, QSAR modelling was performed based on a curated modelling set 67 of molecules from 9 subclasses. The best model was further externally validated with a set of 10 molecules from three studies independent from those used in the modelling set ^[26].

Similar to what was observed for our in-house data, more than 90% of the double prenylated (iso)flavonoids compiled from literature, showed a high anti-MRSA activity ($\text{MIC} \leq 25 \mu\text{g/mL}$, 8-64 μM), whereas half of the mono-prenylated

ones were active. Among the most powerful anti-MRSA agents from literature data (**2**, **20**, **31**, **32**, **50**, **62**, **67**, **78**, **93**, **104** and **106**, **Table S4.1**) ($\text{MIC} \leq 10 \mu\text{g/mL}$, 8-23 μM), only orientanol B (**93**) is mono-prenylated. This molecule showed comparable activity to the in-house tested mono-prenylated isoflavan, 4'-O-methyl-glabridin (**17**). Both compounds are prenylated on the A-ring and possess the same type and amount of substituents, yet in different positions over the backbone (**Figure S4.2**). Structures of representative active anti-MRSA agents per isoflavonoid subclass derived from the extended dataset can be found in **Figure S4.3**.

4.3.3. QSAR model development, selection and external validation

The best GA-MLR-models obtained per number of descriptors and their statistical performance are listed in **Table 4.2**.

Models with four or more descriptors complied with the thresholds of all validation parameters of the QSAR models, whereas models with less descriptors (2-3) gave relatively poor adjusted R^2 's (R^2_{adj}). Usually, a higher number of descriptors results in over-fitted/more complex, less interpretable models (**Table 4.2**). Thus, we chose the four-descriptor model as the best, since it balances well statistical validity, predictivity of the training (Q^2_{LOO} 0.57 and average prediction error of 4%, **Table S4.1**) and the test set (Q^2_{test} 0.75 and average prediction error of 5%, **Table S4.1**) (**Figure 4.2**) and model's interpretability. The model was also externally validated by predicting an independent set of 10 compounds (**1**, **19**, **28-30**, **36**, **37**, **44**, **46**, **47**) coming from three studies [23-25] and low average prediction errors (5%) were obtained (**Table S4.1** and **Figure 4.2**). The applicability domain of the best 4-descriptor model can be found in **Figure S4.4**.

In the chosen four-descriptor model, the hydrophobic volume at the 4th energetic level, i.e. -0.8 kcal/mol (*vsurf_D4*) was the most significant descriptor (p -value 2e^{-10}), followed by the sum of hydrogen bond donor strengths of carbon atoms (*h_emd_C*, p -value 2e^{-4}). In addition, the unbalance between the centre of mass of a molecule and the position of the hydrophilic regions around it (*vsurf_IW7*) and the van der Waals interaction energy (*E_vdw*) were the least significantly correlated descriptors (p -value 6e^{-3}). Definitions of the descriptors can be found in **Tables S4.2**.

Table 4.2. Best GA-MLR models for predicting the antibacterial activity of prenylated (iso)flavonoids against MRSA. n: number of descriptors; R²: coefficient of determination (> 0.6) [31]; R²_{adj}: adjusted R²; Q²_{1,00}: leave-one-out cross-validated coefficient of determination (> 0.5) [31]; Q²_{Test}: correlation coefficient for the test set. All models were significant (*p*-values < 1.0e-7) and no multicollinearity of descriptors was observed (VIF_{max} < 3.2) [32].

n	Equation	R ²	R ² _{adj}	Q ² _{1,00}	Q ² _{Test}
2	$y = 2.79 - 0.16 * h_emd_C + 0.01 * vsurf_D4$	0.56	0.54	0.51	0.73
3	$y = 1.88 - 0.70 * h_pavgQ + 0.01 * vsurf_D4 - 0.05 * vsurf_IW7$	0.60	0.57	0.53	0.78
4	$y = 2.55 - 0.18 * h_emd_C + 0.01 * vsurf_D4 - 0.05 * vsurf_IW7 - 0.05 * E_vdw$	0.64	0.61	0.57	0.75
5	$y = 6.45 + 0.03 * PEOE_VSA_PPOS - 2.23 * vsurf_CW3 - 0.02 * vsurf_IW7 - 1.24 * h_pavgQ + 0.01 * PEOE_VSA + 2$	0.68	0.64	0.60	0.64
6	$y = 6.20 + PEOE_VSA_PPOS - 2.56 * vsurf_CW3 - 0.06 * vsurf_IW7 - 0.89 * h_pavgQ + 0.01 * PEOE_VSA + 2 + 0.03 * vsurf_DD12$	0.69	0.65	0.61	0.65
7	$y = 3.53 + 0.03 * PEOE_VSA_PPOS - 2.70 * vsurf_CW3 - 0.08 * vsurf_IW7 - 0.88 * h_pavgQ + 0.02 * PEOE_VSA + 2 + 0.03 * vsurf_DD12 - 0.31 * PM3_IP$	0.71	0.67	0.60	0.67

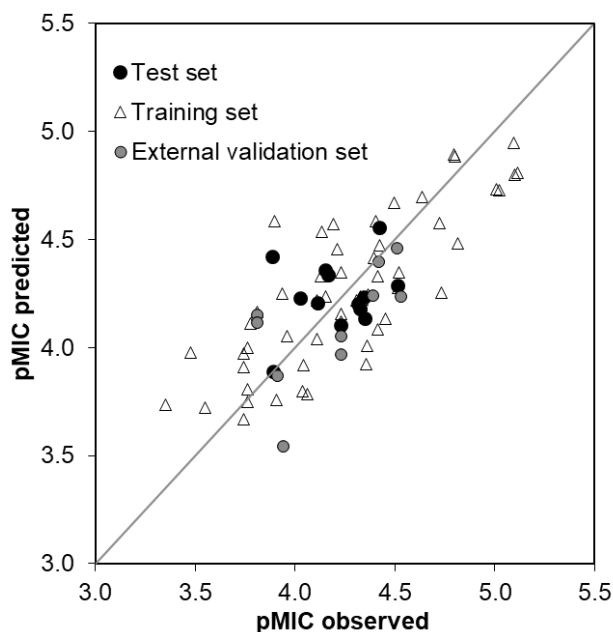


Figure 4.2. Correlation of the experimental and predicted anti-MRSA activity (pMIC, M) of prenylated (iso)flavonoids by using our best 4-descriptor QSAR model for the training, the test and the external validation sets. The applicability domain of the QSAR model can be found in Figure S4.4.

4.3.4. Predicting the level of antibacterial activity of prenylated (iso)flavonoids against other Gram-positive bacteria

The QSAR model developed for MRSA was additionally assessed for its capacity to predict the level of activity (low, moderate, high) of prenylated (iso)flavonoids tested against other Gram-positive bacteria (**Table S4.3**). Thus, activity data (MIC values) of 71 prenylated (iso)flavonoids tested against SA, *Staphylococcus epidermis*, *Bacillus subtilis*, *Enterococcus faecalis* and *Streptococcus mutans* was collected (**Table S4.3** and **Figure S4.5**). The model predicted correctly the level of activity of 73% of the compounds (**Figure S4.6**). This shows that the model is robust enough to be used as a tool for quick screening for potent antibacterial prenylated (iso)flavonoids. Half of the incorrectly predicted molecules were flavanones (**Table S4.3** and **Figure S4.5**), possibly due to the limited structural variation of flavanones in the training and test set (**Table S4.1**) used to develop the model.

4.3.5. Interpretation of most frequently used descriptors in statistically compliant models

To obtain a deeper insight into the molecular properties essential for activity, we analysed the most frequently used descriptors, i.e. present in more than 40% of the statistically compliant models ($R^2_{\text{adj}} > 0.6$ and $Q^2_{\text{LOO}} > 0.5$)^[31] (**Figure 4.3**).

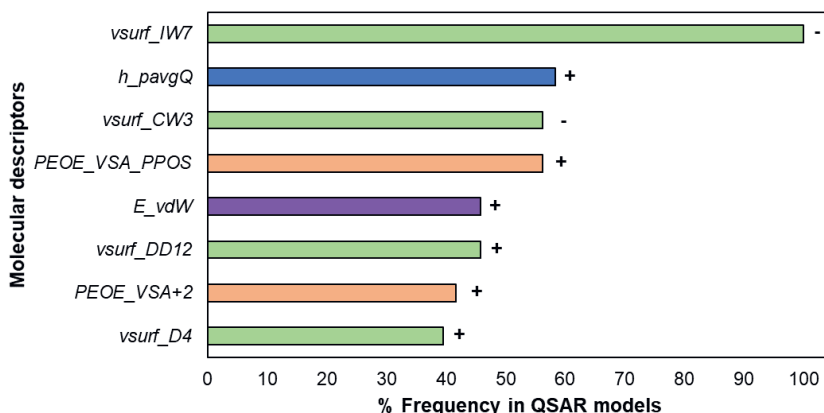


Figure 4.3. Descriptors most frequently selected by the GA to predict the anti-MRSA activity. The positive (+) or negative (-) correlation of each descriptor with anti-MRSA activity is shown next to the bars. Colour coding is used to indicate the different descriptor families. Green indicates the surface area, volume and shape (*vsurf*) descriptors, blue indicates the Hückel-theory (*h*) descriptor, orange represents the partial charge descriptors (*PEOE_VSA*) and purple is used to indicate the energy descriptor. Definitions of the descriptors can be found in **Table S4.2**.

4.3.5.1. Hydrophobic volume and balanced hydrophilic fraction favour anti-MRSA activity

The most frequently used descriptor family included the surface area, volume and shape descriptors, *vsurf* (green colour in **Figure 4.3**). These descriptors were calculated on multiple energetic levels, as volume and shape are influenced by the energy of the molecules^[40].

The descriptor *vsurf_IW7* was present in all statistically compliant models. It represents the hydrophilic integrity moment at -5.0 kcal/mol, an energy level known to be representative for polar and H-bond donor and acceptor regions^[40]. It measures the unbalance between the centre of mass of a molecule and the position of the hydrophilic regions around it. Its negative correlation to the anti-MRSA activity suggests that the polar regions close to the centre of mass or balanced at opposite directions in the molecule favour the activity^[41].

The descriptor *vsurf_CW3* quantifies the ratio between the hydrophilic surface and the total molecular surface^[40] and was one of the most strongly correlated descriptors (4.7e^{-13} - 4.1e^{-09} , **Table S4.4**). Its negative contribution to the anti-MRSA activity indicates that a small hydrophilic fraction favours anti-MRSA activity.

All molecules with $vsurf_CW3$ of $< 1.043 \text{ \AA}^3$ possessed high activity (except dehydroglyceollin IV (**102**) and hispaglabridin A (**25**)).

The $vsurf_DD12$ descriptor quantifies the contact distance of lowest and the 2nd lowest hydrophobic energy points of a molecule. Its positive, although weak contribution to activity (p -value, $4.7e^{-02}$ - $1.5e^{-01}$, **Table S4.4**) implies that the hydrophobically interacting groups or regions should be far away from each other and not localized closely together in the molecule ^[42].

Last, the $vsurf_D4$ descriptor is a measure of the hydrophobic volume at an energy level of -0.8 kcal/mol (known to account for polarizability and dispersion forces) ^[40]. This descriptor was positively correlated to activity indicating that larger hydrophobic surfaces are preferred.

4.3.5.2. (Partial) charges favour anti-MRSA activity of prenylated (iso)flavonoids

Formal positive charge. The second most frequently used, positively correlated descriptor in the QSAR models was the Hückel theory descriptor, h_pavgQ (blue colour in **Figure 4.3**). Hückel theory descriptors take into account local resonance and electron withdrawing effects ^[43]. This descriptor refers to the average total (formal) charge sum across protonation states at pH 7 ^[44], calculated based on the relative concentration of various protonation states of the molecule ^[45]. Isoflavones, (iso)flavanones and 3-aryl coumarins had generally higher values for this descriptor. Possibly, the presence of the carbonyl group on the C-ring of these subclasses enhances the acidity of hydroxyl protons (at C7 and C5) due to stabilization of the negative charge by resonance. In contrast, pterocarpanes, pterocarpenes and isoflavans, lacking this carbonyl group, had low h_pavgQ values. Examples of the correlation of h_pavgQ with the activity can be found in **Figure S4.7**.

Partial positive charge. The 2D partial charge descriptors, $PEOE_VSA_PPOS$ and $PEOE_VSA_+2$ were frequently used, positively correlated variables in the QSAR models (orange in **Figure 4.3**). $PEOE_VSA$ descriptors are calculated based on the Partial Equalization of Orbital Electronegativities method and capture electrostatic interactions ^[46]. $PEOE_VSA_PPOS$ (p -value $3.6e^{-06}$ to $1.4e^{-05}$, **Table S4.4**) refers to the total positive polar van der Waals surface area (in \AA^2), where the partial charge is greater than $+0.200e$. In fact, this descriptor depends on the number of oxygen atoms within the molecule ^[47]. Isoflavones, isoflavanones and 3-aryl coumarins were the most oxygenated subclasses in the dataset and showed large, partially positive surface areas within the molecule ($PEOE_VSA_PPOS > 35 \text{ \AA}^2$). $PEOE_VSA_+2$ (p -value $4.2e^{-03}$ to $1.6e^{-01}$, **Table S4.4**) refers to the sum of van der Waals (vdw) surface area for each atom (in \AA^2) of which the partial charge is between $+0.100e$ and (including) $+0.149e$. Based on the level of significance of these two $PEOE$ descriptors, small partial positive charges are less determinant of anti-MRSA activity compared to larger partial positive charges.

4.3.5.3. Van der Waals surface energy

The energy descriptor E_{vdw} (purple colour in **Figure 4.3**) was also used as a positively correlated explanatory variable. This descriptor represents the van der Waals (vdW) component of the potential energy of the molecules ^[48]. Pterocarpan, pterocarpenes and 2-arylbenzofurans had clearly lower vdW interaction energies ($E_{vdw} < 11.1$ kcal/mol) than the rest of the subclasses. Pterocarpan and pterocarpenes are more rigid molecules than the other (iso)flavonoid subclasses due to the presence of an additional D-ring ^[18]. This higher rigidity should facilitate vdW interactions, due to lower entropic penalties on the rigid molecules compared to more flexible ones ^[49]. 2-Arylbenzofurans, despite the lack of the extra D-ring, contain a furan C-ring, which contributes to increased molecular planarity compared to a pyran ^[50] (**Figure S4.8**). Thus, the more rigid or planar a molecule is, the lower the vdW interaction energy and the lower the activity. This implies that other interactions, most likely electrostatic, are more important for activity.

4.3.6. Pharmacophore modelling

To understand further the effect of prenylation and of other substituents on the antibacterial activity against MRSA, a ligand-based pharmacophore model was developed. The analysis of the fit of the compounds in the 3D-pharmacophore model revealed four structural features mapping the active molecules; two aromatic ring features (orange) corresponding to the A- and B-ring of (iso)flavonoids, one hydrophobic feature representing the prenyl group (green) and a hydrogen donor projection feature referring to the position of a potential hydrogen bond partner (pink) (**Figure 4.4A**). The pharmacophore model constructed for MRSA had a 65% overall accuracy (sum of molecules predicted correctly), a 60% positive accuracy (active molecules predicted correctly) and a 76% negative accuracy (inactive molecules predicted correctly). These accuracies are 20% higher than the accuracies derived when using a previously constructed pharmacophore model on *L. monocytogenes* ^[18]. The hits in pharmacophore search and the quality of fitting of each molecule to the model for MRSA and *L. monocytogenes* are shown in **Table S4.5** and **S4.6**, respectively.

The model predicted correctly all the active prenylated isoflavones, the most abundant subclass of the dataset, 70% of the active isoflavans, 50% of the active pterocarpan and 43% of the active pterocarpenes. **Figure 4.4B** illustrates examples of isoflavones prenylated at different positions with respect to their fitting quality into the pharmacophore model. Prenylated isoflavones on the β -position (A-ring) and δ -position (B-ring) of the isoflavonoid backbone map all the essential pharmacophore features. In contrast, α -prenylation failed to map the hydrophobic moiety (A-ring).

However, the model failed to predict the active di-prenylated isoflavanones (only the di-prenylated members of this subclass were active), while it correctly predicted analogue molecules such as di-prenylated isoflavones and di-prenylated

isoflavans. The simultaneous absence of a double bond in the C-ring and the presence of a carbonyl group in isoflavanones, contrary to isoflavones and isoflavans, respectively, seems to significantly affect the orientation of the B-ring (**Figure S4.8**). This different B-ring orientation could be the reason for the lack of fit of isoflavanones in the pharmacophore. Five molecules (**8**, **25**, **29**, **72** and **77**, **Table S4.1**) were found to be false positives during the pharmacophore search (**Figure S4.9**); These molecules are typical examples of activity cliffs, i.e. structurally similar molecules with large difference in potency ^[51].

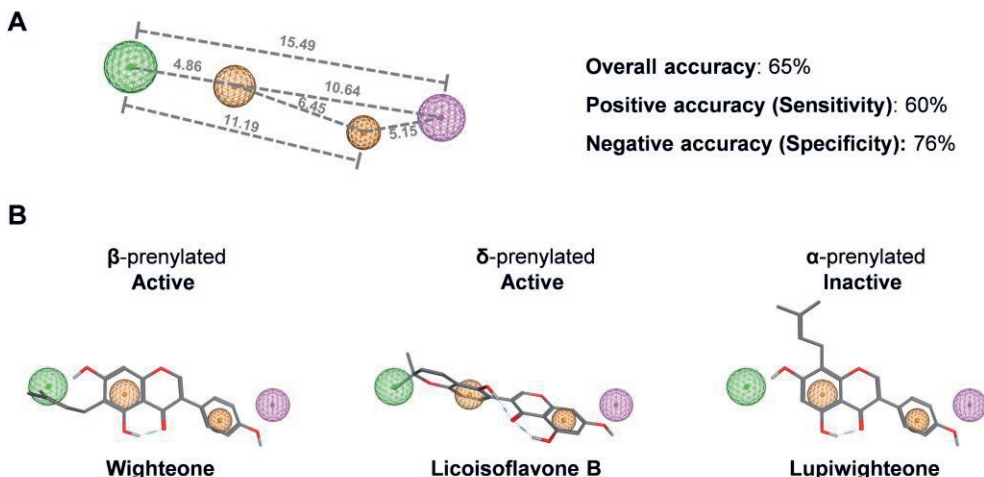


Figure 4.4. Ligand-based pharmacophore model for active anti-MRSA ($\text{MIC} \leq 25 \mu\text{g/mL}$) prenylated (iso)flavonoids. The colour of the spheres represents the following features: orange spheres represent aromatic rings, the green and the pink spheres represent hydrophobic features and hydrogen bond donor projections (i.e. features that denote the presence of possible hydrogen bond partners), respectively. Numbers represent the distance between the features in Ångström. The donor / acceptor projections have a radius of 1.2 Å, the aromatic features have a radius of 0.8 Å and 1.0 Å, left and right respectively and the hydrophobic feature has a radius of 1.2 Å. Percentages correspond to the different prediction accuracies (overall, positive and negative) of the model (**A**). The fitting of molecules in the pharmacophore with respect to their potency are also illustrated (**B**).

4.4. Discussion

4.4.1. Hydrophobicity and electrostatic interactions are the main determinants for the anti-MRSA activity of prenylated (iso)flavonoids

Traditionally, the antimicrobial potency of prenylated (iso)flavonoids was attributed to their increased hydrophobicity mainly due to the presence of the prenyl group ^[11,52]. Generally, the amphiphilic cytoplasmic membrane is hypothesized as the first target of potential antibacterials ^[53]. Prenylated

(iso)flavonoids are small enough to cross the open structure of the bacterial cell wall [54] and hydrophobic enough to access the membrane [55].

In this study, continuous hydrophobicity with balanced hydrophilic groups in the form of the descriptors *vsurf_IW7*, *vsurf_D4* and *vsurf_CW3*, were the most strongly correlated properties to anti-MRSA activity, in accordance with previous results against the Gram-positive *L. monocytogenes* [18]. The contribution of the hydrophobic volume (*vsurf_D4*) and hydrophilic integrity moment (*vsurf_IW7*) to the anti-MRSA activity is illustrated in **Figure 4.5**. Di-prenylated (iso)flavonoids are characterized by an extensive hydrophobic volume, as in molecules (**79**) and (**60**). In most cases, extensive hydrophobic volume accounts for the increased antimicrobial potency of the molecules [18]. Decreasing their hydrophobic volume by removal of one prenyl-group, as in molecules (**77**) and (**59**) indeed decreased the anti-MRSA activity. However, further removal of the C6a hydroxyl-group (molecule (**77**) to (**97**)) (**Figure 4.5A**) restored the hydrophobic volume to a certain extent, reduced the hydrophilic moments in the molecule (*vsurf_IW7*), leading to higher anti-MRSA activity.

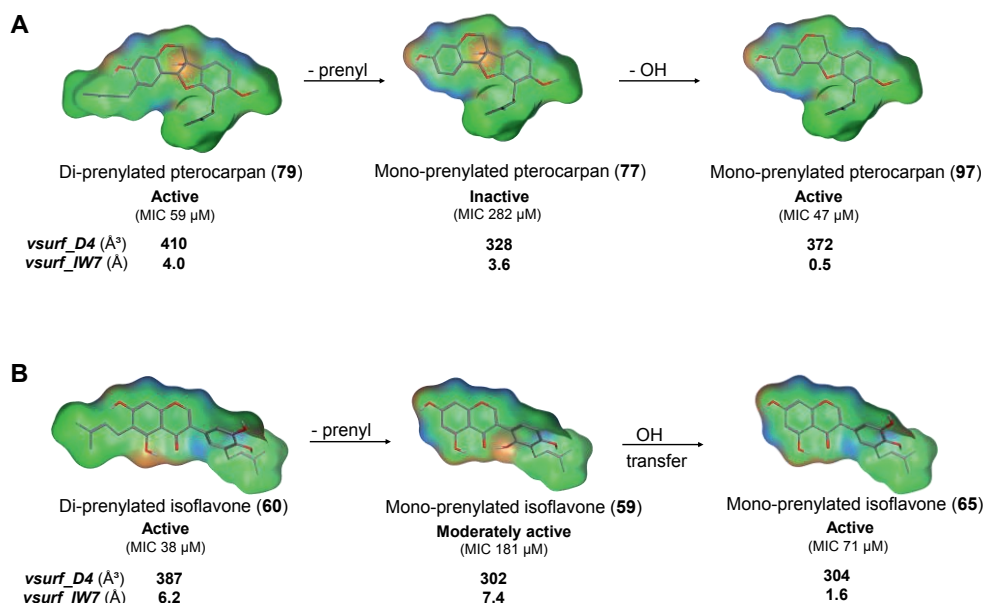


Figure 4.5. Surface maps of a series of active, moderately active and inactive prenylated pterocarpan (**A**) and isoflavones (**B**). (Iso)flavonoids from the same subclass (i.e. **A** or **B**) are analogues, differing only in the presence, absence or relocation of one functional group (indicated by the arrows). These structural differences influence their hydrophobic volume (*vsurf_D4*, \AA^3) and the distribution of the hydrophilic regions (*vsurf_IW7*, \AA) and therefore the anti-MRSA activity. Mildly polar regions are coloured in blue, H-bonding in orange and hydrophobic regions in green.

Interestingly, transferring the OH group from C5' to C6' (molecule (**59**) to (**65**)) (**Figure 4.5B**) restored the balance between the hydrophilic moments in the molecule, enhancing the anti-MRSA potency, even without influencing the hydrophobic volume.

From the above it becomes evident that prenylated (iso)flavonoids scoring low in hydrophobicity can still be active anti-MRSA agents (e.g. molecule **65**). This observation agrees with the findings of our pharmacophore model, where the importance of single, and not necessarily double, prenylation together with a hydrogen bond acceptor were highlighted. Charge was highlighted as the second most important molecular property for the antibacterial activity of prenylated (iso)flavonoids. Large positive partial charges (*PEOE_VSA_PPOS* and *PEOE_VSA+2*) and formal negative charges (*h_pavgQ*) suggest the importance of electrostatic interactions ^[46]. Sadgrove *et al.* (2020) also associated the importance of electrostatic interactions such as hydrogen-bonding with anti-(MR)SA activity ^[20].

4.4.2. New insights in the possible interaction of active anti-MRSA agents with the cytoplasmic membrane

Based on the main molecular properties highlighted by the QSAR study and the pharmacophore model, it is hypothesized that different active mono-prenylated anti-MRSA (iso)flavonoids might be differently taken up by the cell or interact with the membrane. Three ways of interaction of prenylated (iso)flavonoids with the cytoplasmic membrane are proposed (**Figure 4.6**).

4.4.2.1. Acidic prenylated isoflavonoids might interact with both the membrane and with intracellular targets

First, prenylated (iso)flavonoids with high potential to be charged at pH 7 are hypothesized to interact differently from the ones that remain neutral across the pH range. The average total formal charge sum across protonation states at pH 7 ^[44] is represented by the descriptor, *h_pavgQ* (**Table S4.2**). Twenty percent of the active mono-prenylated (iso)flavonoids had an absolute *h_pavgQ* value higher than 0.2. These molecules were considered acidic and both their dissociated and undissociated form were taken into account (**Figure 4.6**, left side). The subclass of isoflavones is the predominant representative subclass (83%) of acidic, active mono-prenylated (iso)flavonoids. All, but one, molecules of this category in our dataset are characterized by the presence of three or more free hydroxyl groups. Prenylated (iso)flavones have been shown experimentally to permeabilize the membrane of MRSA and other Gram-positive bacteria ^[18,56,57]. Yet, the exact mechanism of membrane permeabilization has not been thoroughly investigated.

Recently, Li *et al.* (2018) showed that a very active (MIC 1 µg/mL, 2 µM) di-prenylated xanthone (alpha-mangostin) forms membrane-spanning, intermolecular aggregates primarily through hydrogen bonding ^[55]. This was shown

through molecular dynamic simulation experiments. Aggregate formation ultimately led to membrane destabilization and subsequent water translocation across the membrane, without pore formation ^[55]. This is in line with the membrane permeabilization of Gram-positive bacteria observed by prenylated isoflavones ^[18,57]. Interestingly, it was specifically highlighted that the presence of three hydroxyl groups in alpha-mangostin are crucial for transmembrane aggregate formation, while their absence would make alpha-mangostin soluble in the lipid bilayer ^[55]. The formation of intermolecular hydrogen bonds possibly facilitates the unfavourable presence of polar groups into the hydrophobic interior of the membrane, stabilizing the cluster. Alpha-mangostin is structurally similar to the active isoflavones in our dataset, e.g. a mono-prenylated (wighteone, **74**) and a di-prenylated one (lupalbigenin, **67**), although the xanthone is more planar ^[58] (**Figure S4.10**). The hydrogen bond strengths of mangostin and the two analogue isoflavones were quantified (*h_ema* and *h_emd* descriptors, **Table S4.2**, Molecular Operating Environment, MOE). The sum of hydrogen bond donor (HBD) and acceptor (HBA) strengths for these molecules were comparable (HBD: 10.2 kcal/mol for wighteone, 10.9 kcal/mol for lupalbigenin and 11.4 kcal/mol for mangostin; HBA: 4.6 kcal/mol for the two prenylated isoflavones and 5.6 kcal/mol for the xanthone). Since aggregate formation by the di-prenylated xanthone was shown to be primarily hydrogen-bond driven, possibly this mechanism of action is also employed by prenylated isoflavones given the similar degree of hydrogen-bond capacity.

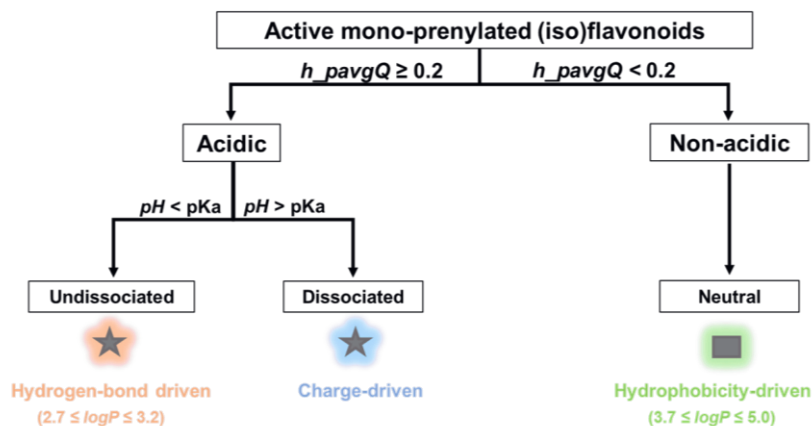
Xanthone transmembrane aggregates were formed after a high enough concentration of the molecule reaches the lipid tail region of the membrane. Although wighteone (**74**) and lupalbigenin (**67**) have similar hydrogen-bond capacities, the presence of only one prenyl group in the former should increase the free energy barrier of membrane penetration compared to the latter ^[38]. Possibly, higher concentrations are needed for mono-prenylated isoflavones to form these aggregates than for their di-prenylated counterparts, something which is also reflected in the higher MICs observed for the former.

The mechanism of membrane activity proposed by Li *et al.* (2018) considered only the undissociated form of the molecule ^[55]. A negative charge in the dissociated acidic isoflavones would be repelled by the polar (phosphate) head groups of the membrane and would not allow membrane penetration ^[55,59]. Instead, the dissociated acidic isoflavones might be transported to the cytosol through transmembrane carrier proteins or by active transport ^[60,61] (**Figure 4.6B**, blue star) similar to what has been shown for other anionic antibiotics, such as carbenicillin and quinolones ^[62]. The proposed membrane transportation of these molecules implies that the membrane is not the only target for their anti-MRSA activity and their mode of action is further complemented by activity inside the cytosol. Recently, a di-prenylated flavone was shown to inhibit the biosynthesis of phosphatidic acids in the cytosol, the repair mechanism of bacterial membranes ^[56] after membrane disruption. Noticeable inhibition (> 99%) of MRSA was

observed within 2 h of exposure to this prenylated flavonoid ^[56], similar to what was found in **Figure 4.1**.

It is therefore proposed that the dissociated and undissociated forms of antibacterial acidic (iso)flavonoids might employ different modes of action (**Figure 4.6B**, orange and blue stars). Internalization of antibacterials in different ways depending on their protonation state has been shown before for Gram-negatives ^[63].

A



B

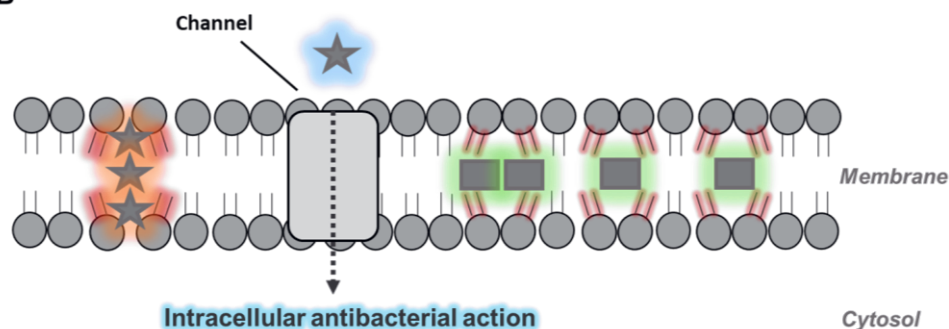


Figure 4.6. Proposed classification of active ($\text{MIC} \leq 25 \mu\text{g/mL}$) prenylated (iso)flavonoids based on their potential to be negatively charged at pH 7. Molecules with high potential to be dissociated at pH 7 ($h_pavgQ \geq 0.2$), i.e. acidic, were considered for their dissociated and undissociated forms separately. Molecules that remain fully undissociated at pH 7 ($h_pavgQ < 0.2$), i.e. non-acidic, were considered neutral (**A**). Hypothesized interactions of active anti-MRSA prenylated (iso)flavonoids with the cytoplasmic membrane (**B**). Stars represent active acidic mono-prenylated (iso)flavonoids, whereas rectangular shapes represent active, neutral mono-prenylated (iso)flavonoids. Different glows around the shapes indicate hypothesized, predominant driving forces that mediate cellular uptake or interaction with the membrane; blue denotes a negative charge, orange indicates strong hydrogen bonding and green glow represents hydrophobicity-driven interaction with the lipid bilayer. The intensity of red shading around phospholipids shows the level of compromise of membrane integrity.

4.4.2.2. *Non-acidic prenylated isoflavonoids might be internalized by the membrane via diffusion*

Hydrogen-bonding, formal charge and hydrophobicity were the main molecular properties determining anti-MRSA activity. It was hypothesized that acidic prenylated isoflavonoids may interact with both the membrane and with intracellular targets, depending on their protonation state. Nevertheless, 80% of the active mono-prenylated isoflavonoids had an absolute h_pavqQ value of less than 0.2, meaning that these molecules remain neutral at the pH of the medium. This category of non-acidic prenylated (iso)flavonoids (**Figure 4.6A**, right side) comprised compounds with less than 3 hydroxyl groups and higher $logP$ values (ranging from 3.7 to 5.0) than the acidic prenylated isoflavonoids ($logP \leq 3.2$ for the undissociated species). It is therefore hypothesized that hydrophobicity becomes the main driver for interaction of these molecules with the membrane ^[55]. Nevertheless, the presence of a few (< 3) hydroxyl groups in these molecules, may also trigger aggregate formation, similarly to the acidic, undissociated (iso)flavonoids. Individually or as aggregates, these molecules might be soluble within the lipid bilayer ^[55], due to their higher hydrophobicity, ultimately disturbing its integrity ^[62] (**Figure 4.6B**, green rectangulars). Contrary to prenylated isoflavones (the acidic group in **Figure 4.6**), a few examples from the non-acidic subclasses were shown not to permeabilize the cytoplasmic membrane, but have been hypothesized to still disrupt its integrity by other means ^[18].

Interestingly, neutral prenylated isoflavonoids can be planar (pterocarpenes) or non-planar (pterocarpans and isoflavans), while acidic isoflavonoids included in this study are all non-planar. Notably, the two most active mono-prenylated isoflavonoids studied were the pterocarpin orientanol B (**93**) (six times more active than its pterocarpene analogue, dehydroglyceollin IV (**102**), **Table S4.1** and **Figure S4.2**) and the isoflavan 4'-O-methyl-glabridin (**17**). Both molecules adopt non-planar conformations (**Figure S4.8**). Planarity has been associated to the extent of insertion in the cytoplasmic membrane and the level of disruption of membrane integrity ^[63-65]. It has been hypothesized that non-planar molecules disrupt membrane integrity more effectively due to better interaction acyl chains ^[55,64,65], possibly leading to higher antimicrobial activity. In contrast, planar, molecules may interact less efficiently with the acyl chains, despite their rapid diffusion into the membrane.

4.5. Conclusion

In this study, QSAR analysis and pharmacophore modelling were performed in a diverse set of prenylated (iso)flavonoids as anti-MRSA agents. A quantitative QSAR model to predict the (level of) activity of prenylated isoflavonoids against MRSA and other Gram positive bacteria was successfully validated. From the QSAR analysis and the pharmacophore model, properties such as formal negative charge and hydrogen bonding or hydrophobicity were found to contribute the most to the

anti-MRSA activity. Information on the contribution of these molecular properties to the anti-MRSA activity can aid the design and development of novel antibacterial agents against Gram-positive bacteria. Last, it is proposed that active prenylated (iso)flavonoids with different primary molecular properties might employ different mechanisms for cell uptake or interaction with the cytoplasmic membrane.

4.6. Acknowledgement

Authors are grateful to John Chapman for critically reading the manuscript.

4.7. References

- [1] Monegro, A. F. & Regunath, H. Hospital acquired infections. in *StatPearls [Internet]* (StatPearls Publishing, 2018).
- [2] Antoci, E., Pinzone, M., Nunnari, G., Stefani, S. & Cacopardo, B. Prevalence and molecular characteristics of methicillin-resistant *Staphylococcus aureus* (MRSA) among subjects working on bovine dairy farms. *Le Infezioni in Medicina: Rivista Periodica di Eziologia, Epidemiologia, Diagnostica, Clinica e Terapia delle Patologie Infettive* **21**, 125-129 (2013).
- [3] Control, C. f. D. & Prevention. *Active bacterial core surveillance report, emerging infections program network, methicillin resistant Staphylococcus aureus*, <http://www.cdc.gov/abcs/reports-findings/survreports/mrsa14.html> (2014).
- [4] ECDC. Antimicrobial resistance surveillance in Europe 2014. Annual Report of the European Antimicrobial Resistance Surveillance Network (EARS-Net). (Stockholm, 2015).
- [5] Organization, W. H. Antibacterial agents in clinical development: an analysis of the antibacterial clinical development pipeline. (2019).
- [6] Lehman, S. M., Mearns, G., Rankin, D., Cole, R. A., Smrekar, F., Branston, S. D. & Morales, S. Design and preclinical development of a phage product for the treatment of antibiotic-resistant *Staphylococcus aureus* infections. *Viruses* **11**, 88 (2019).
- [7] Vestergaard, M., Frees, D. & Ingmer, H. Antibiotic resistance and the MRSA problem. *Gram-Positive Pathogens*, 747-765 (2019).
- [8] Araya-Cloutier, C., Vincken, J.-P., van Ederen, R., den Besten, H. M. & Gruppen, H. Rapid membrane permeabilization of *Listeria monocytogenes* and *Escherichia coli* induced by antibacterial prenylated phenolic compounds from legumes. *Food Chemistry* **240**, 147-155 (2018).
- [9] de Bruijn, W. J., Araya-Cloutier, C., Bijlsma, J., de Swart, A., Sanders, M. G., de Waard, P., Gruppen, H. & Vincken, J.-P. Antibacterial prenylated stilbenoids from peanut (*Arachis hypogaea*). *Phytochemistry Letters* **28**, 13-18 (2018).
- [10] Veitch, N. C. Isoflavonoids of the Leguminosae. *Natural Product Reports* **30**, 988-1027 (2013).
- [11] Botta, B., Menendez, P., Zappia, G., de Lima, R. A., Torge, R. & Delle Monache, G. Prenylated isoflavonoids: Botanical distribution, structures, biological activities and biotechnological studies. An update (1995-2006). *Current Medicinal Chemistry* **16**, 3414-3468 (2009).
- [12] Veitch, N. C. Flavonoid chemistry of the leguminosae. *Recent Advances in Polyphenol Research* **2**, 23-58 (2010).
- [13] Hatano, T., Shintani, Y., Aga, Y., Shiota, S., Tsuchiya, T. & Yoshida, T. Phenolic constituents of licorice. VIII. Structures of glicophenone and glicoisoflavanone, and effects of licorice phenolics on methicillin-resistant *Staphylococcus aureus*. *Chemical & Pharmaceutical Bulletin* **48**, 1286-1292 (2000).
- [14] Sato, M., Tanaka, H., Tani, N., Nagayama, M. & Yamaguchi, R. Different antibacterial actions of isoflavones isolated from *Erythrina poeppigiana* against

- methicillin-resistant *Staphylococcus aureus*. *Letters in Applied Microbiology* **43**, 243-248 (2006).
- [15] Wang, S. Y., Sun, Z. L., Liu, T., Gibbons, S., Zhang, W. J. & Qing, M. Flavonoids from *Sophora moorcroftiana* and their synergistic antibacterial effects on MRSA. *Phytotherapy Research* **28**, 1071-1076 (2014).
- [16] Tanaka, H., Sato, M., Fujiwara, S., Hirata, M., Etoh, H. & Takeuchi, H. Antibacterial activity of isoflavonoids isolated from *Erythrina variegata* against methicillin-resistant *Staphylococcus aureus*. *Letters in Applied Microbiology* **35**, 494-498 (2002).
- [17] Zhou, B. & Wan, C.-X. Phenolic constituents from the aerial parts of *Glycyrrhiza inflata* and their antibacterial activities. *Journal of Asian Natural Products Research* **17**, 256-261 (2015).
- [18] Araya-Cloutier, C., Vincken, J.-P., van de Schans, M. G., Hageman, J., Schaftenaar, G., den Besten, H. M. & Gruppen, H. QSAR-based molecular signatures of prenylated (iso) flavonoids underlying antimicrobial potency against and membrane-disruption in Gram positive and Gram negative bacteria. *Scientific Reports* **8**, 9267 (2018).
- [19] Nandi, S., Ahmed, S. & Saxena, A. Combinatorial design and virtual screening of potent anti-tubercular fluoroquinolone and isothiazoloquinolone compounds utilizing QSAR and pharmacophore modelling. *SAR and QSAR in Environmental Research* **29**, 151-170 (2018).
- [20] Sadgrove, N. J., Oliveira, T. B., Khumalo, G. P., Vuuren, S. F. v. & van Wyk, B. - E. Antimicrobial isoflavones and derivatives from *Erythrina* (Fabaceae): structure activity perspective (sar & qsar) on experimental and mined values against *Staphylococcus Aureus*. *Antibiotics* **9**, 223 (2020).
- [21] van de Schans, M. G., Ritschel, T., Bovee, T. F., Sanders, M. G., de Waard, P., Gruppen, H. & Vincken, J. P. Involvement of a hydrophobic pocket and helix 11 in determining the modes of action of prenylated flavonoids and isoflavonoids in the human estrogen receptor. *ChemBioChem* **16**, 2668-2677 (2015).
- [22] Van De Schans, M. G., Vincken, J.-P., De Waard, P., Hamers, A. R., Bovee, T. F. & Gruppen, H. Glyceollins and dehydroglyceollins isolated from soybean act as SERMs and ER subtype-selective phytoestrogens. *The Journal of Steroid Biochemistry and Molecular Biology* **156**, 53-63 (2016).
- [23] Tanaka, H., Hattori, H., Oh-Uchi, T., Sato, M., Sako, M., Tateishi, Y. & Rizwani, G. H. Three new isoflavanones from *Erythrina costaricensis*. *Natural Product Research* **23**, 1089-1094 (2009).
- [24] Tanaka, H., Sudo, M., Kawamura, T., Sato, M., Yamaguchi, R., Fukai, T., Sakai, E. & Tanaka, N. Antibacterial constituents from the roots of *Erythrina herbacea* against methicillin-resistant *Staphylococcus aureus*. *Planta Medica* **76**, 916-919 (2010).
- [25] Tanaka, H., Atsumi, I., Hasegawa, M., Hirata, M., Sakai, T., Sato, M., Yamaguchi, R., Tateishi, Y., Tanaka, T. & Fukai, T. Two new isoflavanones from the roots of *Erythrina variegata*. *Natural Product Communications* **10**, 1934578X1501000330 (2015).
- [26] Faulon, J.-L. & Bender, A. Handbook of chemoinformatics algorithms. (CRC press, 2010).
- [27] Kennard, R. W. & Stone, L. A. Computer aided design of experiments. *Technometrics* **11**, 137-& (1969).
- [28] de Bruijn, W. J., Hageman, J. A., Araya-Cloutier, C., Gruppen, H. & Vincken, J.-P. QSAR of 1, 4-benzoxazin-3-one antimicrobials and their drug design perspectives. *Bioorganic & Medicinal Chemistry* **26**, 6105-6114 (2018).
- [29] Eriksson, L., Jaworska, J., Worth, A. P., Cronin, M. T., McDowell, R. M. & Gramatica, P. Methods for reliability and uncertainty assessment and for applicability evaluations of classification-and regression-based QSARs. *Environmental Health Perspectives* **111**, 1361-1375 (2003).

- [30] Tanaka, H., Sato, M., Oh-Uchi, T., Yamaguchi, R., Etoh, H., Shimizu, H., Sako, M. & Takeuchi, H. Antibacterial properties of a new isoflavonoid from *Erythrina poeppigiana* against methicillin-resistant *Staphylococcus aureus*. *Phytomedicine* **11**, 331-337 (2004).
- [31] Tropsha, A. Best practices for QSAR model development, validation, and exploitation. *Molecular Informatics* **29**, 476-488 (2010).
- [32] Dolatabadi, M., Nekoei, M. & Banaei, A. Prediction of antibacterial activity of pleuromutilin derivatives by genetic algorithm-multiple linear regression (GA-MLR). *Monatshefte für Chemie-Chemical Monthly* **141**, 577-588 (2010).
- [33] Consonni, V., Ballabio, D. & Todeschini, R. Comments on the definition of the Q(2) parameter for QSAR validation. *Journal of Chemical Information and Modeling* **49**, 1669-1678 (2009).
- [34] Keepers, T. R., Gomez, M., Biek, D., Critchley, I. & Krause, K. M. Effect of *in vitro* testing parameters on ceftazidime-avibactam minimum inhibitory concentrations. *International Scholarly Research Notices* **2015** (2015).
- [35] Brennan-Krohn, T., Smith, K. P. & Kirby, J. E. The poisoned well: enhancing the predictive value of antimicrobial susceptibility testing in the era of multidrug resistance. *Journal of Clinical Microbiology* **55**, 2304-2308 (2017).
- [36] Roy, K., Das, R. N., Ambure, P. & Aher, R. B. Be aware of error measures. Further studies on validation of predictive QSAR models. *Chemometrics and Intelligent Laboratory Systems* **152**, 18-33 (2016).
- [37] Gibbons, S. Anti-staphylococcal plant natural products. *Natural Product Reports* **21**, 263-277 (2004).
- [38] Koh, J.-J., Qiu, S., Zou, H., Lakshminarayanan, R., Li, J., Zhou, X., Tang, C., Saraswathi, P., Verma, C. & Tan, D. T. Rapid bactericidal action of alpha-mangostin against MRSA as an outcome of membrane targeting. *Biochimica et Biophysica Acta (BBA)-Biomembranes* **1828**, 834-844 (2013).
- [39] Coyle, E. A. & Rybak, M. J. Activity of oritavancin (LY333328), an investigational glycopeptide, compared to that of vancomycin against multidrug-resistant *Streptococcus pneumoniae* in an *in vitro* pharmacodynamic model. *Antimicrobial Agents and Chemotherapy* **45**, 706-709 (2001).
- [40] Cruciani, G., Crivori, P., Carrupt, P.-A. & Testa, B. Molecular fields in quantitative structure-permeation relationships: the VolSurf approach. *Journal of Molecular Structure: Theochem* **503**, 17-30 (2000).
- [41] Moorthy, N. H. N., Cerqueira, N. S., Ramos, M. J. & Fernandes, P. A. QSAR analysis of 2-benzoxazolyl hydrazone derivatives for anticancer activity and its possible target prediction. *Medicinal Chemistry Research* **21**, 133-144 (2012).
- [42] Dearden, J. C., Hewitt, M., Roberts, D. W., Enoch, S., Rowe, P., Przybylak, K., Vaughan-Williams, G., Smith, M., Pillai, G. G. & Katritzky, A. R. Mechanism-based QSAR modeling of skin sensitization. *Chemical Research in Toxicology* **28**, 1975-1986 (2015).
- [43] Labute, P., Kossner, M., Ajamian, A., Santavy, M. & Lin, A. Pharmacophore annotation using extended Hückel theory. *Journal of Cheminformatics* **6**, 1-1 (2014).
- [44] Allen, C. H., Mervin, L. H., Mahmoud, S. Y. & Bender, A. Leveraging heterogeneous data from GHS toxicity annotations, molecular and protein target descriptors and Tox21 assay readouts to predict and rationalise acute toxicity. *Journal of Cheminformatics* **11**, 36 (2019).
- [45] Ghafourian, T., Barzegar-Jalali, M., Dastmalchi, S., Khavari-Khorasani, T., Hakimiha, N. & Nokhodchi, A. QSPR models for the prediction of apparent volume of distribution. *International Journal of Pharmaceutics* **319**, 82-97 (2006).
- [46] Labute, P. Derivation and applications of molecular descriptors based on approximate surface area. in *Chemoinformatics* 261-278 (Springer, 2004).
- [47] Potta, T., Zhen, Z., Grandhi, T. S. P., Christensen, M. D., Ramos, J., Breneman, C. M. & Rege, K. Discovery of antibiotics-derived polymers for gene delivery using combinatorial synthesis and cheminformatics modeling. *Biomaterials* **35**, 1977-1988 (2014).

- [48] Bhardwaj, R. M. Control and prediction of solid-state of pharmaceuticals: experimental and computational approaches. (Springer, 2016).
- [49] King, E. M., Gebbie, M. A. & Melosh, N. A. Impact of rigidity on molecular self-assembly. *Langmuir* **35**, 16062-16069 (2019).
- [50] Klymchenko, A. S., Pivovarenko, V. G. & Demchenko, A. P. Perturbation of planarity as the possible mechanism of solvent-dependent variations of fluorescence quantum yield in 2-aryl-3-hydroxychromones. *Spectrochimica Acta Part a-Molecular and Biomolecular Spectroscopy* **59**, 787-792 (2003).
- [51] Bajorath, J. Representation and identification of activity cliffs. (Taylor & Francis, 2017).
- [52] Yazaki, K., Sasaki, K. & Tsurumaru, Y. Prenylation of aromatic compounds, a key diversification of plant secondary metabolites. *Phytochemistry* **70**, 1739-1745 (2009).
- [53] Epand, R. M., Walker, C., Epand, R. F. & Magarvey, N. A. Molecular mechanisms of membrane targeting antibiotics. *Biochimica et Biophysica Acta (BBA)-Biomembranes* **1858**, 980-987 (2016).
- [54] Lambert, P. Cellular impermeability and uptake of biocides and antibiotics in Gram-positive bacteria and mycobacteria. *Journal of Applied Microbiology* **92**, 46S-54S (2002).
- [55] Li, J., Beuerman, R. W. & Verma, C. S. Molecular insights into the membrane affinities of model hydrophobes. *ACS Omega* **3**, 2498-2507 (2018).
- [56] Pang, D., Liao, S., Wang, W., Mu, L., Li, E., Shen, W., Liu, F. & Zou, Y. Destruction of the cell membrane and inhibition of cell phosphatidic acid biosynthesis in *Staphylococcus aureus*: an explanation for the antibacterial mechanism of morusin. *Food & Function* **10**, 6438-6446 (2019).
- [57] Wu, S.-C., Han, F., Song, M.-R., Chen, S., Li, Q., Zhang, Q., Zhu, K. & Shen, J.-Z. Natural flavones from *Morus alba* against methicillin-resistant *Staphylococcus aureus* via targeting the proton motive force and membrane permeability. *Journal of Agricultural and Food Chemistry* **67**, 10222-10234 (2019).
- [58] Negi, J., Bisht, V., Singh, P., Rawat, M. & Joshi, G. Naturally occurring xanthenes: chemistry and biology. *Journal of Applied Chemistry* **2013** (2013).
- [59] Cramariuc, O., Rog, T., Javanainen, M., Monticelli, L., Polishchuk, A. V. & Vattulainen, I. Mechanism for translocation of fluoroquinolones across lipid membranes. *Biochimica et Biophysica Acta (BBA)-Biomembranes* **1818**, 2563-2571 (2012).
- [60] Tommasi, R., Brown, D. G., Walkup, G. K., Manchester, J. I. & Miller, A. A. ESKAPEing the labyrinth of antibacterial discovery. *Nature Reviews Drug Discovery* **14**, 529-542 (2015).
- [61] Franklin, T. & Snow, G. Penetrating the defences: how antimicrobial drugs reach their targets. in *Biochemistry and Molecular Biology of Antimicrobial Drug Action* 107-118 (Springer, 1998).
- [62] Santos, R. S., Figueiredo, C., Azevedo, N. F., Braeckmans, K. & De Smedt, S. C. Nanomaterials and molecular transporters to overcome the bacterial envelope barrier: Towards advanced delivery of antibiotics. *Advanced Drug Delivery Reviews* **136**, 28-48 (2018).
- [63] Li, X.-Z., Plésiat, P. & Nikaido, H. The challenge of efflux-mediated antibiotic resistance in Gram-negative bacteria. *Clinical Microbiology Reviews* **28**, 337-418 (2015).
- [64] Wesołowska, O., Gąsiorowska, J., Petrus, J., Czarnik-Matusiewicz, B. & Michalak, K. Interaction of prenylated chalcones and flavanones from common hop with phosphatidylcholine model membranes. *Biochimica et Biophysica Acta (BBA)-Biomembranes* **1838**, 173-184 (2014).
- [65] van Dijk, C., Driessen, A. J. & Recourt, K. The uncoupling efficiency and affinity of flavonoids for vesicles. *Biochemical Pharmacology* **60**, 1593-1600 (2000).

4.8. Supplementary information

4.8.1. Supplementary figures

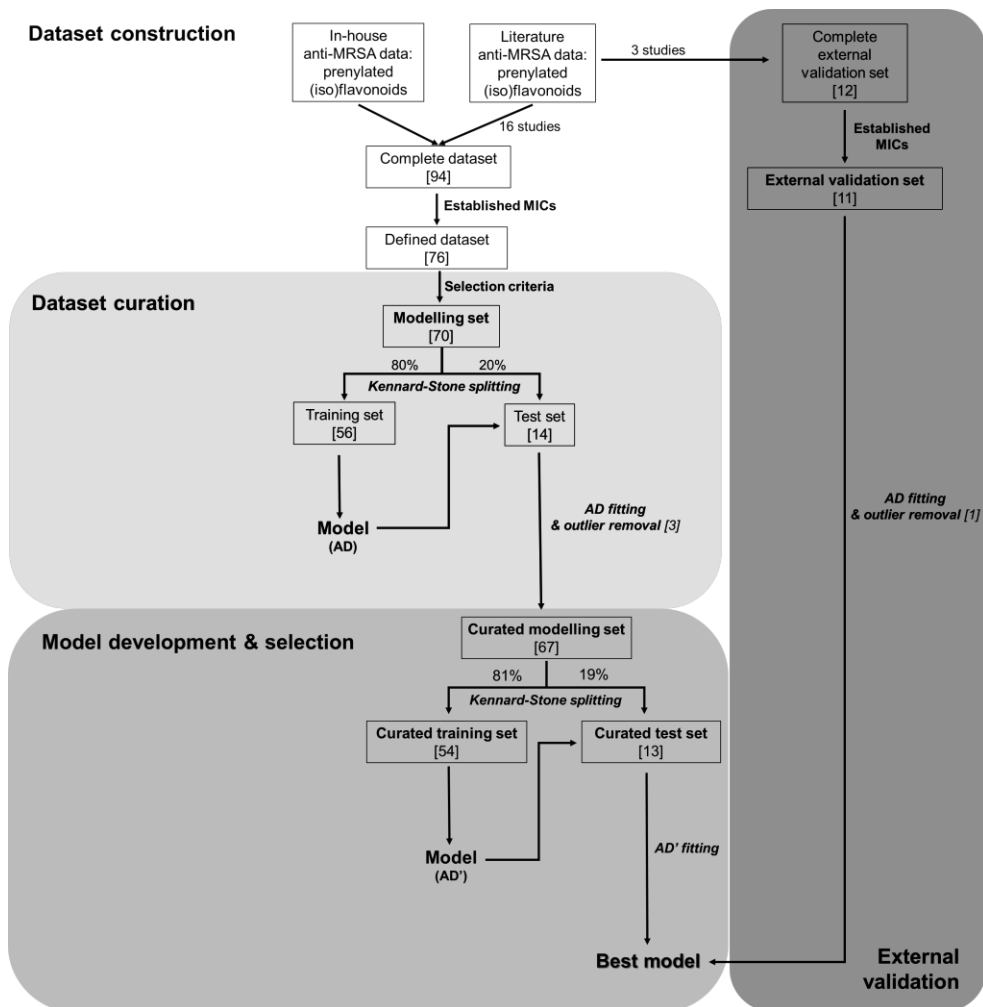


Figure S4.1. Outline of approach followed for QSAR modelling; AD: applicability domain; Numbers in brackets refer to the number of compounds comprised in each set. Colour intensity of the shadings shows the sequence of steps followed for model development, selection and external validation.

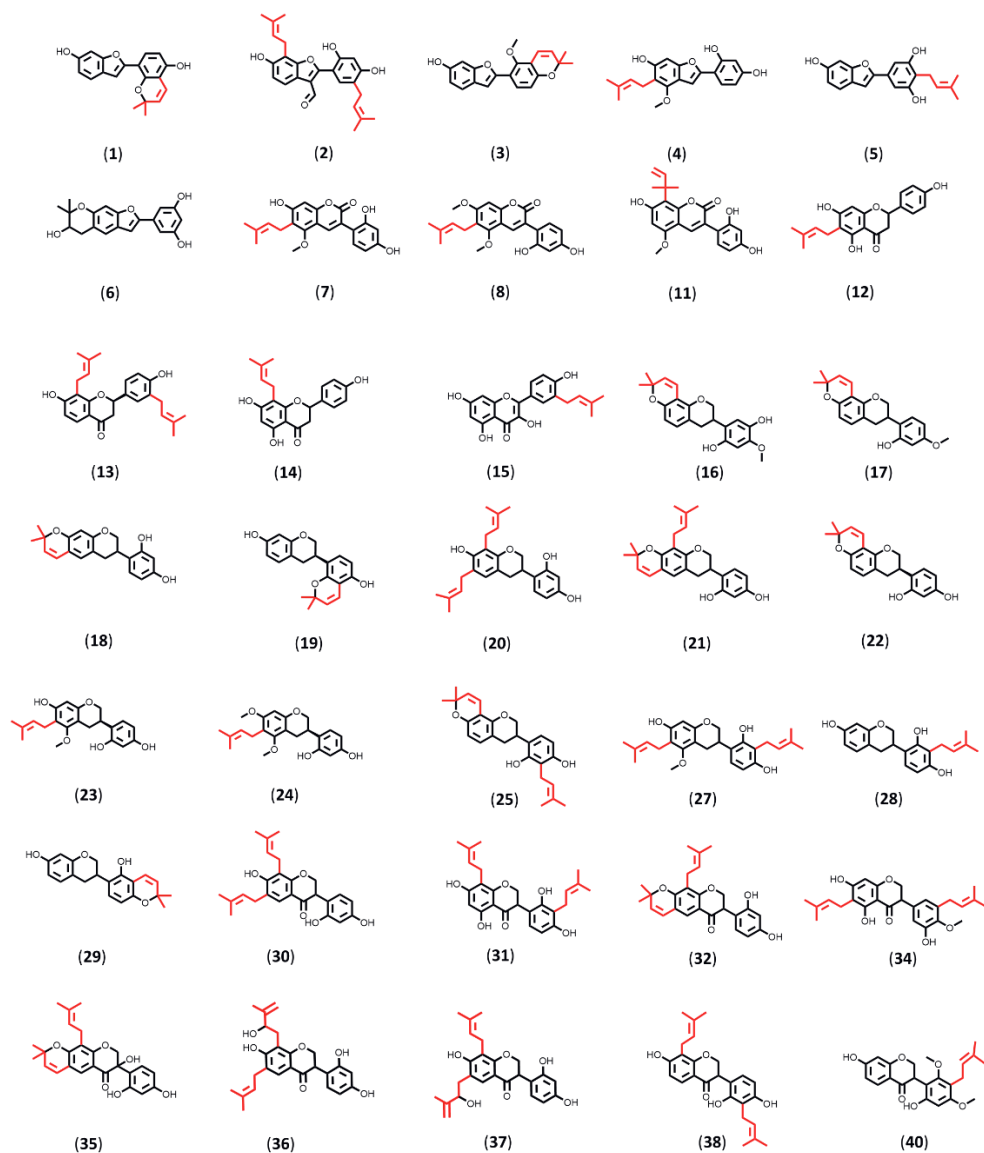


Figure S4.2. Structures of prenylated (iso)flavonoids with established MICs from **Table S4.1**.

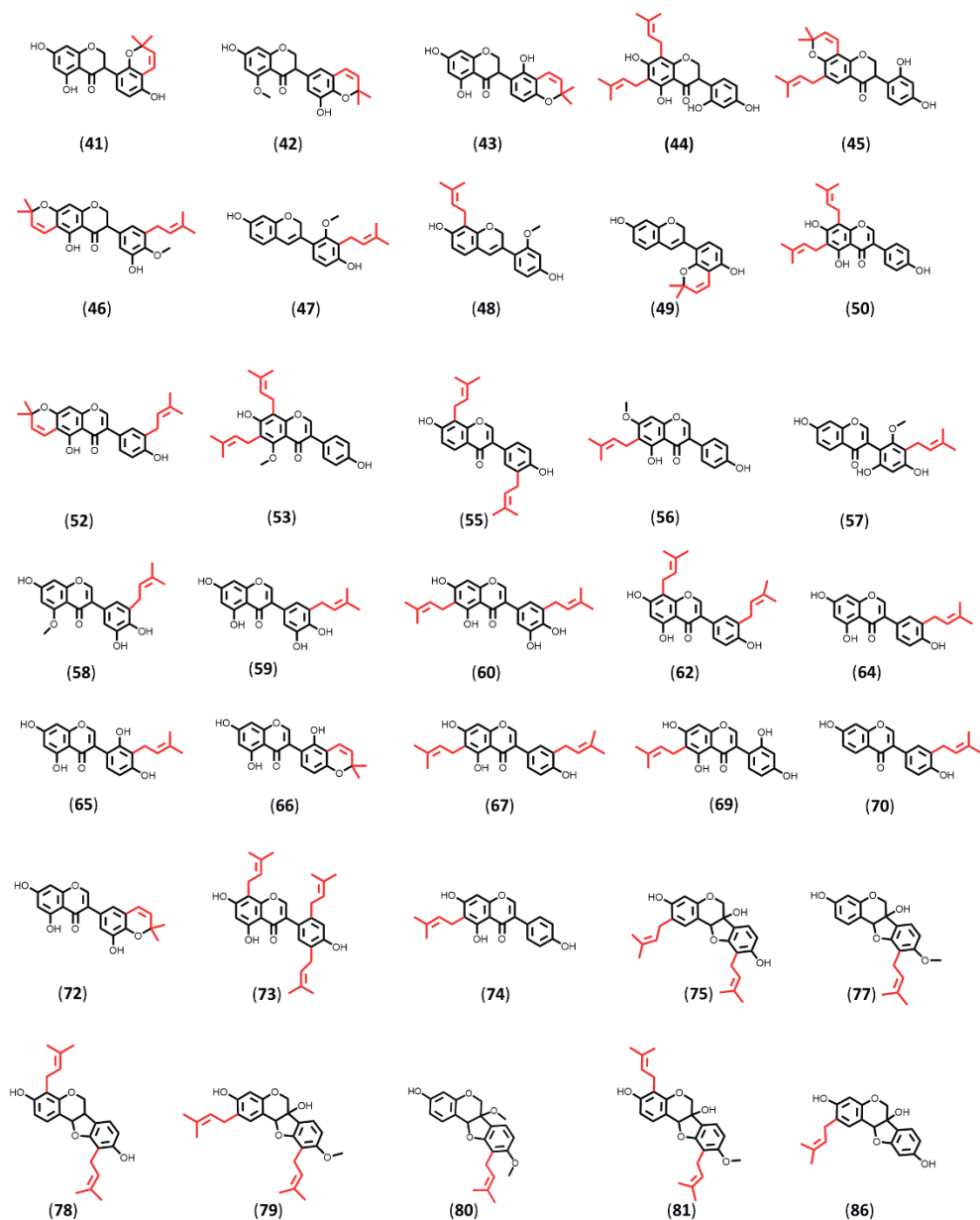


Figure S4.2. Continued

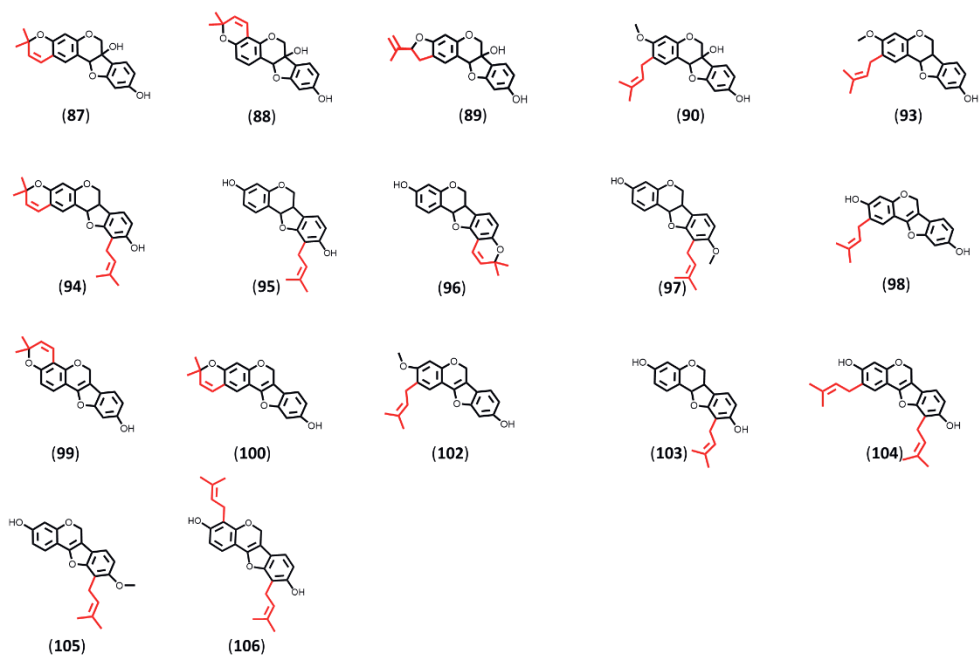


Figure S4.2. Continued

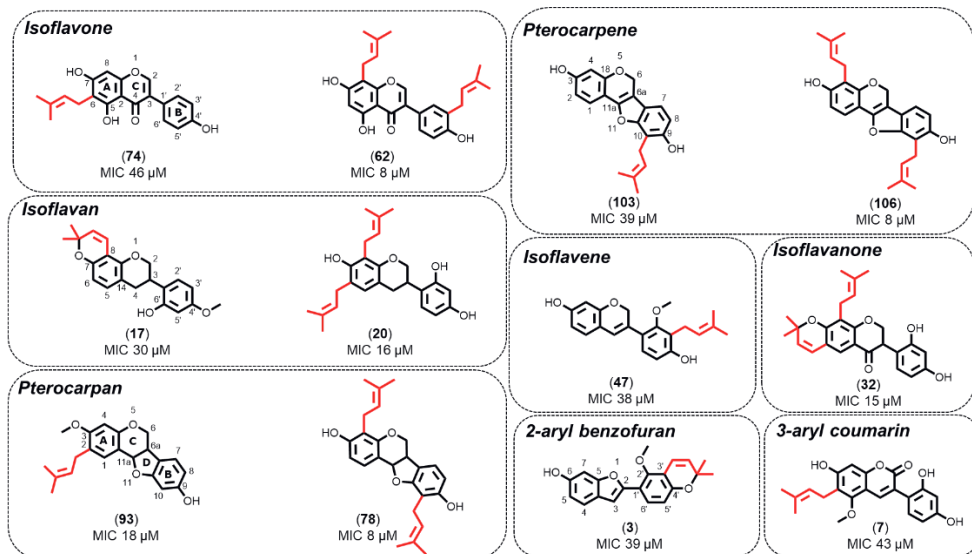


Figure S4.3. Structures of representative active ($\text{MIC} \leq 25 \mu\text{g/mL}$, 8-64 μM) mono- and di-prenylated (iso)flavonoids against MRSA per subclass. Only mono-prenylated derivatives of isoflavenes, 2-aryl benzofurans and 3-aryl coumarins were present in the curated modelling and external validation sets (Table S4.1), whereas only di-prenylated isoflavanones were active anti-MRSA agents. The prenyl groups are highlighted in red.

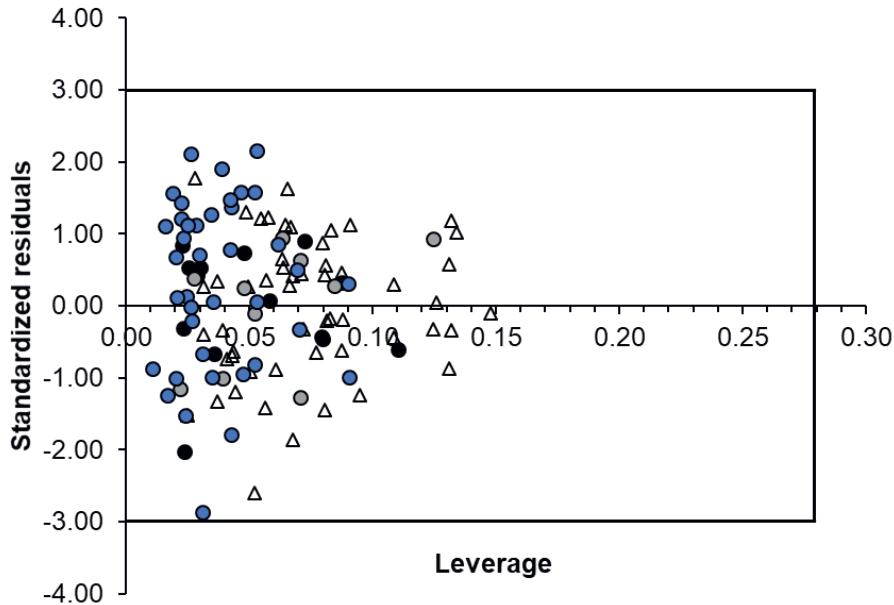


Figure S4.4. Applicability domain of the selected best model for MRSA. The location of molecules from the training (triangles), test (black circles), external validation (grey circles) sets and the set of compounds tested against other Gram-positives (blue circles) are depicted [1].

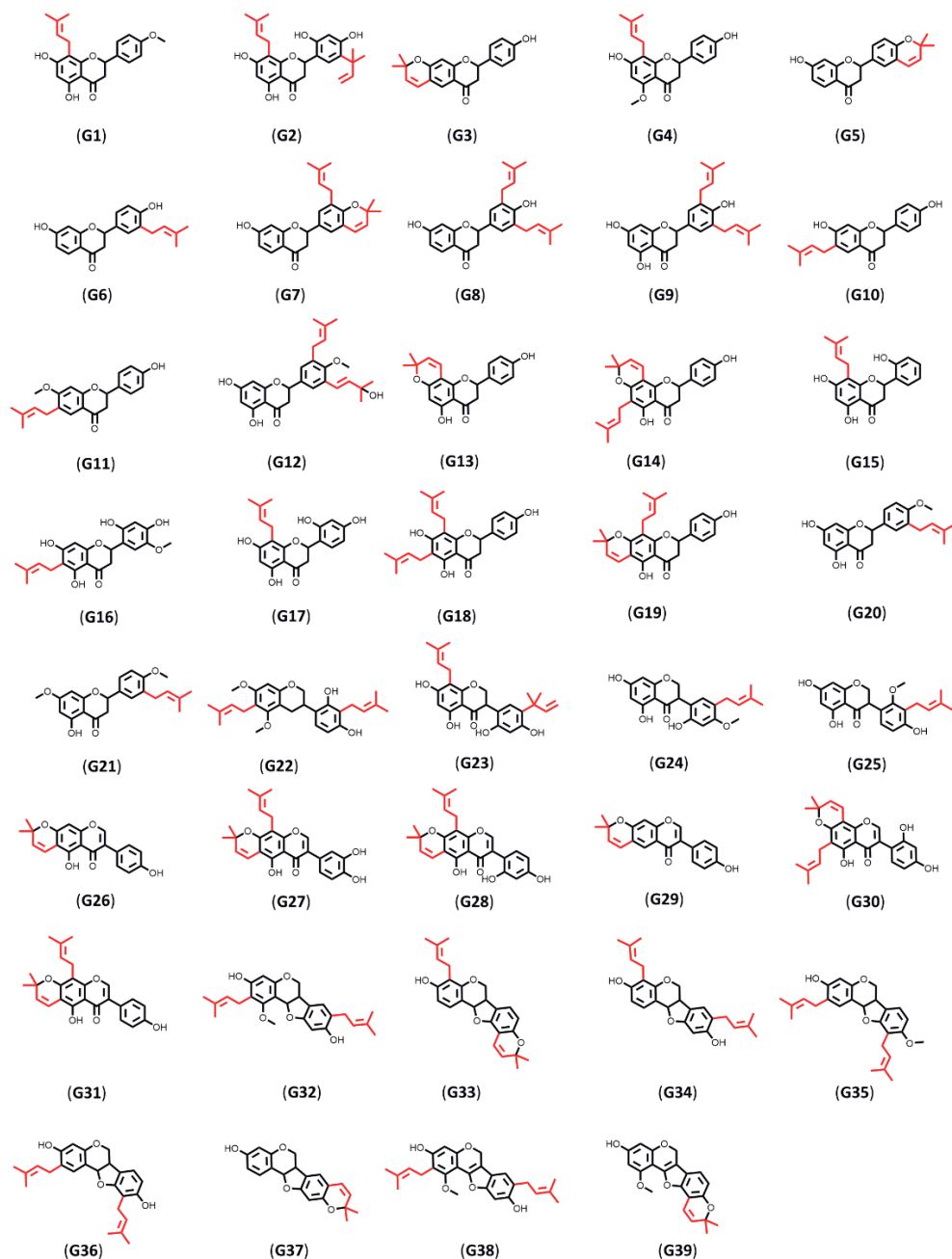


Figure S4.5. Structures of prenylated (iso)flavonoids tested against other Gram-positives (except MRSA) and used to assess the applicability of the best QSAR model developed on MRSA. The structures of the molecules that have also been tested against MRSA can be found in **Figure S4.2**.

Low	G7	8	13	52	56	77	97
	43	57	58	59	72	80	95
Moderate	G24	G26	G39	22	40	41	42
	G1	G6	G9	G12	G14	G23	
High	60	64	66	67	78	105	96
	24	27	31	49	50	53	
	G36	G37	G38	5	7	20	
	G30	G31	G32	G33	G34	G35	
	G21	G22	G25	G27	G28	G29	
	G15	G16	G17	G18	G19	G20	
	G2	G3	G4	G5	G8	G10	G11

Accuracy of prediction of level of activity: 73%

Figure S4.6. Prediction of level of antibacterial activity, ie. low ($\text{MIC} \geq 100 \mu\text{g/mL}$), moderate ($25 < \text{MIC} < 100 \mu\text{g/mL}$) and high ($\text{MIC} \leq 25 \mu\text{g/mL}$) of prenylated (iso)flavonoids against other Gram-positive bacteria by using the best QSAR model obtained for MRSA. Numbers refer to the prenylated (iso)flavonoids of **Table S4.3**; “G” in front of the numbers refer to molecules which have not been tested against MRSA. A yellow glow around the numbers demonstrates that their level of activity was predicted correctly. Compounds for which the predicted activity differed by one two-fold dilution from their experimentally determined one were still considered as correctly predicted [2,3].

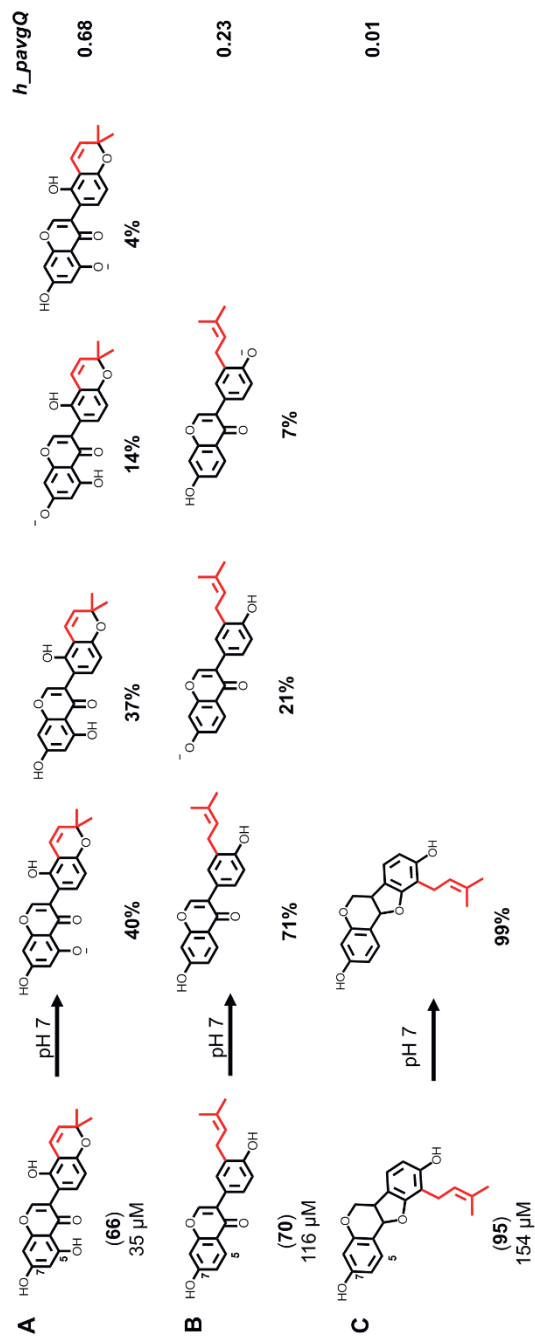


Figure S4.7. Protonation states and their relative abundances at pH 7 of different prenylated isoflavonoids with respect to their anti-MRSA activity and the descriptor, *h_pavgQ*.

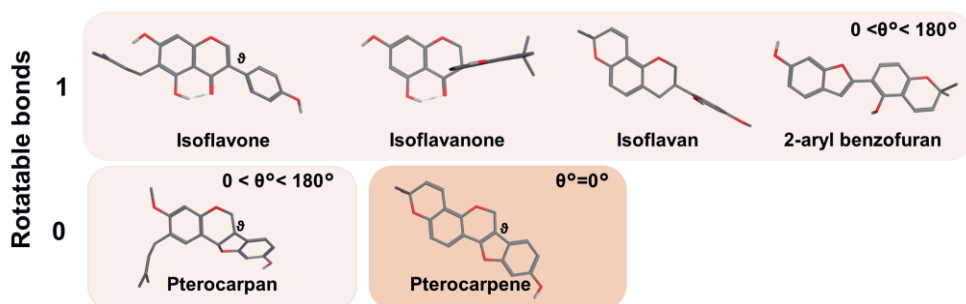


Figure S4.8. Examples of energy minimized structures of mono-prenylated isoflavonoids from selected subclasses. Rotatable bonds refer to the backbone and θ denotes the dihedral bond.

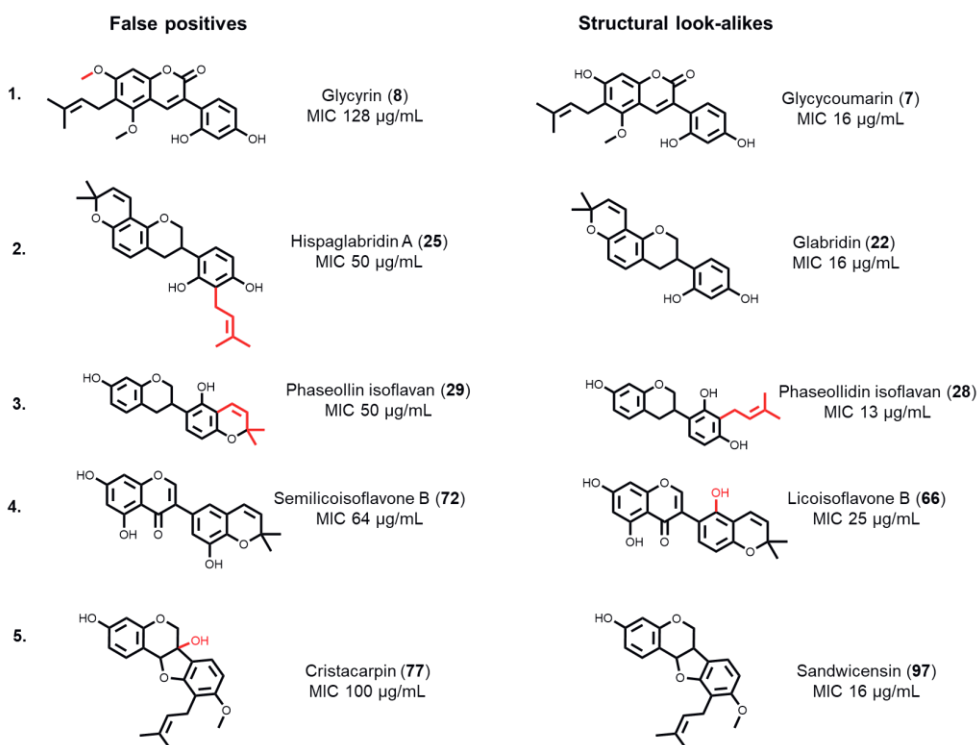
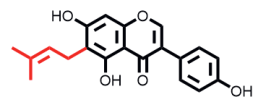
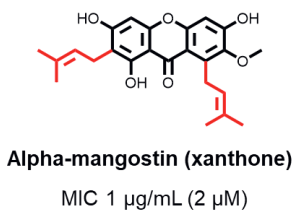
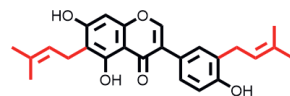


Figure S4.9. False positives (left) in the pharmacophore search. These molecules are “activity cliffs” in the database. Their structural look-alikes are presented on the right and the structural differences that result in substantial change in activity are presented in red.



Wighteone (isoflavone)
MIC 16 µg/mL (46 µM)



Lupalbigenin (isoflavone)
MIC 4 µg/mL (10 µM)

Figure S4.10. Structure and anti-MRSA activity of alpha-mangostin ^[4] in relation to two structurally related prenylated isoflavones, one mono- and one di-prenylated (wighteone and lupalbigenin, respectively).

4.8.2. Supplementary tables

Table S4.1. Anti-MRSA activity of prenylated (iso)flavonoids, experimentally tested and mined from literature. KS stands for the Kennard-Stone splitting, TR stands for the training set, TE for the test set and EV for the external validation set. The % prediction error is defined as $(\text{pMIC}_{\text{observed}} - \text{pMIC}_{\text{predicted}}) / \text{pMIC}_{\text{observed}} \times 100$. Molecules with an asterisk (*) did not comply with the structural criteria (criterion 1 and criterion 2 in Dataset construction, cr.1 and cr.2) used for the QSAR modelling and molecules in grey had unestablished minimum inhibitory concentrations (MIC). The structures of compounds with established MICs can be found in **Figure S4.2**. Di-prenylated (iso)flavonoids are indicated in **bold**. Molecules are sorted based on subclass and ordered alphabetically within each subclass.

ID	(Iso)flavonoid subclass	Name	Set	MIC (µg/mL)	MIC (µM)	% Prediction error	Ref.
1	2-arylbenzofuran	Glabrocoumarone A (Kanzonol U)	EV	13	42	3.4	[5]
2	2-arylbenzofuran	Eryvarin Q	*(cr.2)	6	15	4.7	[6]
3	2-arylbenzofuran	Eryvarin U	TR	13	39	7.4	[7]
4	2-arylbenzofuran	Licocoumarone	TR	16	47	2.1	[8]
5	2-arylbenzofuran	Moracin C	TR	13	40	0.5	[9]
6	2-arylbenzofuran	Moracin P	*(cr.1)	100	306	10.5	[10]
7	3-arylcoumarin	Glycycoumarin	TR	16	43	8.1	[8]
8	3-arylcoumarin	Glycyrin	TR	128	335	14.4	[8]
9	3-arylcoumarin	Glycyrin permethyl ether	-	>128	n.a.	n.a.	[8]
10	3-arylcoumarin	Isorobustone	-	>128	n.a.	n.a.	[11]
11	3-arylcoumarin	Licoarylcoumarin	*(cr.1)	32	87	10.2	[8]
12	Flavanone	6-prenylnaringenin	TR	38	110	2.3	This study
13	Flavanone	Glabrol	*	9	24	2.5	This study
14	Flavanone	Sophoraflavanone B	TR	31	92	5.9	[12]
15	Flavonol	Isolicoflavonol	*(cr.2)	25	71	4.9	[10]
16	Isoflavan	3'-OH-4'-O-methylglabridin	TR	16	44	9.9	This study
17	Isoflavan	4'-O-methylglabridin	TR	10	30	3.8	This study
18	Isoflavan	Eryvarin C	TE	25	77	2.2	[13]
19	Isoflavan	Erythbidin A	EV	50	154	8.9	[5]
20	Isoflavan	Eryzerin C	TR	6	16	1.8	[14,15]

Table S4.1. Continued

ID	(Iso)flavonoid subclass	Name	Set	MIC (µg/mL)	MIC (µM)	% Prediction error	Ref.
21	Isoflavan	Eryzerin D	TR	13	32	3.8	[15]
22	Isoflavan	Glabridin	TR	16	49	2.0	[8]
23	Isoflavan	Glyasperin C	TE	16	45	4.8	[8]
24	Isoflavan	Glyasperin D	TR	16	43	2.7	[8]
25	Isoflavan	Hispaglabridin A	TR	50	127	17.8	This study
26	Isoflavan	Hispaglabridin B	-	>100	n.a.	n.a	This study
27	Isoflavan	Licoricidin	TR	16	38	1.1	[8]
28	Isoflavan	Phaseollidin isoflavan	EV	13	40	0.5	[5]
29	Isoflavan	Phaseollin isoflavan	EV	50	155	8.0	[5]
30	Isoflavanone	2,3-Dihydroauriculatin	EV	25	59	4.2	[16]
31	Isoflavanone	3'-dimethylallyl-kievitone	TR	8	19	3.1	[8]
32	Isoflavanone	Bidwillon B	TR	6	15	6.9	[14,17]
33	Isoflavanone	Costarone	-	>50	59	n.a.	[18]
34	Isoflavanone	Diprenyl-costarone	Outlier	6	14	20.8	[18]
35	Isoflavanone	Eryvarin V	TR	25	59	2.6	[19]
36	Isoflavanone	Eryvarin Y	EV	25	59	0.1	[16]
37	Isoflavanone	Eryvarin Z	EV	50	122	9.0	[16]
38	Isoflavanone	Eryzerin A	TR	25	61	5.7	[15]
39	Isoflavanone	Eryzerin B	-	>50	n.a.	n.a	[14,17]
40	Isoflavanone	Glicoisoflavanone	TR	64	167	8.9	[8]
41	Isoflavanone	Glyasperin F	TR	64	181	2.0	[8]
42	Isoflavanone	Glycyrrhisoflavanone	TR	64	174	1.3	[8]
43	Isoflavanone	Licoisoflavanone	TR	32	90	3.1	[8]
44	Isoflavanone	Orientalol E	EV	13	31	6.5	[16]
45	Isoflavanone	Orientalol F	TE	13	31	5.0	[13]
46	Isoflavanone	Prenyl-costarone	EV	50	115	10.1	[18]
47	Isoflavene	Bidwillol A	EV	13	38	3.4	[5]
48	Isoflavene	Erypoeigin A	TR	25	74	9.8	[20]

Table S4.1. Continued

ID	(Iso)flavonoid subclass	Name	Set	MIC (µg/mL)	MIC (µM)	% Prediction error	Ref.
49	Isoflavone	Glabrene	TR	25	78	2.6	This study
50	Isoflavone	6,8-diprenylgenistein	TR	9	23	1.3	This study
51	Isoflavone	2,3-dehydroklevitane	-	>100	n.a.	n.a	This study
52	Isoflavone	Chandalone	TR	16	40	4.2	[11]
53	Isoflavone	Derrisoflavone A	TR	4	10	5.9	[11]
54	Isoflavone	Erysubin B	-	>25	n.a.	n.a	[21]
55	Isoflavone	Erysubin F	Outlier	100	256	n.a	[6]
56	Isoflavone	Gancaonin G	TE	16	45	2.6	[8]
57	Isoflavone	Glicoricone	TR	64	174	6.3	[8]
58	Isoflavone	Glisoflavone	TR	64	174	0.3	[8]
59	Isoflavone	Glycyrrhisoflavone	TR	64	181	6.1	[8]
60	Isoflavone	Isoangustone A	TE	16	38	3	[8]
61	Isoflavone	Isochandalone	-	>256	n.a.	n.a	[11]
62	Isoflavone	Isoalupalbigenin	TR	3	8	6	[21]
63	Isoflavone	Iso-osajin	-	>100	n.a.	n.a	This study
64	Isoflavone	Isowighteone	TE	32	95	5.1	[8]
65	Isoflavone	Licoisoflavone A	TE	25	71	5.0	This study
66	Isoflavone	Licoisoflavone B	TR	13	35	7.1	[9]
67	Isoflavone	Lupalbigenin	TR	4	10	5.5	[11]
68	Isoflavone	Lupiwighteone	-	>100	n.a.	n.a	This study
69	Isoflavone	Luteone	TR	25	71	2.1	This study
70	Isoflavone	Neobavaisoflavone	TR	38	116	8.1	This study
71	Isoflavone	Scadinone	-	>256	n.a.	n.a	[11]
72	Isoflavone	Semilicoisoflavone B	TR	64	182	4.5	[8]
73	Isoflavone	Strobiliferin	*(cr.2)	36	76	18	[22]
74	Isoflavone	Wighteone (Erythrinin B)	TR	16	46	2.6	This study
75	Pterocarpan	2-(dimethylallyl)-6a-hydroxyphaseollidin	TR	13	31	5.2	[13]
76	Pterocarpan	Anhydrotuberosin	-	>100	n.a.	n.a	This study

Table S4.1. Continued

ID	(Iso)flavonoid subclass	Name	Set	MIC (µg/mL)	MIC (µM)	% Prediction error	Ref.
77	Pterocarpan	Cristacarpan	TR	100	282	4.9	[3]
78	Pterocarpan	Erybraedin A/ 4-prenylphaseollidin	TR	3	8	5.8	[11,14]
79	Pterocarpan	Erystagallin A	TE	25	59	3	[10]
80	Pterocarpan	Erythribyssin A	TR	32	87	6.8	[20]
81	Pterocarpan	Eryzerin E	TR	25	59	2.8	[12]
82	Pterocarpan	Fuscacarpan A	-	>200	n.a.	n.a	[20]
83	Pterocarpan	Fuscacarpan B	-	>200	n.a.	n.a	[20]
84	Pterocarpan	Fuscacarpan C	-	>200	n.a.	n.a	[20]
85	Pterocarpan	Glyceofuran	-	>100	n.a.	n.a	This study
86	Pterocarpan	Glyceollidin II	TE	44	129	0.0	This study
87	Pterocarpan	Glyceollin I	Outlier	100	296	n.a	This study
88	Pterocarpan	Glyceollin II	TR	150	443	11.4	This study
89	Pterocarpan	Glyceollin III	Outlier	100	296	n.a	This study
90	Pterocarpan	Glyceollin IV	TR	44	123	3.8	This study
91	Pterocarpan	Glyceollin V	-	>100	n.a.	n.a	This study
92	Pterocarpan	Glycyrol	-	>128	n.a.	n.a	[5]
93	Pterocarpan	Orientanol B	TR	6	18	10.1	[10]
94	Pterocarpan	Orientanol C	TR	25	64	9	[10]
95	Pterocarpan	Phaseollidin	TR	50	154	9.3	[10]
96	Pterocarpan	Phaseollin	TR	25	78	1.7	[10]
97	Pterocarpan	Sandwicensin	TE	16	47	3.4	[20]
98	Pterocarpane	Dehydroglyceollidin II	TE	22	68	4.1	This study
99	Pterocarpane	Dehydroglyceollin I	TE	16	49	2.6	This study
100	Pterocarpane	Dehydroglyceollin II	TR	19	59	1.8	This study
101	Pterocarpane	Dehydroglyceollin III	-	>100	n.a.	n.a	This study
102	Pterocarpane	Dehydroglyceollin IV	TE	44	130	13.8	This study
103	Pterocarpane	Erypoeigin H	TR	13	39	1.8	[3]
104	Pterocarpane	Erystagallin A	TE	6	16	2.0	[10]
105	Pterocarpane	Eryvarin D	TR	25	74	4.8	[3]
106	Pterocarpane	Eryvarin W	TR	3	8	3.0	[16]

Table S4.2. List of descriptors

No.	Descriptors	Definition
1	<i>a_acc</i>	Number of hydrogen bond acceptor atoms (not counting acidic atoms but counting atoms that are both hydrogen bond donors and acceptors such as -OH).
2	<i>a_aro</i>	Number of aromatic atoms.
3	<i>a_donacc</i>	Number of hydrogen bond donor plus number of hydrogen bond acceptor atoms.
4	<i>a_ICM</i>	Atom information content (mean). This is the entropy of the element distribution in the molecule (including implicit hydrogens but not lone pair pseudo-atoms). Let n_i be the number of occurrences of atomic number I in the molecule. Let $p_i = n_i / n$ where n is the sum of the n_i . The value of <i>a_ICM</i> is the negative of the sum over all I of $p_i \log p_i$.
5	<i>ASA-</i>	Water accessible surface area of all atoms with negative partial charge (strictly less than 0).
6	<i>ASA_H</i>	Water accessible surface area of all hydrophobic ($ q_i < 0.2$) atoms.
7	<i>ASA_P</i>	Water accessible surface area of all polar ($ q_i \geq 0.2$) atoms.
8	<i>ASA+</i>	Water accessible surface area of all atoms with positive partial charge (strictly greater than 0).
9	<i>b_double</i>	Number of double bonds. Aromatic bonds are not considered to be double bonds.
10	<i>b_heavy</i>	Number of bonds between heavy atoms.
11	<i>b_rotN</i>	Number of rotatable bonds. A bond is rotatable if it has order 1, is not in a ring, and has at least two heavy neighbours.
12	<i>balabanJ</i>	Balaban's connectivity topological index.
13	<i>CASA-</i>	Negative charge weighted surface area, ASA- times max ($q_i < 0$).
14	<i>CASA+</i>	Positive charge weighted surface area, ASA+ times max ($q_i < 0$).
15	<i>chiral</i>	Number of chiral centres.
16	<i>DASA</i>	Absolute value of the difference between ASA+ and ASA-.
17	<i>dens</i>	Mass density: molecular weight divided by van der Waals volume as calculated in the <i>vol</i> descriptor.
18	<i>diameter</i>	Largest value in the distance matrix.
19	<i>dipole</i>	Dipole moment calculated from the partial charges of the molecule.
20	<i>E_ang</i>	Angle bend potential energy. In the Potential Setup panel, the term enable (Bonded) flag is ignored, but the term weight is applied.
21	<i>E_ele</i>	Electrostatic component of the potential energy. In the Potential Setup panel, the term enable flag is ignored, but the term weight is applied.
22	<i>E_oop</i>	Out-of-plane potential energy. In the Potential Setup panel, the term enable (Bonded) flag is ignored, but the term weight is applied.
23	<i>E_sol</i>	Solvation energy. In the Potential Setup panel, the term enable parameter (Solvation menu) is ignored, but the term weight is applied.
24	<i>E_str</i>	Bond stretch potential energy. In the Potential Setup panel, the term enable (Bonded) flag is ignored, but the term weight is applied.
25	<i>E_strain</i>	Local strain energy: the current energy minus the value of the energy at a near local minimum. The current energy is calculated as for the E descriptor. The local minimum energy is the value of the E descriptor after first performing an energy minimization. Current chirality is preserved and charges are left undisturbed during minimization. The structure in the dataset is not modified (results of the minimization are discarded).

Table S4.2. Continued

No.	Descriptors	Definition
26	<i>E_tor</i>	Torsion (proper and improper) potential energy. In the Potential Setup panel, the term enable (Bonded) flag is ignored, but the term weight is applied.
27	<i>E_vdw</i>	van der Waals component of the potential energy. In the Potential Setup panel, the term enable flag is ignored, but the term weight is applied.
28	<i>FASA-</i>	Fractional ASA- calculated as ASA- / ASA.
29	<i>FASA_H</i>	Fractional ASA_H calculated as ASA_H / ASA.
30	<i>FASA+</i>	Fractional ASA+ calculated as ASA+ / ASA.
31	<i>FCASA-</i>	Fractional CASA- calculated as CASA- / ASA.
32	<i>FCASA+</i>	Fractional CASA+ calculated as CASA+ / ASA.
33	<i>glob</i>	Globularity, or inverse condition number (smallest eigenvalue divided by the largest eigenvalue) of the covariance matrix of atomic coordinates. A value of 1 indicates a perfect sphere while a value of 0 indicates a two- or one-dimensional object.
34	<i>h_ema</i>	Sum of hydrogen bond acceptor strengths
35	<i>h_emd</i>	Sum of hydrogen bond donor strengths.
36	<i>h_emd_C</i>	Sum of hydrogen bond donor strengths of carbon atoms.
37	<i>h_logD</i>	The octanol/water distribution coefficient at pH 7 calculated as a state average: $\log \sum (10^{h_{\log Pi} - pCi})$.
38	<i>h_pavgQ</i>	The average total charge sum ($Q_i \cdot 10^{-pCi}$) where Q_i is the total formal charge of state i .
39	<i>h_pKa</i>	The pKa of the reaction that removes a proton from the ensemble of states with a hydrogen count equal to the input structure; 14 is reported if there are no states with fewer hydrogens than the input.
40	<i>h_pstrain</i>	The strain energy (kcal/mol) needed to convert all protonation states into the input protonation state: $(kT \ln 10) (pC1 + \log \sum (10^{-pCi}))$
41	<i>KierFlex</i>	Kier molecular flexibility index: $(KierA1) (KierA2) / n$
42	<i>lip_acc</i>	The number of O and N atoms.
43	<i>lip_don</i>	The number of OH and NH atoms
44	<i>logP(o/w)</i>	Log of the octanol/water partition coefficient (including implicit hydrogens). This property is calculated from a linear atom type model [LOGP 1998] with $r^2 = 0.931$, RMSE=0.393 on 1,827 molecules.
45	<i>logS</i>	Log of the aqueous solubility (mol/L). This property is calculated from an atom contribution linear atom type model [Hou 2004] with $r^2 = 0.90$, ~1,200 molecules.
46	<i>npr1</i>	Normalized PMI ratio $pmi1/pmi3$.
47	<i>npr2</i>	Normalized PMI ratio $pmi2/pmi3$.
48	<i>PC-</i>	Total negative partial charge: the sum of the negative q_i
49	<i>PEOE_PC-</i>	Total negative partial charge: the sum of the negative q_i . Q_{PC-} is identical to PC- which has been retained for compatibility.
50	<i>PEOE_RPC-</i>	Relative negative partial charge: the smallest negative q_i divided by the sum of the negative q_i . Q_{RPC-} is identical to RPC- which has been retained for compatibility.
51	<i>PEOE_RPC+</i>	Relative positive partial charge: the largest positive q_i divided by the sum of the positive q_i . Q_{RPC+} is identical to RPC+ which has been retained for compatibility.

Table S4.2. Continued

No.	Descriptors	Definition
52	PEOE_VSA_FHYD	Fractional hydrophobic van der Waals surface area. This is the sum of the v_i such that $ q_i $ is less than or equal to 0.2 divided by the total surface area. The v_i are calculated using a connection table approximation.
53	PEOE_VSA_FNEG	Fractional negative van der Waals surface area. This is the sum of the v_i such that q_i is negative divided by the total surface area. The v_i are calculated using a connection table approximation.
54	PEOE_VSA_HYD	Total hydrophobic van der Waals surface area. This is the sum of the v_i such that $ q_i $ is less than or equal to 0.2. The v_i are calculated using a connection table approximation.
55	PEOE_VSA_NEG	Total negative van der Waals surface area. This is the sum of the v_i such that q_i is negative. The v_i are calculated using a connection table approximation.
56	PEOE_VSA_POS	Total positive van der Waals surface area. This is the sum of the v_i such that q_i is non-negative. The v_i are calculated using a connection table approximation.
57	PEOE_VSA_PPOS	Total positive polar van der Waals surface area. This is the sum of the v_i such that q_i is greater than 0.2. The v_i are calculated using a connection table approximation.
58	PEOE_VSA+0	Sum of v_i where q_i is in the range [0.00,0.05).
59	PEOE_VSA+1	Sum of v_i where q_i is in the range [0.05,0.10).
60	PEOE_VSA+2	Sum of v_i where q_i is in the range [0.10,0.15).
61	PEOE_VSA-0	Sum of v_i where q_i is in the range [-0.05,0.00).
62	PEOE_VSA-1	Sum of v_i where q_i is in the range [-0.10,-0.05).
63	PM3_dipole	The dipole moment calculated using the PM3 Hamiltonian.
64	PM3_E	The total energy (kcal/mol) calculated using the PM3 Hamiltonian [MOPAC].
65	PM3_HF	The heat of formation (kcal/mol) calculated using the PM3 Hamiltonian [MOPAC].
66	PM3_IP	The ionization potential (kcal/mol) calculated using the PM3 Hamiltonian [MOPAC].
67	PM3_LUMO	The energy (eV) of the Lowest Unoccupied Molecular Orbital calculated using the PM3 Hamiltonian [MOPAC].
68	pmi1	First diagonal element of diagonalized moment of inertia tensor.
69	pmi3	Third diagonal element of diagonalized moment of inertia tensor.
70	radius	If r_i is the largest matrix entry in row i of the distance matrix D , then the radius is defined as the smallest of the r_i [Petitjean 1992].
71	rgyr	Radius of gyration.
72	rings	The number of rings.
73	RPC-	Relative negative partial charge: the smallest negative q_i divided by the sum of the negative q_i . Q_{RPC-} is identical to $RPC-$ which has been retained for compatibility.
74	RPC+	Relative positive partial charge: the largest positive q_i divided by the sum of the positive q_i . Q_{RPC+} is identical to $RPC+$ which has been retained for compatibility.

Table S4.2. Continued

No.	Descriptors	Definition
75	<i>SlogP</i>	Log of the octanol/water partition coefficient (including implicit hydrogens). This property is an atomic contribution model [Crippen 1999] that calculates logP from the given structure; i.e., the correct protonation state (washed structures). Results may vary from the logP(o/w) descriptor. The training set for SlogP was ~7000 structures.
76	<i>std_dim1</i>	Standard dimension 1: the square root of the largest eigenvalue of the covariance matrix of the atomic coordinates. A standard dimension is equivalent to the standard deviation along a principal component axis.
77	<i>std_dim2</i>	Standard dimension 2: the square root of the second largest eigenvalue of the covariance matrix of the atomic coordinates. A standard dimension is equivalent to the standard deviation along a principal component axis.
78	<i>std_dim3</i>	Standard dimension 3: the square root of the third largest eigenvalue of the covariance matrix of the atomic coordinates. A standard dimension is equivalent to the standard deviation along a principal component axis.
79	<i>vol</i>	van der Waals volume calculated using a grid approximation (spacing 0.75 Å).
80	<i>vsa_acc</i>	Approximation to the sum of VDW surface areas (Å ²) of pure hydrogen bond acceptors (not counting atoms that are both hydrogen bond donors and acceptors such as -OH).
81	<i>vsa_pol</i>	Approximation to the sum of VDW surface areas (Å ²) of polar atoms (atoms that are both hydrogen bond donors and acceptors), such as -OH.
82	<i>vsurf_A</i>	Amphiphilic moment
83	<i>vsurf_CP</i>	Critical packing parameter
84	<i>vsurf_CW2</i>	Capacity factor at -0.5 kcal/mol.
85	<i>vsurf_CW3</i>	Capacity factor at -1.0 kcal/mol.
86	<i>vsurf_D4</i>	Hydrophobic volume at -0.8 kcal/mol.
87	<i>vsurf_D6</i>	Hydrophobic volume at -1.2 kcal/mol.
88	<i>vsurf_D7</i>	Hydrophobic volume at -1.4 kcal/mol.
89	<i>vsurf_D8</i>	Hydrophobic volume at -1.6 kcal/mol.
90	<i>vsurf_DD12</i>	Contact distances. <i>vsurf_EDmin1</i> , <i>vsurf_EDmin2</i> distance.
91	<i>vsurf_DD13</i>	<i>vsurf_EDmin1</i> , <i>vsurf_EDmin3</i> distance.
92	<i>vsurf_DD23</i>	<i>vsurf_EDmin2</i> , <i>vsurf_EDmin3</i> distance.
93	<i>vsurf_DW12</i>	<i>vsurf_EWmin1</i> , <i>vsurf_EWmin2</i> distance.
94	<i>vsurf_DW13</i>	<i>vsurf_EWmin1</i> , <i>vsurf_EWmin3</i> distance.
95	<i>vsurf_DW23</i>	<i>vsurf_EWmin2</i> , <i>vsurf_EWmin3</i> distance.
96	<i>vsurf_EDmin1</i>	Lowest hydrophobic energy.
97	<i>vsurf_EWmin1</i>	Lowest hydrophilic energy.
98	<i>vsurf_G</i>	Surface globularity
99	<i>vsurf_HB1</i>	H-bond donor capacity at -0.2 kcal/mol.
100	<i>vsurf_HB5</i>	H-bond donor capacity at -0.5 kcal/mol.
101	<i>vsurf_HL1</i>	First hydrophilic-lipophilic balance.
102	<i>vsurf_ID1</i>	Hydrophobic interaction energy (integy) moment at -0.2 kcal/mol.

Table S4.2. Continued

No.	Descriptors	Definition
103	<i>vsurf_ID4</i>	Hydrophobic integrity moment at -0.8 kcal/mol.
104	<i>vsurf_ID6</i>	Hydrophobic integrity moment at -1.2 kcal/mol.
105	<i>vsurf_ID7</i>	Hydrophobic integrity moment at -1.4 kcal/mol.
106	<i>vsurf_ID8</i>	Hydrophobic integrity moment at -1.6 kcal/mol.
107	<i>vsurf_IW1</i>	Hydrophilic integrity moment at -0.2 kcal/mol.
108	<i>vsurf_IW2</i>	Hydrophilic integrity moment at -0.5 kcal/mol.
109	<i>vsurf_IW3</i>	Hydrophilic integrity moment at -1.0 kcal/mol.
110	<i>vsurf_IW6</i>	Hydrophilic integrity moment at -4.0 kcal/mol.
111	<i>vsurf_IW7</i>	Hydrophilic integrity moment at -5.0 kcal/mol.
112	<i>vsurf_R</i>	Surface rugosity
113	<i>vsurf_W1</i>	Hydrophilic volume at -0.2 kcal/mol.
114	<i>vsurf_W3</i>	Hydrophilic volume at -1.0 kcal/mol.
115	<i>vsurf_W7</i>	Hydrophilic volume at -5.0 kcal/mol.
116	<i>vsurf_Wp1</i>	Polar volume
117	<i>vsurf_Wp2</i>	Polar volume at -0.5 kcal/mol.
118	<i>vsurf_Wp3</i>	Polar volume at -1.0 kcal/mol.
119	<i>vsurf_Wp4</i>	Polar volume at -2.0 kcal/mol.
120	<i>vsurf_Wp6</i>	Polar volume at -4.0 kcal/mol.
121	<i>vsurf_Wp7</i>	Polar volume at -5.0 kcal/mol.

Table S4.3. Prenylated (iso)flavonoids with their respective reported and predicted activity (MIC, µg/mL) against Gram -positive bacteria, other than MRSA. The structures of compounds **G1-G39** can be found in **Figure S4.5**. Molecules of which the level of activity (high, moderate, low) was not predicted correctly by the corresponding model are highlighted in red. Di-prenylated (iso)flavonoids are indicated in **bold**. Molecules in grey have been also tested against MRSA (**Table S4.1**). Molecules are sorted based on subclass and ordered alphabetically within each subclass.

ID	(Iso)flavonoid subclass	Name	Highest reported MIC	Predicted MIC	Gram+ bacterium	Ref.
5	2-aryl/benzofuran	Moracin C	13	12	<i>B. subtilis</i> / <i>S. aureus</i> / MRSA	[9]
7	3-arylcoumarin	Glycycoumarin	16	36	<i>S. aureus</i> / MRSA	[8]
8	3-arylcoumarin	Glycytrin	128	40	<i>B. subtilis</i> / <i>S. aureus</i> / MRSA	[8,10]
G1	Flavanone	(2S)-5,7-dihydroxy-4'-methoxy-8-prenylflavanone	32	47	<i>B. subtilis</i>	[24]
G2	Flavanone	2(S)-5'-(1''',1''',-dimethylallyl)-8-(3'',3''-dimethylallyl)-2',4',5,7-tetrahydroxyflavanone	8	28	<i>S. aureus</i>	[25]
G3	Flavanone	5-Dehydroxyparatocarpin K	12	35	<i>S. epidermis</i>	[26]
G4	Flavanone	5-Methylisophorafuranone B (isoxanthohumol)	20	40	<i>S. epidermis</i>	[27]
G5	Flavanone	Abyssinone I	25	32	<i>B. subtilis</i> / <i>S. aureus</i>	[28]
G6	Flavanone	Abyssinone II	50	23	<i>B. subtilis</i> / <i>S. aureus</i>	[28]
G7	Flavanone	Abyssinone III	100	11	<i>B. subtilis</i> / <i>S. aureus</i>	[28]
G8	Flavanone	Abyssinone IV	25	10	<i>B. subtilis</i> / <i>S. aureus</i>	[28]
G9	Flavanone	Abyssinone V	50	15	<i>B. subtilis</i> / <i>S. aureus</i>	[28]
G10	Flavanone	Bavachin (coryfolin)	12	23	<i>S. epidermis</i>	[26]
G11	Flavanone	Bavachinin	6	20	<i>S. epidermis</i>	[26]
G12	Flavanone	Burtinone	62	107	<i>S. aureus</i>	[29]
G13	Flavanone	Citflavanone	>100	59	<i>E. faecalis</i>	[30]
G14	Flavanone	Erythrinenegalone	50	23	<i>E. faecalis</i>	[30]
G15	Flavanone	Kushenol S	5	37	<i>B. subtilis</i>	[31]
G16	Flavanone	Kushenol V	10	30	<i>B. subtilis</i>	[31]
G17	Flavanone	Leachianone G	2	27	<i>B. subtilis</i>	[31]
G18	Flavanone	Lonchocarpol A	6	22	<i>E. faecalis</i>	[30]
G19	Flavanone	Lupinifolin	6	30	<i>B. subtilis</i> / <i>E. faecalis</i>	[30]

Table S4.3. Continued

ID	(Iso)flavonoid subclass	Name	Highest reported MIC	Predicted MIC	Gram+ bacterium	Ref.
G20	Flavanone	Macatrighocarpin A	10	23	<i>B. subtilis</i>	[32]
G21	Flavanone	Macatrighocarpin B	18	21	<i>B. subtilis</i>	[32]
20	Isoflavan	Eryzerin C	10	20	<i>B. subtilis</i> / <i>S. aureus</i> / <i>S. epidermis</i> / MRSA	[33]
22	Isoflavan	Glabridin	31	20	<i>S. aureus</i> / <i>S. mutans</i> / <i>B. subtilis</i> / <i>E. faecalis</i> / MRSA	[8,10,34]
24	Isoflavan	Glyasperin D	16	21	<i>B. subtilis</i> / <i>S. aureus</i> / MRSA	[8,10]
27	Isoflavan	Licoricidin	16	14	<i>B. subtilis</i> / <i>S. aureus</i> / MRSA	[8,10]
G22	Isoflavan	Licorisoflavan A (5-O-Methyllicoricidin)	4	15	<i>S. mutans</i>	[24]
31	Isoflavanone	3'-dimethylallyl-kievitone	8	11	<i>S. aureus</i> / MRSA	[8]
G23	Isoflavanone	Dalversinol A	31	13	<i>S. aureus</i>	[25]
40	Isoflavanone	Glicoisoflavanone	32	30	<i>S. aureus</i> / MRSA	[8]
41	Isoflavanone	Glyasperin F	32	76	<i>S. aureus</i> / MRSA	[8]
42	Isoflavanone	Glycyrrhisoflavanone	32	57	<i>S. aureus</i> / MRSA	[8]
43	Isoflavanone	Licoisoflavanone	32	43	<i>S. aureus</i> / MRSA	[8]
G24	Isoflavanone	Lysisteisoflavanone	62	39	<i>S. aureus</i>	[33]
G25	Isoflavanone	Sophoraisoflavanone A	20	57	<i>S. epidermis</i>	[27]
49	Isoflavene	Glabrene	13	20	<i>B. subtilis</i> / MRSA	[10]
50	Isoflavone	6,8-Diprenyl genistein	2	8	<i>S. mutans</i> / <i>S. aureus</i> / MRSA	[8,35]
G26	Isoflavone	Alpinumisoflavanone	31	34	<i>S. aureus</i>	[33]
G27	Isoflavone	Auriculasin	2	15	<i>B. subtilis</i>	[36]
G28	Isoflavone	Auriculatin	2	11	<i>B. subtilis</i>	[36]
52	Isoflavone	Chandalone	128	10	<i>S. aureus</i> / MRSA	[11]
53	Isoflavone	Derrisisoflavanone	16	8	<i>S. aureus</i> / MRSA	[11]
G29	Isoflavone	Erythrinin A	6	24	<i>S. epidermis</i>	[26]
56	Isoflavone	Gancaonin G	125	21	<i>S. mutans</i> / <i>S. aureus</i>	[8,35]
57	Isoflavone	Glicoricone	64	37	<i>S. aureus</i> / MRSA	[8]
58	Isoflavone	Glisoflavanone	32	66	<i>S. aureus</i> / MRSA	[8]
59	Isoflavone	Glycyrrhisoflavanone	32	38	<i>S. aureus</i> / MRSA	[8]

Table S4.3. Continued

ID	(Iso)flavonoid subclass	Name	Highest reported MIC	Predicted MIC	Gram+ bacterium	Ref.
60	Isoflavone	Isoangustone A	16	12	<i>S. aureus</i> / MRSA	[8]
64	Isoflavone	Isowighteone	16	20	<i>S. aureus</i> / MRSA	[8]
66	Isoflavone	Licoisoflavone B	13	26	<i>S. aureus</i> / MRSA	[10]
67	Isoflavone	Lupalbigenin	4	8	<i>S. aureus</i> / MRSA	[11]
G30	Isoflavone	Millexatin F	2	11	<i>B. subtilis</i>	[36]
G31	Isoflavone	Scandenone	8	11	<i>B. subtilis</i>	[37]
72	Isoflavone	Semilicoisoflavone B	32	44	<i>S. aureus</i>	[8]
G32	Pterocarpan	1-Methoxyficifolinol	4	14	<i>S. mutans</i>	[24]
77	Pterocarpan	Cristacarpin	412	67	<i>B. subtilis</i> / <i>S. aureus</i> / <i>S. epidermis</i> / MRSA	[23,33]
78	Pterocarpan	Erybraedin A/ 4-prenylphaseollidin	2	6	<i>B. subtilis</i> / <i>S. aureus</i> / <i>S. epidermis</i> / MRSA	[33]
G33	Pterocarpan	Erybraedin B	12	8	<i>S. aureus</i>	[38]
G34	Pterocarpan	Erybraedin C	12	6	<i>S. aureus</i>	[38]
G35	Pterocarpan	Erycristin	6	8	<i>S. aureus</i>	[38]
80	Pterocarpan	Erythribyssin A	64	60	<i>S. aureus</i> / MRSA	[23]
G36	Pterocarpan	Erythrabysyn II	3	7	<i>B. subtilis</i>	[28]
G37	Pterocarpan	Isoneorutaneol	25	30	<i>S. aureus</i>	[38]
95	Pterocarpan	Phaseollidin	50	22	<i>S. aureus</i> / <i>B. subtilis</i> / MRSA	[28]
96	Pterocarpan	Phaseollin	13	29	<i>S. aureus</i> / <i>B. subtilis</i> / MRSA	[28]
97	Pterocarpan	Sandwicensin	100	22	<i>S. aureus</i> / <i>B. subtilis</i> / <i>E. faecalis</i> / MRSA	[23,30]
105	Pterocarpene	Eryvarin D	4	16	<i>S. aureus</i> / MRSA	[23]
G38	Pterocarpene	Glycyrrhizol A	1	7	<i>S. mutans</i>	[35]
G39	Pterocarpene	Glycyrrhizol B	32	17	<i>S. mutans</i>	[35]

Table S4.4. Most frequent descriptors used in the top QSAR models and their significance (n: 2 - 7).

Descriptor	<i>p</i>-value
<i>h_emd_C</i>	2.2e^{-04} - 1.7e^{-02}
<i>vsurf_D4</i>	1.0 - 1.9e^{-10}
<i>PEOE_VSA_PPOS</i>	3.6e^{-06} - 1.4e^{-05}
<i>vsurf_CW3</i>	4.7e^{-13} - 4.1e^{-09}
<i>vsurf_IW7</i>	3.5e^{-04} - 3.9e^{-01}
<i>E_vdw</i>	5.8e^{-03}
<i>h_pavgQ</i>	1.7e^{-06} - 1.2e^{-04}
<i>PEOE_VSA+2</i>	4.2e^{-03} - 1.6e^{-01}
<i>vsurf_DD12</i>	4.7e^{-02} - 1.5e^{-01}
<i>PM3_IP</i>	7.1e^{-02}

Table S4.5. Prenylated (iso)flavonoids mapping all features of the pharmacophore model of MRSA. ^a RMSD is the root-mean-square deviation which determines the quality of fitting of each prenylated (iso)flavonoid to the pharmacophore features. ^b True (+) and false (-) positive. Di-prenylated (iso)flavonoids are indicated in **bold**.

ID	(Iso)flavonoid subclass	Name	MIC (µg/mL)	RMSD ^a	Outcome ^b
3	2-arylbenzofuran	Eryvarin U	12	0.64	-
4	2-arylbenzofuran	Licocoumarone	16	0.46	+
5	2-arylbenzofuran	Moracin C	12	0.5	+
7	3-arylcoumarin	Glycycoumarin	16	0.76	+
8	3-arylcoumarin	Glycyrin	128	0.62	+
16	Isoflavan	3'-OH-4'-O-methylglabridin	16	0.68	+
18	Isoflavan	Eryvarin C	25	0.4	+
21	Isoflavan	Eryzerin D	12	0.4	+
22	Isoflavan	Glabridin	16	0.63	+
23	Isoflavan	Glyasperin C	16	0.63	+
24	Isoflavan	Glyasperin D	16	0.78	+
25	Isoflavan	Hispaglabridin A	50	0.64	+
27	Isoflavan	Licoricidin	16	0.64	-
28	Isoflavan	Phaseollin isoflavan	50	0.41	-
35	Isoflavanone	Eryvarin V	25	0.86	+
46	Isoflavanone	Prenyl-costarone	50	0.68	-
49	Isoflavene	Glabrene	25	0.39	+
50	Isoflavone	6,8-diprenylgenistein	9	0.66	+
52	Isoflavone	Chandalone	16	0.56	+
53	Isoflavone	Derrisoflavone A	4	0.68	+
56	Isoflavone	Gancaonin G	16	0.73	+
60	Isoflavone	Isoangustone A	16	0.7	+
62	Isoflavone	Isolupalbigenin	3	0.69	-
65	Isoflavone	Licoisoflavone A	25	0.59	+
66	Isoflavone	Licoisoflavone B	12	0.21	+
67	Isoflavone	Lupalbigenin	4	0.66	-
69	Isoflavone	Luteone	25	0.65	+
72	Isoflavone	Semilicoisoflavone B	64	0.3	-
74	Isoflavone	Wighteone/Erythrinin B	16	0.68	+
75	Pterocarpan	2-(dimethylallyl)-6a-hydroxyphaseollidin	12	0.39	+
77	Pterocarpan	Cristacarpin/Erythrabissin I	100	0.59	+
79	Pterocarpan	Erystagallin A	25	0.59	+
81	Pterocarpan	Eryzerin E	25	0.75	+
96	Pterocarpan	Phaseollin	25	0.92	+
97	Pterocarpan	Sandwicensin	16	0.6	+
99	Pterocarpene	Dehydroglyceollin I	16	0.63	-
105	Pterocarpene	Eryvarin D	25	0.6	+

Table S4.6. Prenylated (iso)flavonoids mapping all features of the pharmacophore model of *L. monocytogenes* [39]. ^a RMSD is the root-mean-square deviation which determines the quality of fitting of each prenylated (iso)flavonoid to the pharmacophore features. ^b True (+) and false (-) positive. Di-prenylated (iso)flavonoids are indicated in **bold**.

ID	(Iso)flavonoid subclass	Name	MIC (µg/mL)	RMSD ^a	Outcome ^b
3	2-arylbenzofuran	Eryvarin U	12	0.72	+
5	2-arylbenzofuran	Moracin C	12	0.73	+
7	3-arylcoumarin	Glycycomarin	16	0.65	+
8	3-arylcoumarin	Glycyrin	128	0.68	-
12	Flavanone	6-prenyl-naringenin	38	0.73	-
16	Isoflavan	3'-OH-4'-O-methylglabridin	16	0.52	+
17	Isoflavan	4'-O-methylglabridin	10	0.52	+
20	Isoflavan	Eryzerin C	6	0.58	+
22	Isoflavan	Glabridin	16	0.52	+
23	Isoflavan	Glyasperin C	16	0.7	+
24	Isoflavan	Glyasperin D	16	0.48	+
25	Isoflavan	Hispaglabridin A	50	0.51	-
27	Isoflavan	Licoricidin	16	0.7	+
29	Isoflavan	Phaseollin isoflavan	50	0.53	-
40	Isoflavanone	Glicoisoflavanone	64	0.47	-
45	Isoflavanone	Orientanol F	12	0.75	+
48	Isoflavene	Erypogin A	25	0.56	+
50	Isoflavone	6,8-diprenylgenistein	9	0.25	+
52	Isoflavone	Chandalone	16	0.36	+
53	Isoflavone	Derrisisoflavone A	4	0.55	+
56	Isoflavone	Gancaonin G	16	0.42	+
57	Isoflavone	Glicoricone	64	0.66	-
58	Isoflavone	Glisoflavone	64	0.82	-
60	Isoflavone	Isoangustone A	16	0.26	+
65	Isoflavone	Licoisoflavone A	25	0.47	+
66	Isoflavone	Licoisoflavone B	12	0.45	+
67	Isoflavone	Lupalbigenin	4	0.25	+
69	Isoflavone	Luteone	25	0.37	+
74	Isoflavone	Wighteone/Erythrinin B	16	0.33	+
78	Pterocarpan	Erybraedin A/ 4-prenylphaseollidin	3	0.52	+
81	Pterocarpan	Eryzerin E	25	0.51	+
90	Pterocarpan	Glyceollin IV	44	0.52	-
93	Pterocarpan	Orientanol B	6	0.66	+
102	Pterocarpene	Dehydroglyceollin IV	44	0.49	-

4.8.3. Supplementary references

- [1] Gramatica, P. Principles of QSAR models validation: internal and external. *QSAR & combinatorial science* **26**, 694-701 (2007).
- [2] Keepers, T. R., Gomez, M., Biek, D., Critchley, I. & Krause, K. M. Effect of *in vitro* testing parameters on ceftazidime-avibactam minimum inhibitory concentrations. *International Scholarly Research Notices* **2015** (2015).
- [3] Brennan-Krohn, T., Smith, K. P. & Kirby, J. E. The poisoned well: enhancing the predictive value of antimicrobial susceptibility testing in the era of multidrug resistance. *Journal of Clinical Microbiology* **55**, 2304-2308 (2017).
- [4] Li, J., Beuerman, R. W. & Verma, C. S. Molecular insights into the membrane affinities of model hydrophobes. *ACS Omega* **3**, 2498-2507 (2018).
- [5] Tanaka, H., Sudo, M., Kawamura, T., Sato, M., Yamaguchi, R., Fukai, T., Sakai, E. & Tanaka, N. Antibacterial constituents from the roots of *Erythrina herbacea* against methicillin-resistant *Staphylococcus aureus*. *Planta Medica* **76**, 916-919 (2010).
- [6] Tanaka, H., Sato, M., Oh-Uchi, T., Yamaguchi, R., Etoh, H., Shimizu, H., Sako, M. & Takeuchi, H. Antibacterial properties of a new isoflavonoid from *Erythrina poeppigiana* against methicillin-resistant *Staphylococcus aureus*. *Phytomedicine* **11**, 331-337 (2004).
- [7] Tanaka, H., Sudo, M. & Hirata, M. Two new isoflavonoids and a new 2-arylbenzofuran from the roots of *Erythrina variegata*. *Heterocycles* **65**, 871-877 (2005).
- [8] Hatano, T., Shintani, Y., Aga, Y., Shiota, S., Tsuchiya, T. & Yoshida, T. Phenolic constituents of licorice. VIII. Structures of glicophenone and glicoisoflavanone, and effects of licorice phenolics on methicillin-resistant *Staphylococcus aureus*. *Chemical & Pharmaceutical Bulletin* **48**, 1286-1292 (2000).
- [9] Fukai, T., Kaitou, K. & Terada, S. Antimicrobial activity of 2-arylbenzofurans from *Morus* species against methicillin-resistant *Staphylococcus aureus*. *Fitoterapia* **76**, 708-711 (2005).
- [10] Fukai, T., Marumo, A., Kaitou, K., Kanda, T., Terada, S. & Nomura, T. Antimicrobial activity of licorice flavonoids against methicillin-resistant *Staphylococcus aureus*. *Fitoterapia* **73**, 536-539 (2002).
- [11] Mahabusarakam, W., Deachathai, S., Phongpaichit, S., Jansakul, C. & Taylor, W. A benzil and isoflavone derivatives from *Derris scandens* Benth. *Phytochemistry* **65**, 1185-1191 (2004).
- [12] Mun, S.-H., Kang, O.-H., Joung, D.-K., Kim, S.-B., Seo, Y.-S., Choi, J.-G., Lee, Y.-S., Cha, S.-W., Ahn, Y.-S. & Han, S.-H. Combination therapy of sophoraflavanone B against MRSA: *in vitro* synergy testing. *Evidence-Based Complementary and Alternative Medicine* **2013** (2013).
- [13] Tanaka, H., Sato, M., Fujiwara, S., Hirata, M., Etoh, H. & Takeuchi, H. Antibacterial activity of isoflavonoids isolated from *Erythrina variegata* against methicillin-resistant *Staphylococcus aureus*. *Letters in Applied Microbiology* **35**, 494-498 (2002).
- [14] Sato, M., Tanaka, H., Oh-Uchi, T., Fukai, T., Etoh, H. & Yamaguchi, R. Antibacterial activity of phytochemicals isolated from *Erythrina zeyheri* against vancomycin-resistant *enterococci* and their combinations with vancomycin. *Phytotherapy Research: An International Journal Devoted to Pharmacological and Toxicological Evaluation of Natural Product Derivatives* **18**, 906-910 (2004).
- [15] Tanaka, H., Oh-Uchi, T., Etoh, H., Sako, M., Asai, F., Fukai, T., Sato, M., Murata, J. & Tateishi, Y. Isoflavonoids from roots of *Erythrina zeyheri*. *Phytochemistry* **64**, 753-758 (2003).
- [16] Tanaka, H., Atsumi, I., Hasegawa, M., Hirata, M., Sakai, T., Sato, M., Yamaguchi, R., Tateishi, Y., Tanaka, T. & Fukai, T. Two new isoflavanones from the roots of *Erythrina variegata*. *Natural Product Communications* **10**, 1934578X1501000330 (2015).

- [17] Sato, M., Tanaka, H., Yamaguchi, R., Kato, K. & Etoh, H. Synergistic effects of mupirocin and an isoflavanone isolated from *Erythrina variegata* on growth and recovery of methicillin-resistant *Staphylococcus aureus*. *International journal of antimicrobial agents* **24**, 241-246 (2004).
- [18] Tanaka, H., Hattori, H., Oh-Uchi, T., Sato, M., Sako, M., Tateishi, Y. & Rizwani, G. H. Three new isoflavanones from *Erythrina costaricensis*. *Natural Product Research* **23**, 1089-1094 (2009).
- [19] Tanaka, H., Atsumi, I., Shiota, O., Sekita, S., Sakai, E., Sato, M., Murata, J., Murata, H., Darnaedi, D. & Chen, I. S. Three new constituents from the roots of *Erythrina variegata* and their antibacterial activity against methicillin-resistant *Staphylococcus aureus*. *Chemistry & biodiversity* **8**, 476-482 (2011).
- [20] Sato, M., Tanaka, H., Yamaguchi, R., Oh-Uchi, T. & Etoh, H. *Erythrina poeppigiana*-derived phytochemical exhibiting antimicrobial activity against *Candida albicans* and methicillin-resistant *Staphylococcus aureus*. *Letters in Applied Microbiology* **37**, 81-85 (2003).
- [21] Sato, M., Tanaka, H., Tani, N., Nagayama, M. & Yamaguchi, R. Different antibacterial actions of isoflavones isolated from *Erythrina poeppigiana* against methicillin-resistant *Staphylococcus aureus*. *Letters in Applied Microbiology* **43**, 243-248 (2006).
- [22] Madan, S., Singh, G. N., Kohli, K., Ali, M., Kumar, Y., Singh, R. M. & Prakash, O. Isoflavonoids from *Flemingia strobilifera* (L) R. Br. roots. *Acta Poloniae Pharmaceutica* **66**, 297-303 (2009).
- [23] Innok, P., Rukachaisirikul, T., Phongpaichit, S. & Suksamrarn, A. Fuscacarpans A-C, new pterocarpanes from the stems of *Erythrina fusca*. *Fitoterapia* **81**, 518-523 (2010).
- [24] Inui, S., Hosoya, T., Shimamura, Y., Masuda, S., Ogawa, T., Kobayashi, H., Shirafuji, K., Moli, R. T., Kozono, I. & Shin-ya, K. Solophenols B-D and Solomonin: New prenylated polyphenols isolated from propolis collected from the solomon islands and their antibacterial activity. *Journal of agricultural and food chemistry* **60**, 11765-11770 (2012).
- [25] Belofsky, G., Percivill, D., Lewis, K., Tegos, G. P. & Ekart, J. Phenolic metabolites of *Dalea versicolor* that enhance antibiotic activity against model pathogenic bacteria. *Journal of natural products* **67**, 481-484 (2004).
- [26] Yin, S., Fan, C.-Q., Wang, Y., Dong, L. & Yue, J.-M. Antibacterial prenylflavone derivatives from *Psoralea corylifolia*, and their structure-activity relationship study. *Bioorganic & Medicinal Chemistry* **12**, 4387-4392 (2004).
- [27] Sohn, H. Y., Son, K. H., Kwon, C. S., Kwon, G. S. & Kang, S. S. Antimicrobial and cytotoxic activity of 18 prenylated flavonoids isolated from medicinal plants: *Morus alba* L., *Morus mongolica* Schneider, *Broussonetia papyrifera* (L.) Vent, *Sophora flavescens* Ait and *Echinosophora koreensis* Nakai. *Phytomedicine* **11**, 666-672 (2004).
- [28] Taniguchi, M. & Kubo, I. Ethnobotanical drug discovery based on medicine men's trials in the African savanna: screening of east African plants for antimicrobial activity II. *Journal of Natural Products* **56**, 1539-1546 (1993).
- [29] Chukwujekwu, J., Van Heerden, F. & Van Staden, J. Antibacterial activity of flavonoids from the stem bark of *Erythrina caffra* thunb. *Phytotherapy Research* **25**, 46-48 (2011).
- [30] Khaomek, P., Ruangrunsi, N., Saifah, E., Sriubolmas, N., Ichino, C., Kiyohara, H. & Yamada, H. A new pterocarpan from *Erythrina fusca*. *Heterocycles* **63**, 879-884 (2004).
- [31] Kuroyanagi, M., Arakawa, T., Hirayama, Y. & Hayashi, T. Antibacterial and antiandrogen flavonoids from *Sophora flavescens*. *Journal of natural products* **62**, 1595-1599 (1999).
- [32] Fareza, M. S., Syah, Y. M., Mujahidin, D., Juliawaty, L. D. & Kurniasih, I. Antibacterial flavanones and dihydrochalcones from *Macaranga trichocarpa*. *Zeitschrift für Naturforschung C* **69**, 375-380 (2014).

- [33] Sadgrove, N. J., Oliveira, T. B., Khumalo, G. P., Vuuren, S. F. v. & van Wyk, B.-E. Antimicrobial isoflavones and derivatives from *Erythrina* (Fabaceae): structure activity perspective (sar & qsar) on experimental and mined values against *Staphylococcus Aureus*. *Antibiotics* **9**, 223 (2020).
- [34] Gupta, V. K., Fatima, A., Faridi, U., Negi, A. S., Shanker, K., Kumar, J., Rahuja, N., Luqman, S., Sisodia, B. S. & Saikia, D. Antimicrobial potential of *Glycyrrhiza glabra* roots. *Journal of ethnopharmacology* **116**, 377-380 (2008).
- [35] He, J., Chen, L., Heber, D., Shi, W. & Lu, Q.-Y. Antibacterial Compounds from *Glycyrrhiza uralensis*. *Journal of natural products* **69**, 121-124 (2006).
- [36] Raksat, A., Maneerat, W., Andersen, R. J., Pyne, S. G. & Laphookhieo, S. Antibacterial prenylated isoflavonoids from the stems of *Millettia extensa*. *Journal of Natural Products* **81**, 1835-1840 (2018).
- [37] Özçelik, B., Orhan, I. & Toker, G. Antiviral and antimicrobial assessment of some selected flavonoids. *Zeitschrift für Naturforschung C* **61**, 632-638 (2006).
- [38] Mitscher, L. A., Okwute, S. K., Gollapudi, S. R., Drake, S. & Avona, E. Antimicrobial pterocarpanes of Nigerian *Erythrina mildbraedii*. *Phytochemistry* **27**, 3449-3452 (1988).
- [39] Araya-Cloutier, C., Vincken, J.-P., van de Schans, M. G., Hageman, J., Schaftenaar, G., den Besten, H. M. & Gruppen, H. QSAR-based molecular signatures of prenylated (iso) flavonoids underlying antimicrobial potency against and membrane-disruption in Gram positive and Gram negative bacteria. *Scientific Reports* **8**, 9267 (2018).

CHAPTER 5

Prenylated (iso)flavonoids as antifungal agents against the food spoiler *Zygosaccharomyces parabailii*

Zygosaccharomyces bailii is one of the most troublesome spoilage yeasts of acidic food products. *Z. bailii* shows resistance towards the traditional food preservatives, weak organic acids. Although some natural antimicrobial agents have been explored as promising alternatives, none of them is active against *Z. bailii* (MIC ≥ 50 $\mu\text{g/mL}$). Prenylated isoflavonoids were investigated for their antifungal properties, including potency and mode of action. The mono-prenylated isoflavonoids, wighteone and glabridin showed fungicidal concentrations of 6.25 $\mu\text{g/mL}$ (18 μM) and 12.5 $\mu\text{g/mL}$ (39 μM), respectively, at the optimal growth pH of the yeast (6.5). Interestingly, the di-prenylated analogues of wighteone and glabridin did not inhibit at all *Z. parabailii* at the highest concentration tested (MIC $\gg 25$ $\mu\text{g/mL}$) at same pH. Furthermore, wighteone and glabridin were found to be 20-40 x more potent (on weight basis) than sorbic acid (MFC 550 $\mu\text{g/mL}$, 4.9 mM) at pH 4.0. Active mono-prenylated isoflavonoids induced killing within 15 min, suggesting potential membrane activity. Membrane permeabilization by these molecules was confirmed by propidium iodide uptake and TEM imaging. Membrane permeabilization was accompanied with leakage of intracellular material. Molecular properties such as the electrostatic energy potential and the hydrophobic integrity moment were correlated to activity through a binary classification quantitative structure-activity relationship (QSAR) model. Altogether, mono-prenylated isoflavonoids can serve as highly potent, novel and natural antifungals against *Z. parabailii* acting by severely compromising the membrane integrity.

Based on: Kalli, S.; Araya-Cloutier, C.; Chapman, J.; Sanders, J-W.; Vincken, J.-P., Prenylated (iso)flavonoids as antifungal agents against the food spoiler *Zygosaccharomyces parabailii*. **Submitted for publication.**

5.1. Introduction

Spoilage yeasts constitute one of the most important challenges in food and drink preservation. The *Zygosaccharomyces bailii* sensu lato clade is probably the most troublesome yeast species complex (Group 1) [1]. This species complex comprises *Zygosaccharomyces bailii* together with two recently revealed, phylogenetically related species (hybrids), namely *Z. parabailii* and *Z. pseudobailii* [2]. *Z. bailii* is strongly associated with spoilage of foods with a high sugar content and/or acidic foods e.g. fruit juices and sauces (pH 3.0-4.0) [3,4], and it is also known for its resistance towards cleaning agents and disinfectants (high concentration of ethanol (> 15% v/v)) [1], impeding the cleaning of food-processing equipment [5,6].

Weak organic acids such as sorbic, acetic and lactic acid are typically used to control the growth of *Z. bailii* [3,7]. They are known to inhibit microbial growth primarily via cytoplasmic acidification [8-11] but other fundamentally different actions have also been proposed [12-15]. *Z. bailii* shows extreme resistance towards them. In particular, *Z. bailii* is approximately 3 times more resistant to acetic and lactic acid than the model yeast, *Saccharomyces cerevisiae* [16-18]. This enhanced resistance has been hypothesized to develop due to (i) cell heterogeneity (preservative heteroresistance), i.e. the ability of a few hyper-resistant cells to cause spoilage [16,19,20], (ii) degradation and metabolism of weak organic acids by the yeast, especially in the presence of sugars [21] and (iii) the proposed efflux of weak organic acids due to the presence of a sorbate pump [22]. Therefore, high amounts of weak organic acids are needed to ensure food safety, but this is prohibited by law and unacceptable to consumers due to the safety complications being associated with them [23]. For example, the limit concentrations approved for use of sorbic acid range from 0.5 to 2 g/L [24] (4.5 to 18 μ M), depending on the food product, but over four times higher concentrations are required to inhibit the growth of *Z. parabailii* [16]. In addition, high concentrations of sorbic acid are associated with strong and undesirable fatty acid odor [25].

Taken together, this indicates that alternative, effective food preservatives which are also well-perceived by consumers, are needed. Some natural compounds have been tested against *Z. bailii*. Octanoic acid, a structural analogue of sorbic acid, has shown a killing concentration of 100 μ g/mL (0.7 mM) [25]. Polygodial, a sesquiterpene isolated from *Polygonum hydropiper* has shown minimum fungicidal concentrations (MFC) of 50 μ g/mL (213 μ M) against *Z. parabailii* [11]. The naturally occurring terpenoid alcohol, geraniol showed an MFC of 800 μ g/mL (4.9 mM) [25]. The terpenoid phenol constituents of herb oils, thymol and carvacrol were found to inhibit the growth of *Z. parabailii* at concentrations of 100 μ g/mL (0.7 mM) [26], whereas anethole tested in another study showed an MFC of 400 μ g/mL (2.7 mM) [25]. Nonetheless, terpenoids are volatile which may restrict their application [27,28]. Notably, none of the aforementioned compounds can be classified as a good antimicrobial (MIC \leq 25 μ g/mL) based on Gibbon's classification system on natural compounds [29]. Nowadays, combinations of natural antimicrobials are increasingly

explored for enhanced antimicrobial potency [11,26]. For example, the antimicrobial potency of the mixture of the terpenoid phenols, thymol and carvacrol with the monoterpene, citral resulted in a 4-fold enhancement of activity for all three molecules [26]. Mechanistically, synergy is thought to occur when the combined agents act in different, yet complementary fashions [26,30].

Prenylated (iso)flavonoids are secondary metabolites predominantly found in the Leguminosae family. Prenylated (iso)flavonoids are already acknowledged for their high potency against bacteria [31,32], molds [33,34] and yeasts [35,36]. The mono-prenylated isoflavan, glabridin, for example, has shown high antimicrobial potency against Gram-positive and Gram-negative bacteria with minimum inhibitory concentrations (MICs) between 10–20 µg/mL (31–62 µM) [31,37] and against *Candida* spp. showing a MIC of 6–64 µg/mL (8–197 µM) [38,39]. Glabridin was shown to exert its antimicrobial action through permeabilization of the microbial membrane [31,38].

To the best of our knowledge, the antimicrobial properties of the highly promising prenylated (iso)flavonoids against *Z. parabailii* have not been evaluated. In this study, we explored the antifungal potency of these molecules and the mode of action of the two most active ones against a food isolate. Lastly, we analyzed the most important molecular properties that influence the antifungal activity of prenylated (iso)flavonoids using a QSAR approach.

5.2. Materials and Methods

5.2.1. Materials and strains

Prenylated (iso)flavonoids (glabrene, 3'-hydroxy-4'-*O*-methyl-glabridin, 4'-*O*-methyl-glabridin, hispaglabridin B, glyceollidin II, dehydroglyceollidin II, dehydroglyceollin I, dehydroglyceollin II, dehydroglyceollin, III, dehydroglyceollin IV and glabrol) were previously purified and chemically characterized [40,41]. Glabridin was supplied by FUJIFILM Wako Pure Chemical Corporation (Neuss, Germany). Propidium iodide (PI), hydrochloric acid (36.5–38.0% v/v) and sorbic acid were purchased from Sigma Aldrich (St. Louis, MO, USA). Potassium sorbate, acetic acid (glacial) and glutaraldehyde 25% w/v in water) were supplied by VWR International B.V. (Amsterdam, the Netherlands). Isowighteone and neobavaisoflavone were purchased from ChemFaces (Wuhan, Hubei, China). Wighteone, lupiwighteone, luteone, and 6,8-diprenygenistein were purchased from Plantech UK (Reading, UK). 6'-Prenylpiscidone was supplied by Carbosynth Ltd. (Berkshire, UK). Yeast extract peptone dextrose broth (YPD) was purchased from Brunschwig Chemie B.V. (Amsterdam, the Netherlands) and bacteriological agar from Oxoid Ltd (Basingstoke, UK), and peptone physiological salt solution (PPS) from Tritium Microbiologie (Eindhoven, the Netherlands). DMSO was purchased from Duchefa Biochemie B.V. (Haarlem, the Netherlands). For transmission electron microscopy glutaraldehyde, paraformaldehyde, OsO₄, UranylLess staining, Spurr's resin and lead citrate were purchased from EMS (Hatfield, USA). Gelatin

(type B, powder) and the ethanol (100% v/v) was supplied by Merck/Sigma-Aldrich and the 96% ethanol from TechniSolv.

Food isolate *Z. parabailii* UL 3699 was kindly provided by Unilever Nederland B.V. (Wageningen, the Netherlands). *Z. parabailii* ATCC 60483 was purchased from the American Type Culture Collection (Wessel, Germany).

5.2.2. Methods

5.2.2.1. Screening of potency of prenylated (iso)flavonoids

Nineteen prenylated (iso)flavonoids were screened for their potency against the food isolate *Z. parabailii*. Yeasts cells were streaked from a $-80\text{ }^{\circ}\text{C}$ glycerol stock onto a YPD agar plate and incubated 48 h at $30\text{ }^{\circ}\text{C}$. One colony was transferred to 10 mL YPD broth and further incubated for 16 h at $30\text{ }^{\circ}\text{C}$. The overnight cultures were diluted 50 times with YPD (final inoculum concentration $4.4 \pm 0.3 \log_{10}$ CFU/mL). Stock solutions of the different prenylated (iso)flavonoids in DMSO (wighteone, glabridin, luteone, isowighteone and 6'-prenyl piscidone) or 70% ethanol (the rest of the compounds) were subsequently diluted with YPD (1-50 $\mu\text{g/mL}$). Equal volumes (100 μL) of yeast inoculum and prenylated (iso)flavonoid solutions in YPD were mixed in a sterile 96-well plate (with a maximum solvent percentage of 2.0%). The 96-well plate was incubated in a Spectramax ID3 (Molecular Devices, Sunnyvale, CA, USA) at $30\text{ }^{\circ}\text{C}$ for 48 h with double orbital, high intensity shaking before each measurement for 5 seconds. The optical density (OD) was measured at 600 nm every 10 min.

Growth was determined by measuring the time to detection (TTD), i.e. the time to reach a change in OD of 0.05 units ^[42]. Potassium sorbate (1.5-3.0 mg/mL) was also tested at the optimal growth pH of the yeast (6.5) for comparison. In addition, negative control (YPD yeast cell suspension with maximum solvent percentage), and blanks were used for optical comparison and sterility control. When ΔOD was less than 0.05, i.e. flat lines after 48 h, viable cell count was performed. In brief, 100 μL from each well was decimally diluted and spread onto an YPD agar plate. Plates were incubated at $30\text{ }^{\circ}\text{C}$ for 48 h after which colonies were counted. The minimum inhibitory concentration (MIC) was determined as the lowest concentration of compound that resulted in a cell count equal or lower than that of the initial inoculum. The minimum fungicidal concentration (MFC) was determined as the lowest concentration of compound that resulted in $> 99\%$ yeast inactivation from the initial inoculum. Prenylated (iso)flavonoids were screened in three biological replicates, each performed in duplicate.

5.2.2.2. Antifungal activity of most active prenylated (iso)flavonoids at acidic pH

The most potent prenylated isoflavonoids found upon screening were tested against *Z. parabailii* UL 3699 and *Z. parabailii* ATCC 60483 at pH 4.0 (or pH 3.0). Overnight cultures were prepared and assayed for 72 h (or 96 h for pH 3.0) as

described above (final inoculum concentration $4.3 \pm 0.3 \log_{10}\text{CFU/mL}$ for UL 3699 and $4.5 \pm 0.2 \log_{10}\text{CFU/mL}$ for ATCC 60483 at pH 4.0, and $4.5 \pm 0.3 \log_{10}\text{CFU/mL}$ for UL 3699 at pH 3.0). The assays were performed in three biological replicates, each performed in duplicate.

5.2.2.3. QSAR binary model

The binary classification QSAR model was chosen (over for e.g. a continuous one) as it can accommodate molecules with non-established MICs (i.e. $> 25 \mu\text{g/mL}$). Incorporation of molecules with unestablished MICs is crucial when small datasets are employed to increase the chemical space used for model development. Chemical structures were extracted from literature and inputted to the modelling software (Molecular Operating Environment, MOE, v.2019.08, Chemical Computing Group) using the canonical SMILES codes from PubChem. If not available, the chemical structure was drawn manually using the PubChem sketcher to obtain the SMILES code before importing to MOE. A conformational search (LowModeMD, RSM gradient 0.1 kcal/mol/\AA , other settings default) was performed for all compounds in the database. The conformation with the lowest energy was further refined using MOPAC force field (RSM gradient $0.01 \text{ kcal/mol/\AA}$).

Optimized chemical structures were used to calculate different molecular descriptors available in MOE. Descriptors were calculated for fully undissociated molecular species. After eliminating descriptors that were identical for all molecules or redundant descriptors (inter-correlation $R_{\text{pearson}} > 0.99$), a total number of 120 descriptors was finally incorporated into the database.

A binary QSAR model was constructed to predict activity of mono-prenylated isoflavonoids, using the QuaSAR-model application of MOE. Genetic algorithm was used to explore which variables best describe the data ^[43]. The binary model was constructed with the two descriptors that were most frequently indicated by the GA as the best predictors of the antifungal potency. Given the number of compounds used (15), only 2 descriptors ^[44] were selected following the principle of "Occam's Razor". This principle supports that a reasonable QSAR model with the smallest number of descriptors should be sought to avoid interpretation complexity ^[45]. As a rule of thumb, the number of descriptors should be maximum 5 times more than the number of data-points ^[46].

In this study, an activity threshold of pMIC of 4.1 ($\text{MIC} \leq 25 \mu\text{g/mL}$) was set to discriminate between actives and inactives. When a MIC range was determined for a molecule, the worst case scenario (highest MIC value of the range) was considered. For the four mono-prenylated isoflavonoids, which showed no change in TTD μg at the maximum concentration tested (i.e. $\text{MIC} > 25 \mu\text{g/mL}$), a MIC value of $100 \mu\text{g/mL}$ was inputted for the analysis. The quality of the binary model was first assessed by the **total accuracy** of the QSAR model, which is the fraction of observations correctly predicted, as well as the **accuracy on actives** (sensitivity) and **accuracy on inactives** (specificity), which are the fractions of correctly predicted sample actives and inactives, respectively. The descriptor importance

was estimated to show the degree to which each descriptor is useful in distinguishing actives from inactives. The model was validated by the leave-one-out cross validation scheme where the cross-validated accuracies (total, active and inactive) were also considered to select the final binary model. Since the size of our experimental set did not allow splitting of the compounds into a training and a test set ^[47], we selected the best model by predicting the activity of an external set of prenylated isoflavonoids tested against other yeasts (*S. cerevisiae* and *Candida albicans*). The external set comprised molecules from the same subclasses as the ones used for model construction, which were within the applicability domain (AD) of the model. The (AD) of the models was calculated by means of the William's plot.

5.2.2.4. Combination studies

The two-dimensional checkerboard microdilution assay ^[48] was used to assess the types of interactions between prenylated isoflavonoids (glabridin and wighteone) and between prenylated isoflavonoids and sorbic acid at pH 4.0 against *Z. parabailii* (UL 3699, inoculum size $4.7 \pm 0.1 \log_{10}\text{CFU/mL}$). Combination experiments with the two prenylated isoflavonoids were performed in 3 biological replicates, each performed in duplicate. Assays between prenylated isoflavonoids and sorbic acid were performed in two biological replicates per combination each performed in duplicate.

Two-fold dilutions of one compound (horizontally) were tested in combination with two-fold dilutions of the other compounds (vertically), in a concentration range based on MIC and MFC determination of the individual compound. The fractional inhibitory fungicidal concentration indices (FICI or FFCI) were calculated based on the checkerboard data obtained after a 72 hour-incubation at 30 °C. The ΣFIC of the combinations refer to $(\text{MIC}_{\text{compound1 in combination}} / \text{MIC}_{\text{compound1 alone}}) + (\text{MIC}_{\text{compound2 in combination}} / \text{MIC}_{\text{compound2 alone}})$. The following criteria were used to determine the type of interaction between the two agents: $\Sigma\text{FIC} \leq 0.5$ synergy; $0.5 < \Sigma\text{FIC} \leq 1.0$ addition; $1.0 < \Sigma\text{FIC} \leq 4$ indifference; $\Sigma\text{FIC} > 4$ antagonism ^[49-51]. The same equation applies for ΣFFCI s determination.

5.2.2.5. Killing kinetics

An overnight yeast culture was diluted to $4.8 \pm 0.3 \log_{10}\text{CFU/mL}$ with acidified YPD (pH 4.0) and mixed with the most active prenylated isoflavonoids, glabridin and wighteone, at their MFC. Samples were incubated in duplicate at 30 °C/300 rpm. At different time points (0, 15 min, 30 min, 45 min, 60 min, 24 h and 48 h), 100 μL of culture medium were taken and decimally diluted in PPS. Dilutions were spread on YPD agar plates and incubated for 48 h at 30 °C, after which, colonies were counted. Sorbic acid at 1.65 mg/mL (=3 x MFC) was used as control antifungal agent. Samples of the sorbic acid-yeast mixture were taken at (0 to 48 h). Experiments were performed in three biological replicates against both yeast strains.

5.2.2.6. Membrane permeabilization

Quantification of membrane permeabilization was performed by measuring the fluorescence signal of propidium iodide (PI). PI is a fluorescence probe that intercalates to DNA through van der Waal's stacking ^[52]. *Z. parabailii* (UL 3699) cell cultures grown for 30 h at 30 °C in YPD were centrifuged at 4,900 rcf, 4 °C for 15 min. The pellet was washed twice with 9 mL PPS. Cells were re-suspended in (acidified, pH 4.0) PPS (cell density $9.2 \pm 0.2 \log_{10}\text{CFU/mL}$). Hundred μL of the cell suspension were incubated at RT with 90 μL of the most active compounds (glabridin or wighteone) at 6.25-50 $\mu\text{g/mL}$ in a black well plate with clear bottoms. To limit the interaction of PI with prenylated isoflavonoids (**Figure S5.1**), yeast cells were pre-incubated with prenylated isoflavonoids for 1 h, prior the addition of PI. Next, 10 μL of PI (4.5 μM final concentration) were added and the fluorescence signal was measured in a Spectramax ID3. Emission of fluorescence was measured every 2 min at 620 nm (bottom read mode) for 2 h, while exciting the samples at 520 nm. Photomultiplier tube detector gain was set to high. As a positive control, cells heated at 99 °C in a thermomixer for 10 min were used. Background fluorescence was accounted for by the use of controls and blanks (live cells with PI, without compounds; prenylated isoflavonoids alone; PI alone; and PPS alone). Viable cell counting was performed after 24 h. Experiments were performed in three biological replicates.

5.2.2.7. Fluorescence microscopy

Z. parabailii (UL 3699) cell suspensions (200 μL) were prepared as described in **5.2.2.6** and mixed with 180 μL stock prenylated isoflavonoids (final concentration 25 $\mu\text{g/mL}$). Different eppendorf tubes were used for the different time-points (from 5 to 180 min). Twenty μL PI (4.5 μM final concentration) were added to each mixture just before visualization of the cells. Cells were visualized with an Olympus BX41 microscope (Olympus, Tokyo, Japan) and a red fluorescent protein (RFP) filter as described elsewhere ^[53]. Viable cell counts were performed at the different time-points. The experiment was performed in two biological replicates.

5.2.2.8. Transmission electron microscopy (TEM)

For TEM analysis, 10^9 CFU/mL *Z. parabailii* cells (UL 3699) grown in acidified YPD (pH 4.0) were treated with glabridin and wighteone at their MFC at these conditions (50 and 25 $\mu\text{g/mL}$, respectively). After specific time of exposure (from 5 to 180 min), (un)treated cells were centrifuged for 5 min at 4,900 rcf at RT. The pellet was fixed with 2.5% (w/v) glutaraldehyde 0.1 M phosphate/citrate buffer, pH 7.2). Fixed cells were collected by centrifugation (4,900 rcf, 5 min) and resuspended in 3% (w/v) gelatin in phosphate buffer (pH 7.2) and allowed to cool until solidified cubes formed. The cubes were manually sliced with a sharp razor blade into pieces of approximately 0.5 x 0.5 x 0.5 mm. The specimens were post-fixed in 1% OsO_4 (in 0.1 M phosphate/citrate buffer, pH 7.2) for 60 min at RT. Subsequently, the

cells were dehydrated with increasing concentrations of ethanol (30%, 50%, 70%, 80%, 90%, 96%, 2x100% [v/v]). The dehydrated cells were then infiltrated in mixtures of 1:2, 1:1 and 1:2 resin:ethanol (30 min with each ratio). Then, the mixture was replaced with resin for 60 min and the cells were resuspended in fresh resin for overnight storage. The resin was polymerized for 8 h at 70 °C. Sections (50 nm coupes) were cut using a Leica EM UC7 microtome (Leica Microsystems B.V., The Netherlands) and post-stained with UranylLess staining and lead citrate. The ultrathin sections were observed with a JEOL JEM-1400plus electron microscope (JEOL USA Inc., USA) at an acceleration voltage of 120 kV. Images correspond to different cells per sample.

5.3. Results

5.3.1. Antifungal potency of prenylated isoflavonoids against *Z. parabailii*

Fifteen mono-prenylated and four di-prenylated (iso)flavonoids were screened for their antifungal potency against *Z. parabailii* (UL 3699) (**Table 5.1** and **Figure S5.2**). Screening was performed at the optimal growth pH of the yeast, 6.5, to ensure that the influence of only one hurdle (i.e. prenylated (iso)flavonoids) on the growth of the yeast was investigated.

Eight mono-prenylated isoflavonoids had a MIC value $\leq 25 \mu\text{g/mL}$, which is associated with a good antimicrobial activity ^[29] (**Table 5.1**). The mono-prenylated isoflavones, wighteone (**9**) and luteone (**7**) and the mono-prenylated isoflavan glabridin (**3**) showed the highest antifungal activity with MICs of 3.13-6.25 $\mu\text{g/mL}$ (9-18 μM), 12.5 $\mu\text{g/mL}$ (35 μM) and 6.25-12.5 $\mu\text{g/mL}$ (19-39 $\mu\text{g/mL}$), respectively. It should be noted that the primary focus of this study is the membrane-activity of prenylated (iso)flavonoids and thus only the undissociated species are considered. However, the highly active isoflavones have low pK_as and are therefore largely dissociated at pH 6.5 (**Table 5.1**), implying that they might also act elsewhere than the membrane.

The four di-prenylated (iso)flavonoids tested in this study were not active against *Z. parabailii*, as they did not induce any significant change in the time to detection (TTD) at the maximum concentration tested (C_{max} 25 $\mu\text{g/mL}$) (**Figure S5.3**). Lack of activity of di-prenylated molecules was independent of the subclass to which they belong (flavanone (**16**), isoflavan (**17**) and isoflavones (**18** and **19**)) or the prenylation patterns they bear (**Figure S2**).

As expected, no activity was found for potassium sorbate at concentrations up to 3,000 $\mu\text{g/mL}$ at pH 6.5 ^[11]. Only the undissociated forms of weak organic acids are membrane permeable and able to cause cytoplasmic acidification which is the generally accepted mode of action of weak organic acids as antimicrobials ^[8-11].

Table 5.1. Antifungal potency (in µg/mL) of mono- and di- prenylated (iso)flavonoids against *Z. parabailii* (UL 3699) at pH 6.5. Ranges in MIC/MFC derive from different values of the replicates. The percentage of undissociated species of prenylated isoflavonoids at pH 6.5 is given in parentheses (only if this is less than 90%) (calculated using MarvinSketch 20.3). (-) means not tested.

No.	Subclass	Compound	MIC	MFC
Mono-prenylated				
1		3'-OH-4'-O-methyl glabridin	>>25	-
2	Isoflavan	4'-O-methyl glabridin	25	-
3		Glabridin	6.25-12.5	12.5
4		Glabrene	25	50
5	Isoflavene	Isowighteone (69%)	12.5-25	25
6		Lupiwighteone (60%)	>>25	-
7		Luteone (58%)	12.5	25
8	Isoflavone	Neobavaisoflavone (65%)	50	-
9		Wighteone (59%)	3.13-6.25	6.25
10		Glyceollidin II	>>25	-
11	Pterocarpan	Dehydrolyceollidin II	25-50	50
12		Dehydroglyceollin I	12.5-25	25
13		Dehydroglyceollin II	25	-
14		Dehydroglyceollin III	>>25	-
15		Dehydroglyceollin IV	>>25	-
Di-prenylated				
16	Flavanone	Glabrol	>>25	-
17	Isoflavan	Hispaglabridin B	>>25	-
18	Isoflavone	6,8-diprenylgenistein (49%)	>>25	-
19		6'-prenyl piscidone (68%)	>>25	-

5.3.2. (Quantitative) structure-activity relationships of mono- prenylated isoflavonoids against *Z. parabailii*

5.3.2.1. Development of binary classification QSAR

To obtain an insight in the overall molecular properties underlying antifungal activity, a QSAR model was developed using the activity data (MICs) of the 15 mono-prenylated isoflavonoids tested (**Table 5.1**). Mono-prenylated isoflavonoids had a range of activities and a variety of structural features (5 different isoflavonoid subclasses and different configuration and position of the prenyl group), aspects important during QSAR modeling. In contrast, the di-prenylated (iso)flavonoids were excluded for the QSAR analysis as they were unanimously inactive, irrespective of their structural features other than prenylation. A binary QSAR model was chosen (over for e.g. a continuous one) as it can accommodate the molecules for which no MIC was established. It should be noted that descriptors were calculated for the undissociated species of prenylated isoflavonoids, since these are expected to interact with the membrane (**Chapter 4**). Genetic algorithm

(GA) was used to select the two variables that best describe the dataset. E_{ele} and $vsurf_ID$ descriptors were the most frequently selected variables by the GA (36% and 57% frequencies, respectively). E_{ele} and $vsurf_ID7$ were used to construct a binary QSAR model which resulted in a 93% total accuracy, discriminating active and inactive compounds with high (cross-validated) accuracies, i.e. $\geq 86\%$ (**Table S5.1**). The choice of the best QSAR model was also based on the quality of prediction of an external set of prenylated isoflavonoids tested against other yeasts (*S. cerevisiae* and *C. albicans*) (**Table S5.2** and **Figure S5.4**), which fell into the applicability domain of the developed model (**Figure S5.5**). The proposed model predicted correctly the activity of 67% of the molecules tested against other yeast species (**Table S5.2**).

E_{ele} refers to the electrostatic component of potential energy (E_{ele}) and $vsurf_ID7$ represents the hydrophobic integrity moment at -1.4 kcal/mol, a measure of unbalance between the centre of mass of a molecule and the barycentre of the hydrophobic regions [54]. Both descriptors were positively correlated to the antifungal activity. The two descriptors had a low correlation coefficient (Pearson coefficient < 0.4) and their importance in the binary model was equally high (35% for E_{ele} and 30% for $vsurf_ID7$).

5.3.2.2. Effect of electrostatic potential energy and hydrophobic integrity moment on the activity of mono-prenylated isoflavonoids

Figure 5.1 demonstrates the effect of location, presence and type of substituents on the electrostatic potential energy and hydrophobic integrity moment and the activity of prenylated isoflavonoids per subclass against *Z. parabailii*.

In isoflavones (**Figure 5.1A**), luteone (**7**), the only studied molecule with 4 free hydroxyl groups had the highest absolute E_{ele} value (**Table S5.3**). The E_{ele} values and the antifungal activity decreased as the number of hydroxyl groups decreased (for example, from (**7**) to (**9**) and from (**5**) to (**8**)) (**Figure 5.1A**). Furthermore, wighteone (**9**) and luteone (**7**), both having A-prenylation, had higher $vsurf_ID7$ values and higher antifungal activity than isowighteone (**5**) (B-ring prenylated) (**Figure 5.1A**). Yet, $vsurf_ID7$ does not distinguish prenylation at different locations of the A-ring since C6-prenylated molecules (as in (**7**) and (**9**)) had the same descriptor value as the C8-prenylated isoflavone (**6**), while the latter showed no activity (**Table S5.3**).

For pterocarpenes (**Figure 5.1B**), methylation of a free -OH group at the C3 (as in dehydroglyceollin IV (**15**) from dehydroglyceollidin II (**11**)) negatively affected E_{ele} and abolished the antifungal activity (**Figure 5.1B**). A furan- over a pyran-prenyl configuration decreased both the E_{ele} and the $vsurf_ID7$, cancelling the antifungal activity of dehydroglyceollin III (**14**) as compared to dehydroglyceollin II (**13**) (**Figure 5.1B**).

In contrast, methylation of isoflavans (**Figure 5.1C**) did not significantly influence E_{ele} , even though it decreased the antifungal activity more than 2-fold (4'-O-methyl glabridin (**2**) compared to glabridin (**3**)) (**Figure 5.1C**). Strikingly,

an additional -OH on the B-ring even decreased the value of the energy descriptor, abolishing the activity, despite the increase in *vsurf_ID7*.

Overall, *E_ele* seems to partially relate to the number of free -OH groups present in the molecules, whereas *vsurf_ID7* seems to correlate more with the location of the prenyl-group. However, isoflavans do not seem to follow the trends observed for isoflavones and pterocarpenes. Possibly, the absence of a double bond at the C-ring and the subsequent discontinued electron distribution might be associated with this deviating behaviour.

It should be noted that the di-prenylated isoflavones and isoflavans tested in this study had electrostatic potential energies (*E_ele*) ranging from -33 to -52 kcal/mol and hydrophobic integrity moments (*vsurf_ID7*) ranging from 0.6-2.0 Å (Table S5.3). These values do not deviate from those of the mono-prenylated (iso)flavonoids, thus, do not explain the absence of activity based on the developed QSAR model.

5.3.3. Influence of low pH on the antifungal activity of prenylated isoflavonoids

Z. parabailii is thought to develop resistance mechanisms at low pH, such as activation of efflux pumps and alteration of membrane permeability [15,16,55]. Thus, it was of high importance to assess the potency of prenylated isoflavonoids at low pH. For this, the molecules which demonstrated potency (MIC ≤ 50 µg/mL) at pH 6.5 were tested at the most relevant pH for products commonly contaminated by *Z. parabailii* (pH 4.0) and at an extreme pH where *Z. parabailii* has been previously shown to survive (pH 3.0) [56-58] (Table 5.2).

Most prenylated isoflavonoids showed slightly higher MICs/MFCs towards lower pH. Prenylated isoflavonoids which were highly potent at pH 6.5 (Table 5.1), i.e. glabridin (**3**), luteone (**7**) and wighteone (**9**) retained their potency also at acidic pH, both at pH 4.0 and 3.0 (Table 5.2). These three molecules showed 2-44 times higher activity (MFCs) than the traditional food preservative, sorbic acid, at acidic pH (Table 5.2). The MICs of sorbic acid at the two acidic pH were in line with the MICs reported by Fujita *et al.* (2005) [11]. Neobavaisoflavone (**8**) and the pterocarpenes (dehydroglyceollin I and II, **12** and **13**) became completely inactive (MICs > 100 µg/mL) at pH 4.0 and thus were not tested at pH 3.0 (Table 5.2). The potency of prenylated isoflavonoids was also confirmed against the reference strain (ATCC 60483) (Table S5.4) at its most relevant pH conditions (pH 4.0).

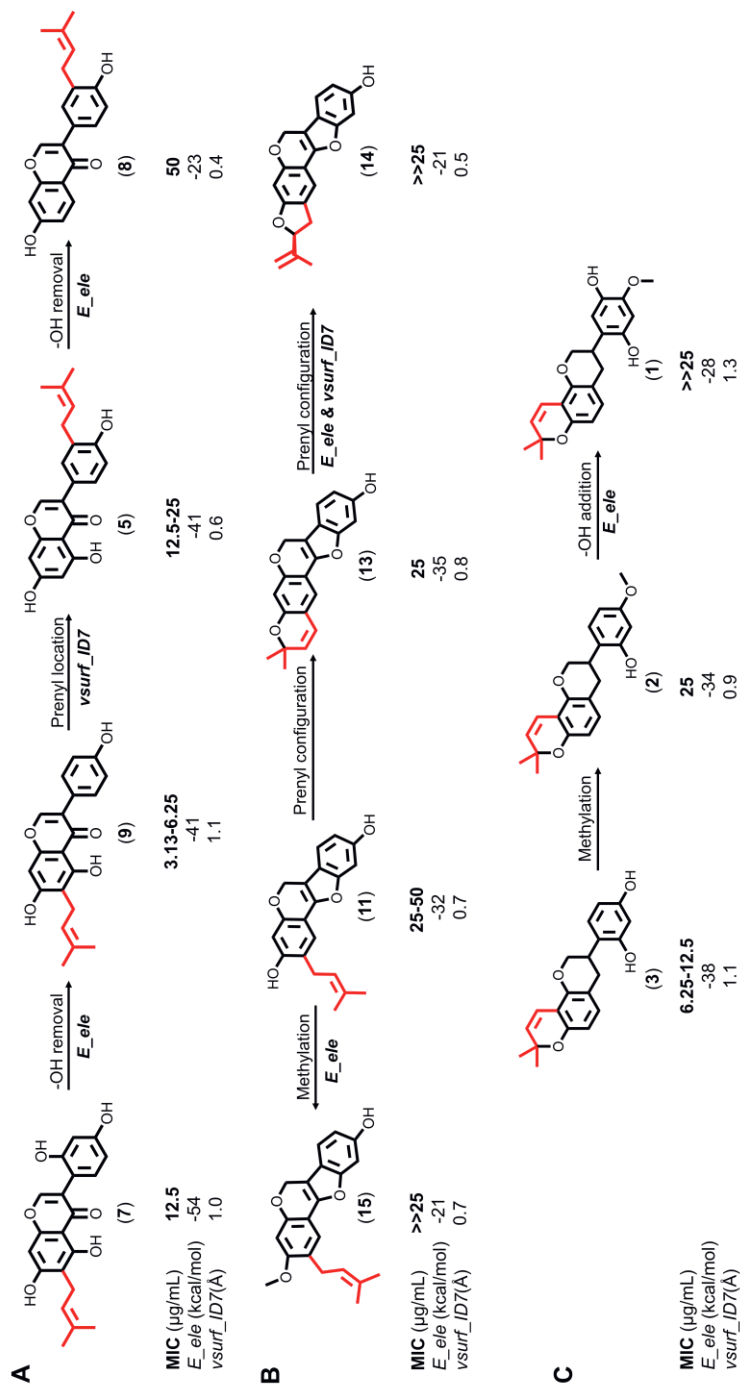


Figure 5.1. Effect of type, location and configuration of substituents on the main two QSAR-derived molecular properties (electrostatic potential, E_ele and hydrophobic integy moment, $vsurf_ID7$) and their subsequent effect on the activity of prenylated isoflavonoids of three subclasses; isoflavones (A), pterocarpenes (B) and isoflavans (C). The structural difference and the affected molecular property are illustrated above and below the arrows respectively.

Table 5.2. Antifungal potency (in $\mu\text{g/mL}$) of mono-prenylated isoflavonoids against *Z. parabailii* (UL 3699) at pH 4.0 and 3.0. Ranges in MIC/MFC derive from different values of the replicates. (-) means not tested. In parentheses, the percentage of undissociated sorbic at each pH is given (calculated using MarvinSketch 20.3). Prenylated isoflavonoids are fully protonated at these pH values.

No.	Subclass	Compound	pH 4.0		pH 3.0	
			MIC	MFC	MIC	MFC
3	Isoflavan	Glabridin	12.5	25	12.5-25	25-37.5
4	Isoflavene	Glabrene	50-75	75	125	150
5	Isoflavone	Isowighteone	50-75	75	50-75	75
7	Isoflavone	Luteone	25-37.5	37.5	25-37.5	37.5
8	Isoflavone	Neobavaisoflavone	>150	-	-	-
9	Isoflavone	Wighteone	6.25-12.5	12.5	12.5	25
12	Pterocarpene	Dehydroglyceollin I	>100	-	-	-
13	Pterocarpene	Dehydroglyceollin II	>100	-	-	-
15	Preservative	Sorbic acid	275 (86%)	550 (86%)	138 (98%)	275 (98%)

* 4'-O-methyl glabridin (**2**) and dehydroglyceollidin II (**11**) were not tested at low pH due to limited purified amounts.

5.3.4. Killing kinetics

The inactivation rate of *Z. parabailii* at pH 4.0 by the two most active prenylated (iso)flavonoids, glabridin (**3**) and wighteone (**9**) at their corresponding MFCs at pH 4.0 (25 and 12.5 $\mu\text{g/mL}$), respectively, is shown in **Figure 5.2**.

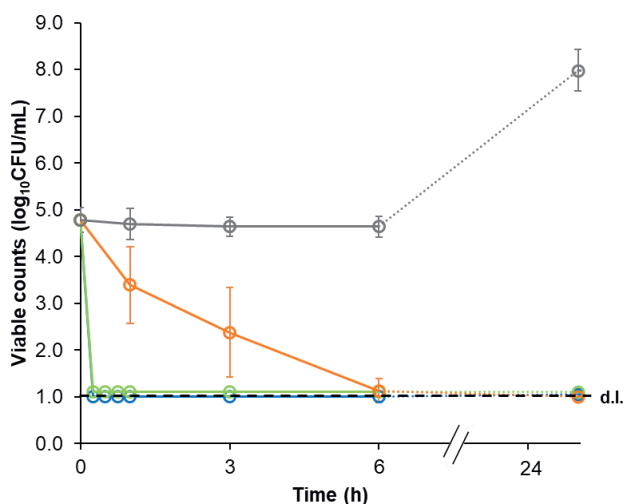


Figure 5.2. Inactivation kinetics of *Z. parabailii* (UL 3699) cells (10^5 CFU/mL) in the presence of 12.5 $\mu\text{g/mL}$ wighteone (green), 25 $\mu\text{g/mL}$ glabridin (blue) and 1650 $\mu\text{g/mL}$ sorbic acid (orange) at pH 4.0. Control cells are shown in grey. d.l. refers to the detection limit.

Within the first 15 min, both prenylated isoflavonoids reduced the viable counts by 99.99% of UL 3699. This fast killing was confirmed with the ATCC 60483 strain (**Figure S5.6**). In contrast, sorbic acid showed slower killing rates for the two isolates. Three to six hours were needed for 99.99% inactivation of UL 3699 isolate by sorbic acid, whereas 24 h were needed for 90-99% inactivation of the ATCC 60483 strain at a sorbic acid concentration of 1,650 µg/mL (**Figure S5.6**). The latter finding is in line with the slow killing activity of sorbic acid (1,600 µg/mL) against *Z. parabailii* (ATCC 60483), which was observed within 12 h ^[11] (no intermediate time-point was obtained between 6 and 24 h in this study).

5.3.5. Combination experiments

Given that prenylated isoflavonoids are thought to act in a different fashion to sorbic acid (putative membrane activity versus cytoplasmic acidification and generation of oxidative stress, respectively) ^[15,31,59], we explored the synergistic potential of their mixture. However, when the two prenylated (iso)flavonoids were (separately) combined with sorbic acid, more than half of the corresponding MFC of the agents was needed to induce complete lethality, suggesting an indifferent effect between the two agents (**Figure S5.7**).

5.3.6. Membrane permeabilization

We assessed the membrane permeabilization capacity of the two most active prenylated isoflavonoids against *Z. parabailii* in a qualitative and a quantitative way. In both cases, the fluorescent probe, propidium iodide (PI) was used to stain damaged cells.

PI staining, and therefore *Z. parabailii* membrane permeabilization, started within 15 min of exposure to the two prenylated isoflavonoids at pH 4.0 (**Figure 5.3A**) and increased with time of exposure. For glabridin-treated cells, intracellular material (most probably including PI) leaked out of the cells within 1 h (**Figure 5.3A**), accompanied with 99.99% decrease in the viable counts (**Figure 5.3C**). Leakage of intracellular material is more pronounced in wighteone-treated cells, as no PI stain was visible after 30 min, accompanied with 99% decrease in cell viability. In contrast, heated cells maintained their integrity (although metabolically inactive as determined by plate counting), retaining the PI taken up intracellularly (**Figure 5.3A**). This is in line with the higher accumulation of PI in cells exposed to glabridin in time compared to those exposed to wighteone, even though these were still lower than in heated cells (**Figure 5.3B**). Similar (quantitative and qualitative) observations were obtained at pH 7.2 (**Figure S5.8** and **S5.9**). Sorbic acid did not cause any PI uptake at pH 4.0 at a concentration sufficient to kill (**data not shown**). These findings agree with the generally accepted mechanism that weak organic acids act through acidification of the cytoplasm by diffusing easily through the membrane.

5.3.7. Transmission electron microscopy

Transmission electron microscopic (TEM) images were obtained after 15 min and 180 min of exposure to the two most active prenylated isoflavonoids. Prenylated isoflavonoids, at their MFC, induced disruption of the membrane integrity compared to the control cells (exemplified in **Figure 5.4**). Glabridin distorted the order in the membrane within the first 15 min (**Figure 5.4A** and **A'**) and induced large discontinuities (pores ^[60]) after 180 min (**Figure 5.4B** and **B'**). Wighteone-treated cells showed membrane elongations engulfing a cluster (**Figure 5.4C**) and some more vaguely visible protrusions together with membrane discontinuities (**Figure 5.4C'**). After 180 min, cells treated with wighteone completely lost their cell membrane (**Figure 5.4D** and **D'**). More representative images can be found in **Figure S5.10**.

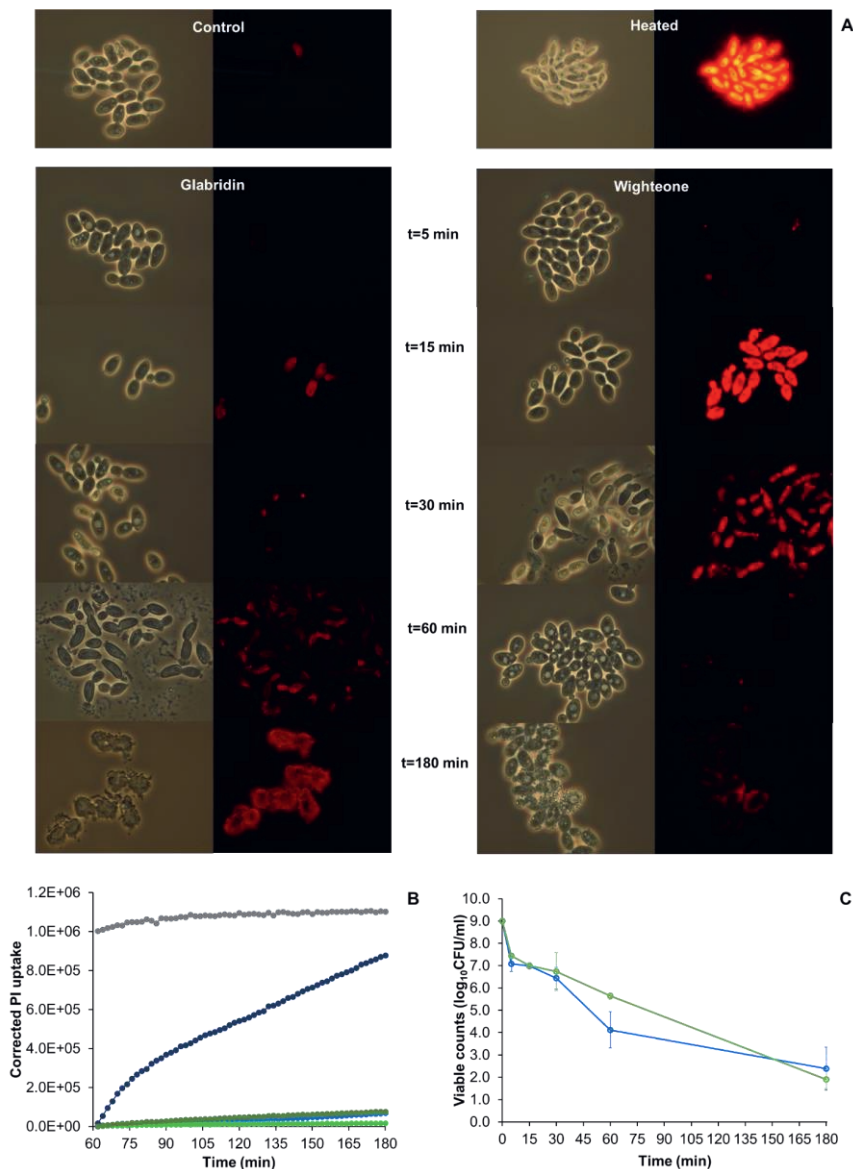


Figure 5.3. Light and fluorescence microscopy images of *Z. parabailii* (UL 3699, 10^9 CFU/mL) at different time points after exposure to 25 µg/mL of glabridin and wighteone. Control and heated cells are shown after 180 min (A). Propidium iodide uptake in time after incubating the yeast cells with different concentrations of glabridin (blue lines) and wighteone (green lines) (light colors correspond to 25 µg/mL and dark colors correspond to 50 µg/mL) for 1 h at pH 4.0. Heated cells served as the positive control and the fluorescence signal of PI from untreated cells was subtracted from the signal of the treated cells (B). Viable cell counting after exposure to 25 µg/mL of glabridin and wighteone over time (blue line represents glabridin and green represents wighteone) (C).

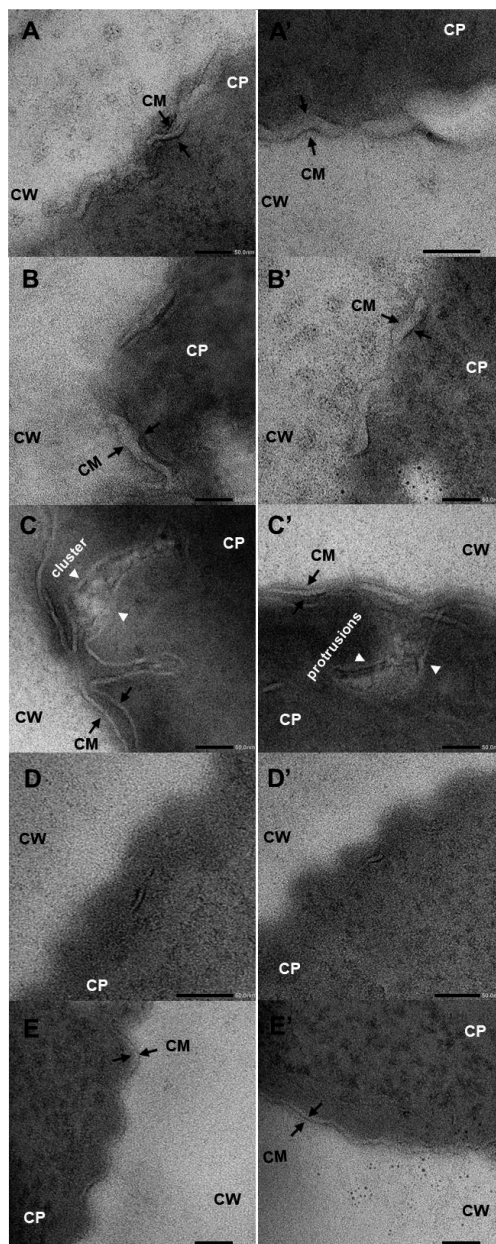


Figure 5.4. Representative TEM images (black scale bars at 50 nm) of cells (10^9 CFU/mL) exposed to 50 µg/mL glabridin (**A, B**) and 25 µg/mL wightone (**C, D**) for 15 (**A, C**) and 180 min (**B, D**), compared to untreated *Z. parabailii* cells (UL 3699) at 180 min (**E**). Letters with a prime refer to duplicates. Arrows point to the cell membrane (CM), CP stands for the cytoplasm and CW designates the cell wall. More images can be found in **Figure S5.10**.

5.4. Discussion

5.4.1. Mono-prenylated isoflavonoids have superior anti-*Z. parabailii* activity to di-prenylated isoflavonoids

Ten mono-prenylated isoflavonoids from four different subclasses showed moderate to good antifungal activity against *Z. parabailii* (MIC \leq 50 $\mu\text{g/mL}$) at pH 6.5. The A-ring prenylated isoflavone, wighteone and the prenylated isoflavan, glabridin, in particular, showed the lowest MICs (MIC $<$ 12.5 $\mu\text{g/mL}$), classifying them as very active antimicrobials [29]. The fungicidal activity of wighteone and glabridin was 4–8 x higher than that of polygodial (MIC 50 $\mu\text{g/mL}$, 213 μM) at pH 6.5, the most potent natural agent against *Z. parabailii* reported so far [11].

In contrast, the di-prenylated analogue of wighteone, 6,8-diprenyl genistein (**18**) and of glabridin, hispaglabridin B (**17**) (along with two other di-prenylated isoflavonoids, (**16**) and (**19**)) did not exert any antifungal activity at Cmax, MIC $>>$ 25 $\mu\text{g/mL}$. The differential activity of mono- and di-prenylated (iso)flavonoids has not been systematically studied in yeasts, and in *Z. parabailii* in particular. Most di-prenylated (iso)flavonoids found in literature were also inactive against other yeast species (for an overview see **Table S5.5**). The absence of activity of isoflavones (**18**) and (**19**) is in line with the absence of activity (up to 60 $\mu\text{g/mL}$) of the structural analogue flavones, morusin (**D1**) and kuwanon C (**D2**) against *C. albicans* [61] (**Figure S5.11**). Similarly, the lack of activity of the flavanone, glabrol (**16**) found in this study, is corroborated by the lack of activity of the flavanones, euchrestafavanone A (**D4**) and lonchocarpol A (**D5**) (MIC $>$ 200 μg , determined by the TLC method) against *Cladosporium herbarum* reported in literature [62] (**Figure S5.11**).

Active mono-prenylated isoflavonoids tested in this study have a *logD* value of \leq 4.5. Possibly, very hydrophobic molecules (*logD* $>$ 5.0) are not able to cross the hydrophilic, complex cell wall of yeasts. Yet, the three di-prenylated (iso)flavonoids reported to inhibit the growth of *S. cerevisiae* and/or *C. albicans* (**D3**, **D7** and **D8**, **Table S5.5**) had *logD* values ranging from 5.0–6.1, implying that there might be additional factors that influence the activity of di-prenylated (iso)flavonoids against yeasts.

5.4.2. The interplay between hydrogen bonding and hydrophobic integrity moment dictates the potency of mono-prenylated isoflavonoids

In **Figure 5.5**, the relationship between the two descriptors derived from the QSAR model (*E_ele* and *vsurf_ID7*) for prenylated isoflavonoids with promising activity (MIC \leq 50 $\mu\text{g/mL}$ at pH 6.5) is displayed. Furthermore, the extent of decrease in activity (ΔMFC) of the compounds at lower pH is depicted with different colors.

Electrostatic interactions (*E_ele*) are expressed through hydrogen-bonding in (iso)flavonoids, given that only the undissociated species are expected to interact

with the membrane [63]. Hydrogen bonding is generally known to stabilize the interacting molecules with the polar head groups of the membrane [64]. Besides, intermolecular hydrogen-bonding between prenylated phenolics has been proposed to shield polarity of the free hydroxyl groups inside the membrane [64] (**Chapter 4**). The location of hydrophobic moieties (shown to be associated with *vsurf_ID7*, in **Figure 5.1**) might be important for effective hydrophobic interactions with the interior (lipid core) of the membrane. These molecular properties are frequently related to antimicrobial activity of prenylated (iso)flavonoids [31,65]. Balance between these two properties is considered optimal for effective interactions with the membrane [25,31,65].

Based on the current set of prenylated isoflavonoids, highly active molecules, such as luteone (**7**), wighteone (**9**) and glabridin (**3**), had *E_ele* values of ≥ 38 kcal/mol and *vsurf_ID7* values of $> 0.9 \text{ \AA}$ (**Figure 5.5** and **Table S5.3**). These molecules are expected to interact well with the membrane via hydrogen-bonding and hydrophobic interactions. Based on **Chapter 4**, molecules (**7**) and (**9**) are expected to form clusters inside the membrane, whereas molecule (**3**) might also do it but to a lesser extent. The B-ring prenylated isoflavone, isowighteone (**5**), scored equally high in *E_ele* as (**7**) and (**9**), but moderately in *vsurf_ID7*, suggesting effective hydrogen-bonding, but without having optimal orientation of the prenyl group, which may affect its interaction with the interior of the membrane. Molecules, such as the A-ring prenylated pterocarpenes (**12** and **13**) and the A-ring prenylated isoflavene (**4**) scored moderately, whereas the B-ring prenylated isoflavone, neobavaisoflavone (**8**) scored low on both descriptors. These molecules are expected to make moderate to poor interactions with the membrane, respectively.

The mono-prenylated (iso)flavonoids with promising activity ($\text{MIC} \leq 50 \text{ }\mu\text{g/mL}$) at pH 6.5 showed a lower, although to different extents, antifungal activity at pH 4.0 (shown in different colors in **Figure 5.5**) irrespective of the subclass. Given the different *pK_a* of the molecules from different subclasses (only isoflavones are charged at pH 6.5), it is unlikely that pH-dependent changes in the compounds are responsible for the decrease in activity. Instead, the cell envelop of *Z. parabailii* is known to undergo remodelling, as a resistant mechanism to cope with acidic stress [55,66]. At low pH, the membrane has been reported to become enriched in saturated (highly ordered [67]) glycerophospholipids and complex sphingolipids, which can result in reduced porosity and diffusion of molecules [68]. Upon re-ordering of the membrane, interactions with prenylated isoflavonoids might be hindered.

Compounds with high scores on both descriptors (*E_ele* > 38 kcal/mol and *vsurf_ID7* $> 0.9 \text{ \AA}$) and thus better proposed interactions with the membrane, showed the least change in activity at lower pH ($\Delta\text{MFC} \leq 2$, green color in **Figure 5.5**). Molecules scoring sub-optimally on one descriptor (such as molecule (**5**)) or on both descriptors (such as molecules (**8**), (**12**) and (**13**)) showed moderate ($2 < \Delta\text{MFC} \leq 3$, orange color in **Figure 5.5**) and detrimental activity change (ΔMFC

> 3, red color in **Figure 5.5**), respectively. The only exception to the above is molecule (**4**). Performing this analysis with more representatives from the different subclasses would help to establish more generalized trends.

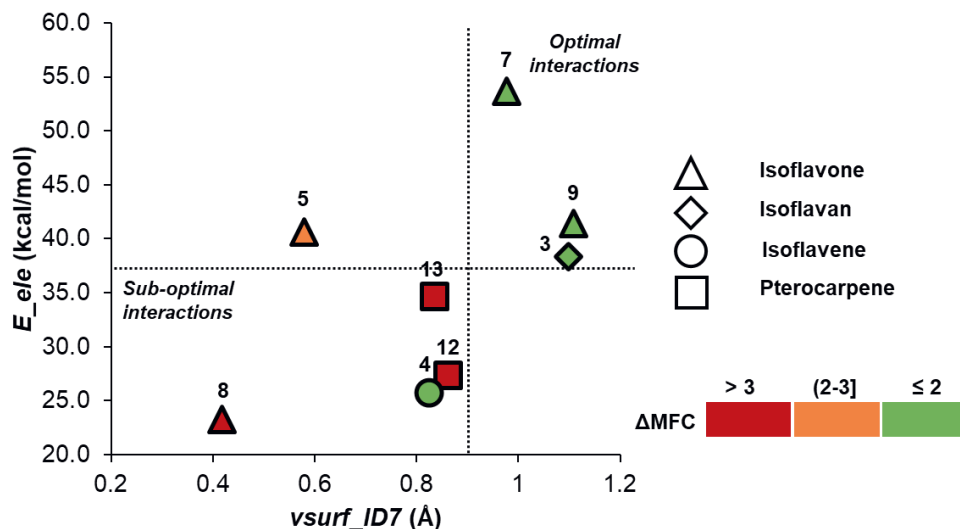


Figure 5.5. Relationship between the two descriptors derived from the QSAR model (E_{ele} and $vsurf_ID7$) and the decrease in the antifungal activity (from pH 6.5 to pH 4.0) of prenylated isoflavonoids with promising potency ($MIC \leq 50 \mu g/mL$) at pH 6.5. The extent of activity decrease upon lowering the pH is shown with different colors; green denotes a $\Delta MFC \leq 2$, orange a $2 < \Delta MFC \leq 3$ and red a $\Delta MFC > 3$. Numbers on top of the symbols refer to compounds and structures in **Figure S5.2** and symbols represent the isoflavonoid subclasses. Dashed lines suggest the descriptor thresholds for optimal and sub-optimal interactions of prenylated isoflavonoids with the membrane.

5.4.3. The most active prenylated isoflavonoids induce different membrane deformations in the cell membrane of *Z. parabailii*

The most potent prenylated isoflavonoids which maintained their high activity also at low pH ($MIC \leq 25 \mu g/mL$) induced rapid killing of the yeast (within 15 min). Membrane permeabilization experiments confirmed fast permeabilization (within 1 h) of the membrane of *Z. parabailii* by glabridin (**3**) and wighteone (**9**), which was accompanied by complete lethality of *Z. parabailii* cells. Fast membrane distortion (within 15 min) after exposure to a killing concentration of the two compounds through TEM imaging corroborated the killing kinetics and the membrane permeabilization. Disruption of the membrane integrity as the primary mode of antimicrobial action of prenylated (iso)flavonoids against *Z. parabailii* confirms what was shown against bacteria and *C. albicans* [38,53,69,70]. Nevertheless, differences in the yeast cell membrane were observed through TEM imaging when

cells were treated with wighteone or glabridin. The membrane elongations and the cluster observed in wighteone-treated yeast cells is reminiscent to endocytosis-dependent changes in the membrane ^[71]. Endocytosis has been associated with the antifungal action of some antimicrobial peptides ^[72]. The possibility of endocytosis-dependent antifungal activity of wighteone and the reason behind the differences induced by the two prenylated isoflavonoids require further investigation.

5.5. Conclusion

This is the first report on the antifungal properties of prenylated (iso)flavonoids against the common food spoilage yeast, *Z. parabailii*. Wighteone and glabridin were the most active prenylated isoflavonoids (MFC 12.5-25 µg/mL, 37-77 µM, respectively at pH 4.0) and their activities are superior to any other natural antifungal reported so far and 20 x higher than sorbic acid against *Z. parabailii*. The antimicrobial properties of prenylated isoflavonoids were correlated with electrostatic potential energy and hydrophobic integrity moment. Wighteone and glabridin scored high on those properties which seem to be related to membrane-activity. The effect of the two molecules on the membrane showed some differences, as visualized through TEM imaging. Prenylated isoflavonoids are promising antimicrobial agents with a distinct mode of action compared to traditional food preservatives. Study of the interaction of prenylated isoflavonoids with other components in food matrices and their potency towards a wider range of *Z. parabailii* strains is necessary to understand their full potential as novel food preservatives.

5.6. References

- [1] Davenport, R. Forensic microbiology for soft drinks business. *Soft Drinks Management International*, 31-33 (1996).
- [2] Suh, S.-O., Gujjari, P., Beres, C., Beck, B. & Zhou, J. Proposal of *Zygosaccharomyces parabailii* sp. nov. and *Zygosaccharomyces pseudobailii* sp. nov., novel species closely related to *Zygosaccharomyces bailii*. *International Journal of Systematic and Evolutionary Microbiology* **63**, 1922-1929 (2013).
- [3] Beuchat, L. Thermal inactivation of yeasts in fruit juices supplemented with food preservatives and sucrose. *Journal of Food Science* **47**, 1679-1682 (1982).
- [4] Stumbo, C. R. *Thermobacteriology in food processing*. (Elsevier, 2013).
- [5] Fleet, G. Spoilage yeasts. *Critical Reviews in Biotechnology* **12**, 1-44 (1992).
- [6] Deak, T. & Beuchat, L. R. Use of indirect conductivity to predict the growth of spoilage yeasts, with special consideration of *Zygosaccharomyces bailii*. *International Journal of Food Microbiology* **23**, 405-417 (1994).
- [7] Martorell, P., Stratford, M., Steels, H., Fernandez-Espinar, M. T. & Querol, A. Physiological characterization of spoilage strains of *Zygosaccharomyces bailii* and *Zygosaccharomyces rouxii* isolated from high sugar environments. *International Journal of Food Microbiology* **114**, 234-242 (2007).
- [8] Krebs, H. A., Wiggins, D., Stubbs, M., Sols, A. & Bedoya, F. Studies on the mechanism of the antifungal action of benzoate. *Biochemical Journal* **214**, 657-663 (1983).
- [9] Neal, A., Weinstock, J. O. & Lampen, J. O. Mechanisms of fatty acid toxicity for yeast. *Journal of Bacteriology* **90**, 126-131 (1965).

- [10] Fujita, K.-i. & Kubo, I. Antifungal activity of octyl gallate. *International Journal of Food Microbiology* **79**, 193-201 (2002).
- [11] Fujita, K.-I. & Kubo, I. Naturally occurring antifungal agents against *Zygosaccharomyces bailii* and their synergism. *Journal of Agricultural and Food Chemistry* **53**, 5187-5191 (2005).
- [12] Piper, P., Mahé, Y., Thompson, S., Pandjaitan, R., Holyoak, C., Egner, R., Mühlbauer, M., Coote, P. & Kuchler, K. The Pdr12 ABC transporter is required for the development of weak organic acid resistance in yeast. *The EMBO Journal* **17**, 4257-4265 (1998).
- [13] Stratford, M. & Anslow, P. Evidence that sorbic acid does not inhibit yeast as a classic 'weak acid preservative'. *Letters in Applied Microbiology* **27**, 203-206 (1998).
- [14] Stratford, M., Plumridge, A., Nebe-von-Caron, G. & Archer, D. B. Inhibition of spoilage mould conidia by acetic acid and sorbic acid involves different modes of action, requiring modification of the classical weak-acid theory. *International Journal of Food Microbiology* **136**, 37-43 (2009).
- [15] Stratford, M., Vallieres, C., Geoghegan, I. A., Archer, D. B. & Avery, S. V. The preservative sorbic acid targets respiration, explaining the resistance of fermentative spoilage-yeast species. *BioRxiv* (2020).
- [16] Stratford, M., Steels, H., Nebe-von-Caron, G., Novodvorska, M., Hayer, K. & Archer, D. B. Extreme resistance to weak-acid preservatives in the spoilage yeast *Zygosaccharomyces bailii*. *International Journal of Food Microbiology* **166**, 126-134 (2013).
- [17] Mira, N. P., Munsterkotter, M., Dias-Valada, F., Santos, J., Palma, M., Roque, F. C., Guerreiro, J. F., Rodrigues, F., Sousa, M. J., Leao, C., Guldener, U. & Sa-Correia, I. The genome sequence of the highly acetic acid-tolerant *Zygosaccharomyces bailii*-derived interspecies hybrid strain ISA1307, isolated from a sparkling wine plant. *DNA Research* **21**, 299-313 (2014).
- [18] Guerreiro, J. F., Mira, N. P. & Sa-Correia, I. Adaptive response to acetic acid in the highly resistant yeast species *Zygosaccharomyces bailii* revealed by quantitative proteomics. *Proteomics* **12**, 2303-2318 (2012).
- [19] van Esch, F. Yeasts in soft drinks and fruit juice concentrates. *Warechemicus (Netherlands)* (1987).
- [20] Steels, H., James, S., Roberts, I. & Stratford, M. Sorbic acid resistance: the inoculum effect. *Yeast* **16**, 1173-1183 (2000).
- [21] Sousa, M. J., Rodrigues, F., Corte-Real, M. & Leao, C. Mechanisms underlying the transport and intracellular metabolism of acetic acid in the presence of glucose in the yeast *Zygosaccharomyces bailii*. *Microbiology* **144** 665-670 (1998).
- [22] Warth, A. Mechanism of resistance of *Saccharomyces bailii* to benzoic, sorbic and other weak acids used as food preservatives. *Journal of Applied Bacteriology* **43**, 215-230 (1977).
- [23] Piper, P. W. Resistance of yeasts to weak organic acid food preservatives. in *Advances in Applied Microbiology* Vol. 77 97-113 (Elsevier, 2011).
- [24] Commission, E. Commission Regulation (EU) No 1129/2011 of 11 November 2011 amending Annex II to Regulation (EC) No 1333/2008 of the European Parliament and of the Council by establishing a Union list of food additives. *Official Journal of the European Union L* **295**, 12.11 (2011).
- [25] Fujita, K. I., Fujita, T. & Kubo, I. Antifungal activity of alkanols against *Zygosaccharomyces bailii* and their effects on fungal plasma membrane. *Phytotherapy Research: An International Journal Devoted to Pharmacological and Toxicological Evaluation of Natural Product Derivatives* **22**, 1349-1355 (2008).
- [26] Rivera-Carriles, K., Argaz, A., Palou, E. & Lopez-Malo, A. Synergistic inhibitory effect of citral with selected phenolics against *Zygosaccharomyces bailii*. *Journal of Food Protection* **68**, 602-606 (2005).
- [27] Mokhtarzadeh, S., Demirci, B., Khawar, K. M. & Kirimer, N. Determination of volatile components in *Thymus vulgaris* L. under *in vitro* conditions. *Journal of Essential Oil Bearing Plants* **21**, 277-281 (2018).

- [28] Mączka, W., Wińska, K. & Grabarczyk, M. One hundred faces of geraniol. *Molecules* **25**, 3303 (2020).
- [29] Gibbons, S. Anti-staphylococcal plant natural products. *Natural Product Reports* **21**, 263-277 (2004).
- [30] Eliopoulos, G. M. & Moellering Jr, R. C. Antibiotic synergism and antimicrobial combinations in clinical infections. *Reviews of Infectious Diseases* **4**, 282-293 (1982).
- [31] Araya-Cloutier, C., Vincken, J. P., van de Schans, M. G. M., Hageman, J., Schaftenaar, G., den Besten, H. M. W. & Gruppen, H. QSAR-based molecular signatures of prenylated (iso)flavonoids underlying antimicrobial potency against and membrane-disruption in Gram positive and Gram negative bacteria. *Scientific Reports* **8**, 9267 (2018).
- [32] Mitscher, L. A., Rao, G. R., Khanna, I., Veysoglu, T. & Drake, S. Antimicrobial agents from higher plants: prenylated flavonoids and other phenols from *Glycyrrhiza lepidota*. *Phytochemistry* **22**, 573-576 (1983).
- [33] Kim, H. J., Suh, H.-J., Lee, C. H., Kim, J. H., Kang, S. C., Park, S. & Kim, J.-S. Antifungal activity of glyceollins isolated from soybean elicited with *Aspergillus sojae*. *Journal of Agricultural and Food Chemistry* **58**, 9483-9487 (2010).
- [34] Ammar, M. I., Nenaah, G. E. & Mohamed, A. H. H. Antifungal activity of prenylated flavonoids isolated from *Tephrosia apollinea* L. against four phytopathogenic fungi. *Crop Protection* **49**, 21-25 (2013).
- [35] Han, Q. B., Qiao, C. F., Song, J. Z., Yang, N. Y., Cao, X. W., Peng, Y., Yang, D. J., Chen, S. L. & Xu, H. X. Cytotoxic prenylated phenolic compounds from the twig bark of *Garcinia xanthochymus*. *Chemistry & Biodiversity* **4**, 940-946 (2007).
- [36] Lima, N. M., Cursino-Hron, L. M., Lima, A. M., Souza, J. V., Oliveira, A. C. d., Marinho, J. V. & Nunez, C. V. Antifungal activity of extracts and phenolic compounds from *Deguelia duckeana*. *Revista Brasileira de Farmacognosia* **28**, 697-702 (2018).
- [37] Fukai, T., Marumo, A., Kaitou, K., Kanda, T., Terada, S. & Nomura, T. Antimicrobial activity of licorice flavonoids against methicillin-resistant *Staphylococcus aureus*. *Fitoterapia* **73**, 536-539 (2002).
- [38] Liu, W., Li, L. P., Zhang, J. D., Li, Q., Shen, H., Chen, S. M., He, L. J., Yan, L., Xu, G. T. & An, M. M. Synergistic antifungal effect of glabridin and fluconazole. *PLoS One* **9**, e103442 (2014).
- [39] Messier, C. & Grenier, D. Effect of licorice compounds licochalcone A, glabridin and glycyrrhizic acid on growth and virulence properties of *Candida albicans*. *Mycoses* **54**, e801-e806 (2011).
- [40] Van De Schans, M. G., Vincken, J.-P., De Waard, P., Hamers, A. R., Bovee, T. F. & Gruppen, H. Glyceollins and dehydroglyceollins isolated from soybean act as SERMs and ER subtype-selective phytoestrogens. *The Journal of Steroid Biochemistry and Molecular Biology* **156**, 53-63 (2016).
- [41] van de Schans, M. G., Ritschel, T., Bovee, T. F., Sanders, M. G., de Waard, P., Gruppen, H. & Vincken, J. P. Involvement of a hydrophobic pocket and helix 11 in determining the modes of action of prenylated flavonoids and isoflavonoids in the human estrogen receptor. *ChemBioChem* **16**, 2668-2677 (2015).
- [42] Aryani, D., Den Besten, H., Hazeleger, W. & Zwietering, M. Quantifying strain variability in modeling growth of *Listeria monocytogenes*. *International Journal of Food Microbiology* **208**, 19-29 (2015).
- [43] Shahlaei, M. Descriptor selection methods in quantitative structure-activity relationship studies: a review study. *Chemical Reviews* **113**, 8093-8103 (2013).
- [44] Shen, Q., Jiang, J.-H., Jiao, C.-X., Shen, G.-I. & Yu, R.-Q. Modified particle swarm optimization algorithm for variable selection in MLR and PLS modeling: QSAR studies of antagonism of angiotensin II antagonists. *European Journal of Pharmaceutical Sciences* **22**, 145-152 (2004).
- [45] Cherkasov, A., Muratov, E. N., Fourches, D., Varnek, A., Baskin, I. I., Cronin, M., Dearden, J., Gramatica, P., Martin, Y. C. & Todeschini, R. QSAR modeling: where

- have you been? Where are you going to? *Journal of Medicinal Chemistry* **57**, 4977-5010 (2014).
- [46] Karelson, M., Karelson, G., Tamm, T., Tulp, I., Jänes, J., Tamm, K., Lomaka, A., Savchenko, D. & Dobcheva, D. QSAR study of pharmacological permeabilities. *ARKIVOC: Online Journal of Organic Chemistry* (2009).
- [47] Tropsha, A. Best practices for QSAR model development, validation, and exploitation. *Molecular Informatics* **29**, 476-488 (2010).
- [48] Norden, C. W., Wentzel, H. & Keleti, E. Comparison of techniques for measurement of in vitro antibiotic synergism. *Journal of Infectious Diseases* **140**, 629-633 (1979).
- [49] Bassolé, I. H. N. & Juliani, H. R. Essential oils in combination and their antimicrobial properties. *Molecules* **17**, 3989-4006 (2012).
- [50] van Vuuren, S. & Viljoen, A. Plant-based antimicrobial studies—methods and approaches to study the interaction between natural products. *Planta Medica* **77**, 1168-1182 (2011).
- [51] Mulyaningsih, S., Sporer, F., Zimmermann, S., Reichling, J. & Wink, M. Synergistic properties of the terpenoids aromadendrene and 1, 8-cineole from the essential oil of *Eucalyptus globulus* against antibiotic-susceptible and antibiotic-resistant pathogens. *Phytomedicine* **17**, 1061-1066 (2010).
- [52] Banerjee, A., Majumder, P., Sanyal, S., Singh, J., Jana, K., Das, C. & Dasgupta, D. The DNA intercalators ethidium bromide and propidium iodide also bind to core histones. *FEBS Open Bio* **4**, 251-259 (2014).
- [53] Araya-Cloutier, C., Vincken, J.-P., van Ederen, R., den Besten, H. M. & Gruppen, H. Rapid membrane permeabilization of *Listeria monocytogenes* and *Escherichia coli* induced by antibacterial prenylated phenolic compounds from legumes. *Food Chemistry* **240**, 147-155 (2018).
- [54] Sharifi, M. & Ghafourian, T. Estimation of biliary excretion of foreign compounds using properties of molecular structure. *The AAPS Journal* **16**, 65-78 (2014).
- [55] Lindahl, L., Genheden, S., Eriksson, L. A., Olsson, L. & Bettiga, M. Sphingolipids contribute to acetic acid resistance in *Zygosaccharomyces bailii*. *Biotechnology and Bioengineering* **113**, 744-753 (2016).
- [56] Pitt, J., Hocking, A. & Beuchat, L. R. Fungi and food spoilage (2nd edn). *Trends in Food Science and Technology* **9**, 89 (1998).
- [57] Pitt, J. & Richardson, K. Spoilage by preservative-resistant yeasts. (1973).
- [58] Berry, J. M. Yeast problems in the food and beverage industry. *Food mycology*, 82-90 (1979).
- [59] Stratford, M., Nebe-von-Caron, G., Steels, H., Novodvorska, M., Ueckert, J. & Archer, D. B. Weak-acid preservatives: pH and proton movements in the yeast *Saccharomyces cerevisiae*. *International Journal of Food Microbiology* **161**, 164-171 (2013).
- [60] Aleksić, M. & Kapetanović, V. An overview of the optical and electrochemical methods for detection of DNA-drug interactions. *Acta Chimica Slovenica* **61**, 555-573 (2014).
- [61] Sohn, H. Y., Son, K. H., Kwon, C. S., Kwon, G. S. & Kang, S. S. Antimicrobial and cytotoxic activity of 18 prenylated flavonoids isolated from medicinal plants: *Morus alba* L., *Morus mongolica* Schneider, *Broussonetia papyrifera* (L.) Vent, *Sophora flavescens* Ait and *Echinosophora koreensis* Nakai. *Phytomedicine* **11**, 666-672 (2004).
- [62] Tahara, S., Katagiri, Y., Ingham, J. L. & Mizutani, J. Prenylated flavonoids in the roots of yellow lupin. *Phytochemistry* **36**, 1261-1271 (1994).
- [63] Cramariuc, O., Rog, T., Javanainen, M., Monticelli, L., Polishchuk, A. V. & Vattulainen, I. Mechanism for translocation of fluoroquinolones across lipid membranes. *Biochimica et Biophysica Acta (BBA)-Biomembranes* **1818**, 2563-2571 (2012).
- [64] Li, J., Beuerman, R. W. & Verma, C. S. Molecular insights into the membrane affinities of model hydrophobes. *ACS Omega* **3**, 2498-2507 (2018).

- [65] Sadgrove, N. J., Oliveira, T. B., Khumalo, G. P., Vuuren, S. F. v. & van Wyk, B. - E. Antimicrobial isoflavones and derivatives from *Erythrina* (Fabaceae): structure activity perspective (sar & qsar) on experimental and mined values against *Staphylococcus Aureus*. *Antibiotics* **9**, 223 (2020).
- [66] Kuanyshev, N., Ami, D., Signori, L., Porro, D., Morrissey, J. P. & Branduardi, P. Assessing physio-macromolecular effects of lactic acid on *Zygosaccharomyces bailii* cells during microaerobic fermentation. *FEMS Yeast Research* **16** (2016).
- [67] Simons, K. & Sampaio, J. L. Membrane organization and lipid rafts. *Cold Spring Harbor Perspectives in Biology* **3**, a004697 (2011).
- [68] Lindberg, L., Santos, A. X., Riezman, H., Olsson, L. & Bettiga, M. Lipidomic profiling of *Saccharomyces cerevisiae* and *Zygosaccharomyces bailii* reveals critical changes in lipid composition in response to acetic acid stress. *PloS One* **8**, e73936 (2013).
- [69] Mun, S.-H., Joung, D.-K., Kim, S.-B., Park, S.-J., Seo, Y.-S., Gong, R., Choi, J.-G., Shin, D.-W., Rho, J.-R. & Kang, O.-H. The mechanism of antimicrobial activity of sophoraflavanone B against methicillin-resistant *Staphylococcus aureus*. *Foodborne Pathogens and Disease* **11**, 234-239 (2014).
- [70] Pang, D., Liao, S., Wang, W., Mu, L., Li, E., Shen, W., Liu, F. & Zou, Y. Destruction of the cell membrane and inhibition of cell phosphatidic acid biosynthesis in *Staphylococcus aureus*: an explanation for the antibacterial mechanism of morusin. *Food & Function* **10**, 6438-6446 (2019).
- [71] Buser, C. & Drubin, D. G. Ultrastructural imaging of endocytic sites in *Saccharomyces cerevisiae* by transmission electron microscopy and immunolabeling. *Microscopy and Microanalysis* **19**, 381-392 (2013).
- [72] Rossignol, T., Kelly, B., Dobson, C. & d'Enfert, C. Endocytosis-mediated vacuolar accumulation of the human ApoE apolipoprotein-derived ApoEdpL-W antimicrobial peptide contributes to its antifungal activity in *Candida albicans*. *Antimicrobial Agents and Chemotherapy* **55**, 4670-4681 (2011).

5.7. Supplementary information

5.7.1. Supplementary figures

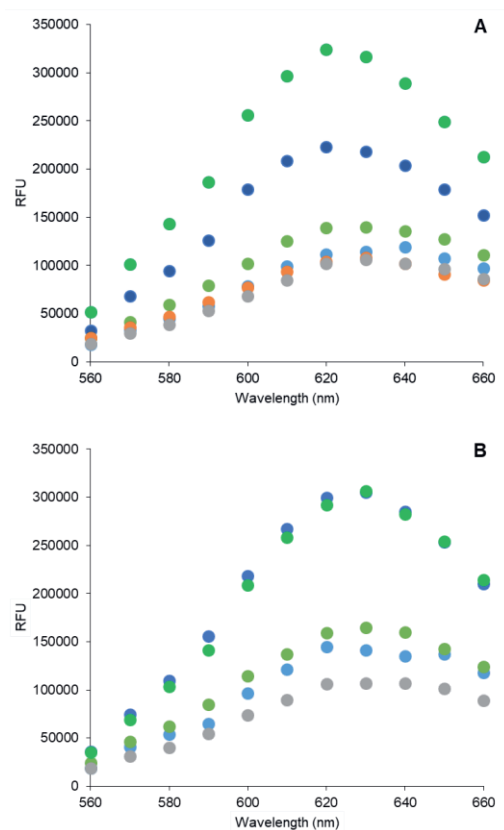


Figure S5.1. Fluorescence spectra (emission of fluorescence at 620 nm and excitation of samples at 520 nm) of mixtures of PI with glabridin (blue) and with wighteone (green) at pH 4.0 (A) and at pH 7.2 (B). PI alone is shown in grey. Colour intensity is related to the concentration of prenylated isoflavonoids; light colour represents a final concentration of 25 µg/mL and darker colour represents a final concentration of 50 µg/mL. The combination of PI with (1,100 µg/mL) sorbic acid is shown in orange and only at the relevant pH (4.0).

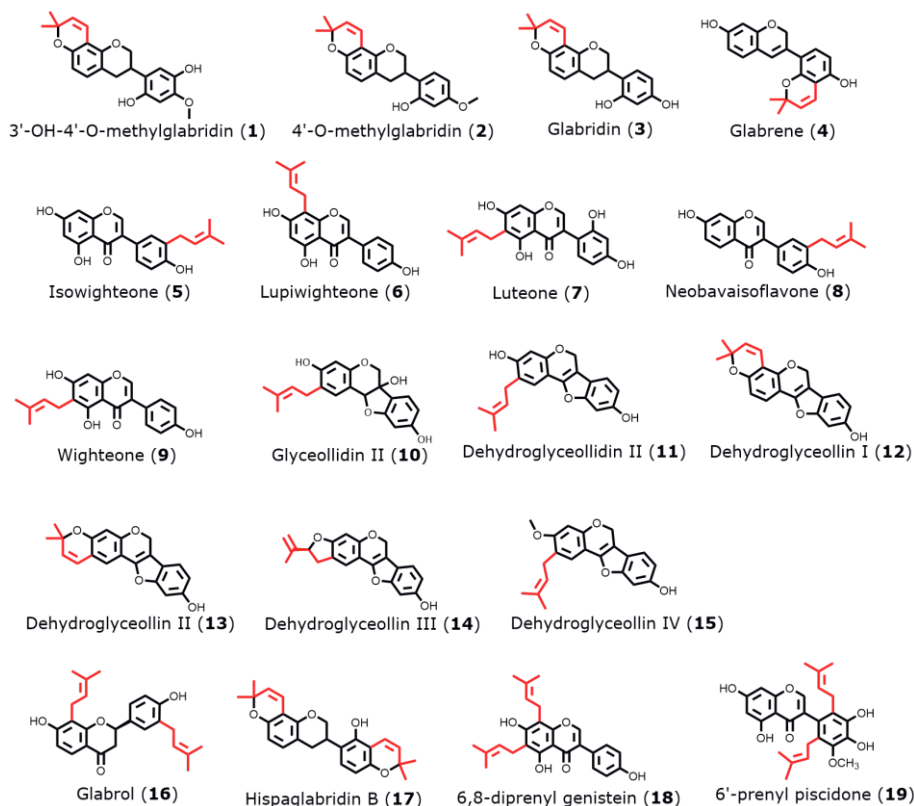


Figure S5.2. Structures of mono-prenylated (iso)flavonoids tested in this study for their antifungal potency against *Z. parabailii* (UL 3699).

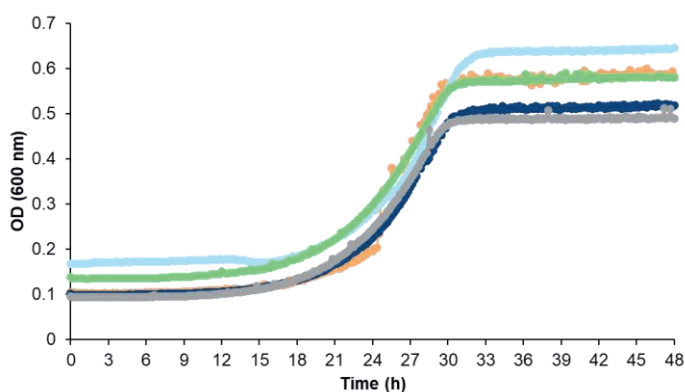


Figure S5.3. Optical density measured at 600 nm of *Z. parabailii* (UL 3699) cells treated with maximum concentration (25 $\mu\text{g/mL}$) of di-prenylated (iso)flavonoids. Orange colour is used for hispaglabridin B, green colour represents glabrol, and blue represents the two isoflavones, 6,8-diprenyl genistein (light) and 6'-prenyl piscidone (dark). Grey colour represents the control yeast cells.

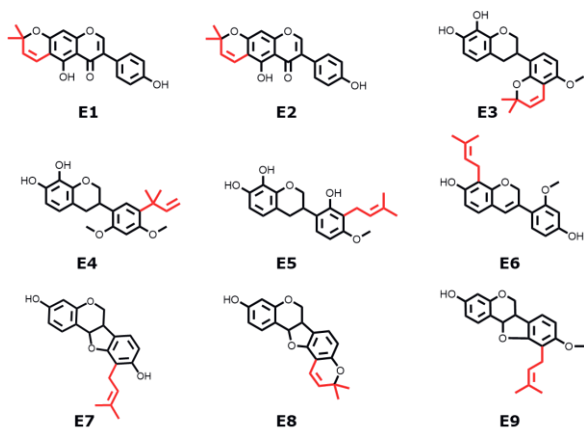


Figure S5.4. Set of prenylated (iso)flavonoids tested against other yeasts (mined from literature) to assess the predictive quality of the binary QSAR model.

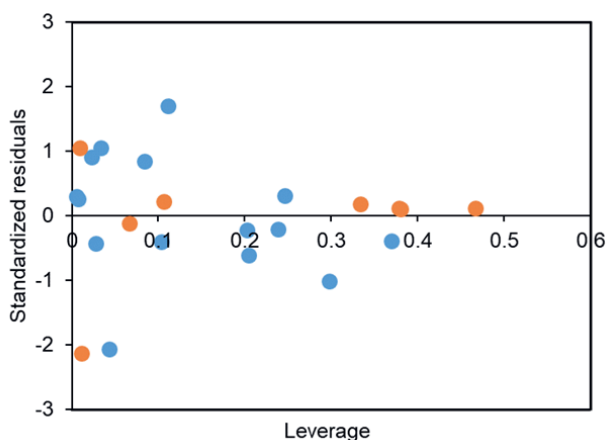


Figure S5.5. Applicability domain of the binary QSAR model for *Z. parabailii*. The in-house data is shown in blue and the external set is displayed in orange. Boundaries were determined based on Gramatica *et al.* (2007) ^[1].

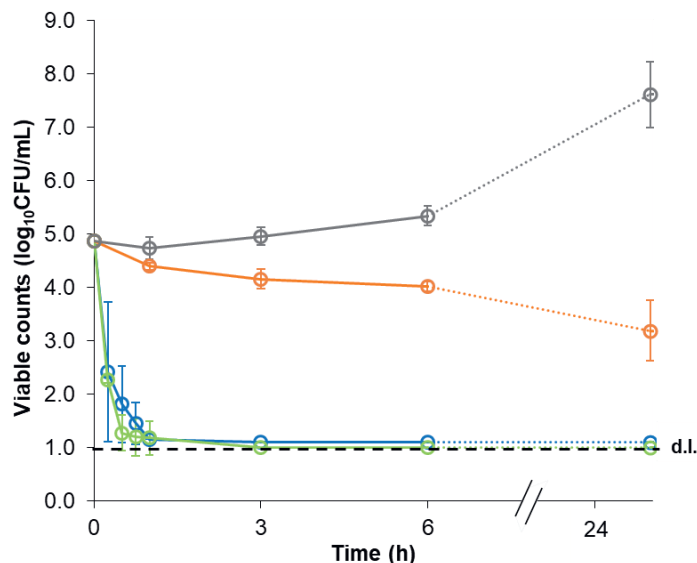


Figure S5.6. Inactivation kinetics of *Z. parabailii* (ATCC 60483) cells (10^5 CFU/mL) in the presence of 12.5 μ g/mL wightone (green), 25 μ g/mL glabridin (blue) and 1,650 μ g/mL sorbic acid (orange) at pH 4.0. Control cells are shown in grey. d.l. refers to detection limit.

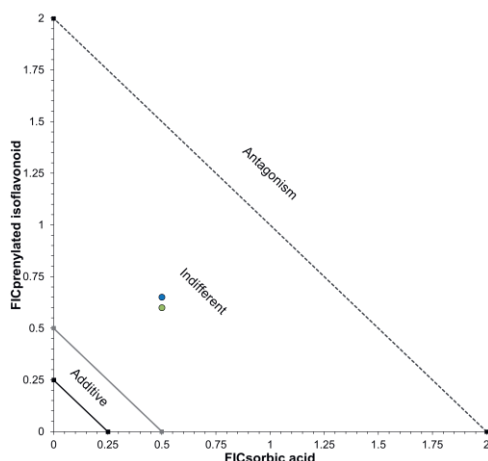


Figure S5.7. Isobolograms of combinations of sorbic acid with glabridin (blue) or wightone (green) at pH 4.0 against *Z. parabailii* (UL 3699), studied with the checkerboard assay. The isobologram was constructed based on the definitions provided by Bassolé *et al.* (2012), van Vuuren *et al.* (2011) and Mulyaningsih *et al.* (2010) [2-4].

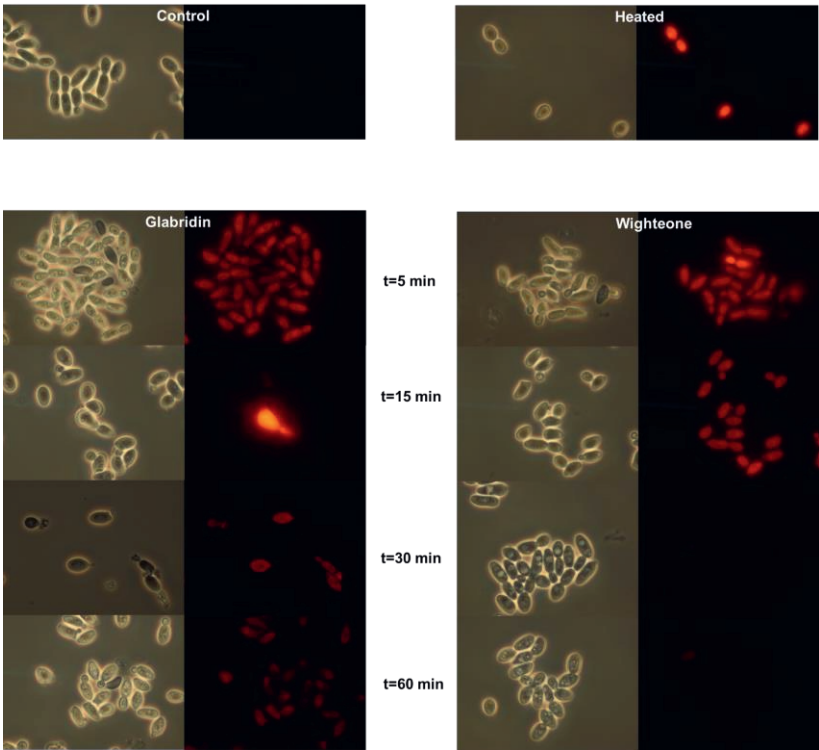


Figure S5.8. Light and fluorescence microscopy images of *Z. parabailii* (UL 3699, 10^9 CFU/mL) after exposure to 25 μ g/mL prenylated isoflavonoids over time at pH 7.2.

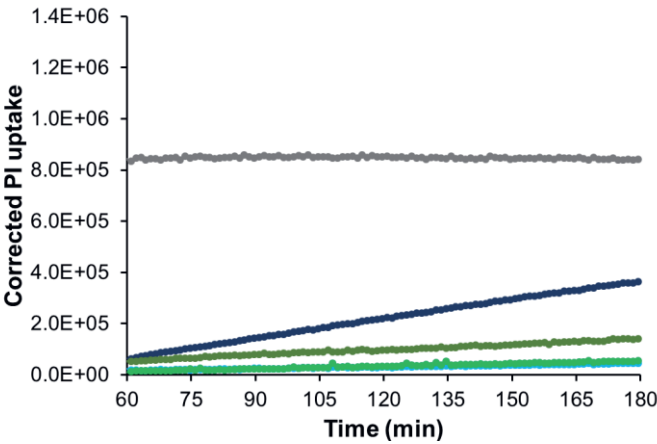


Figure S5.9. Propidium iodide uptake in time after incubating *Z. parabailii* cells (UL 3699) with different concentrations of glabridin (blue lines) and wighteone (green lines) (light colours correspond to 25 μ g/mL and dark colors correspond to 50 μ g/mL) for 1 h at pH 7.2. Heated cells served as the positive control and the PI signal of all treated cells was corrected for the untreated incubated with PI. Data are means of three biological replications.

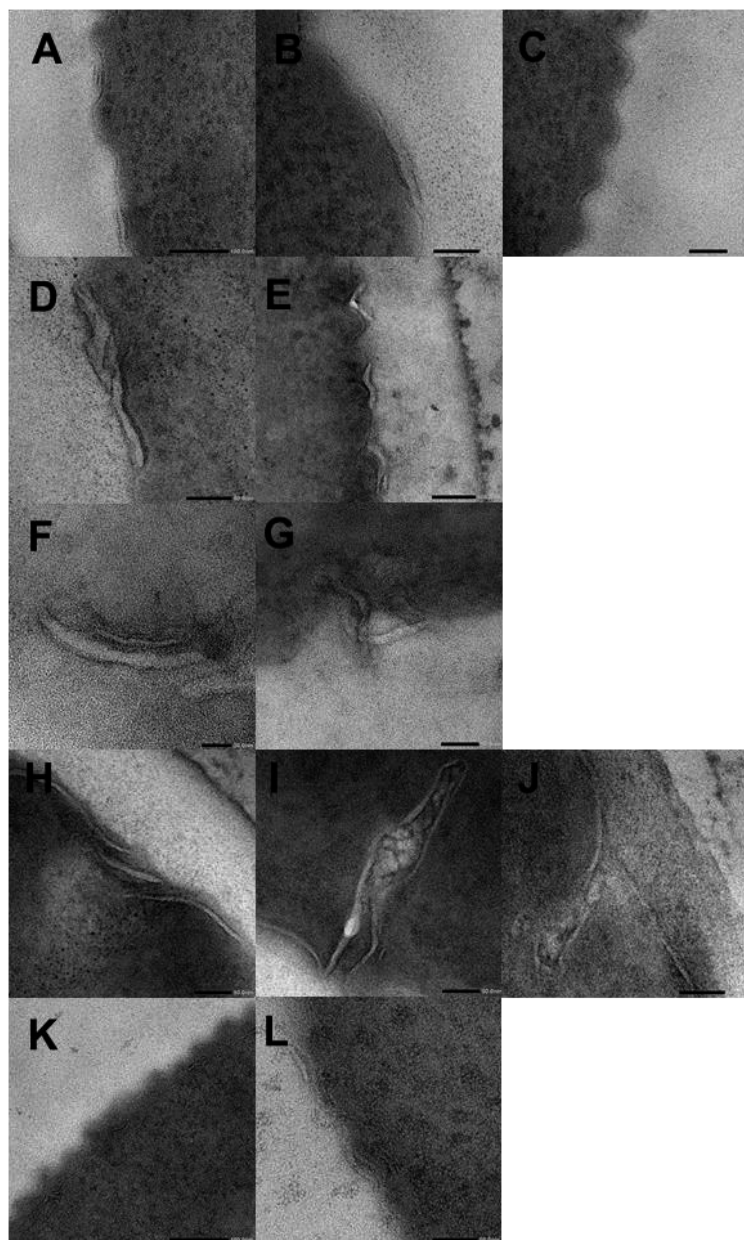


Figure S5.10. TEM images of *Z. parabailii* (UL 3699) cells (10^9 CFU/mL) exposed to 50 μ g/mL glabridin and 25 μ g/mL wighteone for 15 and 180 min, respectively, compared to untreated cells at 180 min. Panels **A-C** show untreated cells at 180 min; scale bars at 100 nm, 50 nm and 50 nm respectively. Panels **D-E** depict glabridin-treated cells for 15 min; scale bars at 50 nm and 100 nm, respectively. Panels **F-G** show glabridin-treated cells for 180 min; scale bars at 20 nm and 50 nm, respectively. Panels **H-J** depict wighteone-treated cells for 15 min; scale bars at 50 nm, and panels **K-L** correspond to wighteone-treated cells for 180 min; scale bars at 100 nm and 50 nm, respectively.

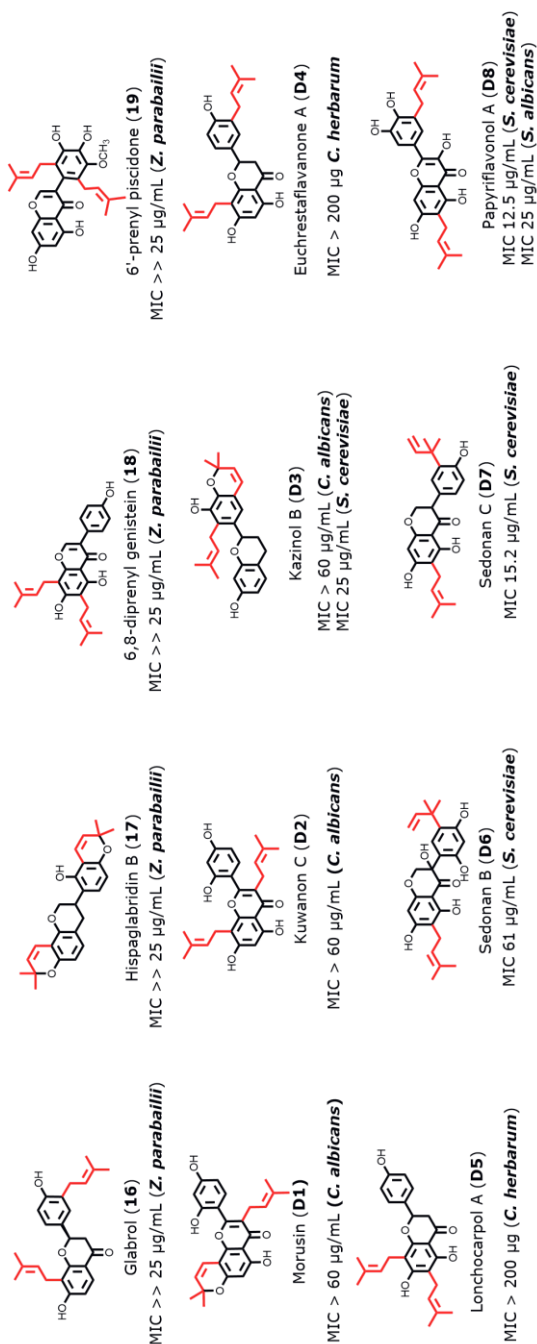


Figure S5.11. Structures of di-prenylated (iso)flavonoids tested against other yeasts mined from literature (**D1-D8**). Di-prenylated (iso)flavonoids tested in this study (**16-19**) are also presented here for comparison. In **bold**, the yeast strain against which di-prenylated (iso)flavonoids were tested is mentioned.

5.7.2. Supplementary tables

Table S5.1. Total and cross-validated accuracies of best binary QSAR model developed in this study, where an activity threshold of 25 µg/mL was used. All accuracies were significant (p -value < 0.05).

Descriptor (relative importance*, contribution)	Accuracy			Cross-validated accuracy		
	Total	Actives	Inactives	Total	Actives	Inactives
<i>vsurf_ID7</i> (30%, +)	93%	100%	86%	87%	88%	86%
<i>E_ele</i> (35%, +)						

Table S5.2. External validation set of best binary QSAR model developed in this study. An activity threshold of MIC ≤ 25 µg/mL was used to discriminate active from inactive molecules. Predicted binary activity > 0.5 classifies the molecule as active. The structures of the compounds can be visualized in **Figure S5.4**.

ID	Name	Subclass	MIC (µg/mL)	pMIC (M)	Predicted binary activity	Microorganism	Ref.
E1	Alpinumisoflavone	Isoflavone	>50	<3.8	n.a.	<i>C. albicans</i>	[5]
E2	Derrone	Isoflavone	7.8	4.6	0.9	<i>Candida spp</i>	[6]
E3	Sedonan D	Isoflavan	30.5	4.1	0.1	<i>S. cerevisiae</i>	[7]
E4	Sedonan E	Isoflavan	15.2	4.4	0.8	<i>S. cerevisiae</i>	[7]
E5	Sedonan F	Isofavan	15.2	4.4	0.6	<i>S. cerevisiae</i>	[7]
E6	Erypoeigin A	Isoflavene	>100	<3.8	0.9	<i>C. albicans</i>	[8]
E7	Phaseollidin	Pterocarpan	>100	<3.8	0.6	<i>S. cerevisiae</i>	[9]
E8	Phaseollin	Pterocarpan	25	4.6	0.6	<i>S. cerevisiae</i>	[9]
E9	Sandwicensin	Pterocarpan	30.5	4.0	0.7	<i>S. cerevisiae</i>	[7]

Table S5.3. Descriptor values of prenylated (iso)flavonoids; Log of the octanol/water partition coefficient ($\log P(o/w)$), electrostatic component of potential energy (E_{ele}), the hydrophobic integy moment ($vsurf_ID7$) and the distribution coefficient at pH 6.5 ($\log D$). All descriptors were calculated with MOE whereas $\log D$ was calculated with MarvinSketch 20.3 (ChemAxon).

No.	Subclass	Compound	pMIC (M)	$\log P(o/w)$	E_{ele} (kcal/mol)	$vsurf_ID7$ (Å)	$\log D$ (pH 6.5)
1	Isoflavan	3'-OH-4'-O-methyl glabridin	3.5	4.1	-28.4	1.3	3.9
2		4'-O-methyl glabridin	4.1	4.5	-34.8	0.9	4.2
3		Glabridin	4.4	4.2	-38.4	1.1	4.1
4	Isoflavene	Glabrene	4.1	4.7	-25.7	0.8	4.0
5	Isoflavone	Isowighteone	4.4	3.0	-40.6	0.6	4.5
6		Lupiwighteone	3.5	2.9	-39.6	0.9	4.4
7		Luteone	4.5	2.7	-53.6	1.0	4.0
8		Neobavaisoflavone	3.8	3.3	-23.3	0.4	4.0
9		Wighteone	4.7	2.9	-41.4	1.1	4.5
10	Pterocarpan	Glyceollidin II	3.5	3.3	-23.2	1.1	3.4
11		Dehydrolyceollidin II	3.8	4.4	-31.5	0.7	4.4
12	Pterocarpene	Dehydroglyceollin I	4.1	4.8	-27.3	0.9	3.9
13		Dehydroglyceollin II	4.1	4.9	-34.6	0.8	3.9
14		Dehydroglyceollin III	3.5	4.3	-18.3	0.5	3.9
15		Dehydroglyceollin IV	3.5	4.6	-21.0	0.7	4.6
16	Flavanone	Glabrol	3.5	4.8	-51.3	0.6	5.9
17	Isoflavan	Hispaglabridin B	3.5	5.8	-33.2	1.0	5.3
18	Isoflavone	6,8-diprenylgenistein	3.5	4.0	-44.3	1.7	6.0
19		6'-prenyl piscidone	3.5	3.7	-52.0	2.0	5.7

Table S5.4. Antifungal potency (in µg/mL) of prenylated isoflavonoids against *Z. parabailii* (ATCC 60483) at pH 4.0. (-) means not tested. Ranges in MIC/MFC derive from different values of the replicates. In parentheses, the percentage of undissociated sorbic at each pH is given (MarvinSketch 20.3, ChemAxon).

No.	Subclass	Compound	MIC	MFC
1	Isoflavan	Glabridin	12.5-25	25
4	Isoflavene	Glabrene	75	100
11	Isoflavone	Isowighteone	75	100
12	Isoflavone	Luteone	37.5-50	50
13	Isoflavone	Wighteone	25	37.5
14	Weak organic acid	Sorbic acid (86%)	275	550

Table S5.5. Overview of di-prenylated (iso)flavonoids and their antifungal activity (MIC in µg/mL) extracted from literature. Structures of all di-prenylated (iso)flavonoids can be found in **Figure S5.11**. *LogD* (pH 6.5) was calculated with MarvinSketch 20.3 (ChemAxon).

No.	Subclass	Compound	MIC	Mw	Yeast strain	<i>logD</i>	Ref.
D1	Flavone	Morusin	>60	420.5	<i>C. albicans</i>	5.2	[10]
D2	Flavone	Kuwanon C	>60	422.5	<i>C. albicans</i>	5.3	[10]
D3	Flavan	Kazinol B	25	392.5	<i>S. cerevisiae</i>	6.1	[10]
			>60		<i>C. albicans</i>		
D4	Flavanone	Euchrestaflavanone A	>200 [#]	408.5	<i>C. herbarum</i>	6.2	[11]
D5	Flavanone	Lonchocarpol A	>200 [#]	408.5	<i>C. herbarum</i>	6.2	[11]
D6	Isoflavanone	Sedonan B	61	440.5	<i>S. cerevisiae</i>	5.2	[7]
D7	Isoflavanone	Sedonan C	15.2	408.5	<i>S. cerevisiae</i>	6.1	[7]
D8	Flavonol	Papyriflavanol A	12.5	438.5	<i>S. cerevisiae</i>	5.0	[12]
			25		<i>C. albicans</i>		[12]

[#] values expressed in µg

5.7.3. Supplementary references

- [1] Gramatica, P. Principles of QSAR models validation: internal and external. *QSAR & Combinatorial Science* **26**, 694-701 (2007).
- [2] Bassolé, I. H. N. & Juliani, H. R. Essential oils in combination and their antimicrobial properties. *Molecules* **17**, 3989-4006 (2012).
- [3] van Vuuren, S. & Viljoen, A. Plant-based antimicrobial studies—methods and approaches to study the interaction between natural products. *Planta Medica* **77**, 1168-1182 (2011).
- [4] Mulyaningsih, S., Sporer, F., Zimmermann, S., Reichling, J. & Wink, M. Synergistic properties of the terpenoids aromadendrene and 1, 8-cineole from the essential oil of *Eucalyptus globulus* against antibiotic-susceptible and antibiotic-resistant pathogens. *Phytomedicine* **17**, 1061-1066 (2010).
- [5] Li, X.-C., Joshi, A. S., ElSohly, H. N., Khan, S. I., Jacob, M. R., Zhang, Z., Khan, I. A., Ferreira, D., Walker, L. A. & Broedel, S. E. Fatty acid synthase inhibitors from plants: isolation, structure elucidation, and SAR studies. *Journal of Natural Products* **65**, 1909-1914 (2002).
- [6] Edziri, H., Mastouri, M., Mahjoub, M. A., Mighri, Z., Mahjoub, A. & Verschaeye, L. Antibacterial, antifungal and cytotoxic activities of two flavonoids from *Retama raetam* flowers. *Molecules* **17**, 7284-7293 (2012).
- [7] Belofsky, G., Kolaczowski, M., Adams, E., Schreiber, J., Eisenberg, V., Coleman, C. M., Zou, Y. & Ferreira, D. Fungal ABC transporter-associated activity of isoflavonoids from the root extract of *Dalea formosa*. *Journal of Natural Products* **76**, 915-925 (2013).
- [8] Sato, M., Tanaka, H., Yamaguchi, R., Oh-Uchi, T. & Etoh, H. *Erythrina poeppigiana*-derived phytochemical exhibiting antimicrobial activity against *Candida albicans* and methicillin-resistant *Staphylococcus aureus*. *Letters in Applied Microbiology* **37**, 81-85 (2003).
- [9] Taniguchi, M. & Kubo, I. Ethnobotanical drug discovery based on medicine men's trials in the African savanna: screening of east African plants for antimicrobial activity II. *Journal of Natural Products* **56**, 1539-1546 (1993).
- [10] Sohn, H. Y., Son, K. H., Kwon, C. S., Kwon, G. S. & Kang, S. S. Antimicrobial and cytotoxic activity of 18 prenylated flavonoids isolated from medicinal plants: *Morus alba* L., *Morus mongolica* Schneider, *Broussonetia papyrifera* (L.) Vent, *Sophora flavescens* Ait and *Echinosophora koreensis* Nakai. *Phytomedicine* **11**, 666-672 (2004).
- [11] Tahara, S., Katagiri, Y., Ingham, J. L. & Mizutani, J. Prenylated flavonoids in the roots of yellow lupin. *Phytochemistry* **36**, 1261-1271 (1994).
- [12] Sohn, H.-Y., Kwon, C.-S. & Son, K.-H. Fungicidal effect of prenylated flavonol, papyriflavonol a, isolated from *Broussonetia papyrifera* (L.) vent. against *Candida albicans*. *Journal of Microbiology and Biotechnology* **20**, 1397-1402 (2010).

CHAPTER

6

General Discussion

As described in the **General Introduction**, prenylated (iso)flavonoids are biosynthesized in plants of the Fabaceae family as part of their defence mechanism. Prenylated (iso)flavonoids are acknowledged for the antimicrobial properties they can exert, rendering them potential candidates as novel therapeutic agents or food preservatives. In this thesis, it was hypothesized that sensitization prior to the traditionally employed fungal elicitation would increase the amounts and diversity of inducible prenylated isoflavonoids in soybean seedlings. Furthermore, given that prenylation-based hydrophobicity is not the only determinant for antimicrobial activity, a systematic, validated QSAR study on 77 analogues was performed to identify other molecular properties important for the activity against the Gram-positive pathogen, MRSA. Prenylated (iso)flavonoids were also shown to be effective antimicrobial against a challenging food spoilage yeast by disrupting its membrane integrity. The main aims of this thesis was (a) to enhance the biosynthesis of prenylated (iso)flavonoids *in planta*, (b) to explore their antimicrobial properties against pathogenic and spoilage microorganisms and (c) to get insights into their mode of antimicrobial action. In this chapter, the following aspects are discussed: (i) the main techniques employed in this thesis focusing on the *in planta* production of prenylated (iso)flavonoids and on QSAR modelling, (ii) the antimicrobial properties of prenylated (iso)flavonoids and insights into their mode of action, (iii) the antimicrobial potency of these compounds against a spore-forming bacterium, and (iv) prospects for the use of these compounds as antimicrobials in clinical and food applications.

6.1. Main considerations with techniques used in this thesis

6.1.1. Priming versus elicitation: two highly intertwined concepts

In **Chapters 2** and **3**, the concept of sensitization of soybean seedlings prior to microbial elicitation was used to enhance the biosynthesis of prenylated isoflavonoids.

In this section, the findings obtained using the pure 'Envy' cultivar are mainly discussed (unless stated otherwise), as the full range of treatments was applied to this cultivar. In **Chapter 2**, soybean seedlings were treated with H_2O_2 and then with FeSO_4 to generate reactive oxygen species (ROS), which are key signalling molecules and are known to promote the plant into a priming state ^[1]. The ROS-treatment alone led to the production of prenylated pterocarpan (glyceollins) in levels lower than those in seedlings elicited with fungus (benchmark treatment) (**Figure 6.1**, light green and dark blue solid lines; event 1). It should be, however, noted that the ROS-treatment induced similar glyceollin amounts to the benchmark in a mixture of different soybean lines (mixCv) (**Chapter 2**). This discrepancy shows the difficulty to distinguish priming from elicitation in all instances. When H_2O_2 was followed by an application of AgNO_3 , the production of glyceollins significantly exceeded that by the benchmark treatment (**Figure 6.1**, dark green solid line; event 1), suggesting that $\text{H}_2\text{O}_2 + \text{AgNO}_3$ is an elicitation treatment. Preliminary evidence suggested that H_2O_2 and AgNO_3 had additive effects in the induction of glyceollins (H_2O_2 alone was 2 x times more effective than AgNO_3 alone). Besides glyceollins, $\text{H}_2\text{O}_2 + \text{AgNO}_3$ additionally triggered the (low) accumulation of prenylated isoflavones (**Figure 6.1**, dark green dashed line; event 1), which were maximally induced upon subsequent microbial elicitation (**Figure 6.1**, dark green dashed line, event 2). This demonstrates that $\text{H}_2\text{O}_2 + \text{AgNO}_3$ had an eliciting effect on glyceollins and a priming effect on prenylated isoflavones, showing once more the difficulty in distinguishing the two concepts.

To be able to assess whether a plant is in a primed state, Martinez-Medina *et al.* (2016) proposed three criteria that need to be asserted: (i) memory (i.e. the information of the priming stimulus is stored until subsequent attack), (ii) fitness costs and (iii) robust defence responses ^[2]. More specifically, several molecular markers related to memory are helpful in identifying the primed state in the model plant, *Arabidopsis*. Increased expression levels of pattern-recognition receptors and of transcription factor genes as well as the accumulation of the mitogen-activated protein kinases, are some indicators that memory has been established ^[3]. Fitness costs refer to the genetic contribution of a plant to the next generation, including plant growth and seed production ^[2]. With respect to robust defence responses in primed plants, these are expressed by longer-lasting activation of defensive traits upon challenge compared to unprimed plants ^[4]. Defensive traits

include defence-related signalling molecules and actual defence responsesI such as the accumulation of secondary metabolites like prenylated (iso)flavonoids [5]. Ideally, quantification of these molecular markers in untreated, “primed”, “elicited”, “primed and elicited” and “sequentially elicited” plants together with an evaluation of the resulting cost–benefit ratio might help to disentangle the concepts of priming and elicitation better [2].

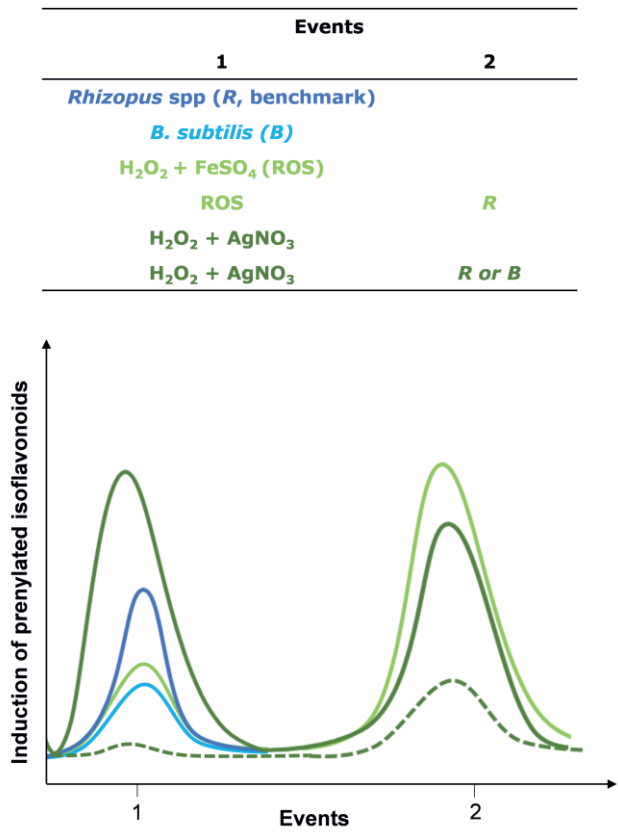


Figure 6.1. Relative response of soybean seedlings (‘Envy’) to the treatments (summarized in the table on top) with respect to production of prenylated isoflavonoids. The colors in the figure correspond to those in the table. The area under the curve represents the extent of induction of prenylated isoflavonoids; solid line = glyceollins, dashed line = prenylated isoflavones. Peak area of event 1 correspond to the accumulation of compounds induced by one event, whereas peak area of event 2 correspond to the accumulation induced by both events.

6.1.2. Is sensitization prior to elicitation the way for enhanced production of prenylated (iso)flavonoids?

In **Chapters 2** and **3**, parameters such as (i) the genetic makeup of the soybean cultivar, regarding its capacity to produce high amounts of diverse metabolites, (ii) the age of the seedlings and (iii) the type of treatment (for example, ROS versus

H₂O₂ + AgNO₃) were explored aiming to increase the quantities and diversity of inducible prenylated isoflavonoids.

Priming with ROS prior to elicitation (ROS + *R*) stimulated the production of glyceollins at a level of 3 mg/g dry weight in mixCv, which was 4-fold higher compared to elicitation alone. These amounts are in the range of *in planta* production of prenylated isoflavonoids normally found with soybean seedlings [6]. However, other studies on elicitation of soybean seedlings obtained an array of prenylated isoflavonoids, even though glyceollins were the predominant molecular species [7,8]. Interestingly, when the 'Envy' cultivar was employed, two observations were made; (a) ROS + *R* was superior to fungal elicitation in the induction of glyceollins, only when applied on seedlings 2 d older than in mixCv and (b) no substantial diversification of prenylated isoflavonoids was achieved by ROS + *R* even though some minor induction of prenylated isoflavones was observed by *R*-elicitation in this cultivar.

Increased diversity was achieved in 'Envy', but not in mixCv (data not shown), when the cultivars were treated with H₂O₂ and AgNO₃ prior to microbial elicitation. The production of prenylated isoflavones in (H₂O₂ + AgNO₃)-treated and subsequently elicited seedlings was not accompanied with further induction of glyceollins, suggesting that the plant might have reached its maximum biosynthetic capacity. Therefore, further fine-tuning the choice of elicitors or growth conditions is not expected to substantially increase the quantities and diversity of compounds of interest in the 'Envy' cultivar.

Another factor that was not considered in this thesis is the exudation of prenylated isoflavonoids that has been reported in several elicited legume species [9-12]. For example, secretion of glyceollin I was 50-fold higher after inoculation with the symbiont *Bradyrhizobium japonicum* compared to the control [12] and lower after inoculation with a phytopathogenic fungus [13]. Possibly, this is also the reason behind the better performance of *B. subtilis* compared to *Rhizopus* spp. observed in (H₂O₂ + AgNO₃)-treated seedlings with respect to prenylated isoflavone induction (**Chapter 3**).

Overall, sensitization of soybean seedlings prior the conventionally employed elicitation by fungus was a step forward in the production of compounds of interest. However, cultivar-dependent parameters such as its capacity to produce diverse metabolites, the optimal time-point of treatment application and the maximum biosynthetic capacity need to be investigated when a new cultivar is employed.

6.1.3. Reflection on QSAR

In this research, *in silico* techniques, such as QSAR and ligand-based 3D-pharmacophore modelling were employed to extend our understanding on the molecular properties underlying the antimicrobial activity of prenylated (iso)flavonoids. Ultimately, it was intended to correlate the outcomes with their mode of action.

6.1.3.1. *Choice of QSAR model type depends on data size and purpose*

In this thesis, two types of QSAR modelling, regression (**Chapter 4**) and classification (binary) (**Chapter 5**), were used based on the objectives of the model and the size of the dataset in each case. In both types, genetic algorithm (GA) was used to find the optimal combination of a low number of descriptors that represents the data in a statistically compliant and readily interpretable way. To increase the dataset used for model development in **Chapter 5**, compounds with experimentally unestablished MIC values were included by imputing a MIC value of 100 µg/mL during modelling. To compensate for the error introduced by MIC imputation, a classification type of QSAR model was chosen. A classification model estimates the probability of activity of each molecule instead of estimating exact MIC values.

In contrast, the extended dataset assembled in **Chapter 4** allowed us to develop a regression model and intentionally exclude compounds with unestablished MIC values. However, exclusion of such compounds results in loss of valuable information. To prevent this, regression analysis with censored data (e.g. MIC values > the highest tested concentrations) is possible and can be employed in QSAR studies ^[14]. Alternatively, a new activity parameter, the growth inhibitory response, has been recently introduced and is based on delayed microbial growth (in h/mM). This parameter can be used to transparently use activity data (without imputation) for the development of regression models ^[15]. The main limitation of this new parameter is that it does not yet allow comparisons with or data mining from literature, but can possibly stand alone when sufficiently large datasets are generated in-house.

6.1.3.2. *Consensus prediction rather than striving for the best model?*

Through GA-MLR the most relevant descriptors explaining the response are captured by providing a large set of possible models with nearly equivalent predictive performance. In **Chapter 4**, the frequency of descriptors in all statistically compliant models was analysed to obtain the full range of the descriptors related to activity and thus to obtain mechanistic insights. Nevertheless, the activity (MIC values) of the compounds was predicted by using only the best QSAR model. This is the most commonly used approach in QSAR modelling ^[16-19]. Nonetheless, certain features might be over- or under-emphasized or be completely ignored during activity predictions by a single QSAR model. Thus for more robust and reliable activity predictions, some authors use consensus predictions where the activities derived from all statistically valid predictive models are considered ^[20,21]. Consensus activity predictions are mostly performed by averaging the predicted activity values derived from the different models (average consensus) ^[22-33]. For example, in the QSAR study of de Bruijn *et al.* (2018), an external set of natural and synthetic antimicrobial 1,4-benzoxazin-3-ones was predicted by using all leave-one-out cross-validated models ^[34]. Only a few authors have tried to give each submodel, either obtained from the same or different modelling methods, a different weight (weighted consensus) ^[25,35,36]. Li *et al.*

(2008) developed different GA-MLR models and grouped them in distinct clusters based on their similarity. From each cluster a top model was selected and used to predict the activities of the compounds of interest. Then, the authors developed a new MLR model using the predicted activities from each top model as independent variables. The different weights of each top model derived from their MLR coefficients in the new model [35]. In contrast, Lei *et al.* (2009) employed a more complicated approach using the leverage values and evaluating the location of each compound in the descriptor space [36,37]. Although it is not clearly established whether the benefits of consensus predictions outweigh their complexity [27], two consensus prediction approaches (the average and a weighted) were employed here to explore whether they can increase the accuracy of prediction of molecules from **Chapter 4**. In **Chapter 4**, 48 statistically compliant models (12 models per number of descriptors (4-7)) were generated by the GA, yielding 18 truly different models (some models appeared more than once). Just by averaging the activities derived from the different models, the average prediction error decreased by 17% and 31% for the training and the external validation set, respectively, while the maximum error of the training and the test set was reduced by 21% and 14%, respectively (**Table 6.1**). When different weights were given to the models by integrating their frequency of appearance in the GA, > 20 % lower maximum prediction errors were obtained in all sets compared to best model of **Chapter 4**.

From the above, it can be proposed that using weighted consensus activity predictions by integrating the frequency of appearance of a model in the GA runs can further increase the accuracy of QSAR activity predictions.

Table 6.1. Prediction errors (%) of the training, test and external validation sets obtained by average consensus and weighted consensus predictions compared to the best QSAR model developed in **Chapter 4**. In **bold**, the decrease in prediction errors (%) after using consensus predictions compared to the prediction using the best model is shown; (-) means no decrease. An average prediction error of 10% is generally acceptable for the training set [38].

Set		Best model (Chapter 4)	Average consensus	Weighted consensus*
Average	Training	5.1	4.2 (17)	4.5 (11)
	Test	4.2	4.1 (1)	4.3 (-)
	External validation	5.0	3.4 (31)	3.6 (28)
Maximum	Training	17.8	14.0 (21)	11.6 (35)
	Test	13.8	11.8 (14)	10.9 (21)
	External validation	10.1	10.2 (-)	7.2 (29)

* Models weighted based on their frequency of appearance in the GA runs

6.1.3.3. Separation of mono- from di-prenylated (iso)flavonoids in *in silico* techniques

For robust QSAR modelling, a dataset should be sufficiently large (at least 25 molecules), the activities should span 3 log units and be normally distributed [39,40]. For these reasons, molecules from different subclasses, including mono- and di-prenylated (iso)flavonoids were pooled in **Chapter 4**, similarly to other QSAR studies [16,17].

In **Chapter 4**, it was shown that different properties were correlated to the antibacterial activity of the different prenylated (iso)flavonoid subclasses. Thus, it would be useful to separate and model the different subclasses separately. However, the limiting step in this approach is the limited number of compounds per subclass available. For example, the most abundant subclass in the large dataset of **Chapter 4** was the isoflavones, encompassing 19 representatives with established MICs (and 6 with non-established MICs).

Likewise, pooling mono- and di- prenylated compounds can distort the actual effect of substituents (presence and distribution) other than prenylation. More specifically, the superiority of double prenylation against Gram-positive bacteria (almost all di-prenylated (iso)flavonoids were highly potent against MRSA), overshadows substituents which might otherwise be detrimental for activity. For example, glycyrrhisoflavone with four -OH groups and one B-ring prenylation was moderately active against MRSA (MIC 64 µg/mL, 181 µM), but when it is additionally prenylated at the A-ring as in isoangustone A, it becomes active (MIC 16 µg/mL, 38 µM), masking the initial unfavourable combination of features. Similarly, even though 6a-OH pterocarpanes are mostly inactive against various microbial species, a di-prenylated 6a-OH pterocarpan (2-(dimethylallyl)-6a-hydroxyphaseollidin) was very active against MRSA (MIC 3 µg/mL, 8 µM), overshadowing the detrimental effect of C6a hydroxylation. The limiting step in performing this kind of splitting to develop QSAR models in **Chapter 4** was that di-prenylated molecules were not normally distributed with respect of activity, since almost all of them were active. To investigate what the effect of this type of splitting would be on the molecular properties surfacing as important for antimicrobials activity, the GA was crudely performed for mono- and di-prenylated (iso)flavonoids from **Chapter 4**, separately. To allow one-to-one comparisons, the GA was also crudely performed for the pooled mono- and di-prenylated compounds (**Table 6.2**). When GA was ran only with mono-prenylated (iso)flavonoids, descriptors encoding properties such as the total negative partial charge and the van der Waals component of the potential energy were most frequently correlated to the activity (69% and 27%, respectively) (**Table 6.2**). In contrast, mostly hydrophobicity-related descriptors such as the octanol/water distribution coefficient at pH 7 and the hydrophobic volume at -1.6 kcal/mol were appearing in the GA for di-prenylated (iso)flavonoids. This indicated that the contribution of di-prenylated molecules in elucidation of molecular properties is limited to hydrophobicity. This is further corroborated with the appearance of *vsurf_CW3*, a

descriptor significantly correlated (R_{pearson} 0.85) to hydrophobicity ($\log P$), when mono- and di-prenylated compounds were pooled together. Considering that the minimum possible number of descriptors is preferred in QSAR models, potentially important information might be lost upon combination of mono- and di-prenylated (iso)flavonoids.

Overall, when the dataset size and the range and distribution of activities of the molecules allow, splitting of mono- from di-prenylated molecules during QSAR modelling would increase the accuracy and interpretability of descriptors.

Table 6.2. Descriptors with their definition, contribution to activity and frequency derived by running the genetic algorithm for mono- and di-prenylated (iso)flavonoids separately and together. The GA was performed twice and 100 models were generated each time.

	Descriptor	Definition	Sign	Frequency
Mono-prenylated (iso)flavonoids	<i>PC-</i>	Negative partial charge	+	69%
	<i>E_vdW</i>	van der Waals component of the potential energy	+	27%
	<i>h_emd</i>	Hydrogen bond donor strengths	+	21%
Di-prenylated (iso)flavonoids	<i>h_logD</i>	octanol/water distribution coefficient at pH 7	+	34%
	<i>vsurf_D8</i>	hydrophobic volume at -1.6 kcal/mol	+	24%
Mono- and di-prenylated (iso)flavonoids	<i>vsurf_CW3</i>	Ratio of hydrophilic surface and the total molecular surface at -1.0 kcal/mol	-	97%
	<i>h_emd_C</i>	Sum of hydrogen bond donor strengths of carbon atoms	-	89%
	<i>RPC-</i>	Relative negative partial charge: the smallest negative q_i divided by the sum of the negative q_i .	-	85%
	<i>h_pavgQ</i>	The average total charge sum ($Q_i \cdot 10^{-pC_i}$) where Q_i is the total formal charge of state i .	+	15%

6.2. Prenylated (iso)flavonoids as antimicrobials

6.2.1. Di-prenylated (iso)flavonoids as specific antimicrobials towards Gram-positive bacteria

The di-prenylated (iso)flavonoids, both experimentally tested and extracted from literature in **Chapter 4**, were found to be promising antibacterials against MRSA. Seventy five percent of them had MIC values of ≤ 25 $\mu\text{g/mL}$, thus being classified as active, whereas 1/3 of them had MIC values of < 10 $\mu\text{g/mL}$, being classified as very active ^[41]. This observation corroborates what is known for other Gram-positive bacteria. Contrarily, di-prenylated (iso)flavonoids tested and mined from literature in **Chapter 5**, were mostly inactive against yeasts. This lack of activity is reminiscent to what has been shown against the Gram-negative bacterium, *E. coli* (even in the presence of an efflux pump inhibitor) ^[16]. The highly ordered, complex outer membrane (OM) of Gram-negative bacteria, ascribed to the presence of lipopolysaccharides and of hydrophilic porins, is thought to limit the influx of hydrophobic molecules ^[16,42]. The yeast cell wall is also characterized by high complexity and crystallinity due to the presence of fibrillar mannoproteins and of a chitin layer, respectively. The architecture of the yeast cell wall limiting the entry of hydrophobic molecules, might also be one of the reasons behind the poor antimicrobial activity of di-prenylated (iso)flavonoids against yeasts as discussed in **Chapter 5**.

6.2.2. Mono-prenylated isoflavonoids as broad spectrum antimicrobials - role of amphiphilic moment

Contrary to di-prenylated (iso)flavonoids, mono-prenylated isoflavonoids showed a wider spectrum of activity, as they were active both as antibacterials against Gram-positive bacteria (including MRSA and *B. subtilis*, the latter shown in section **6.2.4**) and as antifungals against *Z. parabailii* (**Chapter 4** and **5**).

More specifically, the mono-prenylated isoflavonoid, wighteone showed a MIC value of 16 $\mu\text{g/mL}$ against MRSA, in line with its high activity shown for another Gram-positive bacterium, *L. monocytogenes* ^[16]. Wighteone was also active against *Z. parabailii* and *E. coli* (the latter supplied with an efflux pump inhibitor) ^[16] with a MIC value of ≤ 10 $\mu\text{g/mL}$. Similarly, glabridin showed MIC values of ≤ 15 $\mu\text{g/mL}$ against MRSA, *B. subtilis* and *Z. parabailii*, in line with its high activity towards *L. monocytogenes*, *E. coli* and *C. albicans* ^[16,43].

Interestingly, wighteone (A-ring chain-prenylated at C6) is consistently more active than isowighteone (B-ring chain-prenylated) and lupiwighteone (A-ring chain-prenylated at C8), the latter being inactive against the microbial species towards which it has been tested. These prenylated isoflavones differ only in the location of the prenyl group. Likewise, glabridin was more active than 4'-O-methyl glabridin, whereas 3'-OH-4'-O-methyl-glabridin was inactive against *Z. parabailii*

and *E. coli*. These prenylated isoflavans differ in the level of hydroxylation and *O*-methylation. The strict separation of hydrophobic (prenyl) group and polar (hydroxyl) groups (i.e. amphiphilicity) was inversely correlated to activity in **Chapter 4** (in the form of hydrophilic integrity moment, *vsurf_IW7*), in **Chapter 5** (in the form of hydrophobic integrity moment, *vsurf_ID7*) and in the QSAR model developed for *L. monocytogenes* (*vsurf_ID7*)^[16]. The hydrophilic and hydrophobic integrity moments are measures for the distribution of hydrophilic and hydrophobic regions, respectively. Their negative contributions to the activity (**Chapter 4** and **5**) mean that the hydrophilic (or hydrophobic) regions should be equally distributed over the molecule^[44] and thus inversely correlated to the amphiphilic moment.

Figure 6.2 displays the relationship between amphiphilic moments, hydrophobicity and antimicrobial activity of structurally similar prenylated isoflavones and isoflavans. Amphiphilic moments were inversely correlated to the activity of prenylated isoflavones for all microbial species tested (**Figure 6.2**, left). The inactive lupiwighteone has the highest amphiphilic moment among the isoflavones due to the well separated prenyl group (green area in **Figure 6.2**) from the hydrogen bonding regions (pink areas in **Figure 6.2**), compared to wighteone where the prenyl group is in between the hydroxyl groups. In contrast, for prenylated isoflavans, no clear trends could be established between amphiphilic moment and antimicrobial activity (**Figure 6.2**, right). This discrepancy between the two subclasses might lie in the generally higher overall hydrophobicity of the studied isoflavans (*logP* 4.1-4.5) compared to isoflavones (*logP* 2.9-3.0), a molecular property strictly associated with the antibacterial activity of prenylated (iso)flavonoids against Gram-positive bacteria (**Chapter 4** and Araya-Cloutier *et al.* (2018)^[16]). Possibly, the high hydrophobicity of isoflavans cancels the detrimental effects of their amphiphilicity on the antimicrobial activity. Overall, there seems to be a link between amphiphilic moment, molecular hydrophobicity and the antimicrobial activity of prenylated isoflavones and isoflavans.

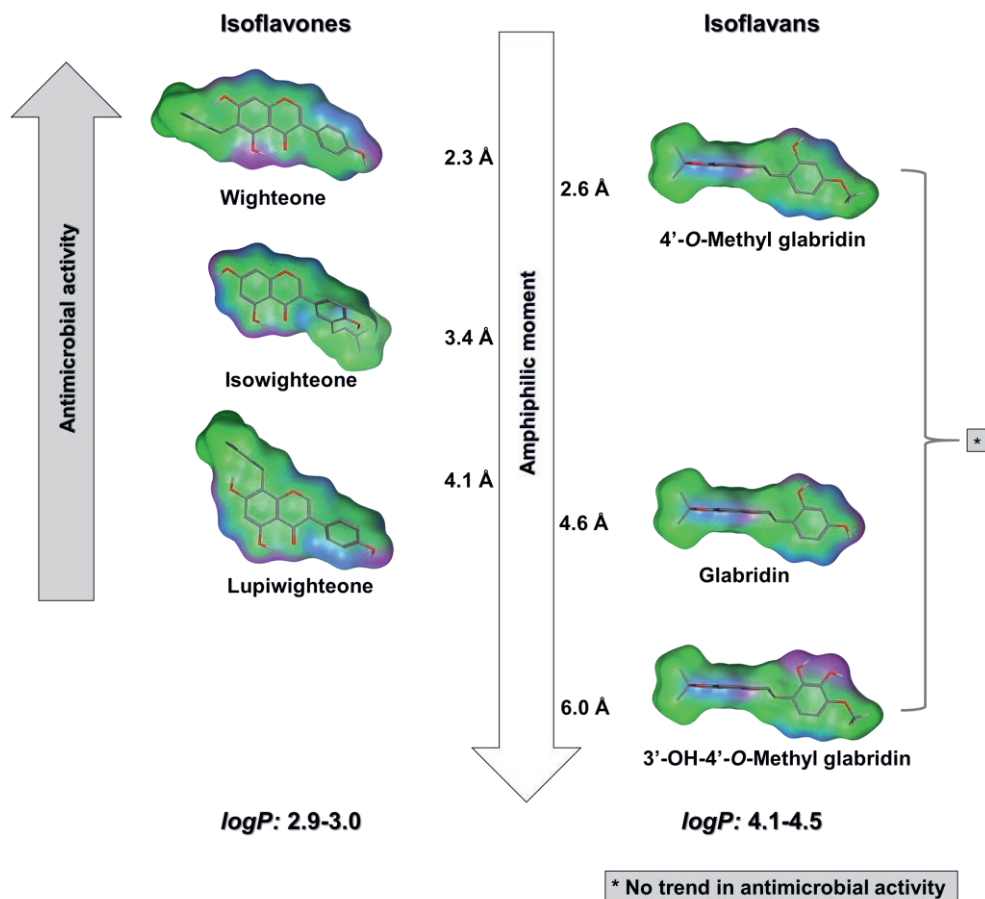


Figure 6.2. Amphiphilic moments (in Å), illustrated with surface maps, and $\log P$ values (both calculated in MOE) of prenylated isoflavans, which differ in the level of hydroxylation and *O*-methylation and prenylated isoflavones differing in the location of the prenyl group, as a function of antimicrobial activity against Gram-positive bacteria. The A-C rings of isoflavones are longitudinal to the plane of the paper, whereas the A-C rings of isoflavans are perpendicular to the plane of the paper for better visualization. Green colour represents hydrophobic areas, whereas pink and blue colours denote hydrogen-bonding and mildly polar areas, respectively.

6.2.3. Mode of action of the mono-prenylated isoflavonoids

In this thesis, it was shown for the first time that the active mono-prenylated isoflavonoids, wighteone and glabridin, act on the membrane of *Z. parvabailii* (Chapter 5). Membrane-activity of prenylated isoflavonoids against various microbial species is the most reported mechanism of action of prenylated (iso)flavonoids in model studies and studies using whole cells [45-48]. In the following sections, it will be discussed (i) how prenylated (iso)flavonoids are

expected to reach the membrane, (ii) how they interact with it and (iii) whether the membrane is the only target for their antimicrobial action.

6.2.3.1. *Is the perception that prenylated (iso)flavonoids act as single molecules oversimplified?*

The relationship between amphiphilic moment (**section 6.2.2**), overall hydrophobicity and the mode of action of mono-prenylated (iso)flavonoids has never been touched upon. Prenylated (iso)flavonoids are expected to hide their hydrophobic parts in a hydrophilic environment through self-aggregation, similar to other hydrophobic or amphiphilic molecules. For example, micellar formation in the extracellular space has been suggested for the amphiphilic antimicrobial peptide, daptomycin ^[49]. Aggregate formation before reaching the lipid bilayer was also shown for the amphiphilic di-prenylated hydroxycinnamic acid, artemillin C, through molecular dynamic simulations. Artemillin C has similar hydrophobicity (*logP* 4.2), size (300 Da) and amphiphilic moment (*vsurf_A* 3.6 Å) to prenylated (iso)flavonoids ^[50] (**Table 6.3**). The di-prenylated xanthone, mangostin (*vsurf_A* 0.6 Å) and its non-prenylated analogue (*vsurf_A* 2.7 Å) were also shown to form aggregates in water, the former through aromatic stacking and hydrogen bonding and the latter exclusively via aromatic stacking ^[51] (**Table 6.3**).

Table 6.3. Molecules from different families that have been shown to aggregate in a hydrophilic environment. Amphiphilic moment, *vsurf_A* (Å) and hydrophobicity, *logP*, were calculated in MOE.

Molecule	Family	<i>vsurf_A</i> (Å)	<i>logP</i>	Molecular weight	Cluster type	Ref.
Daptomycin	Peptide	7.1	-5.7	1620	Micelle	[47]
Artemillin C	Di-prenylated hydroxycinnamic acid	3.6	4.1	300	Aggregate	[48]
Mangostin	Di-prenylated xanthone	0.6	3.9	410	Aggregate	[49]
Xanthone	Xanthone	2.7	1.8	244	Aggregate	[49]
Wighteone	Mono-prenylated isoflavonoid	2.3	2.9	338	Aggregate	This thesis
Lupiwighteone	Mono-prenylated isoflavonoid	4.1	2.9	338	Micelle	This thesis
Glabridin	Mono-prenylated isoflavonoid	4.6	4.2	324	Micelle	This thesis

Based on their amphiphilic moment, prenylated (iso)flavonoids are speculated to self-associate in a micelle or an aggregate, but this needs to be determined. Since no solubility issues were associated with prenylated (iso)flavonoids in hydrophilic growth media at any of the concentrations tested, it is expected that these self-assemblies are soluble. Prenylated isoflavones with low amphiphilic moments (e.g. wighteone) are expected to form aggregates stabilized primarily

through aromatic stacking and possibly hydrogen bonding (**Figure 6.3**, phase 1, left) in analogy to the xanthenes with low amphiphilic moments (**Table 6.3**). In contrast, prenylated isoflavones with higher amphiphilic moments and thus with more clearly defined hydrophobic and hydrophilic moieties, e.g. lupiwighteone, are thought to form micellar-like aggregates (**Table 6.3** and **Figure 6.3**, phase 1, middle). The activity of prenylated isoflavans was less affected by the amphiphilic moment compared to isoflavones (**section 6.2.2**). Nevertheless, because of the high amphiphilic moments of certain members of the isoflavan subclass, such as glabridin and 3'-OH-4'-O-methyl-glabridin, these molecules might also form micellar-like aggregates (**Table 6.3**).

To efficiently interact with the membrane, aggregates should disintegrate when they reach the membrane. Disintegration at the membrane was shown for the aggregates of both daptomycin and artemisin C ^[49,50]. The putative aggregate of wighteone is also expected to dissociate when reaching the membrane (**Figure 6.3**, phase 2, left). Contrarily, micelles of prenylated isoflavonoids may have lower tendency to dissociate, because their hydrophobic parts are more effectively hidden compared to an aggregate, thus prevented from interacting with the membrane (**Figure 6.3**, phase 2, middle). This has been also suggested for stable micelles and strong dimers formed by amphiphilic peptides and their limited interactions with the bacterial membrane, compared to the monomers ^[52,53]. Strong self-association of peptides was shown to have a detrimental effect on their antimicrobial activity ^[53]. This might explain why lupiwighteone is inactive, whereas wighteone is active across all microbial species against which they have been tested. However, this does not explain the high activity of the isoflavan, glabridin, which has an amphiphilic moment similar to lupiwighteone. Possibly, the 3D-configuration of the isoflavan backbone, which is more crooked than that of isoflavones due to the absence of the C2-C3 double bond on the C-ring of the former, might hinder the formation of stable micelles (**Figure 6.3**, phase 1, right). This together with glabridin's higher hydrophobicity might explain why the glabridin micelle might have a higher tendency to dissociate in the membrane compared to the lupiwighteone micelle (**Figure 6.3**, phase 2).

Evidence on the hypothesized clustering propensities of prenylated isoflavonoids can be obtained through cryo-TEM imaging, a readily useful tool to obtain insights on structural and dynamic changes of self-assemblies at nano-scale ^[54]. Preferably, cryo-TEM should be complemented with a quantification method, such as surface tension measurements.

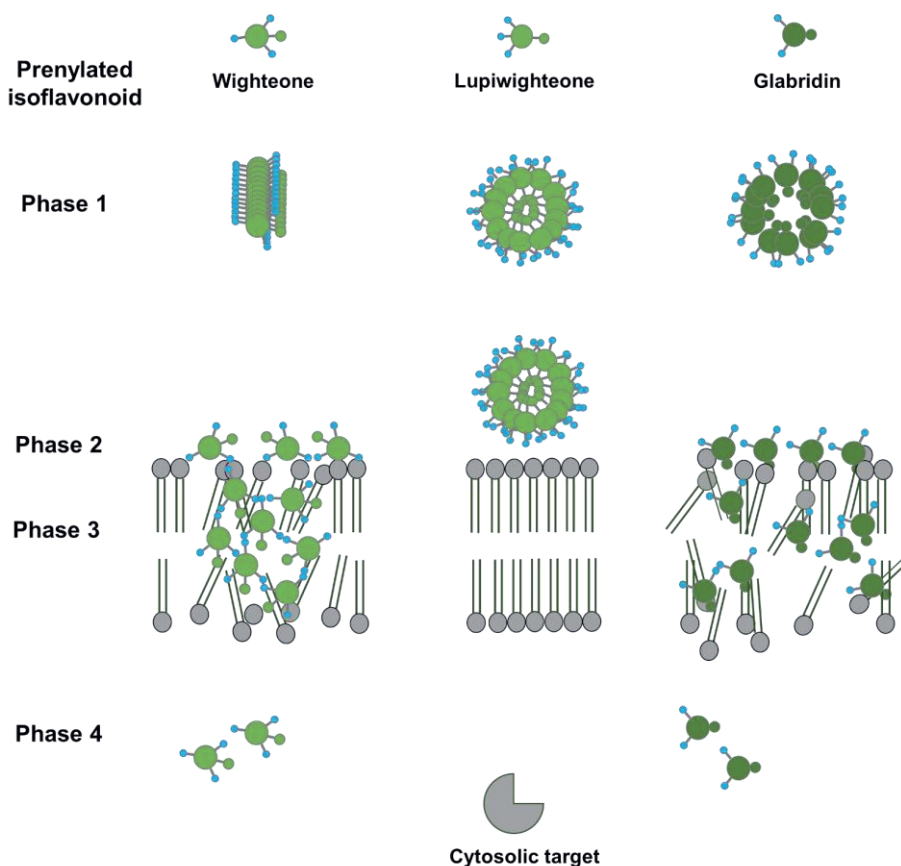


Figure 6.3. Proposed mode of antimicrobial action of mono-prenylated isoflavonoids dissected in 4 different phases: 1, extracellular; 2, membrane surface; 3, interior of the membrane; 4, cytoplasm. Blue dots indicate hydroxyl group. Green small dots represent the prenyl group, whereas larger ones represent the isoflavonoid backbone. A darker green colour indicates higher hydrophobicity of the entire molecule. Ring prenylation is represented by direct attachment of the prenyl group to the backbone, whereas chain prenylation is separated from the backbone.

6.2.3.2. Mono-prenylated isoflavonoids deform the microbial cell membrane differently

Different dominant molecular properties were witnessed to be important for activity in **Chapter 4**. The different properties were reflected in different prenylated (iso)flavonoid subclasses. Thus, it was proposed that subclasses such as isoflavones, isoflavans and pterocarpenes may have differential interactions with the membrane. In **Chapter 5**, differences were observed in the membrane of *Z. parabaillii* cells, when these were treated with the isoflavone, wighteone and the isoflavan, glabridin.

Due to the presumed ease of dissociation of the putative wighteone aggregate, monomeric wighteone enters the membrane. Subsequently, wighteone monomers

are thought to re-cluster again inside the membrane to shield their polarity (**Figure 6.3**, phase 3). Molecules with enhanced hydrogen-bond capacity (≥ 3 free hydroxyl groups), like wighteone, were hypothesized to self-associate through hydrogen-bonding to increase their affinity with the interior of the membrane ^[51] (**Chapter 4**). The hypothesis was based on results obtained from molecular dynamic simulations using modelled membranes with a di-prenylated xanthone ^[51], considering that its hydrogen-bonding capacity is similar to that of prenylated (iso)flavonoids with ≥ 3 free hydroxyl groups (**Chapter 4**). Wighteone is therefore considered an intramembrane cluster inducer. According to Li *et al.* (2018), these kind of intramembrane clusters effectively permeabilized the membrane without pore formation ^[51]. However, some pore formation was observed in the membrane of wighteone-treated *Z. parabailii* cells together with other types of deformation (**Chapter 5**).

In contrast, due to the lower hydrogen-bond forming capacity, glabridin (< 3 free hydroxyl groups) was expected to form intramembrane aggregates to a lesser extent than wighteone (**Chapter 4**) (**Figure 6.3**, phase 3). Opposite to wighteone, glabridin showed catastrophic effects on the membrane of *Z. parabailii* by consistently inducing large discontinuities (pores) (**Chapter 5**). This behaviour is reminiscent to the “detergent model” described for antimicrobial peptides, in which the membrane collapses when the concentration of accumulated molecules is high ^[55]. The detergent model requires interfacial activity of the molecules ^[56]. In general, prenylated (iso)flavonoids are expected to be positioned in the interface of lipid bilayer and the extent of insertion inside the lipid core depends on their hydrophobicity ^[57]. In **Table 6.3**, glabridin was shown to have a higher amphiphilic moment and thus better interfacial activity compared to wighteone.

To obtain further evidence on the interactions of the different prenylated isoflavonoids with the membrane, the thermotropic phase behaviour of liposomal membranes can be followed by means of, for example, differential scanning calorimetry ^[58,59].

6.2.3.3. *Is membrane-permeabilization the only mechanism for killing?*

The main challenge in exploring the mechanism of action of an antibacterial is the difficulty to dissect the primary event from those that follow ^[60].

In **Chapter 5**, it was demonstrated that mono-prenylated isoflavonoids killed *Z. parabailii* cells at their MFC within 15 min. Glabridin destroyed the membrane, promoting higher PI uptake by the yeast cells than wighteone (both at pH 4.0 and 7.2) (**Chapter 5**). In relation to this, wighteone-treated yeast cells at pH 4.0 showed pore formation as well as other types of membrane-deformations, which are reminiscent to those induced during endocytosis (**Chapter 5**). Endocytosis is a phenomenon mediating the internalization of surface receptor/ligand complexes or other surface proteins in yeasts ^[61]. Polar macromolecules are also internalized through endocytosis as an alternative mechanism when they cannot permeate the

membrane ^[62-64]. For example, the fast antifungal activity (within 5 min at its MFC) of the peptide ApoEdpL-W against *C. albicans* was endocytosis-dependent. This was evidenced through inactivation of a gene required for endocytosis and the use of endocytosis inhibitors, both of which reduced the antifungal activity of ApoEdpL-W. The primary mode of action of this peptide was attributed to activity on intracellular targets ^[65]. If part of wighteone is endocytosed into the yeast, then its mode of action might be further complemented intracellularly. To elucidate whether wighteone's activity against *Z. parabailii* is endocytosis-dependent, further investigation by using deletion mutants or different endocytosis inhibitors can be employed ^[65,66].

Araya-Cloutier *et al.* (2017) also showed that although wighteone was a good permeabilizer of *L. monocytogenes* at a concentration > MIC, no permeabilization was observed at its MIC ^[67]. The same author also demonstrated that highly active prenylated (iso)flavonoids (e.g. di-prenylated (iso)flavonoids and mono-prenylated pterocarpenes) did not permeabilize the membrane of Gram-positive and Gram-negative bacteria, implying that membrane permeabilization is not the only mechanism of killing ^[16]. It was hypothesized that prenylated (iso)flavonoids with large hydrophobic volume might migrate deeper in the hydrophobic core, causing rigidification of the membrane ^[16]. However, a few reports have demonstrated cytosolic presence (and activity) of prenylated (iso)flavonoids. For example, the di-prenylated flavonoid, morusin was shown to first disrupt the membrane and then inhibit the phosphatidic acid biosynthesis (phospholipid-repair system), intracellularly ^[68]. In addition, cytoplasmic localization after disruption of the membrane of *Streptococcus mutans* was observed for a di-prenylated flavanone, lupinifolin, by separately assaying cell envelop and cytoplasmic fractions ^[69]. However, no secondary mechanisms of action were explored in this study.

Altogether suggest that membrane-disruption is not the only mechanism of action of prenylated (iso)flavonoids and that their activity might be further complemented in the cytosol (**Figure 6.3**, phase 4). This is in line with **Chapter 4** where we proposed that the anionic species of prenylated compounds with low pKa might traverse the membrane through channels and reach the cytosol. To be able to dissect primary from secondary events in killing by antimicrobials, the subcellular localization of prenylated (iso)flavonoids can be followed by fractionation of the different compartments (i.e. cell wall, membrane and cytoplasmic fractions) ^[69,70] and detection using LC-MS. In parallel, the uptake of PI can be followed in single live cells by time-lapse confocal microscopy ^[65,71]. Furthermore, transcriptome analysis ^[72] and screening of microbial mutant libraries ^[73] can help to reveal cellular responses and to identify the genes required for tolerance/sensitivity to prenylated (iso)flavonoids, respectively.

6.2.4. Prenylated (iso)flavonoids as antibacterial agents against *B. subtilis* cells and spores

B. subtilis is a gram-positive spore-forming bacterium, challenging food preservation. The potency of partially purified prenylated (iso)flavonoids were tested as novel, natural antibacterial agents against vegetative cells and spores of a food isolate of *B. subtilis*.

Table 6.4. Potency of partially purified prenylated (iso)flavonoids against *B. subtilis* (UL 2615) vegetative cells (4.5 log₁₀CFU/mL).

No	(Partially purified) compound	# prenyl groups	Subclass	MIC (µg/mL)	logD (pH 7.2)
1	Glabrene (54% w/w)	1	Isoflavene	25	4.0
2	Glabrol (52% w/w)	2	Flavanone	6.25	5.8
3	4'-O-methyl glabridin (55% w/w)	1	Isoflavan	12.5	4.2
4	Hispaglabridin A (52% w/w)	2	Isoflavan	12.5	5.8
5	Hispaglabridin B (59% w/w)	2	Isoflavan	25	5.3
6	Glabridin (97% w/w)	1	Isoflavan	12.5	4.1

The potency of prenylated (iso)flavonoids against *B. subtilis* cells (**Table 6.4**) resembles the activity against other Gram-positives (**Chapter 4** and Araya Cloutier *et al.* (2018) ^[16]). The partially purified di-prenylated flavanone, glabrol, inhibited cell growth at the lowest concentration tested (MIC 6.25 µg/mL). The two partially purified isoflavans, the mono-prenylated 4'-O-methyl glabridin and the di-prenylated hispaglabridin A inhibited *B. subtilis* cells at a MIC value of 12.5 µg/mL. These three prenylated (iso)flavonoids were the most hydrophobic members of their subgroup (i.e. mono- and di-prenylated). Hydrophobicity, as expected, plays a key role in the activity of prenylated (iso)flavonoids against *B. subtilis*.

Under stressful conditions, *B. subtilis* vegetative cells transform into resilient, dormant structures, called spores, which are particularly troublesome in food industry. Especially in foods with low acidity (pH > 4.6), *B. subtilis* spores (phase-bright structures as manifested by light microscopy) are susceptible to germination (after which they become phase-dark spores) and to outgrowth into vegetative cells (elongated rods) ^[74] causing food spoilage (**Figure 6.4A**). In food industry, mainly thermal treatments are used to inactivate bacterial spores and the milder techniques, sometimes employed nowadays, are not always effective ^[75,76]. In addition, there are no universal food-grade spore germinator inhibitors ^[77]. On the basis that hydrophobicity was previously found to be an important property in inhibiting spores of *B. subtilis* spp. ^[78-80], the most promising partially purified compounds against vegetative cells were tested against the spores.

The di-prenylated flavonoid, glabrol, and the mono-prenylated isoflavonoid, 4'-O-methyl glabridin arrested the germination and outgrowth of the spores at a concentration of 200 µg/mL. Upon exposure of the spores to these prenylated (iso)flavonoids, only non-germinated phase bright spores and no germinated phase dark spores were observed. Furthermore, *B. subtilis* spores treated with prenylated (iso)flavonoid did not grow out even in the presence of germination promoters (a

mixture of alanine and inosine, known to target different germination receptors [81]) (**Figure 6.4B**). This observation suggested that prenylated (iso)flavonoids inhibit the germination step in spores' revival. Alanazi *et al.* (2018) showed that essential oil constituents inhibited the germination of *Clostridium perfringens* spores at 0.05-0.1% (v/v) [82]. Avocado extracts, enriched in fatty acid alcohols, also inhibited the germination of *C. sporogenes* spores at a concentration of 20 µg/mL [83].

Overall, this preliminary qualitative evidence shows that prenylated (iso)flavonoids can serve as a promising new hurdle to control resilient microbial forms, such as the spores of *B. subtilis*. Quantitative determination of the stage at which prenylated (iso)flavonoids inhibit spores' revival and their mode of action await investigation.

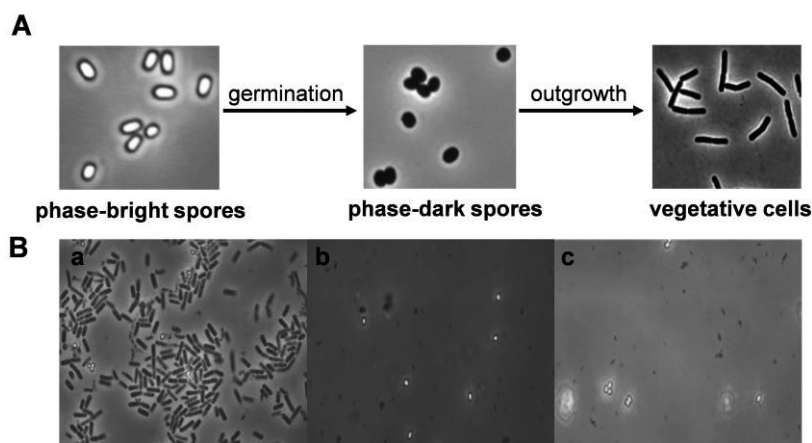


Figure 6.4. Phase contrast microscopy (PCM) imaging demonstrating the morphological changes during *B. subtilis* spore germination and outgrowth [84,85] (**A**) and PCM imaging of exposed *B. subtilis* spores ($8.7 \pm 0.3 \text{ Log}_{10}\text{CFU/mL}$) to two partially purified prenylated (iso)flavonoids at 37 °C for 24 h in the presence of germination promoters (10 mM alanine + 2 mM inosine) (**B**); Untreated (control) spores which grew out into vegetative cells (a), spores treated with 200 µg/mL of partially purified glabrol (b) and 4'-O-methyl glabridin (c).

6.3. Toxicity and applications of prenylated (iso)flavonoids

Based on Davidson *et al.* (2013), an ideal natural antimicrobial needs to (i) be effective at low concentrations in its natural form, (ii) be economical at use levels, (iii) cause no sensory changes to the product, (iv) inhibit a wide array of pathogenic and spoilage organisms and (v) be non-toxic to healthy human cells and beneficial microorganisms [86]. In this regard, despite the high potency of prenylated (iso)flavonoids against problematic Gram-positives ($\text{MIC} \leq 25 \text{ µg/mL}$), no potency ($\text{MIC} > 1,000 \text{ µg/mL}$) was found for a prenylated flavonoid against three probiotic Gram-positive strains, *L. plantarum* [87]. This suggests that prenylated

(iso)flavonoids can be highly specific towards harmful microbial strains. In the following sections, toxicity and potential application of prenylated (iso)flavonoids as food preservatives and therapeutic agents is dealt with.

6.3.1. Toxicity

Promising antimicrobial candidates need to specifically exert their activity towards their target microbial cells at doses that are non-toxic to healthy human cells. Prenylated (iso)flavonoids are generally considered as less toxic than traditional antibiotics and they are not frequently included in lists of known poisonous compounds [88].

Table 6.5 summarizes toxicity information of prenylated (iso)flavonoids. A study on the safety of liquorice flavonoids in an oil preparation (LFO) in human subjects reported that the LFO is safe when administered once daily up to 1,200 mg/day (containing 12 mg of glabridin) up to 4 weeks [89]. The toxicity of pure 6,8-diprenyl eriodictyol and 6-prenyl apigenin was found negligible against silkworms (used as an animal model [90]) at a concentration of 625 µg prenylated flavonoid/g larvae [47]. The di-prenylated flavonol, papyriflavonol A, with strong antifungal activity (MIC values of 12.5-25 µg/mL), showed less than 5% haemolysis of human erythrocytes at concentrations close to their MIC [91]. In the same study, the antibiotic, amphotericin B showed severe haemolysis (53%) even at a low concentration of 6.3 µg/mL. Similarly, the di-prenylated flavanone, lupinifolin did not disrupt the membrane of mammalian red blood cells (RBCs) at concentrations up to 40 µg/mL [92]. Likewise, the di-prenylated xanthone, alpha-mangostin, closely related to prenylated (iso)flavonoids, was found to induce only 7.7-10.5% haemolysis at 1-4 x its MIC against RBCs [93].

Overall, substantial evidence shows that prenylated (iso)flavonoids are not toxic to healthy human cells at the concentrations which were found inhibitory against problematic microorganisms.

6.3.2. Application

6.3.2.1. Application to food

Prenylated (iso)flavonoids are considered advantageous natural metabolites, as (i) they are highly stable compared to for example, prenylated stilbenoids; (ii) they have a subtle colour (white or yellow); (iii) they kill very fast compared to other antimicrobials, such as ITCs [15]. Non-prenylated (iso)flavonoids have been related to bitter taste [94]. Usually the presence of regular levels of salt and sugar, the use of acids and flavours, are debittering strategies implemented in the food industry that can mask this potential bitterness of (iso)flavonoids [95-97]. Nonetheless, preliminary receptomic results from our laboratory (in collaboration with Wageningen Plant Research) showed that glabridin and a liquorice (*G. glabra*) extract at concentrations up to 100 and 200 µg/mL, respectively, did not activate bitter receptors.

Table 6.5. Toxicity information of various prenylated (iso)flavonoids.

Prenylated compound	Subclass	MIC in µg/mL (microorganism)	Toxic effects	Studied organism	Ref.
Glabridin (in complex mixture)	Isoflavan	≤ 15 (various)	< 12 mg/day (4 weeks)	Humans	[89]
6,8-Diprenyl eriodictyol	Flavone	4 (MRSA)	No toxicity at 625 µg prenylated flavonoid/g (24 h)	Silkworms	[47]
6-Prenyl apigenin	Flavone	64 (MRSA)	No toxicity at 625 µg prenylated flavonoid/g (24 h)	Silkworms	[47]
Papyriflavonol A	Flavonol	12.5-25 (<i>C. albicans</i> , <i>S. cerevisiae</i>)	< 5% haemolysis at 10-25 µg/mL and < 11% at 63 µg/mL	Human erythrocytes	[85]
Lupinofolin	Flavanone	8 (<i>S. aureus</i>)	No membrane disruption at C ≤ 40 µg/mL (24 h)	RBCs	[86]

Acidic food emulsions, such as mayonnaise (20% water) are typically spoiled by *Z. parabailii* [98] towards which highly potent mono-prenylated isoflavonoids were found. However, due to the affinity of prenylated (iso)flavonoids for the oil phase, pure prenylated (iso)flavonoids rather than plant extracts could be added at reasonable concentrations to control the growth of *Z. parabailii*. In the best case scenario, wighteone, the most potent prenylated isoflavonoid against this yeast (MFC 12.5 µg/mL at pH 4.0) is selected as a novel, natural food preservative. The amount of wighteone (*logP* of 3.0) that is required to prevent yeast growth in the water phase (20%) is 0.25 g per 100 mL product. To correct for the 2 x higher hydrophobicity of the oil compared to octanol, wighteone should be added at a concentration of 0.5 g per 100 mL mayonnaise. This amount is higher than the 0.1% K-sorbate normally used in mayonnaise. This scenario is mainly restrictive due to the high purification cost of prenylated (iso)flavonoids.

Prenylated (iso)flavonoids could be more promising food preservative alternatives when applied in fat-free, acidic food products containing high concentration of fermentable sugars. These products are also typically spoiled by *Z. parabailii* [98]. Although the solubility of prenylated (iso)flavonoids is considered low, no solubility problems were observed when the compounds were dissolved in hydrophilic growth media for antimicrobial testing at concentrations up to 100 µg/mL. In this type of food products, a legume extract instead of the purified

compounds could be used. Plant extracts are more positively perceived by the consumer and are regarded as clean label ^[86], limiting the costs required for purification. A crude blue lupine extract, for example, is a rich source of different highly potent mono-prenylated isoflavones ^[99]. An ethanolic extract of blue lupine (5.5% of dry weight elicited seedlings) contains around 15 mg of the compounds of interest per g of extract ^[99]. The amount of promising antimicrobials (considering an average MIC of prenylated isoflavones of 30 µg/mL against *Z. parabailii*, **Chapter 5**), which needs to be added in the food product would be 3 mg per 100 mL. Therefore, 0.2 g of dry extract need to be added in 100 mL of food product, which is closer to the K-sorbate levels.

Last, it should be noted that interactions of the prenylated isoflavonoids with other food components might decrease their antimicrobial activity ^[86] and thus these types of interaction need to be further investigated.

6.3.2.2. Application to pharma

Prenylated (iso)flavonoids were found to be promising antimicrobials against MRSA. Based on their hydrophobic nature, prenylated (iso)flavonoids have low bioavailability ^[100]. For example, the bioavailability of xanthohumol (XN) was found to be 33% in rats for a low dose of XN (1.86 mg/kg body weight) and 11% for approximately ten-times higher dose of XN administered by oral gavage ^[100]. Results can be extrapolated to humans ^[101]. These numbers are similar to classical MRSA-targeting antibiotics, such as vancomycin (10% oral bioavailability) whose administration must be via other routes ^[102]. Hence, prenylated (iso)flavonoids may have limited potential to be used as oral drugs.

An alternative topical route of administration has been explored for delivery of several flavonoids ^[103]. Classical antibiotics target biosynthetic processes that occur only in actively growing bacteria ^[104] and they are not effective against slow-growing or dormant cells, as in biofilms ^[105,106]. Consequently, strategies that target active and dormant or slow growing cells are needed ^[107]. Due to their membrane-activity, prenylated (iso)flavonoids could potentially be applied in a topical cream for wounds to prevent biofilm formation. Alternatively, prenylated isoflavonoids can be used as a coating material for medical devices such as catheters in analogy to what has been suggested for antimicrobial peptides that inhibit biofilm formation ^[65].

Certainly, prenylated (iso)flavonoids can also potentiate the activity of traditional antibiotics as they seem to employ fundamentally distinct modes of action. For example, due to the possible indirect effect that these molecules can have on efflux pumps by perturbing the organization of the membrane, similarly to other membrane-active antimicrobials ^[107], prenylated (iso)flavonoids can be synergistically used with antibiotics. For example, a prenylated flavanone inhibited rhodamine 6G efflux and reversed fluconazole-resistance in *Candida albicans*. Furthermore, the synergistic action of glabridin with fluconazole against fluconazole-resistant *C. albicans* ^[108] and with nystatin against the same species has been demonstrated previously ^[43].

Regarding Gram-positive bacteria, morusin reversed oxacillin resistance of MRSA and showed synergy with oxacillin or gentamicin against MRSA. The same molecule reversed tetracycline (functioning inside the cell) resistance of *Staphylococcus epidermidis* [109].

The high potency of mono-prenylated isoflavonoids together with their wide spectrum of activity, their fast killing and presumed low toxicity render these molecules as promising antimicrobials of natural origin. The exact interaction of these molecules with the membrane as well as with cytosolic targets awaits further investigation. Pharmacokinetic characteristics, side bioactivities, emergence of resistance and product/process conditions are some of the points that need to be evaluated for clinical and food applications of prenylated isoflavonoids.

6.4. References

- [1] Graham, T. & Graham, M. Role of hypersensitive cell death in conditioning elicitation competency and defense potentiation. *Physiological and Molecular Plant Pathology* **55**, 13-20 (1999).
- [2] Martinez-Medina, A., Flors, V., Heil, M., Mauch-Mani, B., Pieterse, C. M., Pozo, M. J., Ton, J., van Dam, N. M. & Conrath, U. Recognizing plant defense priming. *Trends in Plant Science* **21**, 818-822 (2016).
- [3] Conrath, U., Beckers, G. J., Langenbach, C. J. & Jaskiewicz, M. R. Priming for enhanced defense. *Annual Review of Phytopathology* **53** (2015).
- [4] Hilker, M., Schwachtje, J., Baier, M., Balazadeh, S., Bäurle, I., Geiselhardt, S., Hincha, D. K., Kunze, R., Mueller-Roeber, B. & Rillig, M. C. Priming and memory of stress responses in organisms lacking a nervous system. *Biological Reviews* **91**, 1118-1133 (2016).
- [5] Balmer, A., Pastor, V., Gamir, J., Flors, V. & Mauch-Mani, B. The 'prime-ome': towards a holistic approach to priming. *Trends in Plant Science* **20**, 443-452 (2015).
- [6] Bhattacharyya, M. & Ward, E. Resistance, susceptibility and accumulation of glyceollins I-III in soybean organs inoculated with *Phytophthora megasperma* f. sp. *glycinea*. *Physiological and Molecular Plant Pathology* **29**, 227-237 (1986).
- [7] Simons, R., Vincken, J.-P., Roidos, N., Bovee, T. F., van Iersel, M., Verbruggen, M. A. & Gruppen, H. Increasing soy isoflavonoid content and diversity by simultaneous malting and challenging by a fungus to modulate estrogenicity. *Journal of Agricultural and Food Chemistry* **59**, 6748-6758 (2011).
- [8] Aisyah, S., Gruppen, H., Madzora, B. & Vincken, J.-P. Modulation of isoflavonoid composition of *Rhizopus oryzae* elicited soybean (*Glycine max*) seedlings by light and wounding. *Journal of Agricultural and Food Chemistry* **61**, 8657-8667 (2013).
- [9] Gagnon, H. & Ibrahim, R. K. Effects of various elicitors on the accumulation and secretion of isoflavonoids in white lupin. *Phytochemistry* **44**, 1463-1467 (1997).
- [10] Recourt, K., van Tunen, A. J., Mur, L. A., van Brussel, A. A., Lugtenberg, B. J. & Kijne, J. W. Activation of flavonoid biosynthesis in roots of *Vicia sativa* subsp. *nigra* plants by inoculation with *Rhizobium leguminosarum* biovar *viciae*. *Plant Molecular Biology* **19**, 411-420 (1992).
- [11] Dakora, F. D., Joseph, C. M. & Phillips, D. A. Alfalfa (*Medicago sativa* L.) root exudates contain isoflavonoids in the presence of *Rhizobium meliloti*. *Plant Physiology* **101**, 819-824 (1993).
- [12] Schmidt, P. E., Parniske, M. & Werner, D. Production of the phytoalexin glyceollin I by soybean roots in response to symbiotic and pathogenic infection. *Botanica acta* **105**, 18-25 (1992).

- [13] Parniske, M., Pausch, G. & Werner, D. Changes in flavonoid pattern of root hairs of *Glycine max* in response to symbiotic infection with *B. japonicum*. *Nitrogen fixation: hundred years after*. Stuttgart: Fisher Verlag **466** (1988).
- [14] Lind, P. QSAR analysis involving assay results which are only known to be greater than, or less than some cut-off limit. *Molecular informatics* **29**, 845-852 (2010).
- [15] Andini, S. *Antimicrobial isothiocyanates from Brassicaceae glucosinolates: Analysis, reactivity, and quantitative structure-activity relationships* PhD thesis, Wageningen University and Research, (2020).
- [16] Araya-Cloutier, C., Vincken, J. P., van de Schans, M. G. M., Hageman, J., Schaftenaar, G., den Besten, H. M. W. & Gruppen, H. QSAR-based molecular signatures of prenylated (iso)flavonoids underlying antimicrobial potency against and membrane-disruption in Gram positive and Gram negative bacteria. *Sci Rep* **8**, 9267 (2018).
- [17] Sadgrove, N. J., Oliveira, T. B., Khumalo, G. P., Vuuren, S. F. v. & van Wyk, B.-E. Antimicrobial isoflavones and derivatives from *Erythrina* (Fabaceae): structure activity perspective (sar & qsar) on experimental and mined values against *Staphylococcus aureus*. *Antibiotics* **9**, 223 (2020).
- [18] Wu, T., He, M., Zang, X., Zhou, Y., Qiu, T., Pan, S. & Xu, X. A structure-activity relationship study of flavonoids as inhibitors of *E. coli* by membrane interaction effect. *Biochimica et Biophysica Acta (BBA)-Biomembranes* **1828**, 2751-2756 (2013).
- [19] Das, S., Majumder, T., Sarkar, A., Mukherjee, P. & Basu, S. Flavonoids as BACE1 inhibitors: QSAR modelling, screening and in vitro evaluation. *International Journal of Biological Macromolecules* **165**, 1323-1330 (2020).
- [20] Zhang, L., Zhu, H., Oprea, T. I., Golbraikh, A. & Tropsha, A. QSAR modeling of the blood-brain barrier permeability for diverse organic compounds. *Pharmaceutical Research* **25**, 1902 (2008).
- [21] Zhu, H., Tropsha, A., Fourches, D., Varnek, A., Papa, E., Gramatica, P., Oberg, T., Dao, P., Cherkasov, A. & Tetko, I. V. Combinatorial QSAR modeling of chemical toxicants tested against *Tetrahymena pyriformis*. *Journal of chemical information and modeling* **48**, 766-784 (2008).
- [22] Asikainen, A., Ruuskanen, J. & Tuppurainen, K. Performance of (consensus) kNN QSAR for predicting estrogenic activity in a large diverse set of organic compounds. *SAR and QSAR in Environmental Research* **15**, 19-32 (2004).
- [23] Asikainen, A. H., Ruuskanen, J. & Tuppurainen, K. A. Consensus kNN QSAR: a versatile method for predicting the estrogenic activity of organic compounds in silico. A comparative study with five estrogen receptors and a large, diverse set of ligands. *Environmental science & technology* **38**, 6724-6729 (2004).
- [24] Gramatica, P., Pilutti, P. & Papa, E. Validated QSAR prediction of OH tropospheric degradation of VOCs: splitting into training- test sets and consensus modeling. *Journal of Chemical Information and Computer Sciences* **44**, 1794-1802 (2004).
- [25] Gramatica, P., Giani, E. & Papa, E. Statistical external validation and consensus modeling: a QSPR case study for Koc prediction. *Journal of Molecular Graphics and Modelling* **25**, 755-766 (2007).
- [26] Sutherland, J. J. & Weaver, D. F. Development of quantitative structure- activity relationships and classification models for anticonvulsant activity of hydantoin analogues. *Journal of Chemical Information and Computer Sciences* **43**, 1028-1036 (2003).
- [27] Hewitt, M., Cronin, M. T., Madden, J. C., Rowe, P. H., Johnson, C., Obi, A. & Enoch, S. J. Consensus QSAR models: do the benefits outweigh the complexity? *Journal of chemical information and modeling* **47**, 1460-1468 (2007).
- [28] Votano, J. R., Parham, M., Hall, L. H., Kier, L. B., Oloff, S., Tropsha, A., Xie, Q. & Tong, W. Three new consensus QSAR models for the prediction of Ames genotoxicity. *Mutagenesis* **19**, 365-377 (2004).
- [29] Li, Y., Shao, X. & Cai, W. A consensus least squares support vector regression (LS-SVR) for analysis of near-infrared spectra of plant samples. *Talanta* **72**, 217-222 (2007).

- [30] Katritzky, A. R., Kuanar, M., Slavov, S., Dobchev, D. A., Fara, D. C., Karelson, M., Acree Jr, W. E., Solov'ev, V. P. & Varnek, A. Correlation of blood–brain penetration using structural descriptors. *Bioorganic & Medicinal Chemistry* **14**, 4888-4917 (2006).
- [31] Horvath, D., Bonachera, F., Solov'Ev, V., Gaudin, C. & Varnek, A. Stochastic versus stepwise strategies for quantitative structure– activity relationship generation how much effort may the mining for successful QSAR models take? *Journal of chemical information and modeling* **47**, 927-939 (2007).
- [32] Wang, J., Krudy, G., Xie, X.-Q., Wu, C. & Holland, G. Genetic algorithm-optimized QSPR models for bioavailability, protein binding, and urinary excretion. *Journal of chemical information and modeling* **46**, 2674-2683 (2006).
- [33] Yap, C., Li, Z. & Chen, Y. Quantitative structure–pharmacokinetic relationships for drug clearance by using statistical learning methods. *Journal of Molecular Graphics and Modelling* **24**, 383-395 (2006).
- [34] de Bruijn, W. J., Hageman, J. A., Araya-Cloutier, C., Gruppen, H. & Vincken, J.-P. QSAR of 1, 4-benzoxazin-3-one antimicrobials and their drug design perspectives. *Bioorganic & Medicinal Chemistry* **26**, 6105-6114 (2018).
- [35] Li, J., Lei, B., Liu, H., Li, S., Yao, X., Liu, M. & Gramatica, P. QSAR study of malonyl-CoA decarboxylase inhibitors using GA-MLR and a new strategy of consensus modeling. *Journal of Computational Chemistry* **29**, 2636-2647 (2008).
- [36] Lei, B., Xi, L., Li, J., Liu, H. & Yao, X. Global, local and novel consensus quantitative structure-activity relationship studies of 4-(phenylaminomethylene) isoquinoline-1, 3 (2H, 4H)-diones as potent inhibitors of the cyclin-dependent kinase 4. *Analytica Chimica Acta* **644**, 17-24 (2009).
- [37] Atkinson, A. C. Plots, transformations and regression; an introduction to graphical methods of diagnostic regression analysis. (1985).
- [38] Roy, K., Das, R. N., Ambure, P. & Aher, R. B. Be aware of error measures. Further studies on validation of predictive QSAR models. *Chemometrics and Intelligent Laboratory Systems* **152**, 18-33 (2016).
- [39] Golbraikh, A. & Tropsha, A. Predictive QSAR modeling based on diversity sampling of experimental datasets for the training and test set selection. *Molecular diversity* **5**, 231-243 (2000).
- [40] Scior, T., Medina-Franco, J., Do, Q.-T., Martínez-Mayorga, K., Yunes Rojas, J. & Bernard, P. How to recognize and workaround pitfalls in QSAR studies: a critical review. *Current Medicinal Chemistry* **16**, 4297-4313 (2009).
- [41] Gibbons, S. Anti-staphylococcal plant natural products. *Natural Product Reports* **21**, 263-277 (2004).
- [42] Nikaido, H. Molecular basis of bacterial outer membrane permeability revisited. *Microbiology and Molecular Biology Reviews* **67**, 593-656 (2003).
- [43] Messier, C. & Grenier, D. Effect of licorice compounds licochalcone A, glabridin and glycyrrhizic acid on growth and virulence properties of *Candida albicans*. *Mycoses* **54**, e801-e806 (2011).
- [44] Cruciani, G., Crivori, P., Carrupt, P.-A. & Testa, B. Molecular fields in quantitative structure–permeation relationships: the VolSurf approach. *Journal of Molecular Structure: THEOCHEM* **503**, 17-30 (2000).
- [45] Tsuchiya, H. & Iinuma, M. Reduction of membrane fluidity by antibacterial sophoraflavanone G isolated from *Sophora exigua*. *Phytomedicine* **7**, 161-165 (2000).
- [46] Sianglum, W., Muangngam, K., Joycharat, N. & Voravuthikunchai, S. P. Mechanism of action and biofilm inhibitory activity of lupinifolin against multidrug-resistant enterococcal clinical isolates. *Microbial Drug Resistance* **25**, 1391-1400 (2019).
- [47] Dzoyem, J. P., Hamamoto, H., Ngameni, B., Ngadjui, B. T. & Sekimizu, K. Antimicrobial action mechanism of flavonoids from *Dorstenia* species. *Drug Discoveries & Therapeutics* **7**, 66-72 (2013).
- [48] Selvaraj, S., Krishnaswamy, S., Devashya, V., Sethuraman, S. & Krishnan, U. M. Influence of membrane lipid composition on flavonoid–membrane interactions:

- Implications on their biological activity. *Progress in Lipid Research* **58**, 1-13 (2015).
- [49] Straus, S. K. & Hancock, R. E. Mode of action of the new antibiotic for Gram-positive pathogens daptomycin: comparison with cationic antimicrobial peptides and lipopeptides. *Biochimica et Biophysica Acta (BBA)-Biomembranes* **1758**, 1215-1223 (2006).
- [50] Pazin, W. M., da Silva Olivier, D., Vilanova, N., Ramos, A. P., Voets, I. K., Soares, A. E. E. & Ito, A. S. Interaction of Artepillin C with model membranes. *European Biophysics Journal* **46**, 383-393 (2017).
- [51] Li, J., Beuerman, R. W. & Verma, C. S. Molecular insights into the membrane affinities of model hydrophobes. *ACS omega* **3**, 2498-2507 (2018).
- [52] Zhang, Y., Algburi, A., Wang, N., Kholodovych, V., Oh, D. O., Chikindas, M. & Uhrich, K. E. Self-assembled cationic amphiphiles as antimicrobial peptides mimics: Role of hydrophobicity, linkage type, and assembly state. *Nanomedicine: Nanotechnology, Biology and Medicine* **13**, 343-352 (2017).
- [53] Chen, Y., Guarnieri, M. T., Vasil, A. I., Vasil, M. L., Mant, C. T. & Hodges, R. S. Role of peptide hydrophobicity in the mechanism of action of α -helical antimicrobial peptides. *Antimicrobial Agents and Chemotherapy* **51**, 1398-1406 (2007).
- [54] Newcomb, C. J., Moyer, T. J., Lee, S. S. & Stupp, S. I. Advances in cryogenic transmission electron microscopy for the characterization of dynamic self-assembling nanostructures. *Current Opinion in Colloid & Interface Science* **17**, 350-359 (2012).
- [55] Wimley, W. C. Describing the mechanism of antimicrobial peptide action with the interfacial activity model. *ACS Chemical Biology* **5**, 905-917 (2010).
- [56] Rathinakumar, R., Walkenhorst, W. F. & Wimley, W. C. Broad-spectrum antimicrobial peptides by rational combinatorial design and high-throughput screening: the importance of interfacial activity. *Journal of the American Chemical Society* **131**, 7609-7617 (2009).
- [57] Wesółowska, O., Gąsiorowska, J., Petrus, J., Czarnik-Matusiewicz, B. & Michalak, K. Interaction of prenylated chalcones and flavanones from common hop with phosphatidylcholine model membranes. *Biochimica et Biophysica Acta (BBA)-Biomembranes* **1838**, 173-184 (2014).
- [58] Hendrich, A. B., Malon, R., Pola, A., Shirataki, Y., Motohashi, N. & Michalak, K. Differential interaction of *Sophora* isoflavonoids with lipid bilayers. *European Journal of Pharmaceutical Sciences* **16**, 201-208 (2002).
- [59] Kostecka-Gugała, A., Latowski, D. & Strzałka, K. Thermotropic phase behaviour of α -dipalmitoylphosphatidylcholine multibilayers is influenced to various extents by carotenoids containing different structural features-evidence from differential scanning calorimetry. *Biochimica et Biophysica Acta (BBA)-Biomembranes* **1609**, 193-202 (2003).
- [60] O'Grady, F. in *Antibiotics and Chemotherapeutic Agents*. (SAGE Publications).
- [61] Riezman, H. Yeast endocytosis. *Trends in cell biology* **3**, 273-277 (1993).
- [62] Mukhopadhyay, D. & Riezman, H. Proteasome-independent functions of ubiquitin in endocytosis and signaling. *Science* **315**, 201-205 (2007).
- [63] Geli, M. I. & Riezman, H. Endocytic internalization in yeast and animal cells: similar and different. *Journal of Cell Science* **111**, 1031-1037 (1998).
- [64] Riezman, H., Munn, A., Geli, M. & Hicke, L. Actin-, myosin- and ubiquitin-dependent endocytosis. *Experientia* **52**, 1033-1041 (1996).
- [65] Rossignol, T., Kelly, B., Dobson, C. & d'Enfert, C. Endocytosis-mediated vacuolar accumulation of the human ApoE apolipoprotein-derived ApoEdPL-W antimicrobial peptide contributes to its antifungal activity in *Candida albicans*. *Antimicrobial Agents and Chemotherapy* **55**, 4670-4681 (2011).
- [66] El-Mounadi, K., Islam, K. T., Hernández-Ortiz, P., Read, N. D. & Shah, D. M. Antifungal mechanisms of a plant defensin MtDef4 are not conserved between the ascomycete fungi *Neurospora crassa* and *Fusarium graminearum*. *Molecular Microbiology* **100**, 542-559 (2016).

- [67] Araya-Cloutier, C. *Antibacterial prenylated isoflavonoids and stilbenoids: quantitative structure-activity relationships and mode of action* PhD thesis, Wageningen University, (2017).
- [68] Pang, D., Liao, S., Wang, W., Mu, L., Li, E., Shen, W., Liu, F. & Zou, Y. Destruction of the cell membrane and inhibition of cell phosphatidic acid biosynthesis in *Staphylococcus aureus*: an explanation for the antibacterial mechanism of morusin. *Food & Function* **10**, 6438-6446 (2019).
- [69] Limsuwan, S., Moosigapong, K., Jarukitsakul, S., Joycharat, N., Chusri, S., Jaisamut, P. & Voravuthikunchai, S. P. Lupinifolin from *Albizia myriophylla* wood: A study on its antibacterial mechanisms against cariogenic *Streptococcus mutans*. *Archives of Oral Biology* **93**, 195-202 (2018).
- [70] Petiti, M., Houot, L. & Duché, D. Cell fractionation. in *Bacterial Protein Secretion Systems* 59-64 (Springer, 2017).
- [71] Jang, W. S., Bajwa, J. S., Sun, J. N. & Edgerton, M. Salivary histatin 5 internalization by translocation, but not endocytosis, is required for fungicidal activity in *Candida albicans*. *Molecular Microbiology* **77**, 354-370 (2010).
- [72] Gerits, E., Blommaert, E., Lippell, A., O'Neill, A. J., Weytjens, B., De Maeyer, D., Fierro, A. C., Marchal, K., Marchand, A. & Chaltin, P. Elucidation of the mode of action of a new antibacterial compound active against *Staphylococcus aureus* and *Pseudomonas aeruginosa*. *PloS One* **11**, e0155139 (2016).
- [73] Fujita, K., Matsuyama, A., Kobayashi, Y. & Iwahashi, H. The genome-wide screening of yeast deletion mutants to identify the genes required for tolerance to ethanol and other alcohols. *FEMS yeast research* **6**, 744-750 (2006).
- [74] Sinai, L., Rosenberg, A., Smith, Y., Segev, E. & Ben-Yehuda, S. The molecular timeline of a reviving bacterial spore. *Molecular cell* **57**, 695-707 (2015).
- [75] Warda, A. K., Xiao, Y., Boekhorst, J., Wells-Bennik, M. H., Groot, M. N. N. & Abee, T. Analysis of germination capacity and germinant receptor (sub) clusters of genome-sequenced *Bacillus cereus* environmental isolates and model strains. *Applied and Environmental Microbiology* **83** (2017).
- [76] Cho, W.-I. & Chung, M.-S. *Bacillus* spores: a review of their properties and inactivation processing technologies. *Food Science and Biotechnology* **29**, 1447-1461 (2020).
- [77] Abee, T., Groot, M. N., Tempelaars, M., Zwietering, M., Moezelaar, R. & van der Voort, M. Germination and outgrowth of spores of *Bacillus cereus* group members: diversity and role of germinant receptors. *Food microbiology* **28**, 199-208 (2011).
- [78] van Melis, C., Almeida, C. B., Kort, R., Groot, M. N. & Abee, T. Germination inhibition of *Bacillus cereus* spores: impact of the lipophilic character of inhibiting compounds. *International Journal of Food Microbiology* **160**, 124-130 (2012).
- [79] Cortezzo, D., Setlow, B. & Setlow, P. Analysis of the action of compounds that inhibit the germination of spores of *Bacillus* species. *Journal of Applied Microbiology* **96**, 725-741 (2004).
- [80] Yasuda-Yasaki, Y., Namiki-Kanie, S. & Hachisuka, Y. Inhibition of *Bacillus subtilis* spore germination by various hydrophobic compounds: demonstration of hydrophobic character of the L-alanine receptor site. *Journal of Bacteriology* **136**, 484-490 (1978).
- [81] Hornstra, L. M., de Vries, Y. P., de Vos, W. M., Abee, T. & Wells-Bennik, M. H. gerR, a novel ger operon involved in L-alanine-and inosine-initiated germination of *Bacillus cereus* ATCC 14579. *Applied and Environmental Microbiology* **71**, 774-781 (2005).
- [82] Alanazi, S., Alnoman, M., Banawas, S., Saito, R. & Sarker, M. R. The inhibitory effects of essential oil constituents against germination, outgrowth and vegetative growth of spores of *Clostridium perfringens* type A in laboratory medium and chicken meat. *Food microbiology* **73**, 311-318 (2018).
- [83] Hernandez-Brenes, C., Garcia-Cruz, M. I., Gutierrez-Urbe, J. A., Benavides-Lozano, J. A. & Rodriguez-Sanchez, D. G. Antimicrobial, antibacterial and spore

- germination inhibiting activity from an avocado extract enriched in bioactive compounds. (2013).
- [84] Üstök, F. I., Packman, L. C., Lowe, C. R. & Christie, G. Spore germination mediated by *Bacillus megaterium* QM B1551 SleL and YpeB. *Journal of Bacteriology* **196**, 1045-1054 (2014).
 - [85] Arjes, H. A., Vo, L., Dunn, C. M., Willis, L., DeRosa, C. A., Fraser, C. L., Kearns, D. B. & Huang, K. C. Biosurfactant-mediated membrane depolarization maintains viability during oxygen depletion in *Bacillus subtilis*. *Current Biology* **30**, 1011-1022 (2020).
 - [86] Davidson, P. M., Critzer, F. J. & Taylor, T. M. Naturally occurring antimicrobials for minimally processed foods. *Annual Review of Food Science and Technology* **4**, 163-190 (2013).
 - [87] Lee, J.-H., Kim, Y.-G., Khadke, S. K., Yamano, A., Woo, J.-T. & Lee, J. Antimicrobial and antibiofilm activities of prenylated flavanones from *Macaranga tanarius*. *Phytochemistry* **63**, 153033 (2019).
 - [88] Šmejkal, K. Cytotoxic potential of C-prenylated flavonoids. *Phytochemistry Reviews* **13**, 245-275 (2014).
 - [89] Aoki, F., Nakagawa, K., Kitano, M., Ikematsu, H., Nakamura, K., Yokota, S., Tominaga, Y., Arai, N. & Mae, T. Clinical safety of licorice flavonoid oil (LFO) and pharmacokinetics of glabridin in healthy humans. *Journal of the American College of Nutrition* **26**, 209-218 (2007).
 - [90] Hamamoto, H., Tonoike, A., Narushima, K., Horie, R. & Sekimizu, K. Silkworm as a model animal to evaluate drug candidate toxicity and metabolism. *Comparative Biochemistry and Physiology Part C: Toxicology & Pharmacology* **149**, 334-339 (2009).
 - [91] Sohn, H.-Y., Kwon, C.-S. & Son, K.-H. Fungicidal effect of prenylated flavonol, papyriflavonol a, isolated from *Broussonetia papyrifera* (L.) vent. against *Candida albicans*. *Journal of Microbiology and Biotechnology* **20**, 1397-1402 (2010).
 - [92] Yusook, K., Weerananantapan, O., Hua, Y., Kumkrai, P. & Chudapongse, N. Lupinifolin from *Derris reticulata* possesses bactericidal activity on *Staphylococcus aureus* by disrupting bacterial cell membrane. *Journal of Natural Medicines* **71**, 357-366 (2017).
 - [93] Koh, J.-J., Qiu, S., Zou, H., Lakshminarayanan, R., Li, J., Zhou, X., Tang, C., Saraswathi, P., Verma, C. & Tan, D. T. Rapid bactericidal action of alpha-mangostin against MRSA as an outcome of membrane targeting. *Biochimica et Biophysica Acta (BBA)-Biomembranes* **1828**, 834-844 (2013).
 - [94] Roland, W. S., Vincken, J.-P., Gouka, R. J., van Buren, L., Gruppen, H. & Smit, G. Soy isoflavones and other isoflavonoids activate the human bitter taste receptors hTAS2R14 and hTAS2R39. *Journal of Agricultural and Food Chemistry* **59**, 11764-11771 (2011).
 - [95] Keast, R. S. & Breslin, P. A. Modifying the bitterness of selected oral pharmaceuticals with cation and anion series of salts. *Pharmaceutical Research* **19**, 1019-1026 (2002).
 - [96] Munin, A. & Edwards-Lévy, F. Encapsulation of natural polyphenolic compounds; a review. *Pharmaceutics* **3**, 793-829 (2011).
 - [97] Szejtli, J. & Szenté, L. Elimination of bitter, disgusting tastes of drugs and foods by cyclodextrins. *European journal of pharmaceuticals and biopharmaceutics* **61**, 115-125 (2005).
 - [98] Thomas, D. & Davenport, R. *Zygosaccharomyces bailii*—a profile of characteristics and spoilage activities. *Food Microbiology* **2**, 157-169 (1985).
 - [99] Araya-Cloutier, C., den Besten, H. M., Aisyah, S., Gruppen, H. & Vincken, J.-P. The position of prenylation of isoflavonoids and stilbenoids from legumes (Fabaceae) modulates the antimicrobial activity against Gram positive pathogens. *Food Chemistry* **226**, 193-201 (2017).
 - [100] Legette, L., Ma, L., Reed, R. L., Miranda, C. L., Christensen, J. M., Rodriguez-Proteau, R. & Stevens, J. F. Pharmacokinetics of xanthohumol and metabolites in

- rats after oral and intravenous administration. *Molecular nutrition & food research* **56**, 466-474 (2012).
- [101] Legette, L., Karnpracha, C., Reed, R. L., Choi, J., Bobe, G., Christensen, J. M., Rodriguez-Proteau, R., Purnell, J. Q. & Stevens, J. F. Human pharmacokinetics of xanthohumol, an antihyperglycemic flavonoid from hops. *Molecular Nutrition & Food Research* **58**, 248-255 (2014).
- [102] Patel, S., Preuss, C. V. & Bernice, F. in *StatPearls [Internet]* (2020).
- [103] Shelke, S., Shinkar, D. & Saudagar, R. Topical gel: a novel approach for development of topical drug delivery system. *International Journal of Pharmacy & Technology* **5**, 2739-2763 (2013).
- [104] Chopra, I., Hesse, L. & O'Neill, A. J. Exploiting current understanding of antibiotic action for discovery of new drugs. *Journal of Applied Microbiology* **92**, 4S-15S (2002).
- [105] Blair, J. M., Webber, M. A., Baylay, A. J., Ogbolu, D. O. & Piddock, L. J. Molecular mechanisms of antibiotic resistance. *Nature Reviews Microbiology* **13**, 42-51 (2015).
- [106] Costerton, J. W., Stewart, P. S. & Greenberg, E. P. Bacterial biofilms: a common cause of persistent infections. *Science* **284**, 1318-1322 (1999).
- [107] Uppu, D. S., Konai, M. M., Sarkar, P., Samaddar, S., Fensterseifer, I. C., Farias-Junior, C., Krishnamoorthy, P., Shome, B. R., Franco, O. L. & Haldar, J. Membrane-active macromolecules kill antibiotic-tolerant bacteria and potentiate antibiotics towards Gram-negative bacteria. *PLoS One* **12**, e0183263 (2017).
- [108] Liu, W., Li, L. P., Zhang, J. D., Li, Q., Shen, H., Chen, S. M., He, L. J., Yan, L., Xu, G. T. & An, M. M. Synergistic antifungal effect of glabridin and fluconazole. *PLoS One* **9**, e103442 (2014).
- [109] Aelenei, P., Rumbu, C. M., Horhoge, C. E., Lobiuc, A., Neagu, A.-N., Dunca, S. I., Motrescu, I., Dimitriu, G., Aprotosoia, A. C. & Miron, A. Prenylated phenolics as promising candidates for combination antibacterial therapy: Morusin and kuwanon G. *Saudi Pharmaceutical Journal* **28**, 1172-1181 (2020).

Summary

Antimicrobial persistence and resistance of clinical- and food-associated microorganisms to traditional antimicrobials has accelerated the search for novel antimicrobial agents. Furthermore, the negative reputation of traditional preservatives, such as e.g. sorbic acid, among consumers accelerates the quest for novel ones. The Leguminosae family is one of the richest sources of novel, promising, natural antimicrobials. Prenylated (C5-isoprenoid substituted) (iso)flavonoids are accumulated in legumes as a part of plant's defence mechanism. Prenyl substitution is usually responsible for the antimicrobial function of (iso)flavonoids, due to the highly lipophilic character it brings on to the molecules. Molecular hydrophobicity is known to increase the affinity towards biological targets. However, accumulating evidence suggests that hydrophobicity cannot be the only determinant of the activity of prenylated (iso)flavonoids. In this thesis, it was attempted to reveal other key molecular properties important for activity and to correlate these with the mechanism of action of prenylated (iso)flavonoids. Prior to this, a novel method of elicitation was explored to increase the content and diversity of these molecules in the well-studied legume, soybean.

In **Chapter 1**, the background and objectives of this PhD research are provided. The problem posed by key pathogenic and food spoilage microorganisms, as well as the opportunities offered by plants, especially those of the Leguminosae family, to combat these microorganisms is described. Overviews of different methods employed to stimulate the biosynthesis of prenylated (iso)flavonoids *in planta* and of their antimicrobial potency are provided. Last, the importance of *in silico* tools in antimicrobial research is highlighted.

In **Chapter 2**, sensitization of soybean seedlings prior to the traditional fungal elicitation was employed to enhance the production of glyceollins in two soybean cultivars (mixCv and 'Envy'). Liquid chromatography coupled to mass spectrometry was used to identify and quantify the prenylated isoflavonoids and their precursor isoflavonoids in the differently treated seedling extracts. Reactive oxygen species (ROS), key molecules in plant's signal transduction, were shown to be twice as effective than physical agents (i.e. wounding) in sensitizing soybean seedlings. Furthermore, the ROS-treatment showed specificity towards the production of prenylated pterocarpans (glyceollins). The ROS treatment prior elicitation with *Rhizopus* spp. induced 8.6 ± 0.9 and 4.6 ± 0.3 μmol glyceollins per g dry weight (DW) seedlings, being 4 and 1.3 times higher than with fungal elicitation without prior treatments in the mixCv and 'Envy' cultivar, respectively.

In **Chapter 3**, the ROS-sensitization treatment was extended by using the long-lived ROS representative, H_2O_2 , in combination with AgNO_3 as an effort to diversify the array of inducible prenylated compounds in 'Envy' from **Chapter 2**. H_2O_2 + AgNO_3 without any subsequent treatments was as effective as the treatment described in **Chapter 2** for the production of glyceollins. This suggested that the microbial agent is not necessary for the biosynthesis of glyceollins in soybeans, showing possibilities to circumvent the very intricate host-microbe relationship.

Subsequent microbial elicitation of the (H₂O₂ + AgNO₃)-treated seedlings diversified the prenylated (iso)flavonoids by triggering the additional production of two prenylated isoflavones and of a prenylated coumestan. The rhizobacterium, *B. subtilis*, induced 30% higher accumulation of prenylated isoflavones than the classical, phytopathogenic fungus, *Rhizopus* spp., in (H₂O₂ + AgNO₃)-treated seedlings. The most strongly induced prenylated isoflavone, 6-prenyl daidzein was predicted to be a very promising antibacterial by using a previously developed quantitative structure-activity relationship (QSAR) model for *L. monocytogenes* and *E. coli*.

In **Chapter 4**, the antimicrobial potency of prenylated (iso)flavonoids from liquorice and soybean against methicillin-resistant *Staphylococcus aureus* (MRSA) was explored and the killing time of the most active ones was established to be 2 h at their minimum bactericidal concentration (MBC). Then, antimicrobial activity data of other prenylated (iso)flavonoids against MRSA obtained from literature was assembled to create a large dataset for robust QSAR modelling. A set of 77 molecules was used to develop QSAR models, to select the best one and to externally validate it. The developed QSAR model (R^2_{adj} 0.61, Q^2_{Loo} 0.57 and Q^2_{test} 0.75) was also used to classify prenylated (iso)flavonoids tested against other Gram-positives as good, moderate and poor antibacterials. Seventy three % of these molecules were correctly classified, suggesting that the model can be used as a tool to predict the potency of prenylated (iso)flavonoids against Gram-positive bacteria. In addition, a 3D-pharmacophore model was constructed to give an insight in important molecular features for anti-MRSA activity. The *in silico* analyses showed that properties such as formal charge, hydrogen-bonding and hydrophobic volume underlie antibacterial activity. These properties were correlated to mode of action of prenylated (iso)flavonoids. Prenylated (iso)flavonoids from different subclasses were proposed to interact differently with their bacterial main target (i.e. the cytoplasmic membrane), depending on their main molecular properties. Last, the importance of formal charge implied potential secondary cytosolic activity of prenylated (iso)flavonoids with low pKa.

In **Chapter 5**, the antimicrobial properties of 19 prenylated (iso)flavonoids were assayed for the first time against the food spoilage yeast, *Zygosaccharomyces parabailii*. Mono-prenylated (iso)flavonoids were active (minimum inhibitory concentration, MIC \leq 25 $\mu\text{g/mL}$) against *Z. parabailii* at the normal pH of the growth medium, whereas their di-prenylated analogues were not. A binary QSAR model was constructed using the electrostatic component of potential energy and the hydrophobic integrity moment as positively correlated descriptors to antifungal activity. The model showed high cross-validated accuracies (total, on actives and on inactives) of $> 85\%$. Furthermore, at a pH relevant for *Z. parabailii* (pH 4.0), wighteone and glabridin showed a MIC \leq 12.5 $\mu\text{g/mL}$, making them the most active natural antifungals against *Z. parabailii* known to date. The mode of action of these compounds was explored by determining their killing rate and employing assays to

determine their membrane activity at this pH. Wighteone and glabridin were found to interact quickly (within 15 min) with the membrane, yet in different ways.

In **Chapter 6**, the main findings of this thesis are discussed. Main considerations with techniques used to enhance the biosynthesis of prenylated (iso)flavonoids and *in silico* modelling of their activity were addressed. Progressive insights into their mode of action by merging the findings of **Chapters 4** and **5** are provided. Finally, prospects of prenylated (iso)flavonoids as novel therapeutics and as food preservatives are elaborated.

To summarize, sensitization of soybean seedlings with abiotic agents enhanced and diversified the synthesis of prenylated isoflavonoids from different subclasses. A robust QSAR regression model was developed and evidenced to be a useful tool for the prediction of antibacterial activity of new compounds not only limited to MRSA, but also applicable to other Gram-positive bacteria. These different properties were also proposed to mediate differential cellular uptake and interactions with the cytoplasmic membrane. Different membrane activity was shown by two of the most active antimicrobial prenylated isoflavonoids against *Z. parabailii*. Potential secondary cytosolic activity of prenylated (iso)flavonoids needs to be further explored. The properties derived from the QSAR models developed for MRSA and *Z. parabailii* can be considered during the design of novel prenylated (iso)flavonoids as antimicrobial agents.

Acknowledgements

After four years involving an everlasting pandemic, it is time to express my appreciation to the people without whom I would not have made it or contributed to a fun and caring atmosphere.

Jean-Paul, the boss. I should start by thanking you for your impressive patience with my theatrical and sarcastic attitude; that was not an easy task considering that this attitude was escalating over the years. Furthermore, your guidance, motivational spirit and support on the PhD itself but also on personal matters were definitely some of the key aspects of finalizing this PhD on time! Your presence and our short (and long) talks in an empty building at the final phase of the PhD, really kept me going. I cannot thank you enough for giving me the opportunity to work on a topic that I was absolutely keen on since my MSc thesis and for the opportunity to collaborate with my other two favorite people, Carla and Wouter.

Carla, the small boss. Our scientific discussions and your unstoppable passion for science, your patience with my (occasional) recalcitrance and your calmness during crisis are some of the things I want to thank you for. On top of these, I admire you as a person and I truly appreciate you as a friend.

Wouter, I started by not knowing how to write down your name. Now, we have very creative nicknames for each other. I am greatly thankful for your constant help, support and encouragement from the first day of my MSc thesis until the last one of my PhD.

John Chapman and Jan-Willem Sanders, I would like to thank you for constant support and your readiness to help with anything I needed.

Jos Hageman, thank you for your contribution to the QSAR study on MRSA and for patiently answering all my questions.

Moreover, I would like to extend my appreciation to the entire FCH group. I am grateful for the nice moments and memories I had with the people of FCH during and outside working hours.

Jolanda, FCH's safety belt. Besides your help to every organizational matter and the moral support, I would like to specially thank you for all the chewing gums you gave me and the chocolates we exchanged.

Mirjam, the warm-hearted one. Thank you Mirjam for always being approachable and truly helpful for everyone in need. I will never forget your visit at my place to bring me a movie and chocolates together with a sweet note, when I had to quarantine.

Special thanks to the initial members of the office X0132 (formerly known as 1.03), Alexandra, Bianca and Suzanne. You were the best officemates I could have asked for. I appreciate the different qualities you gave to this office and your encouragement even after you left it. Αλεξάνδρα, σε ευχαριστώ για την αδιάκοπη στήριξη σε όλα τα επίπεδα αυτά τα 4 χρόνια. Με μια σου λέξη, γινόσουν η φωνή της λογικής που χρειαζόμουν. Μαζί με τον Ηλία ήσασταν πάντοτε (ηθικά κυρίως λόγω των συνθηκών) παρόντες σε ό,τι χρειάστηκα. Of course, the composition of the

office largely changed over the years, so I would like to also thank Renske, Tibo, Loes, Roelant, Έλενα and Marina who in one way or another all contributed to a fun office. Roelant, I enjoyed teaching you Greek. You were such a great learner (of course!). Besides, I totally appreciate your immense help and frustration-sharing with the LC-MS systems. Έλενα, αν και ήμασταν ελάχιστα στο ίδιο γραφείο, αυτό δεν μας σταμάτησε από το να κάνουμε όμορφες συζητήσεις, να μου δίνεις χρήσιμες συμβουλές για τα πάντα και φυσικά να μου δίνεις το περίσσευμα από το φαγητό σου.

Katharina, *Cantharellus cibarius*. Canthy mou, I have laughed so much with you and I truly enjoyed our talks, walks and the time we have spent together. I deeply appreciate your help and care when I needed it, by bringing me food, my desktop and even my office chair.

Silvia, thank you for your constant help, our interesting discussions on our topics the last 4 years and of course the "interplay".

Zhibin, the gentleman. We started our PhD projects together and you were always a few steps ahead. It was fun working with you on the opposite sides of the same lab-bench in the phytolab and next to each other in the microlab where you performed all this magic in the anaerobic chamber. Last, I greatly appreciate all your help in the last organizational parts of the thesis.

Δημήτρη, συνοδοιπόροι σε όλο το MSc, στην απόφαση μας να μην κάνουμε διδακτορικό και στο ότι τελικά επιστρέψαμε στο FCH για να κάνουμε διδακτορικό. Το σάντουιτς με τα Captain iglo και το Aperol ήταν ένα από τα highlights, του κατά τ'άλλα επεισοδιακού, PhD trip.

Judith, thanks for putting my name in all the activities that I did not subscribe timely and the encouraging words whenever you were passing by my office at the final stage of the PhD. Sarah, thanks for making a chocolate stash in your office so that I could satisfy my sweet tooth without exaggerations. Natalia, I appreciate the regular updates when there was new, good stuff in the stash.

Yiran Lin, Ben Skiller, Myrthe Leermarker, Sanne Folkertsma, Janniek Ritsema, Yiyun Liu and Eva van der Burgt, thank you for contributing to my research as part of your BSc or MSc studies. It was a pleasure and a great learning process for me to work with all of you.

Last but not least, I would like to thank our technicians for all those times they assisted me in technical matters.

Moreover, I need to express my appreciation to the people outside FCH.

Εβίτα, σε ευχαριστώ για τα γέλια μέχρι δακρύων που με έκαναν να ξεχνώ οποιαδήποτε δυσκολία μέσα στη μέρα, τις καθησυχαστικές σου κουβέντες σε περιόδους κρίσης και την έμπρακτη βοήθεια σου σε διάφορα ζητήματα. Μαρία, σε ευχαριστώ για τα νόστιμα και θρεπτικά λαδερά σου.

Βασίλω, ♪ on a dark desert highway. Σε ευχαριστώ κυρίως για τη χρονιά 2017-2018 που ακούσαμε αυτό το τραγούδι 1000 φορές.

Rob van Dam, your positive energy and smile whenever I was passing by your office to get some extra vitamins, were always a refreshing break for me.

Χρήστο, σε ευχαριστώ που με ενθάρρυνες από τα «μπαλκόνια» του 1^{ου} ορόφου.

Ingrid, thank you for your hospitality when I had to prepare my countless media at the FHM kitchen.

Δεν θα μπορούσα να μην ευχαριστήσω τις φίλες μου στην Ελλάδα, Αφροδίτη (Τίτη), Αφροδίτη (Camay), Τερέζα, Σοφία, Μυρτώ, Γιάννα και Μαριφίλη, που συνέβαλλαν σημαντικά στο να γεμίζω μπαταρίες τα Χριστούγεννα και τα καλοκαίρια που κατάφερνα να ξεφύγω από το PhD.

Επίσης θέλω να εκφράσω την απεριόριστη ευγνωμοσύνη στην οικογένεια μου που ήταν αρωγός και σε αυτή μου την προσπάθεια.

Μαμά μου, πάντα διακριτικά δίπλα μου. Σ'ευχαριστώ για τις ενέσεις αισιοδοξίας, ενθάρρυνσης και γέλιου. Ήταν πολύ σημαντικό για μένα που ήρθες όταν σε είχα πεθυμήσει πολύ, εν μέσω της πανδημίας.

Νονάκα μου, τίποτα δεν θα γινόταν χωρίς τη βοήθεια σου 7 χρόνια πριν. Πάντα μας εντυπωσιάζεις με το πόσο «μέσα σε όλα» είσαι.

Γιώργο, σε ευχαριστώ για την πολύτιμη ηθική στήριξη, ενθάρρυνση και τα γέλια μέχρι δακρύων όλα αυτά τα χρόνια παρόλη την απόσταση.

Ραϋμόνδε, σε ευχαριστώ για τις συμβουλές σου στο cover και που με άφηνες να δουλεύω στον διαστημικό υπολογιστή σου, όποτε και να σου το ζητούσα.

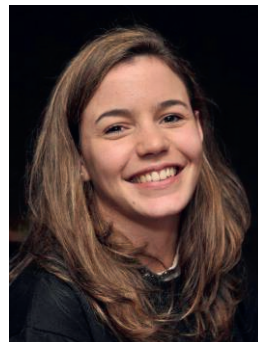
Τέλος, θέλω ολόψυχα να ευχαριστήσω τον άνθρωπο που μου στάθηκε όσο κανείς. Αγαπημένε μου Κωσταντίνε, μοναδικέ μου Όρο, ό,τι και αν γράψω δεν είναι αρκετό για να περιγράψει την υπερπολύτιμη βοήθεια, την ουσιαστική στήριξη και τη βαθιά πίστη σου σε εμένα. Έκανες όλη τη διαδικασία του διδακτορικού πιο εύκολη, πιο εφικτή. Σε ευχαριστώ πραγματικά γιατί ανέχτηκες κάθε παραξενιά και δυσκολία, εκλογίκευσες κάθε ανησυχία και ενδιαφέρθηκες αληθινά για κάθε κομμάτι αυτής μου της προσπάθειας. Εύχομαι να μου δίνεται για πολύ καιρό ακόμα η ευκαιρία να σου δείχνω πόσο σημαντικός είσαι στη ζωή μου.

Σύλβια

About the author

Curriculum vitae

Sylvia Kalli-Angel was born on September 18, 1991 in Athens, Greece. In 2009, she started her studies in Chemistry at the National and Kapodistrian University of Athens (UoA), Greece. Her bachelor thesis focused on the organic synthesis of heterocyclic amines with potential bioactivity. After that, she did an internship at the General Chemical State Laboratory of Greece, where she performed chemical analyses in food and water samples. In 2014, she started her MSc studies in Food Technology with a specialization in Food Ingredient Functionality, Wageningen University, the Netherlands. Her thesis focused on the effect of abiotic elicitation on the modification of phytochemical content of legumes. The thesis was performed at the Laboratory of Food Chemistry, Wageningen University. As part of her MSc study program, she did an industrial internship at FrieslandCampina DOMO, Wageningen, the Netherlands, where she explored the development of a new concentrated medical nutrition model. After graduating in 2016, she joined the Laboratory of Food Chemistry as an educational assistant. In 2017, she started her PhD research at the Laboratory of Food Chemistry. The results of her PhD research are presented in this thesis. Sylvia continues to work at the Laboratory of Food Chemistry as a postdoctoral researcher.



✉ : sylviakalli.18@gmail.com



List of publications

Kalli Sylvia; Araya-Cloutier, Carla; Chapman, John; Sanders, Jan-Willem; Vincken, Jean-Paul. Prenylated (iso)flavonoids as antifungal agents against the food spoiler *Zygosaccharomyces parabailii*. *Submitted for publication*.

Kalli Sylvia; Araya-Cloutier, Carla; Hageman, Jos; Vincken, Jean-Paul. Prenylated (iso)flavonoids as agents against methicillin-resistant *Staphylococcus aureus* - Insights into the molecular properties underlying antibacterial activity. *Submitted for publication*.

Kalli Sylvia; Araya-Cloutier, Carla; de Bruijn, Wouter; Chapman, John; Vincken, Jean-Paul. 2020. Induction of promising antibacterial prenylated isoflavonoids from different subclasses by sequential elicitation of soybean. *Phytochemistry*, 179: 112496.

Kalli Sylvia; Araya-Cloutier, Carla; Lin, Yiran; de Bruijn, Wouter; Chapman, John; Vincken, Jean-Paul. 2020. Enhanced biosynthesis of the natural antimicrobial glyceollins in soybean seedlings by priming and elicitation. *Food Chemistry* 317: 126389.

Overview of completed training activities

Discipline specific activities

Courses

Advanced food analysis	VLAG, Wageningen, 2017
Food and biorefinery enzymology	VLAG, Wageningen, 2017
International chemical design and discovery course	CMBI, Nijmegen, 2017
Applied statistics	VLAG, Wageningen, 2018
Chemometrics	VLAG, Wageningen, 2018
PhD VLAG scientific lectures	VLAG, Wageningen, 2020

Conferences

Biochemistry, molecular aspects and pharmacology of bioactive natural products ^a	PSE, Budapest, 2019
IMEKOFOODS	PSE, online, 2020
Plant derived natural products as pharmacological and nutraceutical tools	PSE, online, 2020

General courses

VLAG PhD week	VLAG, Baarlo, 2017
The essentials of scientific writing & presenting	WGS, Wageningen, 2017
Introduction to R	VLAG, Wageningen, 2018
Scientific writing	WGS, Wageningen, 2018
Career orientation	VLAG, Wageningen, 2019

Optionals

Research proposal preparation	FCH, Wageningen, 2017
PhD study trip 2018 ^{a,b}	FCH, Italy and Austria, 2018
BSc and MSc thesis student supervisions, presentations, and colloquia	FCH, Wageningen, 2017-2020
PhD presentations	FCH, Wageningen, 2017-2020

^a Poster presentation.

^b Oral presentation.

Abbreviations: CMBI, Center for Molecular and Biomolecular Informatics. FCH, Laboratory of Food Chemistry, Wageningen University. PSE, Phytochemical Society of Europe. VLAG, Graduate School for Food Technology, Agrobiotechnology, Nutrition, and Health Sciences. WGS, Wageningen Graduate Schools.

The research described in this thesis was performed at the Laboratory of Food Chemistry, Wageningen University & Research, the Netherlands.

Funding for this work was provided by Unilever's global Foods Innovation Centre in Wageningen, the Netherlands.

Financial support from Wageningen University for printing this thesis is gratefully acknowledged.

Cover design by Sylvia Kalli-Angel
Printed by ProefschriftMaken, the Netherlands
Edition: 180 copies

Sylvia Kalli-Angel, 2021

